DISSERTATION

CHANNEL CHANGES DOWNSTREAM

OF THE HAPCHEON RE-REGULATION DAM

IN SOUTH KOREA

Submitted by

Young Ho Shin

Department of Civil and Environmental Engineering

In partial fulfillment of the requirements

For the Degree of Doctor of Philosophy

Colorado State University

Fort Collins, Colorado

Fall 2007

UMI Number: 3299783

INFORMATION TO USERS

The quality of this reproduction is dependent upon the quality of the copy submitted. Broken or indistinct print, colored or poor quality illustrations and photographs, print bleed-through, substandard margins, and improper alignment can adversely affect reproduction.

In the unlikely event that the author did not send a complete manuscript and there are missing pages, these will be noted. Also, if unauthorized copyright material had to be removed, a note will indicate the deletion.

UMI®

COLORADO STATE UNIVERSITY

August 13, 2007

WE HEREBY RECOMMEND THAT THE DISSERTATION PREPARED UNDER OUR SUPERVISION BY YOUNG HO SHIN ENTITLED CHANNEL CHANGES DOWNSTREAM OF THE HAPCHEON RE-REGULATION DAM IN SOUTH KOREA BE ACCEPTED AS FULFILLING IN PART REQUIREMENTS FOR THE DEGREE OF DOCTOR OF PHILOSOPHY.
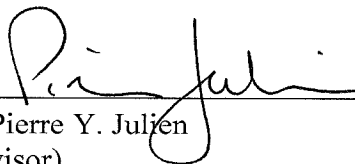
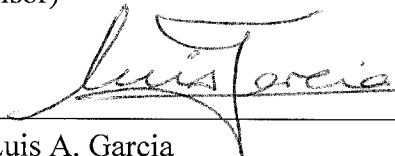Committee on Graduate Work

_____
Dr. Chester C. Watson

_____
Dr. Ellen E. Wohl

_____
Dr. Neil S. Grigg

_____
Dr. Pierre Y. Julien
(Advisor)

_____
Dr. Luis A. Garcia
(Department Head)

ii

ABSTRACT OF DISSERTATION

CHANNEL CHANGES DOWNSTREAM OF THE HAPCHEON RE-REGULATION DAM IN SOUTH KOREA

The Hwang River is a tributary of the Nakdong River and it covers a drainage area of 1,329 km^2 in South Korea. The Hapcheon Main Dam and re-regulation Dam, located 6.5 km downstream of the main dam, were completed in 1989. The purpose of the lower dam is to regulate the downstream flows of the daily three-hour peak hydro power generation at the main power station. The study reach is 45 km long from the Hapcheon re-regulation Dam to the confluence with the Nakdong River. As almost 20 years passed since the Hapcheon Dam was completed, it seems important to monitor the river changes downstream of the dam.

The Hwang River has experienced channel adjustments such as changes in channel width, bed material sizes, vegetation expansion, and island formation after the construction of the two dams. These channel changes were caused by changes in flow regime and sediment transport after dam construction. Based on reservoir sediment deposition in 2002, the Hapcheon Main Dam trapped approximately 600,000 m^3 of sediment per year since the completion of the dam in 1989. The two dams also dramatically reduced annual peak flows from 654.7 m^3/s to 126.3 m^3/s (19.3 % of pre-dam condition).

The main objectives of this study are as follows;

- Identify past spatial and temporal trends and the corresponding response of the channel before and after dam construction

- Analyze and predict future channel changes in lateral and vertical variations such as channel width, bed slope, bed material, and expansion of islands and vegetation

- Analyze and evaluate the channel changes due to flow pulses by the operation of the Hapcheon Re-regulation Dam

An analysis of a time series of aerial photographs taken in 1982, 1993, and 2004 showed that the non-vegetated active channel width narrowed an average of 152 m (47 % width reduction since 1982). Also, the non-vegetated active channel area decreased an average of 6.6 km^2 (44 % reduction since 1982) between 1982 and 2004, with most changes occurring after dam construction. The average median bed material size increased from 1.07 mm in 1983 to 5.72 mm in 2003, and the bed slope of the reach decreased from 0.000943 in 1983 to 0.000847 in 2003. The riverbed vertical degradation is approximately 2.6 m for a distance of 15 km below the re-regulation dam.

Since the dam construction, the channel moved toward a new stable/equilibrium condition. The analysis of aerial photographs and field surveys shows that the 2004 channel width was on average 1.5 times greater than the estimated equilibrium width from the Julien and Wargadalam (1995) hydraulic geometry equations. It is expected from the result of GSTAR-1D steady simulations that the thalweg elevation will reach a stable condition around 2013~2015, 25 years after the dam construction in 1989.

Although the Hapcheon Re-regulation Dam attenuated peak flows, there are daily flow pulses due to peak hydropower generation and sudden sluice gate opening and closing during flood seasons. The effects of these pulses of water level and discharge downstream of the re-regulation dam are analyzed using the unsteady sediment transport numerical model (GSTAR-1D). The daily pulses and flood peaks exert a greater impact on downstream channel geometry than steady discharge conditions. The sediment transport rates (tons/day) of daily pulses and flood peaks were 121 % and 115 % of their respective daily and flood averages.

Young Ho Shin

Department of Civil and Environmental Engineering

Colorado State University

Fort Collins, CO 80523

Fall 2007

ACKNOWLEDGEMENTS

TABLE OF CONTENTS

LIST OF TABLES

LIST OF FIGURES

LIST OF SYMBOLS

A_{act} = Non-vegetated active channel area (km^2)

A_{sid} = Island area (km^2)

A_{veg} = Vegetated area (km^2)

B = Bed elevation at time, t

B_o = Bed elevation at time, t_0

D_{50} = Median bed material size (mm)

dA_{act} = Change of non-vegetated active channel area (km^2)

dA_{sid} = Change of Island area (km^2)

dA_{veg} = Vegetated area (km^2)

dW_{act} = Rate of change of non-vegetated active channel width (m/year)

h = Flow depth (m)

k_l = Empirical rate constants

MI = Mobility Index

P = Sinuosity

Q = Flow discharge (m3/s)

Q_{bv} = Bed load discharge (m^3/

Q_{peak} = Average peak discharge (m^3/s)

Q_{bank} = Average bankfull discharge (m^3/s)

$Q_{peak} S$ = Total stream power for peak discharge (m^3/s)

$Q_{bank} S$ = Total stream power for bankfull discharge (m^3/s)

Q_s = Sediment discharge (m^3)

Q_H = Peak pulse flow (m^3)

Q_L = Minimum pulse flow (m^3)

$\bar{Q}$ = Average pulse flow (m^3)

S = Channel slope (m/m)

V = Flow velocity (m/s)

V_{s_pulse} and V_{s_avg} = Sediment volume of flow pulse and flow average (m^3)

W_{act} = Non-vegetated active channel width (m)

W_e = Equilibrium channel width (m)

W_o = Non-vegetated active channel width (m) at time, t

1 INTRODUCTION

The rainfall season in Korea is during summer and most of the runoff occurs from June to September. For this reason, the water flow in rivers is frequently insufficient throughout the year. Also, water demand has dramatically increased due to the development of heavy chemical industry which started in the early 1970's and caused a concentration of population in urban areas. The contamination of river water worsened by increasing factories and domestic wastewater. The Korean government started the national comprehensive development program to develop water resources and reduce flood damage. A preliminary investigation (1966) and a feasibility study (1970) for the Nakdong River Basin Development Project suggested the construction of several multi-purpose dams for water supply, flood control, and hydropower generation. Accordingly, MOCT and KOWACO built 5 multi-purpose dams and 1 estuary barrrage in the Nakdong River basin. These are: Andong dam (1977), Hapcheon dam (1989), Nakdong estuary barrage (1990), Imha dam (1993), Namgang dam (2001), and Milyang dam (2001).

It has been well known that dams can cause numerous effects on downstream river channels. These changes may affect among others, riverbed elevation, channel width and depth, bed-particle sizes and armoring, vegetation expansion, and other morphological changes in the river. As 20 years have passed since some dams were completed, it seems important to monitor the river changes downstream of those dams.

The Hwang River, a tributary of Nakdong River, was selected as the study reach for the 45 km reach from the Hapcheon Re-regulation Dam to the confluence with the Nakdong River because there is some evidence to suggest that channel bed degradation, bed material coarsening, channel narrowing and vegetation expansion may be in progress downstream of the Hapcheon Re-regulation Dam. Also, among those dams for which 20 years ave passed since dam completion, the Hapcheon Dam only has the re-regulation dam at 6 km downstream from the main dam to regulate the discharge from the main power station by peak power generation and has relatively plentiful data for analysis and

prediction of downstream channel changes. Although the re-regulation dam attenuates flow pulses from the main dam, flow pulses still exist during typical floods due to periodical water gate opening and closing. These flow pulses may accelerate the downstream channel changes.

The basic studies (MOCT, 1983, 1993 and 2003, and MOCT and KOWACO, 2004) were conducted by the Korean government (MOCT, Ministry of Construction and Transportation) and a government agency (KOWACO, Korea Water Resources Corporation). These studies included climate change, land use change, surveying of the river channel, and estimating bed material as part of the river channel management plan and river basin investigation. These studies showed several evidences of channel bed degradation and bed material coarsening during the thirteen-year period immediately after completion of the dam.

Also, several researchers investigated the effect of flow regime changes on the river morphology and vegetation cover in the downstream river reach after the Hapcheon Dam construction (Choi et al., 2004; Woo et al., 2004a, b). They analyzed the changes in bed elevation, channel cross-sections and vegetation expansion by this flow regime change. However, these studies mainly focused on the effects of the dam construction at the present time such as channel degradation and vegetation expansion on sand bars without prediction of future channel changes because the available data were so limited at that time. There was also no consideration of the effects of the flow pulses caused by the operation of Hapcheon Re-regulation Dam. These pulses may more significantly affect the downstream channel geometry than steady discharges from the re-regulation dam and the effects should be determined. It is also important to predict the future changes in hydraulic geometry and define where new equilibrium and stability conditions may be reached.

This dissertation proposes a contribution toward better understanding of river regulation below dams, and the response to varying water and sediment inputs. Because dams influence the two primary factors (water and sediment) that determine the shape, size, and overall morphology of a river, they represent fundamental interventions in the fluvial system (Grant et al., 2003; Xu, 1990). This dissertation thoroughly documents the

changing inputs to the downstream river system of the Hwang River before and after construction of the Hapcheon Dam. It a specially considers the downstream effects of water pulses by the operation of re-regulation dams. Also, this dissertation provides documentation of the effects of dams in the future river system management and reservoir operation strategy.

The main objectives of this research are to:

(1) Identify spatial and temporal trends and the corresponding response of the channel before and after dam construction. This will be specially added to the variation of hydrology and sediment regimes, and channel response (changes in bed material, bed elevation, active channel width, vegetation expansion and channel planform).

(2) Analyze and predict channel changes over time until 2023 in lateral and vertical variations such as channel width, bed slope, bed material, and expansion of islands and vegetation. This will include equilibrium concepts, statistical and numerical analyses.

(3) Analyze and evaluate the channel changes due to flow pulses by the operation of the Hapcheon Re-regulation Dam. This will include the development of a relationship between flow pulses and channel changes.

The dissertation consists of eight chapters. An introduction is presented in Chapter 1. Chapter 2 reviews the literature on the concept of equilibrium, and previous studies about channel adjustment and effects of dam construction. The site descriptions, characteristics, and database of the Hwang River and Nakdong River are described in Chapter 3. The historic geomorphic analysis of the study reach is presented in Chapter 4. An analysis and prediction of future channel changes are discussed in Chapter 5. Chapter 6 contains an analysis of the downstream effects due to flow pulses by the re-regulation dam operations. The summary and conclusions are found in Chapter 7.

2 LITERATURE REVIEW

Human disturbances have modified the nature and rate of river adjustments, altering the spatial and temporal distribution of river forms and processes (Brierley and Fryirs, 2005). Dam construction is one of the significant human disturbances in river systems. The impact of a particular scheme on the fluvial environment will vary with the size and purpose of the dam and its physical setting, but in general both upstream and downstream adjustments can be expected (Knighton, 1998). This chapter presents a review of geomorphic and environmental adjustment by human disturbances to river channels located downstream of dams.

2.1. Equilibrium Concept

Prediction of the downstream channel adjustments after dam construction requires understanding of the equilibrium concept. The prediction of channel adjustment by natural and human disturbed changes is important for designing hydraulic structures and river channel management. However, the researches related to channel responses were started by fluvial geomorphologists instead of hydraulic engineers (Woo, 2002). The definition of equilibrium in the dictionary is as follows (Wohl, 2005);

Equilibrium exists in any system when the phases of the system do not undergo any change of properties with the passage of time, and provided that the phases have the same properties when the same conditions, with respect to the variants, are again reached by a different procedure.

The first part of this definition is most applicable to fluvial geomorphology (Wohl, 2005). The idea of equilibrium was first introduced to geomorphology by Gilbert (1877), then modified by Mackin (1948), Leopold & Maddock (1953), and Wolman (1955). Renwick (1992) described equilibrium, disequilibrium, and non-equilibrium with the following definitions and Figure 2-1:

4

Equilibrium – not a static state but form displays relatively stable characteristics to which it will return after disturbance;

Disequilibrium – adjustment is towards equilibrium, but because response times are relatively long, there has not been sufficient time to reach such a state;

Non-equilibrium – there is no net tendency toward equilibrium and therefore no possibility of identifying an average or characteristic condition.
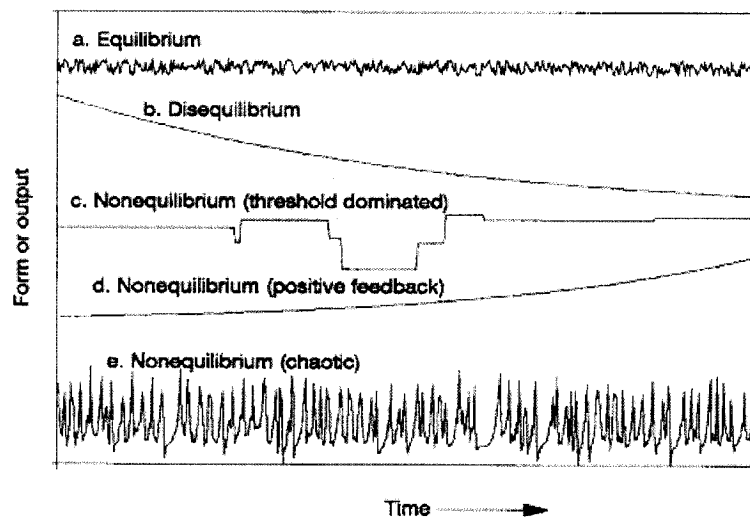
Figure 2-1. Examples of equilibrium, disequilibrium, and non equilibrium landform behavior (Renwick, 1992, Figure 1)

Thorn and Welford (1994) explained neutral equilibrium, unstable equilibrium, stable equilibrium, and metastable equilibrium with the following definitions and Figure 2-2:

Neutral equilibrium arises when a small displacement of an object results in no net force on that object.

Unstable equilibrium occurs when an object is located in a position where a small displacement results in a net force acting in the same direction as the initial displacement

Stable equilibrium stands in direct contrast to unstable equilibrium.

5

Metastable equilibrium occurs when an object is located in a position where small perturbations result in stable behavior.
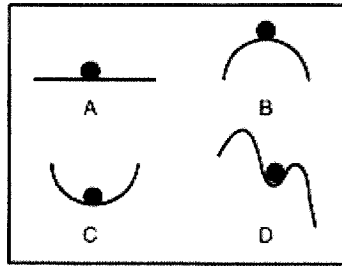
Figure 2-2. Schematic diagram of an object in neutral equilibrium (A), unstable equilibrium (B), stable equilibrium (C), and metastable equilibrium (D). The underlying surface may be considered to be a potential energy surface (Thorn and Welford, 1994, Figure 1)

Also, several definitions for equilibrium are in Table 2-1.

Table 2-1. Equilibrium concepts (Downs and Gregory, 2004, p. 78)

Term used	Context or meaning	Example reference
Equilibrium	Widely used in relation to aspects of environment to connote stability whereby the system does not undergo any further change, the sum of all the forces acting is equal to zero, input of mass and energy is equal to the outputs from the subsystem, and there is no net transfer of mass or energy between phases (e.g. gas and liquid). Types include: • Static equilibrium – no change over time • Stable equilibrium – the tendency of the variable to return to its original value • Unstable equilibrium – the tendency of the variable to respond to system disturbance by adjustment to a new value • Metastable equilibrium - a combination of stable and unstable except that variable settles on new value only after crossing threshold value of returns to original value	Chorley and Kennedy (1971)

Continued Table 2-1

Term used	Context or meaning	Example reference
Steady state	A situation whereby input, output and properties of system remain constant over time.	Richards (1982)
Dynamic equilibrium	Used to signify a situation fluctuating about some apparent average state where that average state is itself also changing over time. Used for grade, which is the condition of a channel that has a gradient such that a perfect balance occurs between erosion, resistance, transport and deposition resulting in a channel profile. Most natural stream channels are in dynamic equilibrium with the prevailing flow conditions. Engineers developed in regime to signify where this equilibrium condition obtained. From regime theory of alluvial canals channel form is relatively constant despite variations in flow over periods of 2-10 years.	Blench (1957)
Quasi-equilibrium	An apparent balance between opposing forces and resistances. A tendency towards natural equilibrium state but not realized. Approximate equilibrium would be less confusing.	Leopold and Maddock (1953) Graf (1988)
Disequilibrium	Tendency towards equilibrium but has not been sufficient time to reach the equilibrium state. Alternating flood and drought dominated regimes in New South Wales give instability and incomplete adjustment before the next regime.	Renwick (1992) Warner (1994)
Nonequilibrium	No net tendency towards equilibrium so that no possibility of identifying an average or characteristic condition. Equilibrium conditions in middle reaches of Australian dryland rivers but nonequilibrium conditions in aggradational lower reaches.	Renwick (1992) Tooth and Nanson (2000)
Multiple equilibria	When several possible equilibrium states may arise from particular environmental conditions.	Phillips (2003)

2.2. Equilibrium Approaches

Lane (1955) proposed the qualitative relationship for adjustment in an alluvial river channel. This relationship is commonly visualized as Lane's balance (Figure 2-3). Lane's balance is simple and qualitative but gives very valuable information (Woo, 2002).

$$Q\,S \;\propto\; Q_s d_{50} \qquad\qquad (2\text{-}1)$$

Where: Q = water discharge, S = slope, Q_s = bed material load, and

$$d_{50} = \text{median size of the bed material}$$

This relationship shows that changes in bed material load, bed material size and flow discharge will induce adjustments of channel slope to achieve equilibrium state (Lane 1954, 1955; Schumm, 1969).
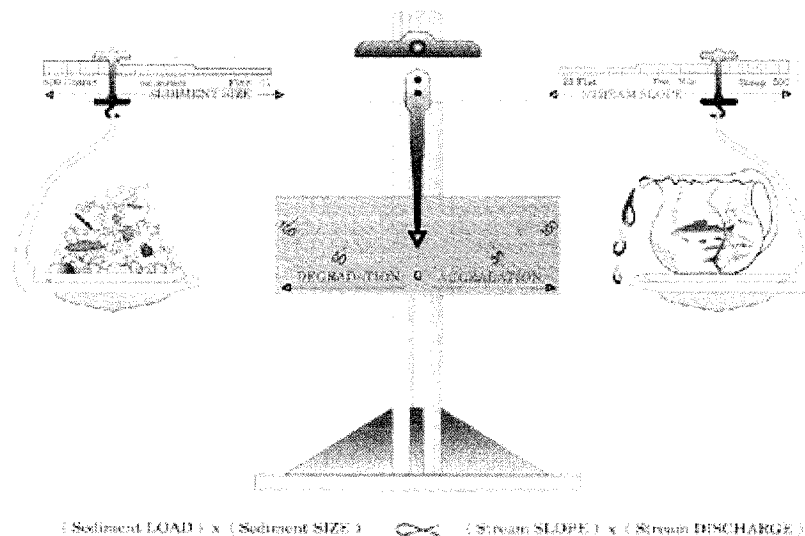
Figure 2-3. Lane's balance (after E.W. Lane, 1955, Figure 1)

Mackin's explanation of how a graded stream responds to changes in the controlling variables is easily illustrated by Lane's balance, which shows how a change will tend to produce a response in stream characteristics such that equilibrium is restored (Watson et

al., 2005). When a stream is in dynamic equilibrium, it has adjusted these four variables such that the sediment transported into the reach is also transported out, without aggradation or degradation (Watson et al. 2005). This approach was extended by developing an approach to river metamorphosis based on empirical relationships obtained from 36 stable alluvial channels in semiarid and humid areas of the Great Plains of the United States and Riverine Plain of New South Wales, Australia (Schumm, 1969), as follows:

$$Q_w \approx \frac{W \ d \ ML}{S} \tag{2-2}$$

$$Q_s \approx \frac{W \ ML \ S}{d \ P} \tag{2-3}$$

Where: W = channel width, d = water depth,

Q_w = water discharge, Q_s = bed material load,

ML = meander wavelength, S = bed slope, and

P = Sinuosity

Schumm (1969) obtained the following equations. A plus or minus exponent indicates increase or decrease of discharge or bed material load.

$$Q_w^+ \approx \frac{W^+ \ d^+ \ ML^+}{S^-} \tag{2-4}$$

$$Q_w^- \approx \frac{W^- \ d^- \ ML^-}{S^+} \tag{2-5}$$

$$Q_s^+ \approx \frac{W^+ \ ML^- \ S^+}{d^- \ P^-} \tag{2-6}$$

$$Q_s^- \approx \frac{W^- \ ML^- \ S^-}{d^+ \ P^+} \tag{2-7}$$

Brandt (2000a) developed a classification and qualitative predictive model of channel changes downstream of dams based on a synthesis of the literature. Jiongxin (2001) established a conceptual model for predicting the tendency of alluvial channel adjustment induced by human activities. This model has been tested using data from natural rivers and a laboratory model river, and can be used to explain the complex behavior of channel adjustment after reservoir construction. According to Downs and Gregory (2004), the above approximation *"indicated how possible changes could occur but was limited in that there may be correlation between the component variables that are not always appropriate and comprehensive, and that several outcomes may be possible from any situation. For example, in the case that water discharge increases as a result of catchment land use change then a positive response could occur in numerous of the parameters, including:* $Q_w^+ = \dfrac{W^+ \cdot d^+ \cdot ML^+}{S^-}$ *"*.

The ASCE Task Committee on Hydraulics, Bank Mechanics, and Modeling of River Width Adjustment (1998) grouped the existing quantitative methods for describing equilibrium river morphology as empirical (regime theory and power laws), extremal hypotheses, and rational or mechanistic approaches. The modern approach is more quantitative and stems directly from the empirical work on hydraulic geometry (Leopold and Maddock, 1953; Wolman, 1955). To construct stable irrigation canals in India and Pakistan, they used regime relationships (Julien, 2002). Empirical regime relationships have been proposed by Kennedy (1895), Lacey (1929), Simons and Albertson (1963), and Blench (1969). The regime equations of Kennedy (1895) are a simple power function of velocity as a function of flow depth. Leopold and Maddock (1953) proposed the following hydraulic geometry relationships:

$$W = aQ^b \qquad\qquad (2\text{-}8)$$

$$D = cQ^f \qquad\qquad (2\text{-}9)$$

$$V = kQ^m \qquad\qquad (2\text{-}10)$$

where: W = stream width, Q = discharge,

10

$$D = \text{depth, and} \quad V = \text{velocity}$$

According to the Knighton (1998, p.173), the exponents of the above equations, b, f, m are around 0.5, 0.4, and 0.1, respectively, depending on data sources and applicable condition. However, the regression coefficients, a, c, and k vary widely. Later versions of these simple hydraulic geometry relationships add the median bed sediment size (d_{50}) to improve the predictive power of the equations, and appear in the following format (Watson et al., 2005):

$$W = k_1 Q^{k2} d_{50}^{k3} \tag{2-11}$$

$$D = k_4 Q^{k5} d_{50}^{k6} \tag{2-12}$$

$$S = k_7 Q^{k8} d_{50}^{k9} \tag{2-13}$$

Engineers applied this theory primarily to predict a stable form for irrigation canals during the first half of the 1900's. The equations 2-8~10 were derived originally for canals with a steady flow and fine sediment and consist of a set of empirical equations which can be manipulated to give the width (W), depth (D), and slope (S) of an approximately stable live-bed channel whose cross-sectional form is maintained by a local balance between erosion and deposition. The more important equations are (Knighton, 1998):

$$P = 4.84 Q^{1/2} \tag{2-14}$$

$$R = 0.41 Q^{1/3} D^{-1/6} \tag{2-15}$$

$$V = 0.50 Q^{1/6} D^{1/6} \tag{2-16}$$

$$S = 0.00065 Q^{-1/6} D^{5/6} \tag{2-17}$$

Where, V, Q and D are, respectively, mean velocity, discharge and bed material size (in mm), and $P \approx W$ and $R \approx h$ for large channel (Lacey, 1929).

There are many other similar equations such as Lindley (1919), Lacey (1929), Simons and Albertson (1963) and Blench (1969) for the design of straight irrigation canals with sandy beds and sandy or cohesive banks, and Kellerhals (1967) and Hey (1982) for natural rivers (Wharton, 1995). Some more recent studies have taken more of an analytical approach than Leopold and Maddock (1953). For instance, Julien and Wargadalam's (1995) hydraulic geometry equations are "semi-theoretical" equations developed by simplifying Julien's (1988) theoretically based equations (Wargadalam 1993), as shown in Equation 2-19~23.

Another method is the hyperbolic function by developed Williams and Wolman (1984) to predict width change downstream from a dam in the following form:

$$\frac{W_t}{W_o} = \left(\frac{t}{a+bt}\right) + 1 \qquad (2\text{-}18)$$

Where, W_t = active channel width at time t, W_o =active channel width at onset of narrowing, a and b = empirically determined constants

An exponential function was developed by Simon (1992) to predict spatial trends in aggradation and degradation through time. The exponential function that describes the dimensionless change in bed elevations was applied to the Obion-Forked Deer and Toutle River systems. Richard (2000) and Richard et al. (2005) also developed exponential functions to estimate equilibrium channel width and predict future channel changes. The hypothesis is that the magnitude of the slope of the width vs. time curve increases with deviation from the equilibrium width, W_e:

$$\frac{\Delta W}{\Delta t} = -k_1(W - W_e) \qquad (2\text{-}19)$$

Where, ΔW = change in active channel width (m), during the time period Δt; and Δt = time period (years)

Differentializing equation (5-8) results in the following equation:

$$\frac{dW}{dt} = -k_1(W - W_e) \qquad (2\text{-}20)$$

12

Rearranging and integrating equation (4-2):

$$\int_{W_0}^{W} \frac{dW}{(W - W_e)} = \int_0^t -k_1 dt$$

$$\ln(W - W_e) - \ln(W_0 - W_e) = -k_1 t \big|_0^t$$

$$\ln\left(\frac{W - W_e}{W_0 - W_e}\right) = -k_1 t \tag{2-21}$$

$$\left(\frac{W - W_e}{W_0 - W_e}\right) = e^{-k_1 t}$$

$$W - W_e = (W_0 - W_e) \cdot e^{-k_1 t}$$

The result is an exponential function:

$$W = W_e + (W_0 - W_e) \cdot e^{-k_1 t} \tag{2-22}$$

where: k_1 = rate constant, W_e = Equilibrium width toward which channel is moving, W_o = Channel width at time, t_o; and W = Channel width at time, t.

Phillips (1990, 1991) suggested that channel adjustment is characterized by multiple modes of adjustment rather than a single 'equilibrium' response. Recently, Julien and Wargadalam (1995) determined approximative empirical values for the flow depth h, surface width W, average flow velocity V and friction slope S from a large data set, including data from 835 rivers and canals. The downstream hydraulic geometry for non-cohesive alluvial channels for hydraulically rough turbulent flows is

$$h = 0.133 Q^{\frac{1}{3m+2}} d_s^{\frac{6m-1}{6m+4}} \tau_*^{\frac{-1}{6m+4}} \tag{2-23}$$

$$W = 0.512 Q^{\frac{2m+1}{3m+2}} d_s^{\frac{-4m-1}{6m+4}} \tau_*^{\frac{-2m-1}{6m+4}} \tag{2-24}$$

$$V = 14.7 Q^{\frac{m}{3m+2}} d_s^{\frac{2-2m}{6m+4}} \tau_*^{\frac{2m+2}{6m+4}} \tag{2-25}$$

13

$$S = 12.4Q^{\frac{-1}{3m+2}} d_s^{\frac{5}{6m+4}} \tau_*^{\frac{6m+5}{6m+4}} \qquad (2\text{-}26)$$

$$\tau_* = 0.121Q^{\frac{2}{5+6m}} d_s^{\frac{-5}{5+6m}} s^{\frac{4+6m}{5+6m}} \qquad (2\text{-}27)$$

Where: Q=equilibrium or dominant flow discharge in cubic meters per second

$d_s = d_{50}$ = median grain size in meters

$$\tau_* = \frac{\gamma hS}{(\gamma_s - \gamma)d_{50}} = \text{Shields parameter}$$

$$m = \frac{1}{\ln(12.2h/d_{50})} = \text{resistance exponent}$$

When Manning's equation is applicable, $m = 1/6$, a simplified form is obtained as

$$h \cong 0.133Q^{0.4}\tau_*^{-0.2} \qquad (2\text{-}28)$$

$$W \cong 0.512Q^{0.53}d_s^{-0.33}\tau_*^{-0.27} \qquad (2\text{-}29)$$

$$V \cong 14.7Q^{0.07}d_s^{0.33}\tau_*^{0.47} \qquad (2\text{-}30)$$

$$S \cong 12.4Q^{-0.4}d_s\tau_*^{1.2} \qquad (2\text{-}31)$$

$$\tau_* \cong 0.121Q^{0.33}d_s^{-0.83}S^{0.83} \qquad (2\text{-}32)$$

The hydraulic geometry of stable channels is obtained from the above equations when $\tau_* \cong 0.047$ (Julien, 1998 and 2002).

Rosgen (2002) develops a stream channel stability assessment methodology. This assessment procedure involves a stream channel stability prediction and validation methodology on a hierarchical framework. However, Wohl (2004) examined the limits of downstream hydraulic geometry relationships by applying data sets from 10 mountain rivers in the United States, Panama, Nepal, and New Zealand.

Another approach for predicting channel morphology is the extremal hypothesis approach. Extremal hypotheses are physically based because they rely on principles of energy and power. They are hypotheses rather than governing relationships because they are based on variational arguments in which some parameter is minimized or maximized (Phillips, 1991). Extremal approaches have been strongly criticized because they can produce results or implications which are unrealistic or inconsistent with common flow and transport relations, because they do not consider mechanisms of width adjustment, and because they may imply unrealistic shear stresses (Griffiths, 1984; Ferguson, 1986). Sediment transport equation and alluvial friction are combined with a third relationship to determine channel width and to predict regime or equilibrium conditions. This relationship has been expressed in terms of the maximization or minimization of a parameter, such as stream power, energy dissipation rate, or sediment concentration (ASCE Task Committee, 1998). These hypotheses with a more physical basis have been proposed as conditions for equilibrium (Knighton, 1998):

(1) minimum unit stream power (minimized VS) (Yang, 1976);

(2) minimum stream power (minimize γQS) (Chang, 1980);

(3) minimum energy dissipation rate (minimize $(\gamma Q + \gamma_s Q_s)LS$) (Brebner and Wilson, 1967; Yang et al., 1981);

(4) minimum Froude number (minimize $V/\sqrt{gD}$), which approximates to minimization of the kinetic energy/potential energy ratio (Yalin, 1992; Jia, 1990);

(5) maximum sediment transport rate (Kirkby, 1977; Ramette, 1979; White et al., 1982);

(6) maximum friction factor (maximize $ff \Leftrightarrow$ minimize V^2/DS) (Davies and Sutherland, 1980)

Where, Q, Q_s, V, S, D, ff are hydraulic variables (discharge, sediment discharge, velocity, slope, depth, resistance), L is stream length, g is the acceleration due to gravity, and γ, γ_s are the specific weights of water and sediment, respectively.

2.3. Channel Response to Changes in Water Flow and Sediment Transport

The general issues of channel responses to change in water and sediment inputs are discussed in many textbooks and in particular in the literature on hydraulic geometry and regime theory (Ferguson, 1986; Hey, 1979; Huang and Nanson, 2000; Lamberti, 1992; Miller, 1991a, b; Simon and Thorne, 1996; Yang, 1992). Hydraulic geometry is explicitly concerned with adjustment at a cross-section (at-a-station) or downstream in response to changes in imposed flows and sediment inputs (Phillips et al., 2005). A few researchers (e.g. Brandt, 2000b; Xu, 1990) have attempted to explicitly link principles of hydraulic geometry and regime theory to effects of dams. Xu's (1990, 1996, 2001) model of complex response downstream from reservoirs predicts, for a case where clear water scour occurs, a three-stage adjustment process. First is a decrease in width/depth ratio and channel slope, coupled with an increase in sinuosity. Feedbacks in stage two lead to increasing w/d ratios and decreasing sinuosity, with a slowdown in the rate of slope change.

Dam construction can produce adjustment of river channels as sediment trapped above the dam results in clearer water immediately downstream of the dam (Downs and Gregory 2004). Petts (1984, pp. 24-5) identified the three orders of impact:

- first-order impacts occur simultaneously with dam closure, and affect the transfer of energy and material into, and within, the downstream river, and therefore include impacts on processes, flow regime, sediment load, water quality and plankton;

- second-order impacts are changes in channel structure and primary production that result from the modification of first-order impacts, according to local conditions, and depend upon the characteristics of the river prior to dam closure. These impacts may require a time period of between 1 and 100 years or more to achieve a new 'equilibrium' state, and they therefore influence the channel form, substrate composition, macrophytes and periphyton;

16

- third-order impacts on fish and invertebrates may occur after a considerable time lag, and reflect all the first- and second-order changes. The fish population is also influenced by the changes of the invertebrate community that provide the major food supply for many species. There may be several phases of population adjustment and readjustment, particularly in response to the second-order factors.

Table 2-2 shows impacts of river regulation in terms of creation of a dam, lake and below dam or reservoir (Downs and Gregory, 2004). Most research related to the downstream impacts of dam construction considered a reduction in the magnitude of flood peaks. For example, the 50-year flood on central European rivers has been reduced in magnitude by 20% (Lauterbach and Leder, 1969) and the 10-year flood on the Colorado River below Glen Canyon dam has been reduced by 75% (Dolan et al., 1974). Also, Williams and Wolman (1984) showed that flood peak has been reduced in magnitude as much as 90% in 21 reservoir sites in the central and southwestern United States. Page et al. (2005) evaluated the effect of altered flow regime on the frequency and duration of bankfull discharge of the Murrumbidgee River in Australia. In this research, flood peak significantly decreased and bankfull discharge with return periods of 1.25 and 2 years was reduced by between 29 and 37% from Gundagai downstream to Hay and by more than 50% at the Balranald gauging station after dam completion.

Dams have been shown to act as sediment sinks, reducing the turbidity of the river downstream (Grimshaw and Lewin, 1980). Reservoirs are effective sediment traps, with commonly over 90% of total load (Knighton, 1998). Since the completion of Hoover Dam in 1935, the average annual suspended load has declined from about 130 million tons to under 100 thousand tons (Meade and Parker, 1985).

A common response to the release of sediment-free water below dams is degradation of the channel bed, typically at rates much higher than in natural rivers (Knighton, 1998). Williams and Wolman (1984) studied changes in mean channel-bed elevation, channel width, bed-material sizes, vegetation, water discharges, and sediment loads downstream from 21 dams constructed on alluvial rivers in the United States.

Table 2-2. Impacts of river regulation (Downs and Gregory, 2004, p 95)

Impact	Consequence	Results
Creation of dam	Introduction of barrier - to downstream transfers - to upstream migration of fish	Sediment accretion in reservoir
Creation of lake	Water balance changed	Average runoff reduced and evaporation increased
	Loss of river, wetland and terrestrial ecosystems Barrier to funeral migration (e.g. of fish or caribou) Limnological changes	
Below dam or reservoir	Changes of flows	Reduced seasonal variability and reduced flood magnitudes
	- sediment loads	Bedload transport reduced, suspended load reduced (William and Wolman, 1984)
	- water quality - water temperatures	Significant changes Reduced seasonal and diurnal variability
	Loss of floodplain-channel interactions	Floodplain less frequently inundated with implications for riparian plant communities
	Change of channel morphology	Scour downstream of dam because of clear water erosion; downstream changes in channel capacity, width, depth, width/depth ratio, sinuosity, meander wavelength (Gregory, 1987)
	Change of instream hydraulic characteristics Change of autogenic:allogenic energy sources	
	Change of channel ecology	Reduction of abundance and diversity of macroinvertebrates; fish species change

In this study, bed degradation varied from negligible to about 7.5 m in the 287 cross sections. In general, most degradation occurred during the first decade or two after dam closure (Williams and Wolman, 1984). Simon et al. (2002) investigate the effects of the altered flow regime and bed degradation on bank stability by two independent bank-stability analyses (one for planar failures, the other for rotational failures) downstream of the Fort Peck dam on the Missouri River. They also analyzed channel migration rates using maps and photographs.

One degradation process of the channel bed is armoring downstream of dams. Armoring refers to coarsening of the bed-material size as a result of degradation of well-graded sediment mixtures (Julien, 2002). Also, Kassem and Chaudhry (2005) explained that armoring is a grain sorting process in which larger size particles an armor coat on the channel bed, reducing further degradation. Shen and Lu (1983) examined the development of bed armoring and derived three simple regression equations to predict the median size, d_{30} and d_{84}, of the final armoring bed material size distribution for different gradation of the initial bed material and flow conditions. Major increases of bed sediment sizes had been reported within sand-bed reaches, dominated by sediments of 100-200 μm being converted to coarse-sand and gravel-bed reaches (Petts, 1984). Karim et al. (1983) developed a one-dimensional approach for bed armoring in alluvial channels and Karim and Holly (1986) applied this approach to simulate a 20-year bed degradation in the Missouri River downstream of Gavins Point Dam. The research result shows good agreement with the observed bed characteristics. Also, Kassem and Chaudhry (2002, 2005) developed the two-dimensional, semi-coupled numerical model and upgraded it to compute the bed topography in curved alluvial channels with unsteady flow and non-uniform sediment.

Shields et al. (2000) examined channel migration at the Missouri River for 200 km downstream of the Fort Peck Dam. According to this research, channel activity for the period 1971-91 averaged 1.8 m/yr and values for a given bend ranged as high as 11 m/yr. Jiongxin (1997) dealt with the evolution of mid-channel bars in a braided channel. The results showed that the characteristics of mid-channel bars can be related to factors such as channel boundary conditions, energy expenditure, and bank erosion. Richard and Julien (2005) and Richard et al. (2005) measured the lateral mobility of the Rio Grande below Cochiti Dam, New Mexico, using a geographic information system from digitized aerial photos of the non-vegetated active channel between 1918 and 2001. Simon et al. (2002) conducted two types of bank bank-stability analyses to compare the stability of the 17 study sites. The first one is a commercially available rotational failure analysis (SLOPE/W, 1998) and the Agricultural Research Service (ARS) method for planar failures. According to this research, the closure of Fort Peck Dam has resulted in a

fourfold reduction of the average rate of long-term channel migration between the dam and the North Dakota border.

Phillips et al. (2005) described and explained river channel cross-sectional change in the Trinity River, Texas, downstream of Livingston Dam to test theoretical models of channel adjustment. Also, Wellmeyer et al. (2005) quantified downstream impacts of Livingston dam on flow regime and channel planform in the same river. Grams and Schmidt (2005) examine bed and bank adjustment in the 105 km downstream Flaming Gorge Dam in Green River. They show that the average channel width reduced 10-30%. Assani and Petit (2004) studied the impacts of hydrological modifications below the Butgenbach dam. In this research, the following modifications have been identified: a doubling of the channel width in 45 years, a reduction in the number of riffles and pools, an increase in the number of gravel bars and islets and increase in bedrock outcrops in the channel. Pohl (2004) evaluated the impact of two dams of moderate size on the downstream channel system. To determine bed material mobility, the relationship between the shear stress and the critical shear stress was evaluated by applying the two-year and ten-year flood event. Wang and Hu (2004) examined impacts of large dams on upstream and downstream in China. Wohl and Rathburn (2003) suggested a five-step procedure to mitigate sedimentation hazard downstream from reservoirs. Grant et al. (2003) proposed a conceptual and analytical framework for predicting geomorphic response of rivers to dams. Juracek (2000) analyzed channel stability of the Neosho River channel since the completion of the John Redmond dam using aerial-photograph and stream-gage information.

Petts and Gurnell (2005) reviewed research progress and further directions in dams and geomorphology. According to this review, research advanced by improved data sets, especially including long time-series of high quality data from field monitoring and remote sensing, and increasingly intensive field survey program in the final two decades of the last century. The application of remote-sensing techniques, supported by new developments in data analysis and interpretation, not only led to important developments in fluvial geomorphology but also to new research on large rivers and to supporting the integration of geomorphology and ecology. Ward et al. (1999, 2001) think that there is

no doubt that advances in understanding fluvial metamorphosis remain constrained by the failure fully to develop an accurate comprehension of the spatio-temporal heterogeneity of channel dynamics and their ecological interactions in unaltered rivers. In Williams and Wolman's (1984) study of regulated rivers, vegetation increased following dam closure in most cases. Also, Merritt and Cooper (2000) reported that along one reach of the Green River within 10 years of the Flaming Gorge Dam closure, nearly 90% of the previously active point bar surfaces had been colonized by riparian vegetation and average channel width had been reduced by 13% (19 m). USGS (1999) measured pH and oxygen concentration at Lees Ferry located downstream of Glen Canyon Dam before and after the flood. The results show that the daily range was about 50 to 80% smaller immediately after the flood.

2.4. Vegetation, Surface Water, and Channel Changes

Riparian Vegetation and Channel Adjustment

Vegetation expansion is a common and important phenomenon for channel adjustment in regulated river channels by dam construction due to reducing peak flow. The establishment of vegetation in the active channel may facilitate accretion and reduced channel capacity by increasing hydraulic roughness and increasing sediment deposition rates (Merritt and Cooper, 2000).

Shafroth et al. (2002) studied the Bill Williams River in western Arizona, USA, to understand dam-induced changes in channel width and in the areal extent, structure, species composition, and dynamics of woody riparian vegetation. Also, they conducted parallel studies along a reference system, the Santa Maria River, an unregulated major tributary of the Bill Williams River.

Merritt and Cooper (2000) evaluated the effects of river damming on geomorphic processes and riparian vegetation through field studies along the regulated Green River and the free-flowing Yampa River in northwestern Colorado, USA by GIS analysis of

21

historical photographs, hydrologic and sediment records, and measurement of channel planform. Figure 2-4 shows the model of channel response to flow regulation on the Green River in Browns Park by Merritt and Cooper (2000).

Johnson (1997) sampled and analyzed nine Platte River reaches to evaluate equilibrium state of riparian vegetation. In this study, the Platte River in central Nebraska responded to water development by rapid channel narrowing and expansion of native riparian woodland. Woodland expanded most rapidly in the 1930s and 1950s. Open channel and woodland area stabilized in the 1960s and have remained stable for most reaches into the mid-1990s, despite relatively low and infrequent peak flows in the past decade.
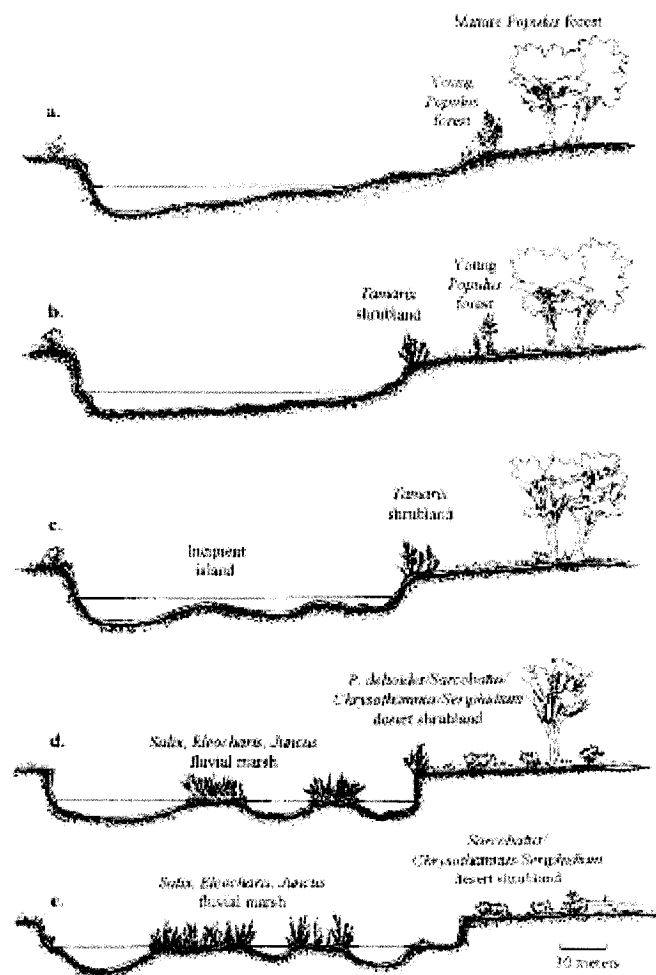
Figure 2-4. Model of channel response to flow regulation on the Green River in Browns Park from 1938 through the present inferred from planform geometry (Merritt and Cooper, 2000, Figure 8)

Williams and Wolman (1984) mapped vegetation changes in selected reaches downstream from 10 dams. In this study, vegetation cover in and along the channel downstream from the dams usually increased following dam closure. Also, they evaluated that vegetation had covered as much as 90% of the channel bottomland in some cases and seven of the ten areas showed an increased growth of more than 50%.

Other studies relating channel narrowing and vegetation development were conducted by Friedman et al. (1996), Martin and Johnson (1987), Van Looy and Martin (2005), Tal et al. (2003), Friedman and Lee (2001) and Gurnell et al. (2001).

Relationship of surface water, groundwater and channel adjustment

From a geomorphologic perspective, subsurface hydraulic erosion is an important geomorphic process in the head watershed, because soil piping and water discharge via the pipes significantly affect hydrology, channel initiation, and slope evolution (Fox, 2006). In this manner, Fox (2006) developed an empirical sediment transport model for seepage erosion of noncohesive sediment on near-vertical streambanks. A seepage erosion transport model for conductive, noncohesive soil layers was derived based on a dimensionless sediment discharge and dimensionless seepage flow shear stress.

Simon et al. (2002) performed two independent bank-stability analyses (one for planar failures, the other for rotational failures) on 17 outside meanders of the Missouri River, eastern Montana.

Wynn et al. (2004) studied the effects of woody and herbaceous vegetation on stream bank erosion. They determined the erodibility of rooted stream bank soils and evaluated the relative effects of vegetation type, root density, and freeze-thaw cycling on the erodibility of stream banks. Also, they developed regression equations for prediction of soil erodibility (K_d) for Appalachian headwater streams in southwest Virginia, USA.

Groundwater and surface water are not isolated components of the hydrologic system, but instead interact in a variety of physiographic and climatic landscapes. Thus, development or contamination of one commonly affects the other. Therefore, an

understanding of the basic principles of interactions between groundwater and surface water (GW–SW) is needed for effective management of water resources (Sophocleous, 2002). The lateral, subsurface flow can potentially result in erosion of unconsolidated material at the face of a streambank if the outflow is sufficient to mobilize particles away from the streambank (Dunne, 1990; Higgins, 1982, 1984; Zaslavsky and Kassiff, 1965; Terzaghi, 1943). Subsurface flow can erode in two ways (Fox, 2006): (1) through the development of a critical body force or drag force that entrains particles in water seeping through and out of porous medium, causing either liquefaction or Coulomb failure; and (2) through application of shear stress to the margins of macropores, which may have originated independently of the water flow (Jones, 1997; Zaslavsky and Kassiff, 1965).

Brunke and Gonser (1997) point out that clogging exerts severe impacts on the renewal of groundwater through river-bank filtration and the development and colonization of invertebrates and fish. Figure 2-5 shows a diagram of stream-aquifer relationships.
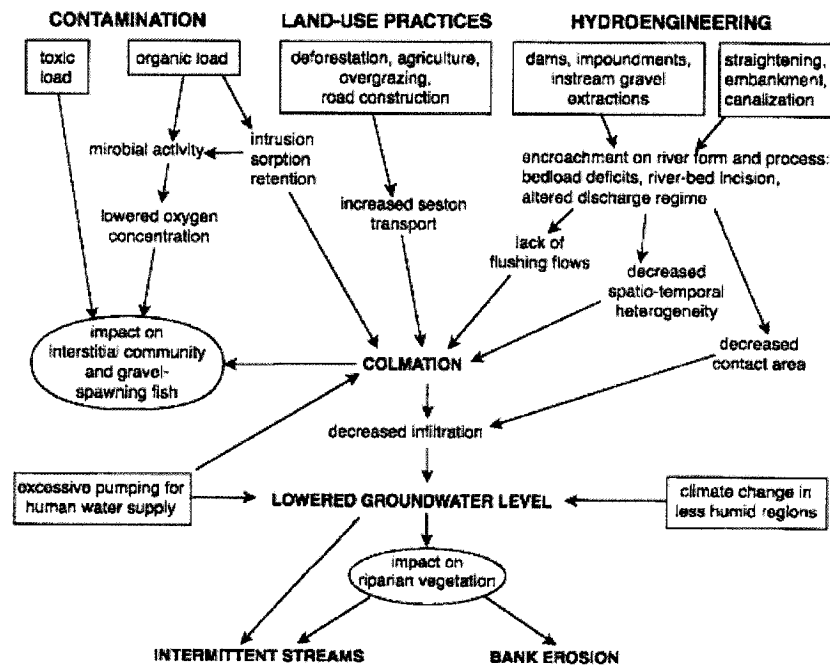
Figure 2-5. Human-induced impacts that promote clogging of stream-bed sediments, and their ecological consequences (Brunke and Gonser, 1997, Figure 5)

The same authors also refer to a case study where the mechanical opening of a clogged section of the stream bed of the Rhine River, Germany, near a drinking-water bank-filtration site induced a 1-m rise in the water table near the river, but after a few weeks, the opened section had become sealed again. They also indicate that river-bed incision results from bed-load deficits due to sediment retention by impoundments and from increased transport capacity following channel straightening. Figure 2-5 shows a diagram of human-induced impacts that promote clogging of stream-bed sediments, and their ecological consequences (Brunke and Gonser, 1997).

2.5. Incipient Motion Analysis

Incipient motion of streambed material is a fundamental process with applications to a wide variety of research problems such as paleohydraulic reconstruction (Church, 1978), placer formation (Komar and Wang, 1992; Li and Komar, 1992), canal design (Lane, 1955), flushing flows (Milhous, 1990; Kondolf and Wilcock, 1992), and assessment of aquatic habitat (Buffington, 1995; Montgomery et al., 1996). Due to the stochastic nature of sediment movement along an alluvial bed, it is difficult to define precisely at what flow condition a sediment particle will begin to move (Yang, 2003). In spite of these difficulties, many researchers made significant progress on this study of incipient motion, both theoretically and experimentally.

One of the approaches for incipient motion is the shear stress approach. White (1940) assumed that the slope and lift force have insignificant influence on incipient motion, and hence can be neglected compared with other factors. The drag force is proportional to the product of bed shear stress and the square diameter of the particle, i.e.,

$$F_D = C_1 \tau d^2 \qquad (2\text{-}33)$$

Where, τ = shear stress, d = particle diameter, and, C_1 =constant

If the distance above the point of rotation to the point of action is proportional to the particle diameter, then the overturning moment is

25

$$M_o = C_1 C_2 \tau d^3 \qquad (2\text{-}34)$$

Where, C_2 =constant

The resisting moment is the product of the submerged weight of the particle $C_3(\gamma_s - \gamma_f)d^3$ and its moment arm $C_4 d$, i.e.,

$$M_R = C_3 C_4 (\gamma_s - \gamma_f)d^4 \qquad (2\text{-}35)$$

Where, C_3 and C_4 =constant, and γ_s and γ_f = specific weights of sediment and fluid, respectively

A particle will start to move when the shear stress is such that $M_O = M_R$. This value is called the critical shear stress. So, we can get following equation.

$$\tau_c = C_5(\gamma_s - \gamma_f)d \qquad (2\text{-}36)$$

Where, C_5 = constant and τ_c = critical shear stress at incipient motion

Another shear stress approach was proposed by Shields (1936). He believed that it was very difficult to express analytically the forces acting on a sediment particle. He applied dimensional analysis to determine some dimensionless parameters and established his diagram for incipient motion as Figure 2-6. The dimensionless shear stress τ_* , called the Shields parameter, is as follows:

Shields parameter, $\qquad \tau_* = \dfrac{\tau_0}{(\gamma_s - \gamma_f)d_s} = \dfrac{\rho_f u_*^2}{(\gamma_s - \gamma_f)d_s} \qquad (2\text{-}37)$

Where, τ_0 = boundary shear stress, u_* = shear velocity, ρ_f = mass density of a fluid, γ_s =specific weight of a sediment particle, γ_f =specific weight of a fluid mixture, d_s =particle size

The critical value of the Shields parameter τ_{*c} corresponding to the beginning of motion ($\tau_0 = \tau_c$) depends on whether laminar or turbulent flow conditions prevail around the

26

particle. Besides the angle of repose, one should consider the ratio of sediment size to the laminar sublayer thickness expressed either as d_s / δ or as the grain shear Reynolds number, $R_{e*} = u_* d_s / v_f$ (Julien, 1998).

$$\textit{Critical Shields parameter,} \quad \tau_{*c} = \frac{\tau_c}{(\gamma_s - \gamma_f)d_s} \quad (2\text{-}38)$$

Critical Shields parameter was approximated as follows (Julien, 1998):

$$\tau_{*c} = 0.5 \tan \Phi \quad\quad \textit{when } d_* < 0.3 \quad\quad\quad (2\text{-}39)$$

$$\tau_{*c} = 0.25 d_*^{-0.6} \tan \Phi \quad \textit{when } 0.3 < d_* < 19 \quad\quad (2\text{-}40)$$

$$\tau_{*c} = 0.013 d_*^{0.4} \tan \Phi \quad \textit{when } 19 < d_* < 50 \quad\quad (2\text{-}41)$$

$$\tau_{*c} = 0.06 \tan \Phi \quad\quad \textit{when } d_* > 50 \quad\quad\quad (2\text{-}42)$$

$$\text{Where,} \quad d_* = d_s \left[\frac{(G-1)g}{v_f^2} \right]^{1/3} \quad\quad (2\text{-}43)$$

Where, τ_c = critical shear stress, γ_s =specific weight of a sediment particle, γ_f =specific weight of a fluid mixture, d_s =particle size, d_* =dimensionless particle diameter, v_f = kinematic viscosity of a fluid, G =specific gravity, g = gravitational acceleration

Also, there are many other approaches related to incipient motion analysis. For example, Fortier and Scobey's (1926), Hjulstrom's (1935) and Yang's (1973) approach based on critical velocity, Bagnold's (1956) approach based on critical stream power, Meyer-Peter et al.'s (1934) based on critical unit discharge developed to estimate incipient motion analysis. However, the evaluation of the critical flow conditions for sediment motion is most often performed through the critical shear stress approach (Shields, 1936), even though other approaches have been proposed, as previously mentioned (Lenzi et al., 2006).
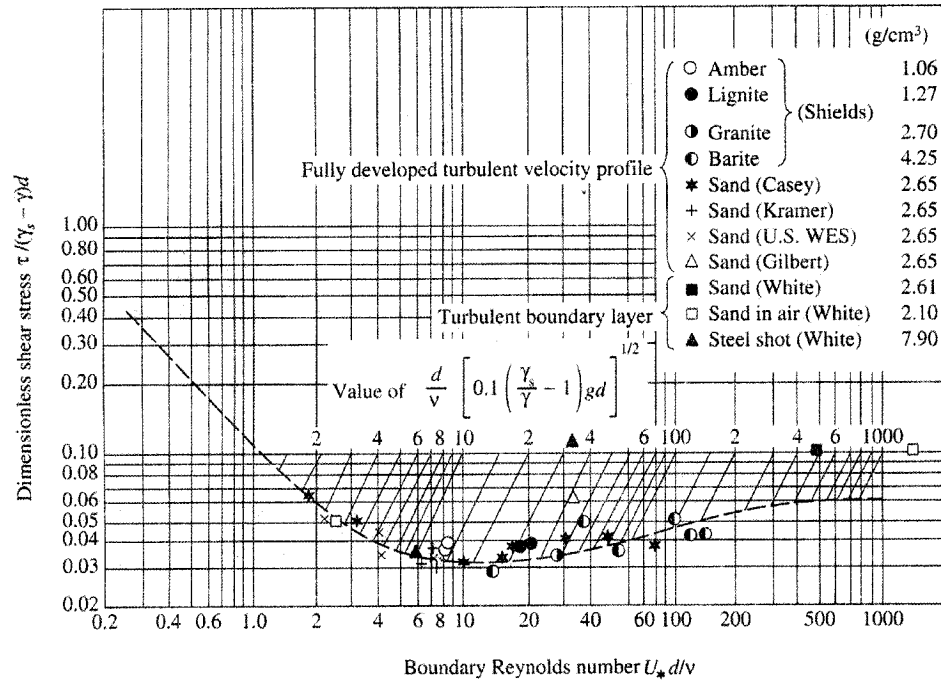
Figure 2-6. Shield diagram for incipient motion (Vanoni, 1975)

Batalla and Martin-Vide (2001) determined the threshold conditions for initiation of motion in a poorly sorted sandy gravel-bed river in Spain. Also, Lenzi et al. (2006) determined threshold of motion using two methods such as the displacement of marked clasts and the flow competence approach, which uses the largest grain size diameter transported by each flood event. Marsh et al. (2004) compared four different methods for predicting the incipient motion conditions of a uniform sand bed. The four methods, the Shields diagram, an empirical approach, a method derived from resolution of rotational forces, and a simplified resolution of rotational forces with a variable lift force coefficient, were used to predict the incipient motion conditions for 97 experimental runs taken from seven independent experimental flume studies. Cao et al. (2006) develop an explicit formulation of the Shields diagram, enabling the critical Shields parameter to be determined directly from fluid and sediment characteristics without resorting to any trial and error procedure or iteration. Mohammadi (2005) and Shvidchenko (2001) conducted experimental study of the incipient motion in fixed bed channel and sand/gravel channel, respectively.

28

3 DESCRIPTION OF THE STUDY REACH AND DATABASE

This chapter contains description and data about the study reach downstream of the Hapcheon Re-regulation Dam. The first section presents a brief explanation of the study reach which includes geological features, land use, and a detailed description of the Hapcheon Main Dam and Re-regulation Dam. A description of the data utilized in this dissertation follows. In order to facilitate the geomorphic analysis, the study reach of the Hwang River has been divided into three sub-reaches.

3.1. Description of the Study Reach

There is large seasonal variation in precipitation which results in frequent flooding during the wet season (June to September) and severe droughts during the low flow season (October to May) in Korea. With these precipitation features, the flow conditions in the rivers are unstable, as indicated by a large coefficient of river regime (the ratio of maximum to minimum stream flow) ranging from 300 to 400, which is far greater than the typical range of 3 to 34 for other countries. This large variation creates problems in river management associated with flood control and water supply. Table 3-1 summarizes river regime for several rivers around the world. This study reach is located on the Hwang River, a tributary to the Nakdong River. The reach extends from the Hapcheon Re-regulation Dam to the Nakdong River confluence. The Nakdong River is the longest river in South Korea. The river length is 506 km and the basin area of the river is 23,394 km^2, the second largest after the Han River (32,200 km^2). It is located in the southeastern part of the Korean Peninsula and generally flows from north to south. The bed material is mostly sands except in the upper mountain area where it is composed of gravel and cobble. This river basin contains 6 multi-purpose dams which began construction in the 1970's starting from the Andong Dam (1977), Hapcheon Dam (1989), Nakdong estuary barrage (1990), Imha Dam (1993), Namgang Dam (2001), and Milyang Dam (2001). The purposes of these dams are for flood control, water supply and hydroelectric power generation.

Table 3-1. Comparisons of coefficients of river regime (the ratio of maximum to minimum stream flow)

River	Country	Coefficients of River Regime
Han	Korea	390
Nakdong	Korea	260
Missouri	USA	75
Seine	France	34
Nile	Egypt	30
Yangtze	China	22
Rhine	Germany	16
Thames	England	8

The Hwang River flows from west to east. It is located at the western part of the Nakdong River basin (Figure 3-1). The river length is 107.6 km and the basin area of the river is 1,329 km^2.
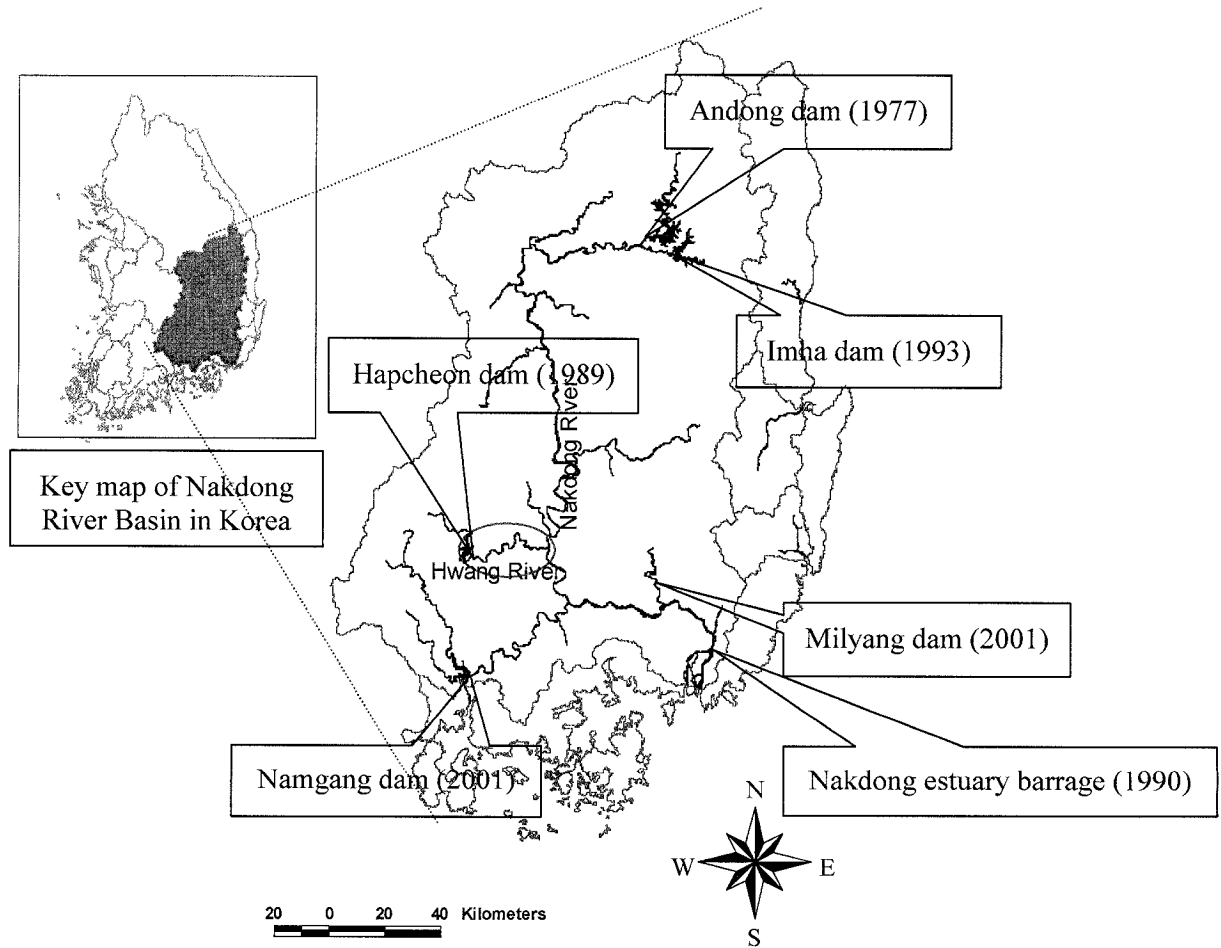
Figure 3-1. Nakdong River Basin and the study reach (red circled area) in Hwang River
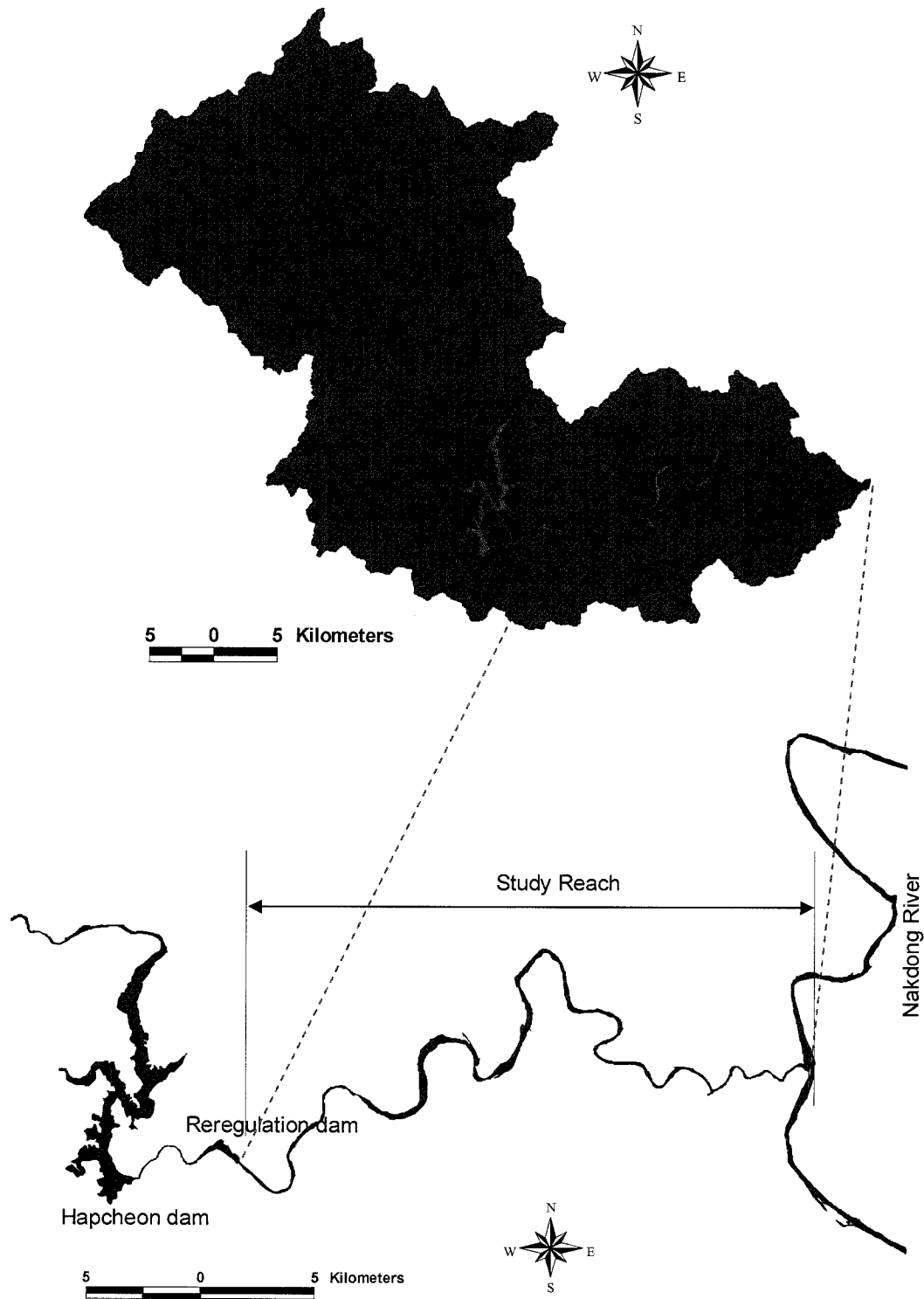
Figure 3-2. The Hwang River basin and study reach from the Hapcheon Re-regulation Dam to confluence with the Nakdong River (45 km)

31

Figure 3-2 provides a more detailed map of the Hwang River basin and study reach from the Hapcheon Re-regulation Dam to the Nakdong River. The study reach is 45 km long, with a basin area of 372.4 km^2. It is 28% of the total Hwang River basin (1329 km^2). The Hapcheon Main Dam was constructed in the narrow canyon of the Hwang River. The dam is located about 16 km north of the Hapcheon City. The purpose of the dam was to reduce flood damage and provide water supply to downstream of the Nakdong River as well as the Busan City and Masan City, etc. It is a concrete gravity dam with a total fill volume of 891×10^6 m^3. The basin area of the dam is 925 km^2. The dam dimensions are 96 m in height and 472 m in length, and it has a reservoir storage capacity of 790 $\times 10^6$ m^3. In addition, there is the re-regulation dam located 6.5 km downstream of the main dam to regulate the discharge from the main hydro power station. The main power station is located 2 km upstream from the re-regulation dam and operates only 3 hours per day except during flood season. The maximum discharge of the main power station is 119 m^3/s (1,285,200 m^3/day) and the Re-regulation Dam regulates this 3-hour discharge as approximately 15 m^3/s per day. Figure 3-4 shows a schematic of the study reach. Four tributaries join the Hwang River at 6, 14, 30, and 38 km. In addition, there are two water level gaging stations, Hapcheon at 11.1 km and Jukgo at 37.8 km from the re-regulation dam.
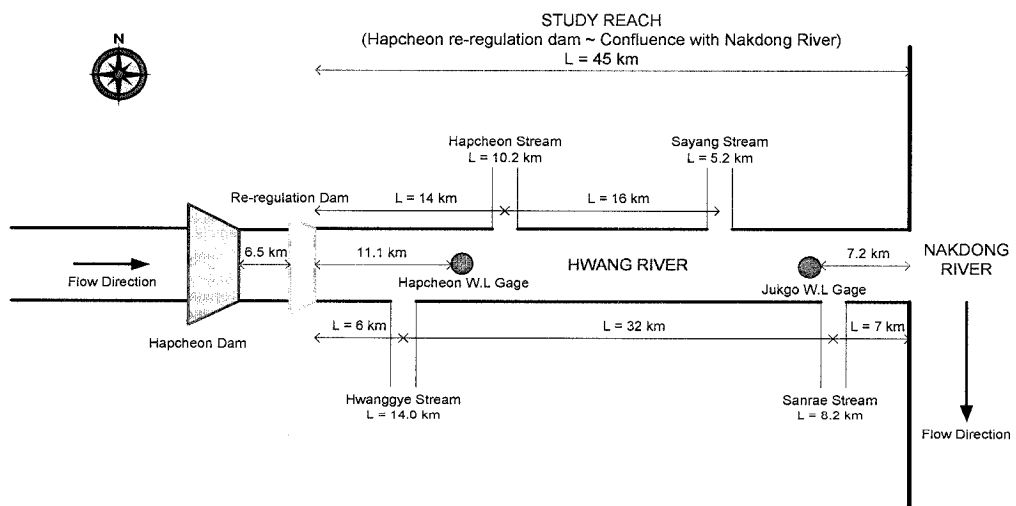
Figure 3-3. Schematic diagram of Study reach in the Hwang River from the Hapcheon Re-regulation Dam to confluence with the Nakdong River

Figure 3-4 shows satellite images of the reach between the Hapcheon Main Dam and re-regulation Dam, and the study reach between Hapcheon Re-regulation Dam and confluence with the Nakdong River. Hapcheon city is located about 10 km downstream from the re-regulation dam. It is the biggest city in the study reach.
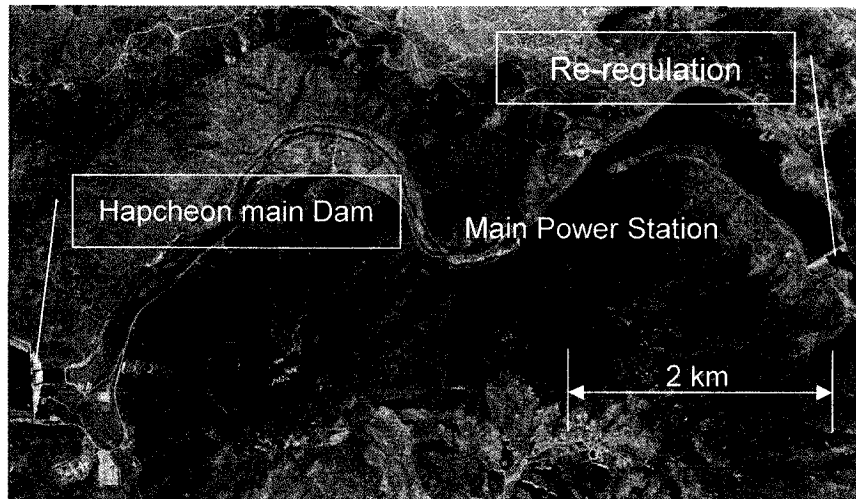
(a) Satellite image between the Hapcheon Main Dam and Re-regulation Dam
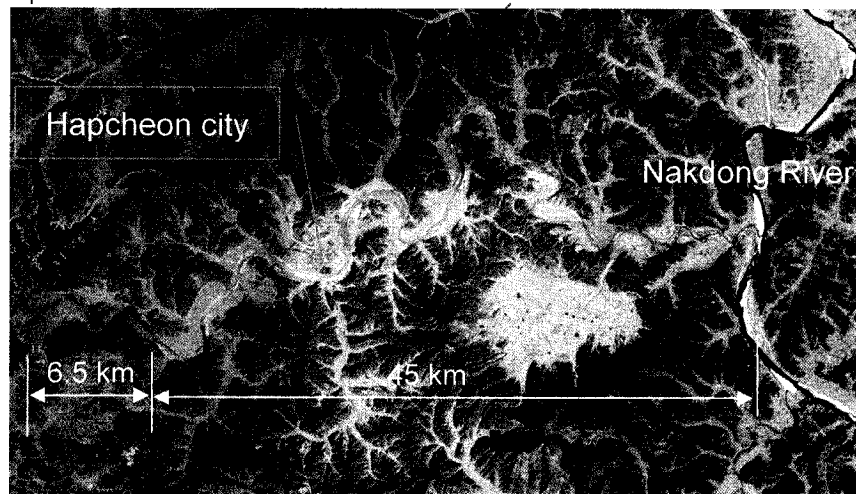
(b) Satellite image of entire study reach between the Hapcheon Main Dam and confluence with the Nakdong river

Figure 3-4. Satellite images taken in 2004 for the reach (6.5 km) between the Hapcheon Main Dam and Re-regulation Dam (a), and the study reach (45 km) between the re-regulation dam and confluence with the Nakdong river (b)

Figure 3-5 (a) shows the Hapcheon Main Dam site (before construction) and the Hapcheon Main Dam (after construction). Also, Figure 3-5 (b) shows the Hapcheon Re-regulation Dam site and the Re-regulation Dam. Table 3-2 provides detailed configuration of the Hapcheon Main Dam and Re-regulation Dam.
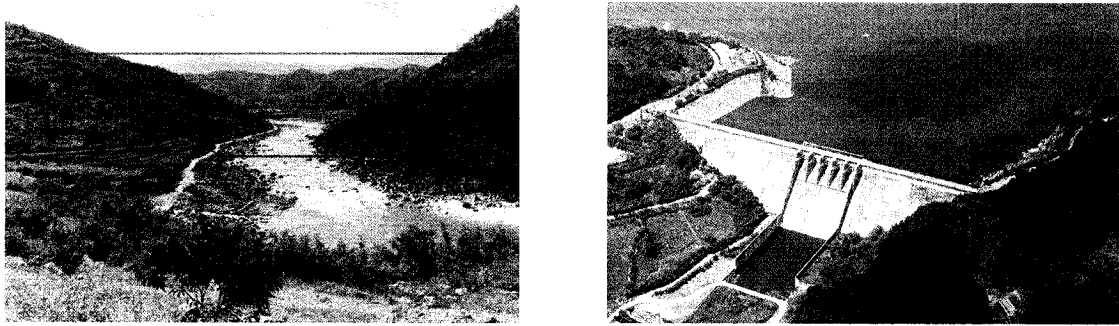
(a) Hapcheon Main Dam site (left) and Hapcheon Main Dam (right)
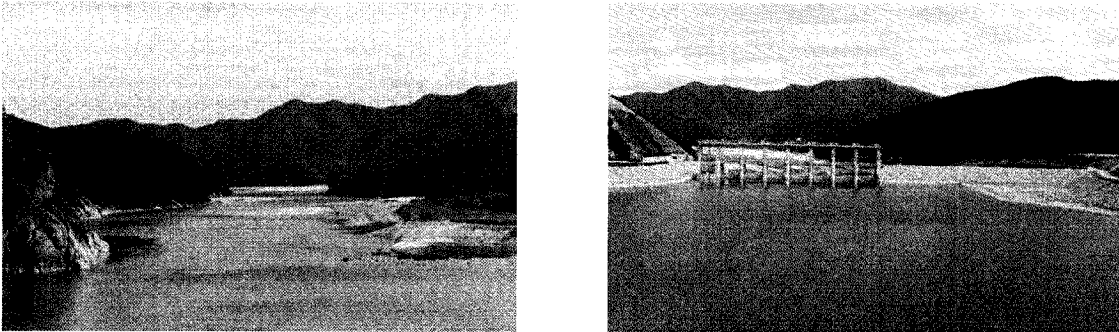
(b) Hapcheon Re-regulation Dam site (left) and Hapcheon Re-regulation Dam (right)

Figure 3-5. Hapcheon Main Dam (a) and Re-regulation Dam (b)

The construction of the Hapcheon Main Dam and re-regulation Dam began in April 1982 and was completed in December 1989. It has a 101 MW hydropower plant which utilized the geographic characteristics of the region by constructing a diversion tunnel to increase the head for the maximum possible power generation. The re-regulation dam is located 2 km downstream from the main power station. It is a concrete structure of the length 130.5 m at the left bank and rockfill type of the length 145 m at the right bank. The overall height is 29 m and contains a total volume of 188×10^3 m^3. The effective storage capacity is 1.4×10^3 m^3. The purpose of this re-regulation dam is to regulate the flow from the main power station from 119 m^3/s for 3 hours to approximately 15 m^3/s for 24 hours.

Table 3-2. Configuration of the Hapcheon Main Dam and Re-regulation Dam

1) General
  - Location : Hwang River (tributary of the
      Nakdong river)
  - Catchment area : 925 km^2
  - Annual mean inflow : 911.4 million m^3
	2) Main Dam
	  - Height : 96 m
	  - Length : 472 m
	  - Dam crest elevation : EL.181.0 m
	  - Type : Concrete gravity dam

3) Re-regulation Dam
  - Height : 29 m
  - Length : 275.5 m
  - Type : Concrete & Rockfill dam
  - Location : 6.5 km downstream of the
      main dam
	4) Reservoir of Main Dam
	  - Flood water level : EL.179.0 m
	  - Normal water level : EL.176.0 m
	  - Lowest water level : EL.140.0 m
	  - Gross storage capacity : 790 million m^3
	  - Effective storage capacity :
	             560 million m^3
	  - Flood control capacity : 80 million m^3
	  - Reservoir area : 25.0 km^2

5) Power Generation (Main dam)
  - Installed Capacity : 101,000 kW
  - Annual Energy Output: 232.4 GWh
  - Maximum Turbine Discharge :
            119 m^3/sec
  - Rated Head : 95.0 m
	6) Power Generation (Re-regulation dam)
	  - Installed Capacity : 1,200 kW
	  - Maximum Turbine Discharge :
	            20 m^3/sec
	  - Rated Head : 7.3 m

7) Water Supply
  - Annual Water Supply : 599 million m^3 - Municipal & Industrial : 520 million m^3
  - Irrigation : 32 million m^3 - Environmental Flow : 47 million m^3	

The geology of the Hwang River Basin is composed of igneous, metamorphic, granite and sedimentary rocks. Ninety five percent of the river basin is composed of granite and metamorphic rocks and the other five percent is composed of other igneous rocks and sedimentary rocks. The granite and metamorphic rocks are located in the central and northern regions of the river basin. However, sedimentary rocks are found in the vicinity of the confluence with the Nakdong River (MOCT, 2003). Figure 3-6 shows the geological map of the Hwang River Basin.
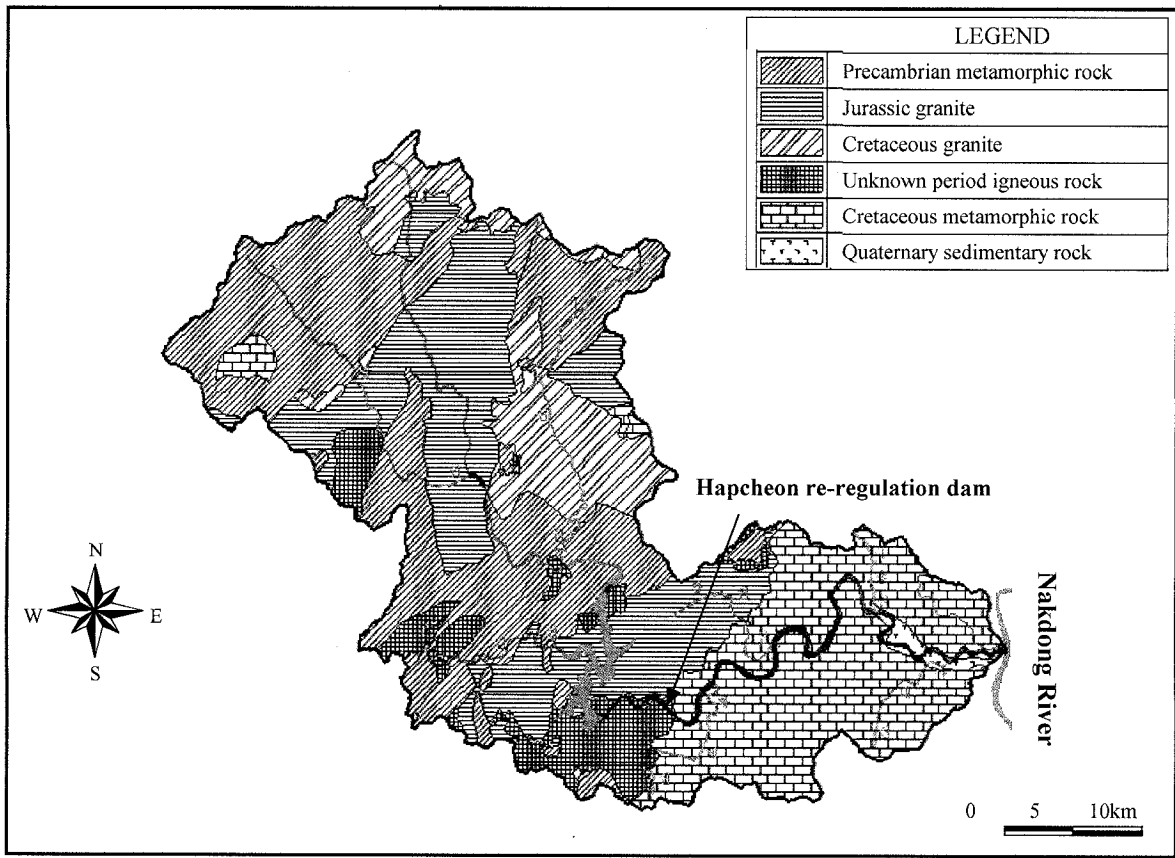
Figure 3-6. Geological map of the Hwang River Basin (MOCT, 2003)

The total land area of the Hwang River Basin is 1,344.2 km². The current land use of the river basin is summarized in Figure 3-7 and Table 3-3. Forest area is the dominant land use (74.17%) in this river basin. The agricultural area is second, with rice paddy fields composing more than 70% of the total agricultural area.
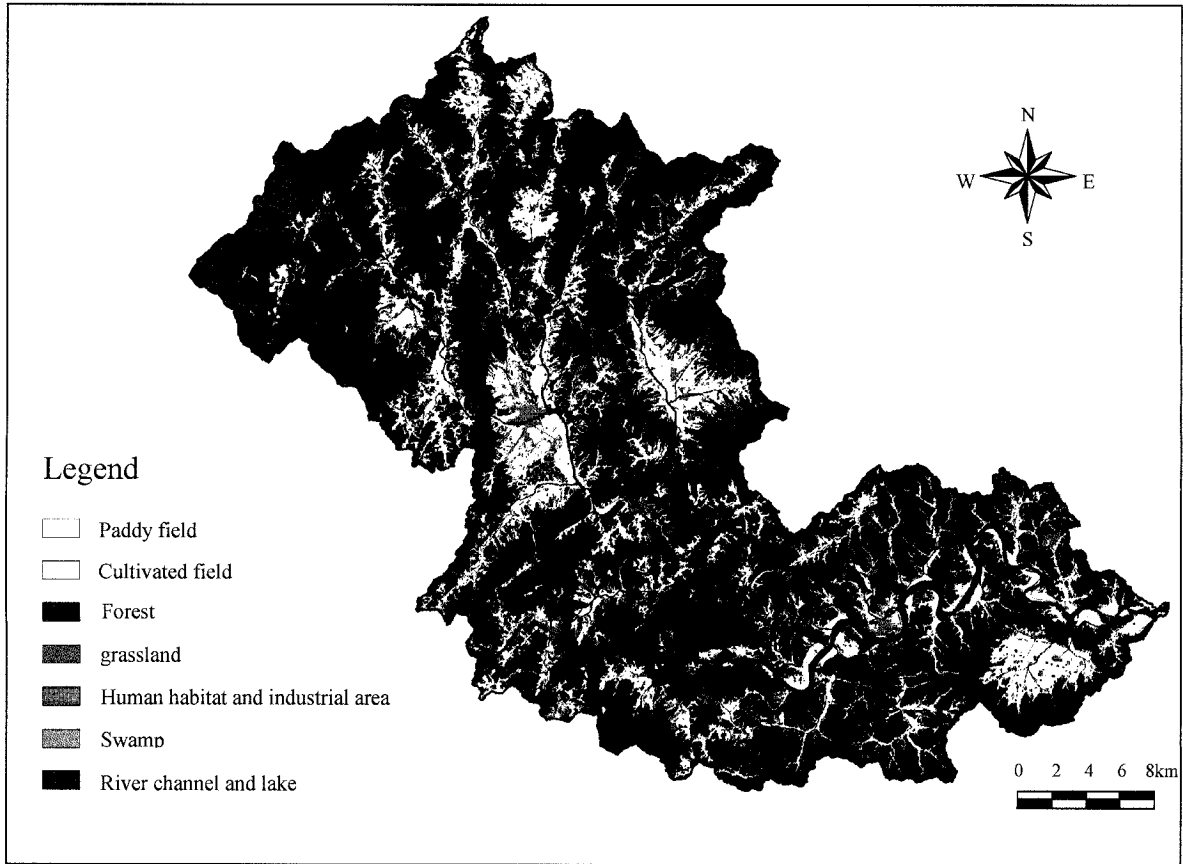
Figure 3-7. Map of land use of the Hwang River Basin (MOCT, 2003)

Table 3-3. Land use of the Hwang River Basin

	Total	Agricultural area			Human habitat	Industrial area	Forest	Others
		Subtotal	Paddy field	Cultivated field				
Area (km²)	1344.2	208.04	143.43	64.70	14.04	0.98	997.03	124.10
Percent (%)	100.0	15.48	10.66	4.81	1.04	0.07	74.17	9.23

3.2. Data of the Study Reach

Most of the data collection began on the Hwang River in 1983 with the national river channel maintenance plan to protect properties from flood damage by the Ministry of Construction of Korea, which is known as the Ministry of Construction and Transportation (MOCT) since 1996. Data are generally collected every 10 years and focused on maintenance and construction of levees along the channel, especially downstream of the Hapcheon Re-regulation Dam to reduce flood damage. Data include cross-section surveys, bed material size surveys, flow discharge, meteorological data, water quality and environmental conditions such as distribution of animals and plants. There are three major data sets for this study reach (1983, 1993, and 2003). Aerial photos taken in 1982, 1993 and 2004 were gathered from the National Geographic Information Institute of Korea to quantify and compare channel adjustment before and after dam construction. Also, discharge data were gathered from the MOCT and KOWACO gaging stations (from 1969 to 2005).

Cross-section Surveys

Cross-section survey data were measured in 1983, 1993, and 2003 for this study reach. The cross-section survey data set from 1983 was obtained from the National Water Management Information System (WAMIS) of Korea website. It consists of Microsoft Excel spreadsheets and was converted to HEC-RAS to facilitate analysis of flow condition. The cross-section survey data sets from 1993 were only available in a survey report, so only thalweg elevation data were available with numeric formation. Finally, the cross-section survey data sets from 2003 contained HEC-RAS geometric input files (MOCT, 2003), so they were directly used in the analysis to study flow conditions. The cross-section surveys were collected approximately 500 m apart for a total of 100 cross-sections in 1983 and 1993. However, in 2003 the cross-section surveys were collected 250 m apart, with a total of 210 cross-sections.

Aerial Photos (1:12,000)

Aerial photos are available for 1982 (May 26 to 28), 1993 (June 5 to September 6), and 2004 (December 7 to 9). The aerial photos were obtained from the National Geographic Information Institute of Ministry of Construction and Transportation of Korea. These photos are strictly image files without any information coordinate system to recognize the locations and to measure lengths and areas. Therefore, a geometric correction process was performed to quantify and identify the location of the active channel, active channel width, area, vegetated islands, and numerous other important features. These aerial photos were digitized by using ERDAS IMAGINE software from the Digital Elevation Model (DEM) to get X, Y coordinates to determine location site and measure the length and area. After processing, the images, the active channel area, cross-section survey lines, vegetated area, and island area were drawn on the aerial photos using ArcView 3.2 software. Then, active channel width, active channel areas, vegetated area and island area were also measured using this software for each sub-reach.

Figure 3-8 provides a sample of the digitized aerial photos taken in 1982, 1993, and 2004 with non-vegetated active channel area and survey lines of 1993.

1 0 1 2 Kilometers

N
W — E
S

1993_survey_line_sub.shp
1982_active_channel_sub1.shp
1982_active_channel_sub2.shp
1982_active_channel_sub3.shp
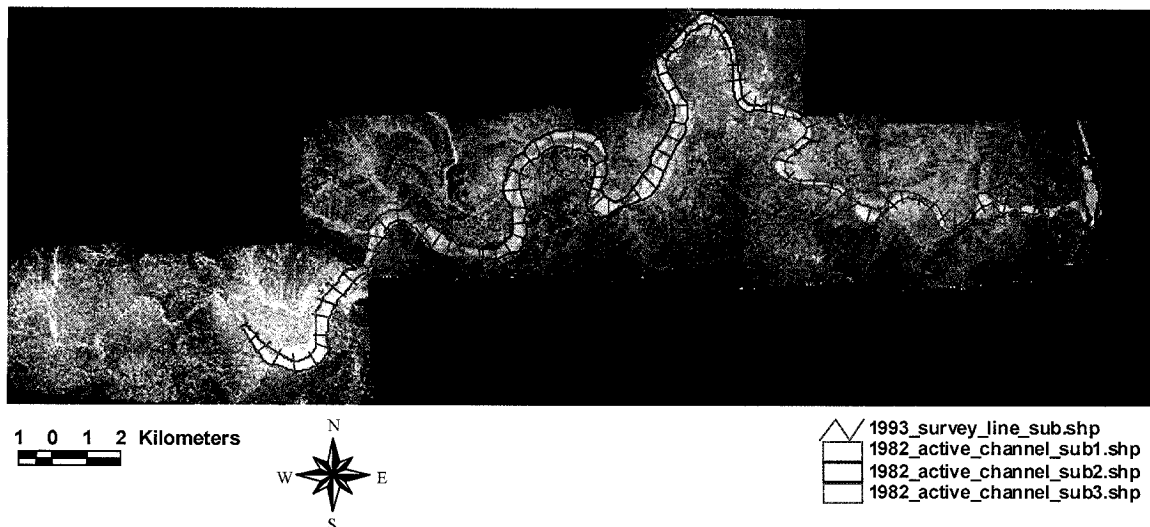
(a) Aerial photo taken in 1982 with active channel area and survey lines
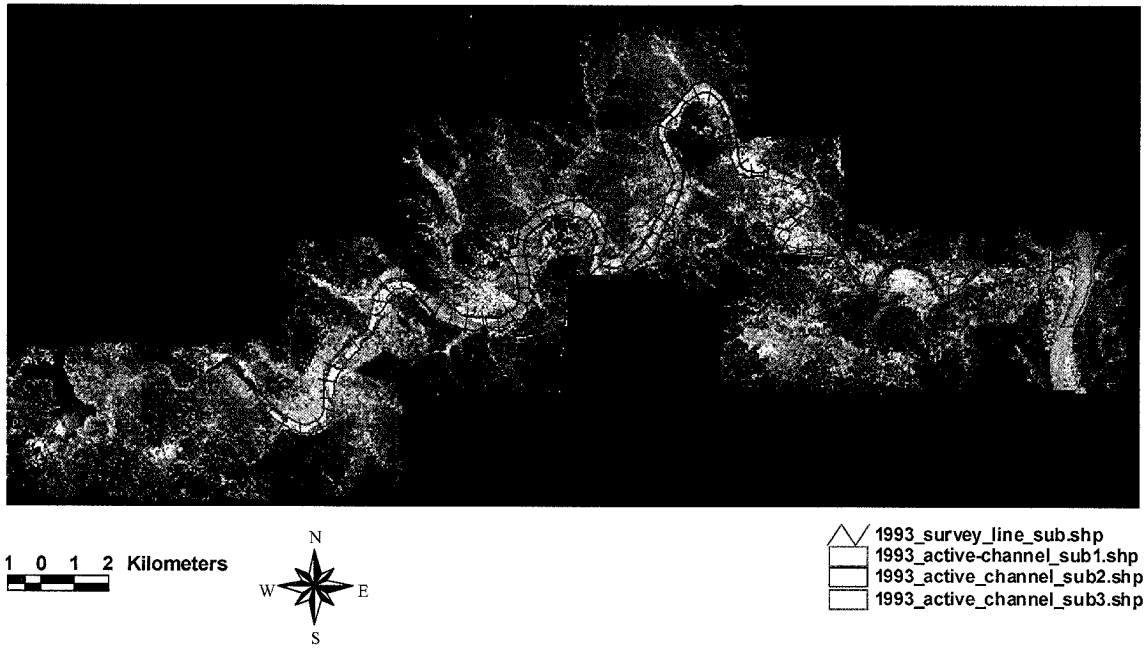
(b) Aerial photo taken in 1993 with active channel area and survey lines
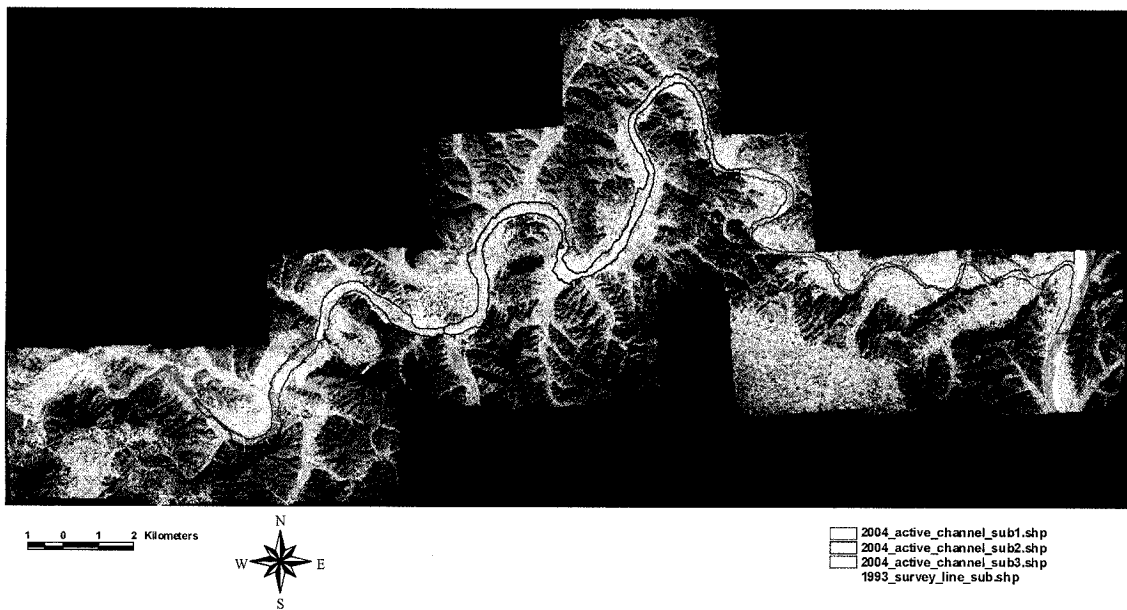
(c) Aerial photo taken in 2004 with active channel area and survey lines

Figure 3-8. Cross-section survey lines of 1993 and aerial photos taken in 1982 (a), 1993 (b), 2004 (c)

Discharge Records

Daily stream data along the study reach were available from 1969 to present at KOWACO and MOCT gaging stations. The flow discharge data were collected at the Changri Station, which changed its name to the Hapcheon Re-regulation Dam gaging station operated by KOWACO after 1989 (after the dam completion). In addition, hourly and 30 minute data were available since 1996. There are two water level gaging stations downstream of the Hapcheon Re-regulation Dam, Hapcheon and Jukgo gaging stations, operated by MOCT since 1962. However, there were missing data and errors in the conversion from water level to discharge using the stage-discharge rating curves by MOCT. Therefore, most analyses were conducted using the data of the Hapcheon Re-regulation Dam gaging station.

Sediment Sampling and Bed Material Size Measurement

Bed material samples were collected during the same time as cross-section surveys by MOCT (1983, 1993, 2003). The dates of the available data are summarized in Table 3-4.

Table 3-4. List of measured bed material size of the study reach

Year	Number of cross-section	Interval (km)
1983	13	4
1993	46	1
2003	25	2

Suspended sediment sampling was performed at the Changri gaging station (the Hapcheon Dam site) in 1969 to get sufficient data for the construction of the Hapcheon Dam by FAO/UNDP and KOWACO (1971). They measured sediment data in the Hwang River in 1969 (12 samples) and 1970 (37 samples) at Hapcheon Dam site as a pre-investment survey to forecast sedimentation for the eighteen dam sites proposed in the Nakdong River basin, including the Hwang River for the Hapcheon Dam. There are

no other sediment related data measured after this study in the Hwang River except the survey of the reservoir sediment deposition of the Hapcheon Main Dam in 2002 by KOWACO (2002). However, the survey was an indirect measurement to estimate the sediment transport rate of the study reach. More detailed data configuration related to sediment transport will be explained in Chapter 4.

3.3. Definition of the Study Reach and Sub-reaches

In order to facilitate analysis of the study reach, the reach was divided into three sub-reaches based on channel characteristics and sub watershed related to the tributaries. The reach definitions and lengths are described in Table 3-5. Sub-reach 1 is approximately 11.0 km from the Hapcheon Re-regulation Dam to the Namjung Bridge (Hapcheon Water Level Gaging Station). Sub-reach 2 is 19.5 km from the Namjung Bridge to the Sayang Stream and sub-reach 3 is 14.5 km from the Sayang Stream to the Confluence with Nakdong River. Figure 3-9 and Tables 3-5 and 3-6 provide descriptions of the sub-reaches and locations of the tributaries downstream of the Hapcheon Re-regulation Dam.

2   0   2 Kilometers

N
W — E
S

2004_active_channel_sub1.shp
2004_active_channel_sub2.shp
2004_active_channel_sub3.shp
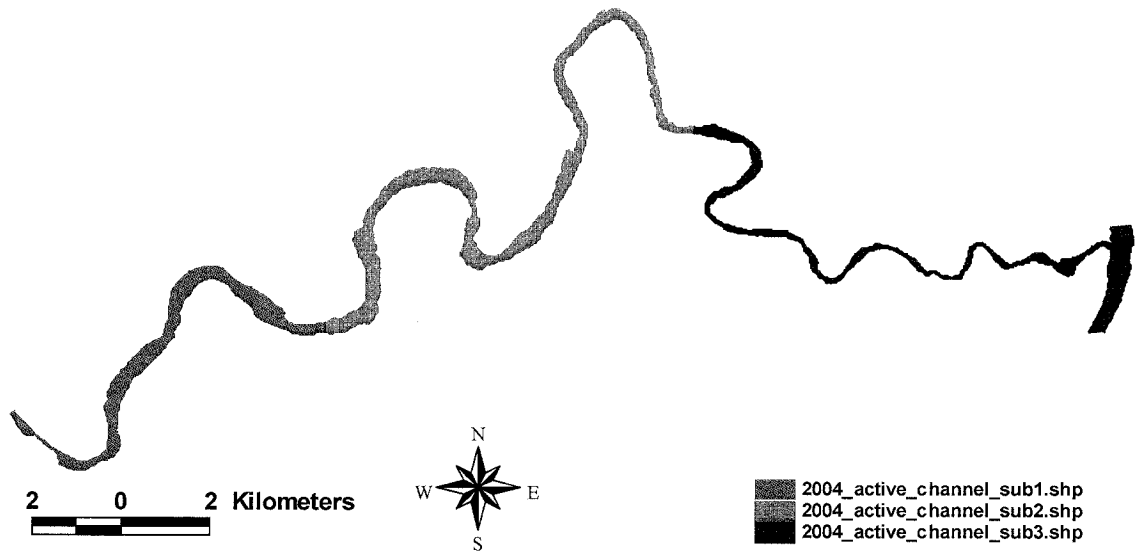
Figure 3-9. Reach definition

Table 3-5. Reach definition and lengths

Reach	Description	Valley Length (km)	Average Thalweg Length (km)
1	Hapcheon Re-regulation Dam ~ Namjung Bridge (Hapcheon Water Level Gaging Station)	6.9	11.0 (34.0~45.0 km)
2	Namjung Bridge (Hapcheon Water Level Gaging Station) ~ Sayang Stream	10.5	19.5 (14.5~34.0 km)
3	Sayang Stream ~ Confluence with the Nakdong River	8.0	14.5 (0~14.5 km)

- ( ) : Location of the each sub-reach

Table 3-6. Locations of tributaries in the study reach

Sub-reach	Tributaries	Location
1	- Hwanggye stream	40.0~39.5 km
2	- Hapcheon stream	31.5~31.0 km
3	- Sayang stream	15.0~14.5 km
	- Sanrae stream	5.0~4.5 km

3.4. Summary

The 45 km study reach is located in the Hwang River from the Hapcheon Re-regulation Dam to the confluence with the Nakdong River. After dam construction, there were many changes to the geomorphology, flow regime, bed material, vegetation, and ecology downstream of the dam.

The data sets include water discharge, sediment transport, channel slope, bed material size, cross section surveys, and digitized GIS coverages of the active channel from aerial photos. The data were measured by different government agencies (MOCT, KOWACO) beginning in 1982 and continuing through 2004. Additionally, to aid in the study of the spatial variability of response within the study reach, the reach was divided into 3 sub-reaches to quantify parameters and analyze the change in these parameters. The geomorphic analyses in this dissertation are based on channel changes between digitized coverages of the non-vegetated active channel. The channel changes are presented in the following chapters.

4 ANALYSIS OF CHANNEL GEOMORPHIC CHANGES

A quantitative analysis is conducted to understand changes that have occurred spatially and temporally in the study reach. This will give information about the channel geomorphic change due to dam construction. The water discharge, total sediment transport rate and channel slope were analyzed. Also, the vertical response of the bed material and bed elevation of the channel were quantified. Then, lateral response of channel width and sinuosity are measured by digitized aerial photos taken in 1982, 1993 and 2004. The other data were measured in 1983, 1993 and 2003.

4.1. Hydrologic Regime

The study of the historic discharge record of the study reach is summarized as three main goals:

1) Identification of temporal trend in daily and annual peak discharge regime,

2) Identification of the impacts of the Hapcheon Re-regulation Dam on flow duration and annual peak discharge change, and

3) Determination of bankfull discharge for each return interval.

The results for each are presented in the following sections.

In order to understand natural change in this study reach, the rainfall pattern is considered before analyzing the flow discharge. There are six water level gaging stations and eight rain gaging stations in the Hwang River basin, as shown in Figure 4-1. Two water level gaging stations are located downstream of the Hapcheon Re-regulation Dam (Hapcheon and Jukgo gaging stations). The mean annual rainfall calculated by data from 1972 to 2001 of the Hwang River basin is 1,232.3 mm (MOCT, 2003). Figure 4-2 shows

mean annual rainfall of the Hwang River basin (1972~2001), pre (1972~1988) and post dam (1989~2001). It shows that the mean annual rainfall increased from 1,218 mm to 1,252 mm after dam construction.
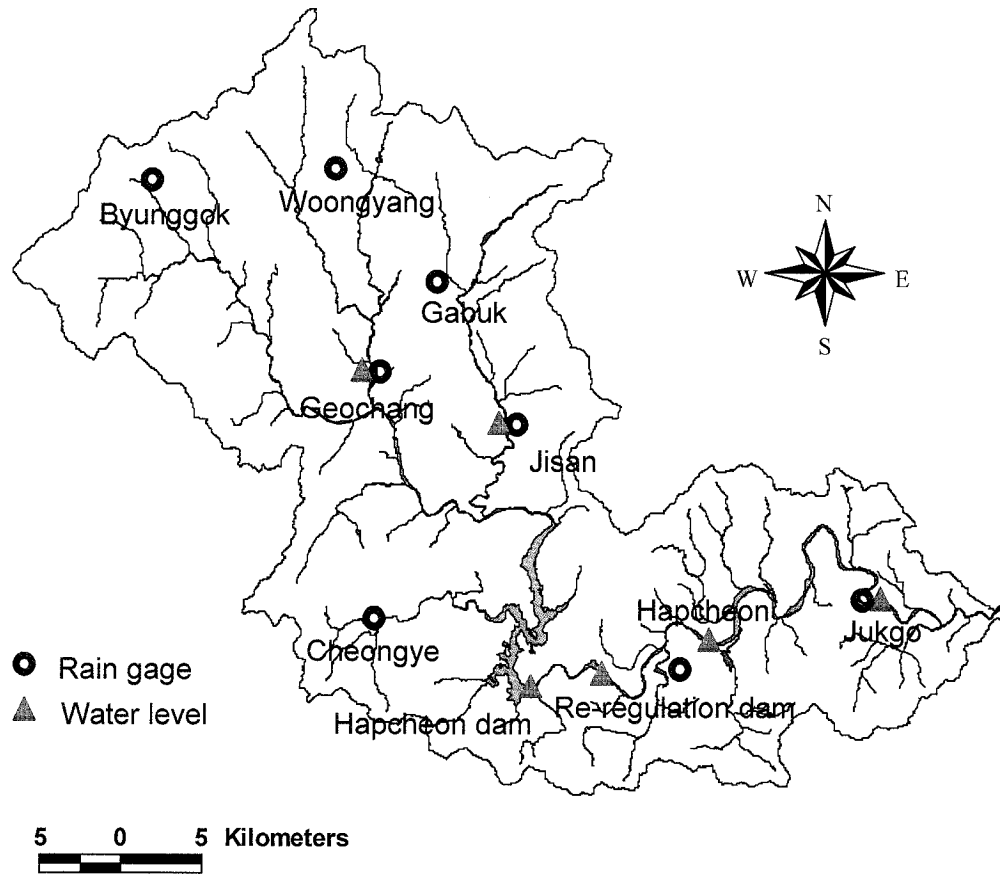
Figure 4-1. Location map of the gaging stations in the Hwang River basin

Daily discharge data at the Hapcheon Re-regulation Dam site were used to construct a flow duration curve and check the variation of daily peak discharge before and after dam construction. Before dam construction, there was the Changri water level gaging station at the present Hapcheon Re-regulation Dam site, so daily stage-discharge data at the Changri station were used for the period before dam construction and discharge from the Hapcheon Re-regulation Dam were used for the period after dam construction. The data are available for 30 years from 1969 to 1981 and from 1989 to 2005 to describe the pre and post-dam periods, respectively. The mean annual peak discharge decreased from

654.7 m³/sec to 126.3 m³/sec after dam construction (Figure 4-3 and Table 4-1). However, the annual minimum discharge increased from 2.6 m³/sec to 4.1 m³/sec. Figure 4-4 shows daily discharge at the Hapcheon Re-regulation Dam site from 1969 to 2005.
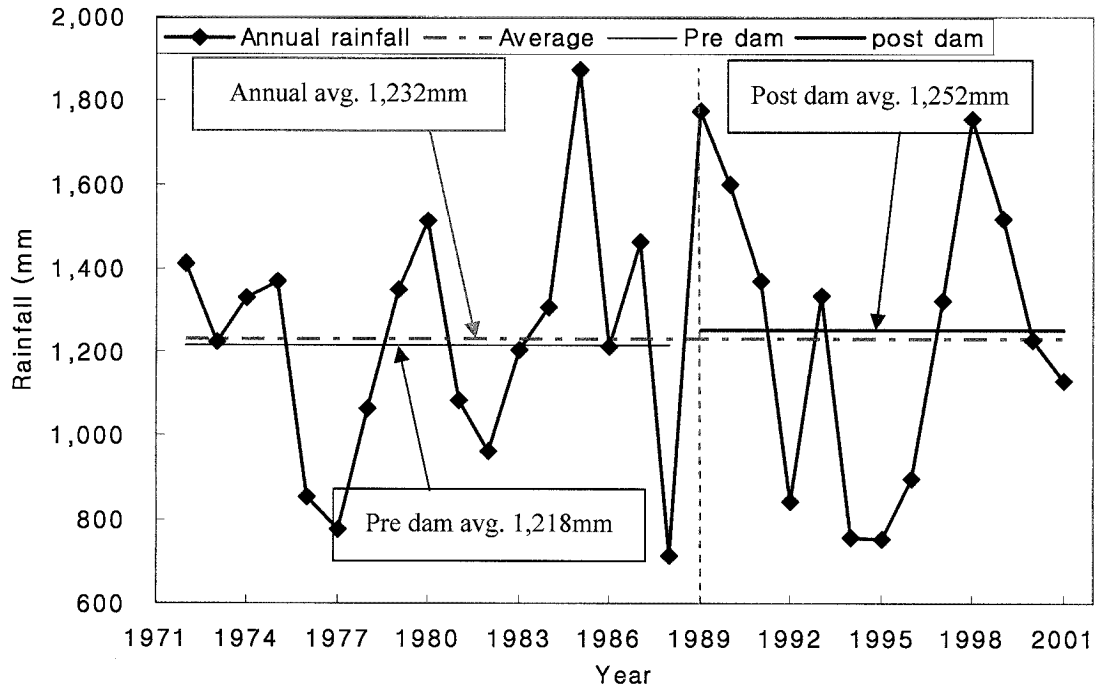
Figure 4-2. Variation of annual rainfall in Hwang River basin before and after the Hapcheon Dam

Table 4-1. Mean daily, annual peak and minimum discharge at the Hapcheon Re-regulation Dam site

Period	Mean daily discharge (m³/s)	Mean annual peak discharge (m³/s)	Mean annual minimum discharge (m³/s)
Pre-dam (1969~1981)	28.7	654.7	2.6
Post-dam (1989~2005)	22.1	126.3	4.1
Overall (1969~2005)	25.0	355.3	3.5
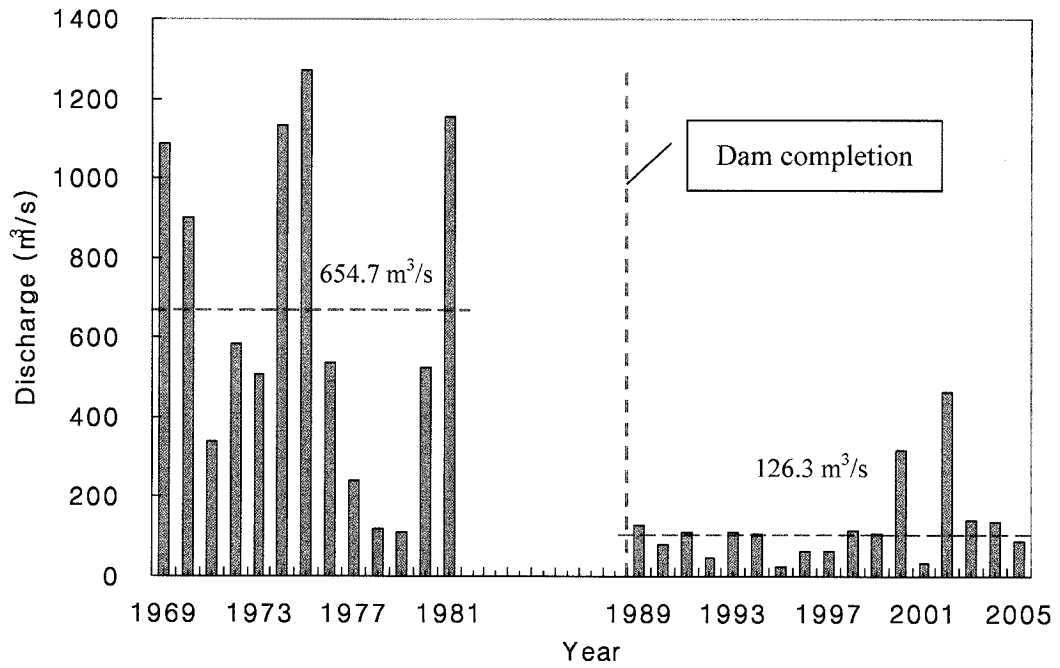
Figure 4-3. Annual peak discharge at the Hapcheon Re-regulation Dam site from 1969 to 2005
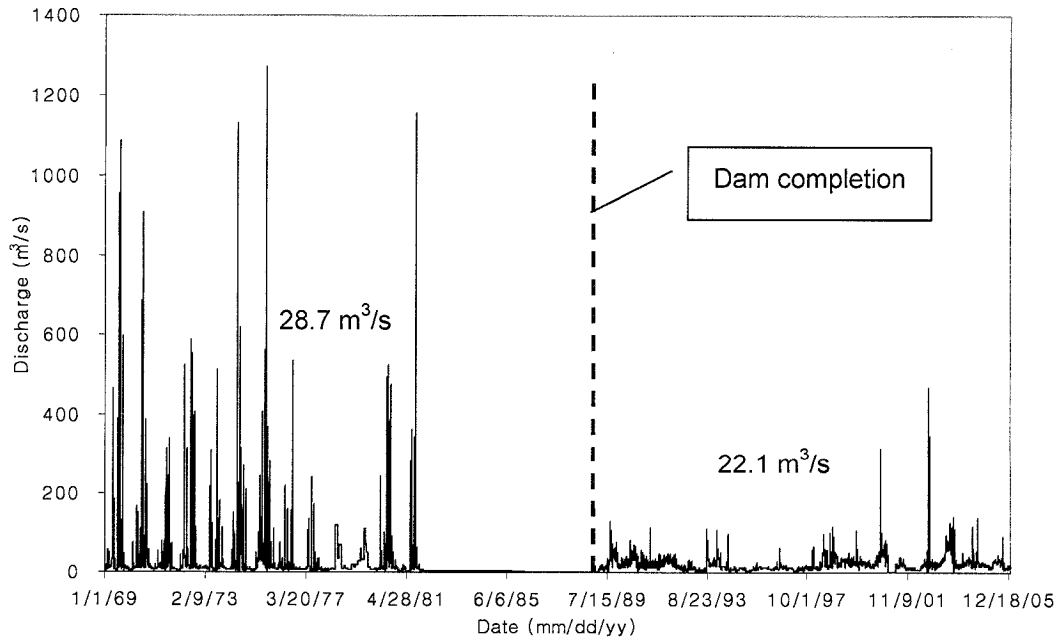
Figure 4-4. Daily discharge at the Hapcheon Re-regulation Dam site (1969 to 2005)

The distribution of monthly mean discharge is shown in Figure 4-5. The monthly mean discharge for the pre-dam period varies greatly throughout the year. It is a little over 5 m^3/s in December and January, but it is 36 m^3/s in July during flood season. However, monthly mean discharge for the post-dam period shows little variation throughout the years. The lowest discharge was about 15 m^3/s and the highest discharge was a little more than 20 m^3/s because the re-regulation dam attenuated peak flood.
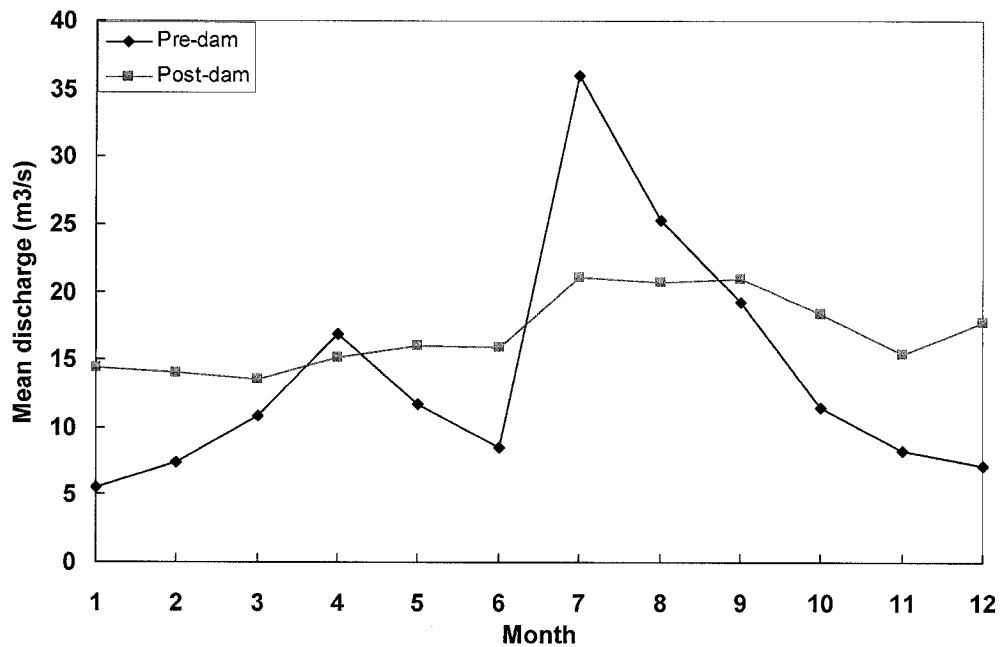
Figure 4-5. Monthly mean discharge at the Hapcheon Re-regulation Dam site from 1969 to 2005

The cumulative discharge is approximately 23,000 million m^3 from 1969 to 2005 at the Hapcheon Re-regulation Dam site (no data for 7-year period, 1982~1988) and it is 11,780 million m^3 before dam construction period. From Figure 4-6, we can find that the slope of the cumulative discharge of the post-dam period is somewhat lower than the slope of pre-dam period.

Flow duration distributions, generated from daily flow discharges, are a useful indicator of temporal variability in the record. The slope of these curves indicates how

flashy or steady the discharge record is for a period of time. Figure 4-7 shows flow duration curves for the pre and post-dam period. It shows that high flows, with percent exceedance lower than 22%, are decreased after dam completion. Low flow, with percent exceedance over 22%, are increased after dam completion. Table 4-2 shows percent exceedance of flow duration of pre and post-dam period.

$y = 1.81 x - 47395$
$R^2 = 0.98$

$y = 2.39 x - 59446$
$R^2 = 0.99$

Pre-dam (1969~1981)
Post-dam(1989~2005)
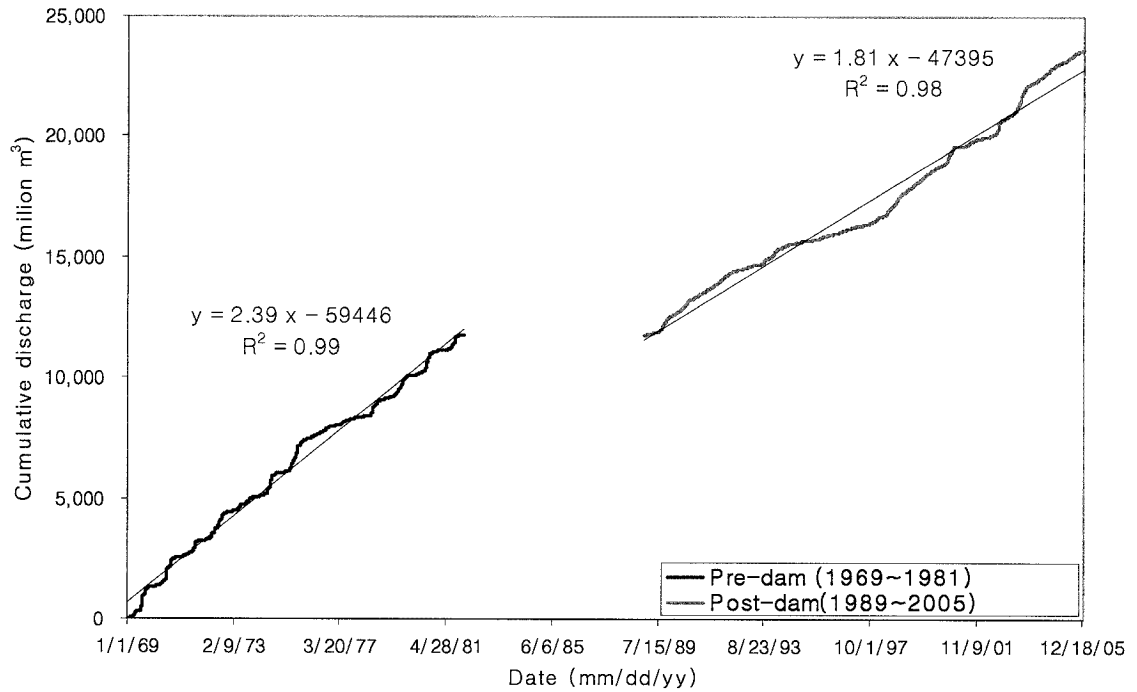
Figure 4-6. Cumulative flow at Hapcheon Re-regulation Dam site (1969~2005)

Table 4-2. Compare the flow duration (percent exceedance) of Pre-dam and Post-dam period

% exceedance	Pre-dam (1969~1981)	Post-dam (1989~2005)
0.02	1271.8	462.3
5	110.2	61.7
10	60.5	44.9
22	26.9	27.9
50	10.1	16.2
80	6.0	8.2
97.5	3.1	0.3
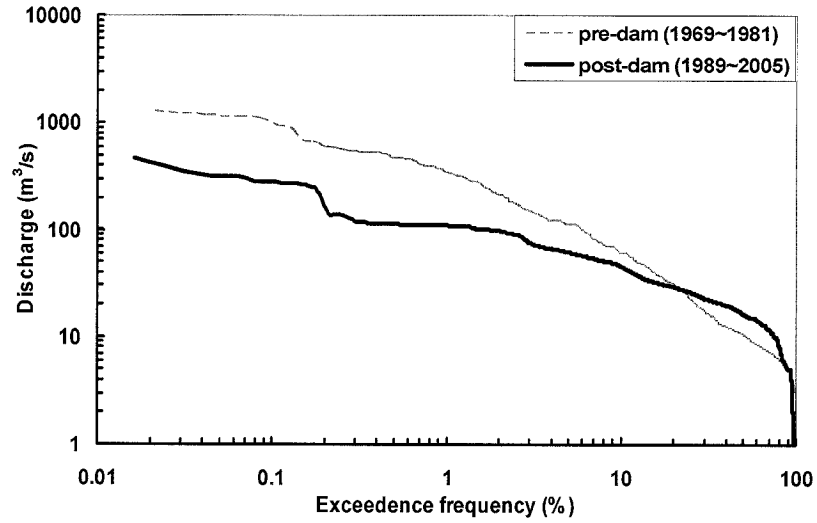
Figure 4-7. Flow duration curves at the Hapcheon Re-regulation Dam site from 1969 to 2005

Figure 4-8 shows comparison of typical discharge hydrographs at the Hapcheon Re-regulation Dam site before and after dam completion, in 1981 and 2002, respectively. Generally, the precipitation in Korea is concentrated in summer (from June to September), as mentioned in the previous chapter. It shows that the peak discharge was dramatically decreased after dam construction by regulating discharge during the flood season.
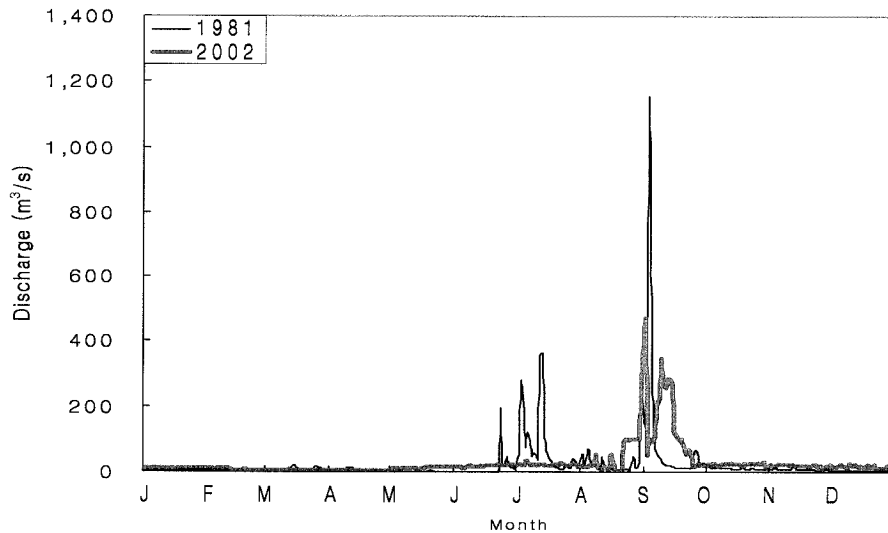
Figure 4-8. Comparison of discharge hydrographs of 1981 and 2002 at the Hapcheon Re-regulation Dam

Bankfull discharge (1.58 yr discharge frequency) of the Hwang River was estimated as 110.9 m³/s at the Hapcheon Re-regulation Dam site for the entire period (1969~2005). Bankfull discharge of the pre-dam period was estimated as 509.8 m³/s and 86.3 m³/s for the post-dam period. The bankfull discharge of the post-dam period is just 17% of the pre- dam period. Figure 4-9 and Table 4-3 show the variation of bankfull discharge before and after dam construction.

Table 4-3. Bankfull discharge of Hwang River before and after dam construction by recommended frequencies using discharge at Hapcheon Re-regulation Dam site

Discharge Frequency	Overall (m³/s)	Pre-dam (m³/s)	Post-dam (m³/s)
1.5 year	110.2	447.5	80.4
1.58 year	110.9	509.8	86.3
2 year	133.5	535.9	107.7

• Overall : 1969~2005, Pre-dam : 1969~1981, Post-dam : 1989~2005
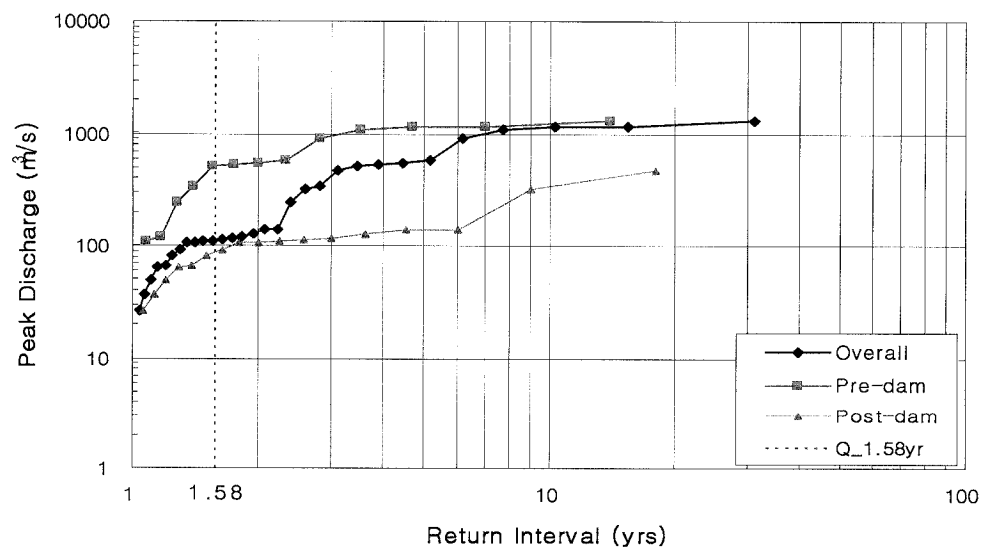
Figure 4-9. Peak discharge vs. Return interval at the Hapcheon Re-regulation Dam site for 1969~2005 period

4.2. Sediment Transport

FAO/UNDP and KOWACO (1971) measured sediment transport in the Hwang River in 1969 (12 samples) and 1970 (37 samples) at the Hapcheon Dam site as a pre-investment survey to forecast sedimentation in the eighteen dams proposed in the Nakdong River basin, including the Hapcheon Dam. There are no other sediment-related data measured after this study in the Hwang River. These studies dealt with sediment transport in rivers only. Erosion on the hills could not be measured but was considered to be the natural cause of sediment transport. These studies also only considered the suspended load of the sediment. Bed load was assumed to be 10% of the suspended load. In this study, it was assumed that sediment transport in the Nakdong River Basin is mainly caused by precipitation. Therefore, a new method based on sediment sampling and combined river discharge and rain recording was developed to calculate sediment transport to match the geographical conditions of the Nakdong River Basin. The method departs from the "sediment-rating curve – flow duration curve" method for calculating sediment transport. The different method is necessary because long period river flow data were not available and the runoff distribution is unusual as high flood peaks can appear and disappear within less than one day. In 1969 and 1970, respectively, 12 and 37 sediment samples were taken for analysis of sediment concentration at the Changri station, which is the Hapcheon Dam site. Sediment transport was calculated using rainfall and sediment relationships.

Figure 4-10 shows a location map of the sediment transport sampling site at Changri, Hapcheon Dam site, in the Hwang River. Also, Table 4-4 shows sediment transport related to particular storm conditions observed at the Changri sampling site (the Hapcheon Dam site) in the Hwang River (FAO/UNDP and KOWACO, 1971). In 1969, the total precipitation was 896 mm during 5 months (Apr. 25 ~ Sept. 24) and the calculated total sediment transport was 1,595.6 ton/km^2. In 1970, however, the total precipitation was 439 mm and the calculated total sediment transport was 516.0 ton/km^2 during a month (Jul. 5 ~ Aug. 7), as shown in Table 4-5.

Table 4-4. Sediment transport related to particular storm conditions observed at the Changri sampling site (the Hapcheon Dam site) in the Hwang River (FAO/UNDP and KOWACO, 1971)

Year	Date	Maximum intensity of precipitation (mm/hr)	Total precipitation (average) (mm)	Total sediment Transport (ton/km^2)	Total sediment Transport Ton
1969	25-Apr	-	(58)	56.2	52,000
	5-May	-	(48)	8.7	8,000
	8-Jul	85/18 = 4.7	90	102.2	94,500
	13-Jul	35/6 = 5.8	43	4.1	3,800
	20-Jul	77/12 = 6.4	74	38.5	35,600
	31-Jul	133/6 = 22.2	116	268.0	248,000
	3-Aug	37/9 = 4.1	45	141.8	131,000
	5-Aug	66/6 = 11.0	67	158.0	146,000
	7-Aug	97/15 = 6.4	107	395.0	367,000
	15-Sep	131/24 = 5.5	138	149.1	138,000
	24-Sep	-	(110)	274.0	254,000
	Total		**896**	**1,596.6**	**1,477,900**
1970	5-Jul	-	127	169.3	156,600
	14-Jul	-	67	11.7	10,800
	16-Jul	-	99	226.5	209,520
	17-Jul	-	54	74.7	69,120
	18-Jul	-	20	16.3	15,120
	7-Aug	-	72	17.5	16,200
	Total		**439**	**516.0**	**477,360**

Table 4-5. Sediment transport measured at the Changri sampling site (the Hapcheon Dam site) in the Hwang River during 1969 – 1970 and interpolated to a year with average precipitation. (FAO/UNDP and KOWACO, 1971)

Year	Total Sediment Transport Annually (ton/km^2)	Total Sediment Transport Annually (10^6 ton)	Total Sediment Transport Annually Total (mm)	Annual Precipitation of Storms which Produced Sediment Transport (mm)	Annual Precipitation of Storms which Produced Sediment Transport (% of total)
1969	1,596	1.478	1,661	896	54
1970	516	0.477	1,373	439	32
average expected	1,056		1,517	668	44
l.p. average	798	0.739	1,150	(516)	

Abbreviations: l.p. average = long period average
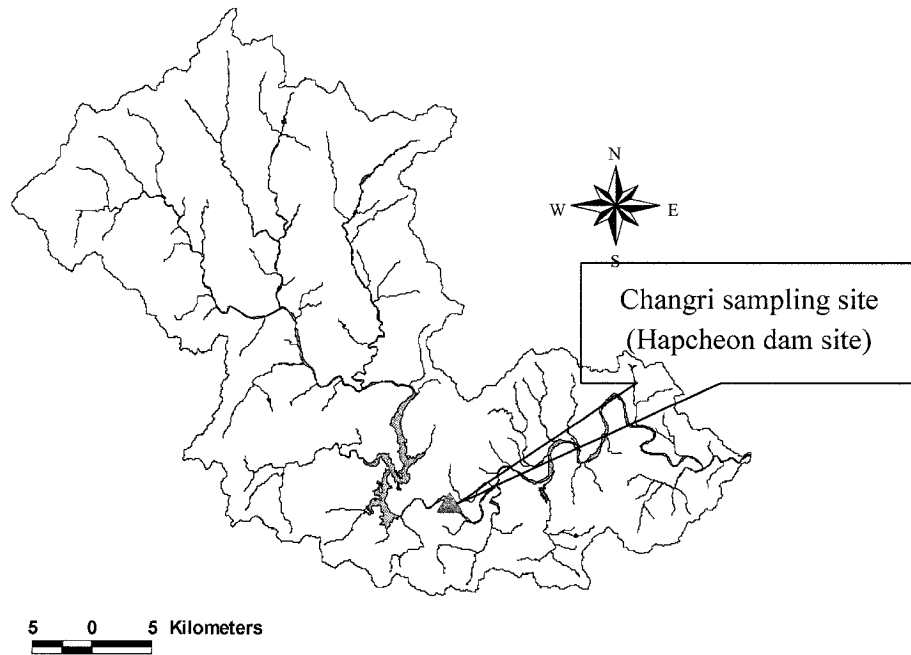
Figure 4-10. Location map of sediment transport sampling site at the Changri (the Hapcheon Dam site) in 1969 and 1970

Figure 4-11 shows a relationship of precipitation and total sediment transport at the Hapcheon Dam site (previously the Changri gaging station). It is analyzed by using precipitation and sediment transport data of 1969 and 1970, as shown in Table 4-5. It shows a quite good relationship of total precipitation and total sediment transport at Hapcheon Dam site. However, the relationship of precipitation intensity and total sediment transport does not show a good relationship because there are only eight data sets, so it is not enough to get a good relationship (see Figure 4-12). After the KOWACO/FAO/UNDP study, MOCT (1993) estimated the total sediment transport rate and made a relationship of discharge-sedimentation at the confluence with the Nakdong River by comparing four empirical equations. The Engelund & Hansen (1972), Shen & Hung (1972), Ackers & White (1973) and Van Rijn (1984) empirical equations were used because there are no measured data in this river basin, as shown in Table 4-6. The Engelund & Hansen (1972) method was selected to compute the total sediment transport rate of this river basin. According to this method, the rate of sediment load was 777 m^3/year/km^2 and the total sediment load was 289,320 m^3/year (obtained by multiplying

the sediment load and river basin area, 372.34 km^2). Table 4-7 shows total sediment load in the Hwang River versus the water discharge and duration at the confluence with the Nakdong River in 1993.
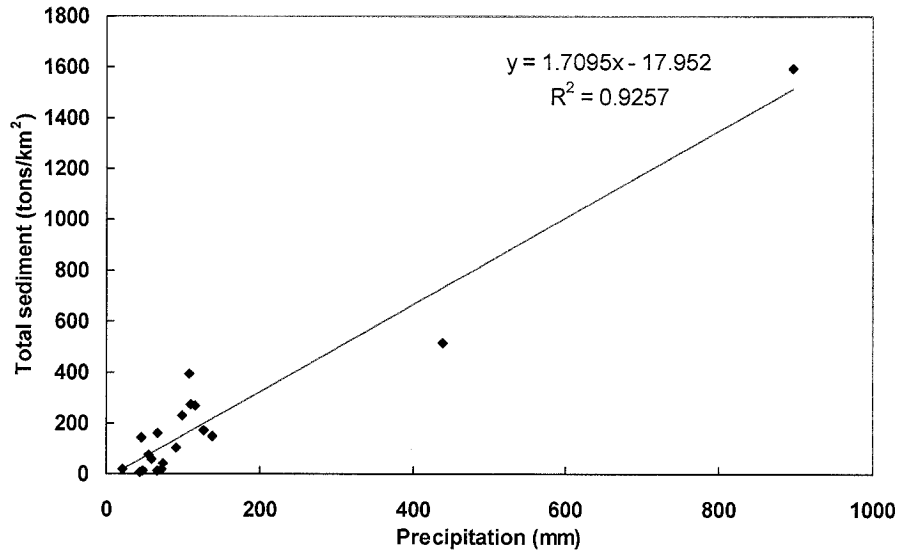
Figure 4-11. Relationship of precipitation and total sediment transport at the Hapcheon Dam site (the Changri gaging station)
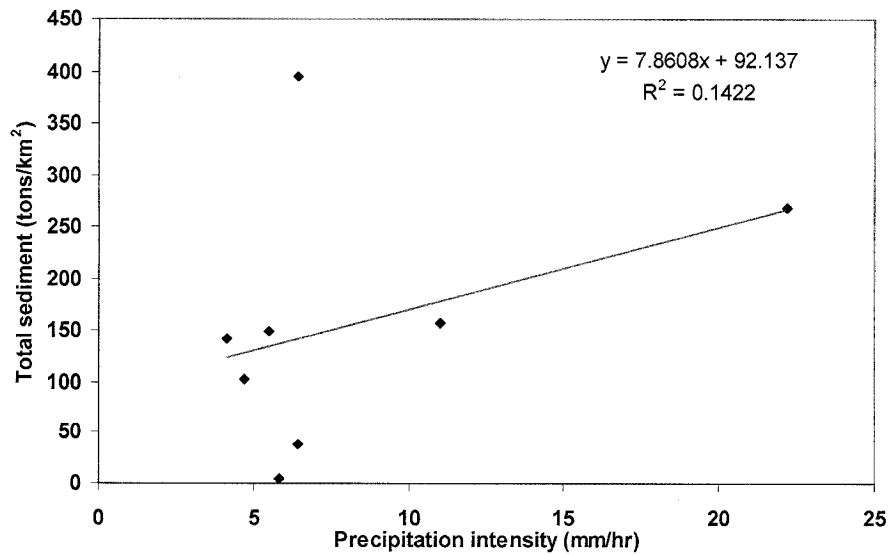
Figure 4-12. Relationship of precipitation intensity and total sediment transport at the Hapcheon Dam site (the Changri gaging station)

Table 4-6. Rate of sediment load for each method (MOCT, 1993)

Method	Engelund & Hansen	Shen & Hung	Ackers & White	Van Rijn
Rate of sediment load (m^3/year/km^2)	777	669	693	1,309

Table 4-7. Annual sediment load according to the discharge (MOCT, 1993)

Discharge (m^3/sec)	Duration (day)	Sediment load (ton/day)	Total sediment load (ton)
20.5	90	465	41,850
23.5	79	586	46,294
30.0	102	884	90,168
42.5	38	1,580	60,040
75.0	56	4,010	224,560
Total	365		462,912

KOWACO in 2002 surveyed sediment deposition of the Hapcheon Main Dam reservoir for the first time since the Hapcheon Main Dam completion in 1989. According to the survey, the amount of reservoir sediment deposition in the Hapcheon Main Dam for 14 years from July 1988 to July 2002 was 8,279,000 m^3. From this, the sediment loading rate was estimated as 639 m^3/km^2/year (1,022 ton/km^2/year by applying unit volume of sediment weight is 1,600 kg/m^3). MOCT (2003) also estimated total sediment load by applying and comparing nine empirical sediment transport equations including Engelund & Hansen, Ackers & White and Yang's method. From the result, MOCT finally selected Yang's method for this river basin because it was thought that the bed material of the Hwang River is composed of sand. The estimated total sediment load was 324 m^3/km^2/year (520 ton/ km^2/year). From Table 4-9, the estimated total sediment load declined from 1,477,900 ton/year in 1969 to 120,638 ton/year in 2003 due to the reduction of river basin area and interception of sediment transport by the Hapcheon Dam construction.

The sediment transport rate is estimated by comparing the rate of sediment load estimated from the survey results of reservoir sediment deposition of the Hapcheon Main Dam in 2002 and five different sediment transport equations (Table 4-10). Yang's (1973) method shows the most similar rate of sediment load compared with the 2002 survey result. The estimated total sediment load was 738 m^3/km^2/year, as shown in Table 4-10.

Table 4-8. Sediment load in the Hwang River Basin from 1969 to 2003

Year	Point	Basin Area (km^2)	Rate of Sediment Load $(ton/km^2/year)$	Total sediment Load (thousand ton/year)	Method
1969	Hapcheon dam site	925	1,597	**1,478**	**Measured** suspended load+ Assumed bed material load (10% of suspended load)
1970	"	925	516	**477**	"
2002	"	925	1,022	**946**	**Survey of the reservoir**
1993	Confluence With Nakdong River	372	1,244	**463**	**Empirical method** for total sediment load estimation (Engelund & Hansen method)
2003	"	372	520	**194**	**Empirical method** for total sediment load estimation (Yang's method)

Table 4-9. Estimated total sediment load by applying basin area from the result of the survey of reservoir sediment deposition of the Hapcheon Main Dam in 2002

Reach	Basin area (km^2)	Rate of sediment load $(m^3/km^2/year)$ / $(tons/km^2/year)$	Total sediment load (thousand m^3/year) / (thousand tons/year)
2002 survey	925	639 / 1,022	591 / 946
Sub-reach1	108.5	639 / 1,022	69 / 111
Sub-reach2	159.4	639 / 1,022	102 / 163
Sub-reach3	104.5	639 / 1,022	67 / 107
Entire	372.4	639 / 1,022	238 / 381

- Rate of sediment load = 639 m^3/km^2/year = 1,022 tons/ km^2/year

- Assume, Unit volume of sediment weight = 1,600 kg/m^3

Table 4-10. Estimated total sediment load by using empirical sediment transport equations at confluence with the Nakdong river (thousand tons/year)

	2002 survey	Engelund and Hansen (1972)	Ackers and White (1973)	Yang (1973)	Yang (1979)	Van Rijn (1984)
10^3 tons/year	381	673	1,194	440	541	1,268
Tons/km^2/year	1,022	1,806	3,207	1,181	1,452	3,405
M^3/km^2/year	639	1,129	2,004	738	908	2,128

- 2002 survey : estimated from survey result of reservoir sediment deposition of the Hapcheon Dam

Yang's equation generally does well at estimating sediment transport rate for a sand bed alluvial river channel. Figure 4-13 shows the sediment-discharge rating curve of the Hwang River at the confluence with the Nakdong River estimated using Yang's (1973) empirical sediment transport equation. From regression, the sediment-discharge rating curve is $Q_s = 9.77Q^{1.49}$. Table 4-11 shows the estimated total sediment load (tons/year) computed using the empirical sediment transport equation of Yang (1973) corresponding to each amount of water discharge at the confluence with the Nakdong River. The estimated sediment load (tons/year) was approximately 440 thousand tons/year (Table 4-11).
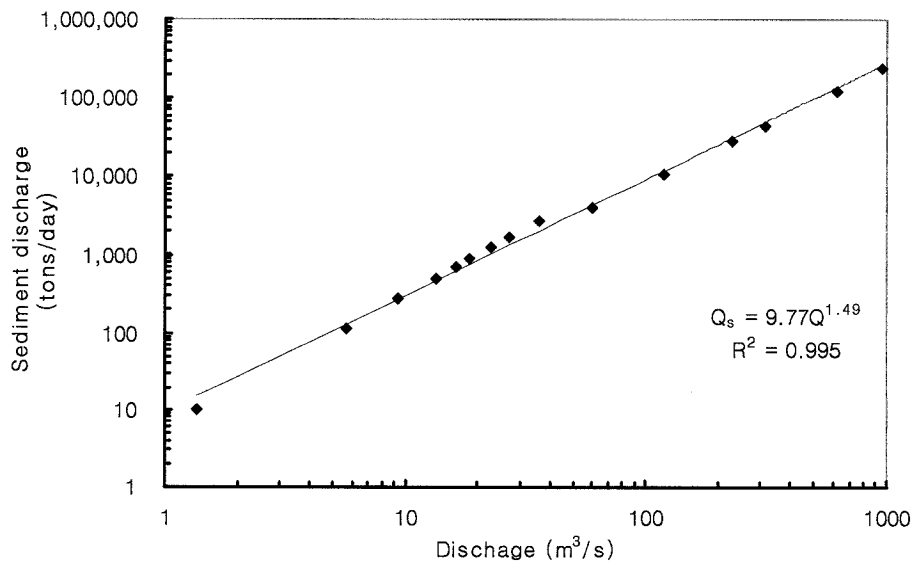
Figure 4-13. Sediment – discharge rating curve at the confluence with the Nakdong River by Yang's (1973) method

Table 4-11. Estimated total sediment load by using Yang's (1973) empirical sediment transport equation at confluence with the Nakdong River after dam construction

Time interval (%)	Interval midpoint (%)	Interval, Δp (%)	Discharge, Q (m^3/s)	Sediment, Qs (tons/day)	days	Sediment load (tons/year)
(1)	(2)	(3)	(4)	(5)	(6)	(7)
0.00-0.02	0.01	0.02	462.3	89,492	0.07	6,533
0.02-0.1	0.06	0.08	316.9	51,051	0.29	14,907
0.1-0.5	0.3	0.4	120.1	12,061	1.46	17,609
0.5-1.5	1	1	109.4	10,500	3.65	38,325
1.5-5.0	3.25	3.5	72.1	5,650	12.78	72,176
5-15	10	10	44.9	2,794	36.5	101,983
15-25	20	10	29.2	1,474	36.5	53,792
25-35	30	10	22.8	1,020	36.5	37,237
35-45	40	10	19.7	821	36.5	29,965
45-55	50	10	16.2	614	36.5	22,404
55-65	60	10	14.4	515	36.5	18,805
65-75	70	10	11.8	383	36.5	13,986
75-85	80	10	8.2	223	36.5	8,141
85-95	90	10	5.0	107	36.5	3,902
95-98.5	96.25	3.5	1.0	10	12.78	125
Total						439,900

4.3. Bed Material

The first measurement of bed material size in this study reach was conducted by MOCT in 1983 as part of the river channel management and maintenance plan. After 1983, MOCT conducted periodic bed material size surveys every 10 years in 1993 and 2003. Figure 4-14 shows the variation of bed material size along the study reach from the Hapcheon Re-regulation Dam to the confluence with the Nakdong River. The bed material size is finer than before dam completion (1983) in the vicinity of confluence with the Nakdong River (0~5 km reach) in 2003. However, it is coarser than before dam completion at just below the Hapcheon Re-regulation Dam (5 km downstream reach from the re-regulation dam).
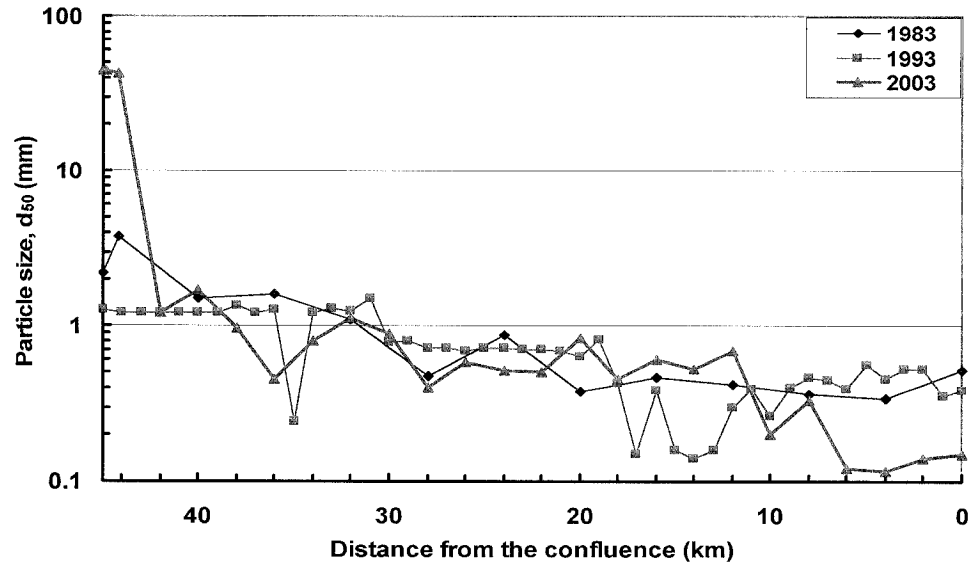
Figure 4-14. Variation of bed material size (median, d_{50}) along the study reach from the Hapcheon Re-regulation Dam to the confluence with the Nakdong River

The average median particle size increased from 1.07 mm in 1983 to 5.72 mm in 2003. Table 4-12 shows the median particle sizes along with measured years of 1983, 1993, and 2003 (MOCT, 1983, 1993, 2003). Sub-reach 1 was the coarsest reach following the dam construction in 2003 due to armoring immediately downstream of the re-regulation dam. Sub-reach 3 was the finest reach among the three sub-reaches in 2003. Table 4-13 shows median particle size in the vicinity of just below the Hapcheon Re-regulation Dam at 45, 44.15 and 40 km from the confluence with the Nakdong River. The median particle size was coarsening to over 42 mm at 44.15 and 45 km from the confluence (immediately downstream of the re-regulation dam). This indicates that the channel bed material changed from sand to gravel and the bed changed to an armored condition.

Table 4-12. Average and median particle sizes, d_{50}, in millimeter along with measured years of 1983, 1993, 2003 for the study reach

Reach	1983	1993	2003
Sub-reach 1	2.24	1.15	16.89
Sub-reach 2	0.65	0.73	0.65
Sub-reach 3	0.41	0.38	0.28
Entire	1.07	0.72	5.73

61

Table 4-13. Median particle size in the vicinity of just below the Hapcheon Re-regulation Dam at 40, 44.15 and 45 km from the confluence with the Nakdong River

Distance from the confluence (km)	Year	d_{50} (mm)
40.00	1983	1.50
	1993	1.22
	2003	1.70
44.15	1983	3.71
	1993	1.21
	2003	42.00
45.00	1983	2.16
	1993	1.27
	2003	44.00

Figure 4.15 shows particle size distribution along the study reach in 1983, 1993, and 2003. Generally, the bed material of the study reach is composed of sand of size 0.125~2.0 mm. There are no major differences in bed material size along the study reach between 1983 and 1993. However, it is coarser than before dam completion at just below the Hapcheon Re-regulation Dam at 45, 44.15 and 40 km from the confluence in 2003 and finer than before dam completion in the vicinity of the confluence.

4.4. Bed Slope and Bed Elevation

The vertical response of the study reach was measured by changes in bed slope and bed elevation. Figure 4-16 and Table 4-14 show variation of bed slope of each sub-reach for pre and post dam conditions (1983, 1993, and 2003). The bed slope of the whole reach decreased after dam completion from 0.000943 in 1983 to 0.000847 in 2003. An average degradation of bed elevation is 2.6 m along the 45~30 km (0~15 km from the re-regulation dam) reach from the confluence with the Nakdong River and an average of 1.0 m along the entire reach after dam completion.
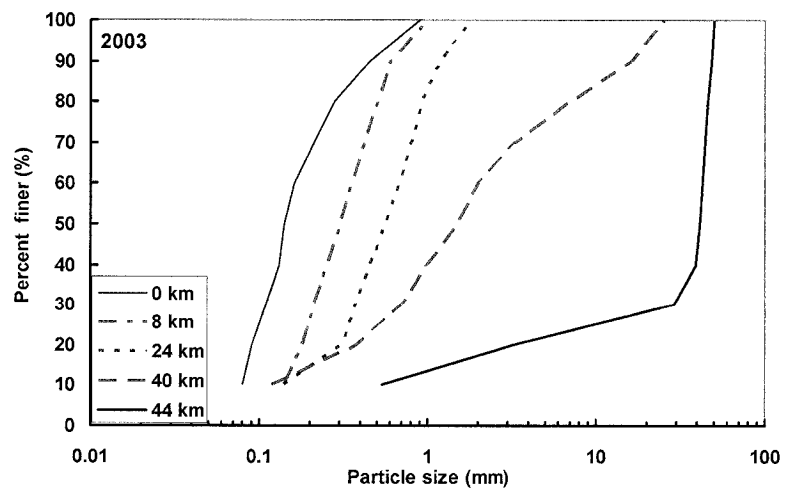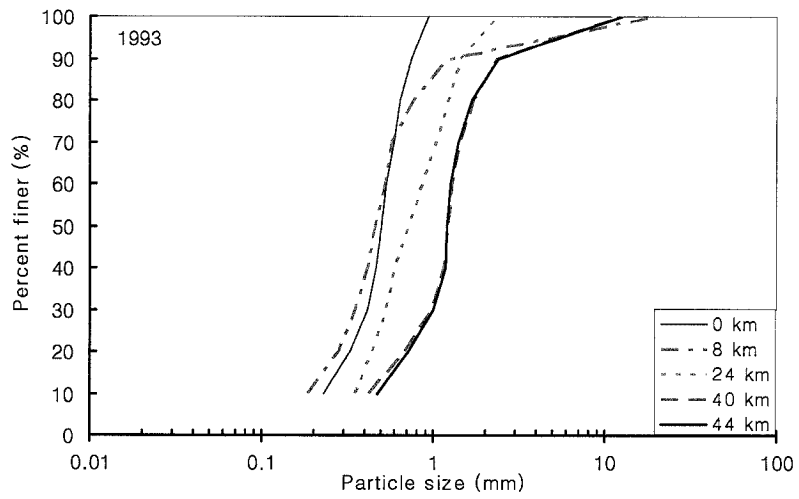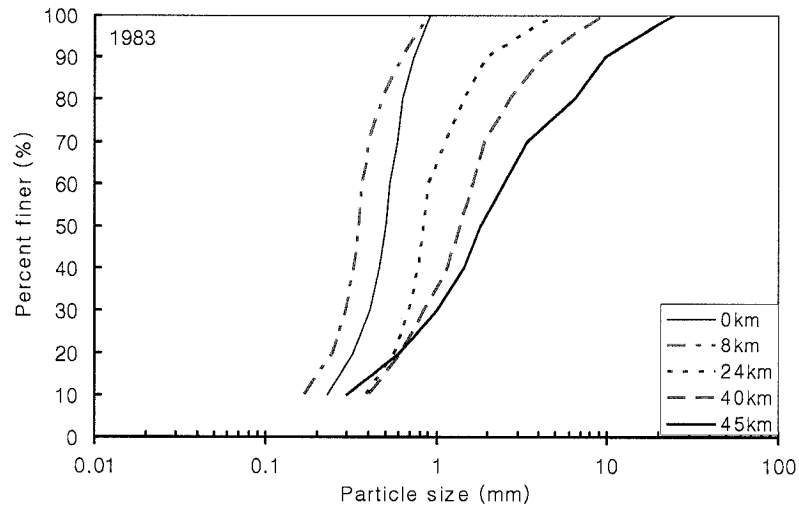
Figure 4-15. Particle size distributions along the study reach in 1983, 1993, and 2003

Table 4-14. Variation of average bed slopes along the study reach

Reach	Bed slope		
	1983 (pre-dam)	1993 (post-dam)	2003 (post-dam)
Sub-reach 1	0.001434	0.001713	0.001445
Sub-reach 2	0.000989	0.000967	0.000850
Sub-reach 3	0.001638	0.001288	0.001581
Entire	0.000943	0.000898	0.000847
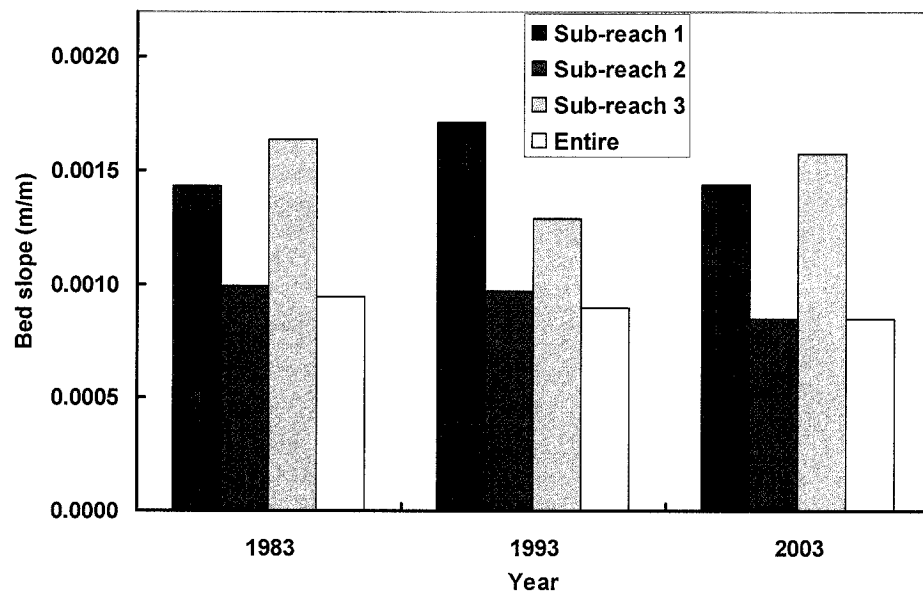
Figure 4-16. Variation of average bed slopes in 1983, 1993 and 2003

Figure 4-17 shows the variation of the longitudinal profile from the Hapcheon Re-regulation Dam to the confluence with the Nakdong River. The bed elevation (thalweg elevation) aggraded at and near the confluence with the Nakdong River, from 0 km to 5 km but degraded in the upper region, from 20 km to 45 km. The central region from 5 km to 20 km remained generally unchanged. The bed aggradation in the reach 0 km to 5 km caused a decrease in flow velocity and increase in vegetation growth on sand bars.
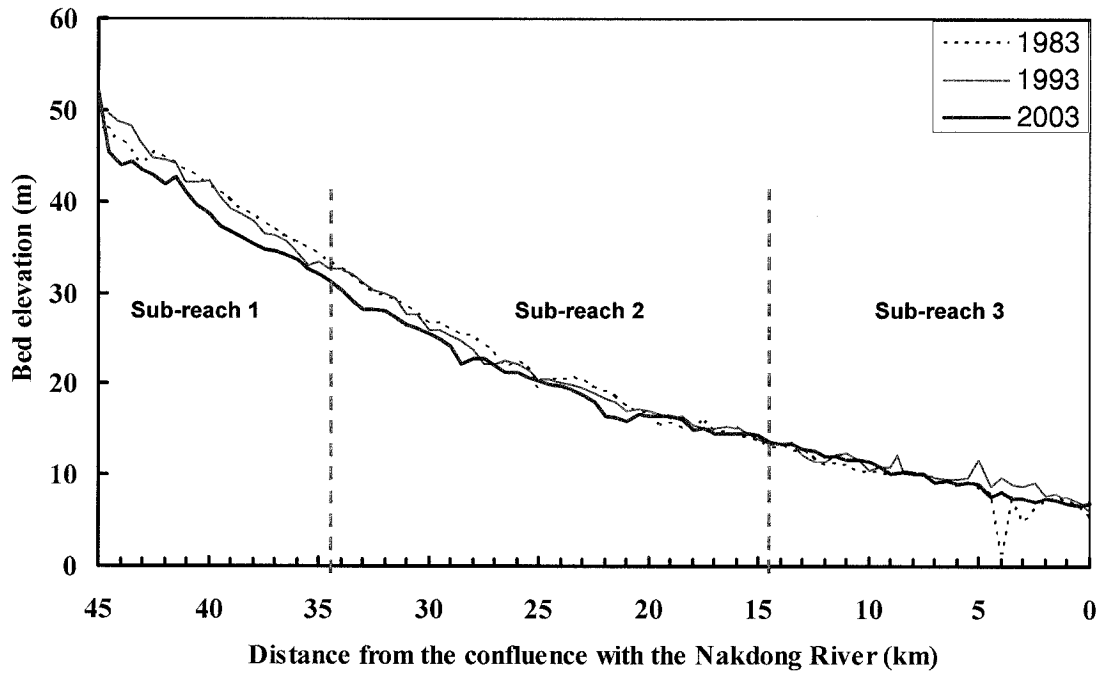
Figure 4-17. Variation of longitudinal profiles downstream of the Hapcheon Re-regulation Dam (45 km) to the confluence with the Nakdong River (0 km) in 1983, 1993, and 2003

4.5. Lateral Response

Change in channel width, cross-section and channel pattern such as sinuosity and planform are described in the following sections.

Channel width

Figures 4-18 (a) and (b) show the variation of bottom width and top width of study reach in 1983, 1993, and 2003, respectively. The bottom widths are estimated by plotting the measured water depths observed at low flow. The bottom widths increased along the reach from the confluence with the Nakdong River to 5 km in the upstream direction following the dam completion. It is estimated that the reason is related to developing and fixing sand bars in the river channel due to the flow regime change after dam completion. The bottom width maintained stability at the reach between 5 and 15 km from the confluence with the Nakdong River. It also increased at the reach between 15 and 30 km and decreased noticeably at the reach between 30 and 45 km. Figure 4-18(c) shows variation of the rate of bottom width and top width along the channel. The average of these rates varied by 0.35 in 1983, 0.54 in 1993 and 0.49 in 2003.
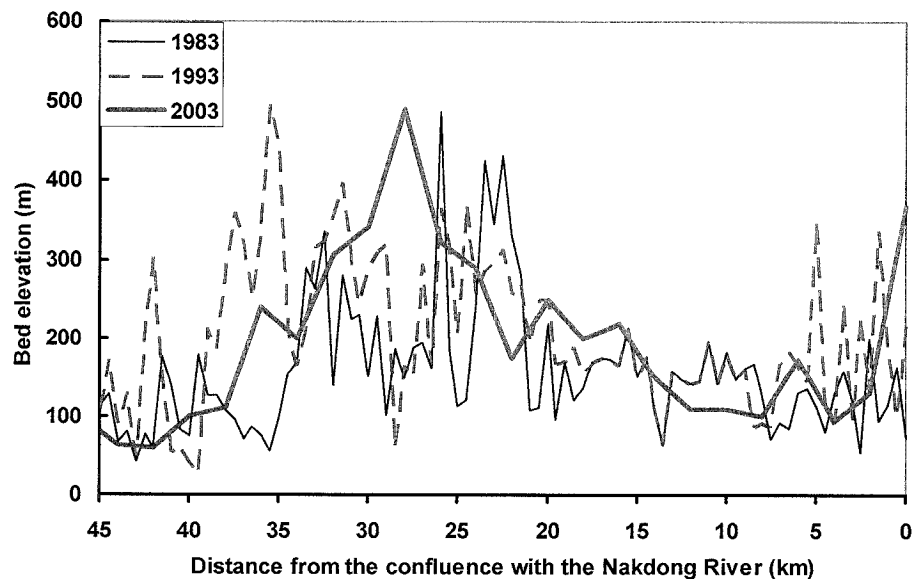
(a) bottom width
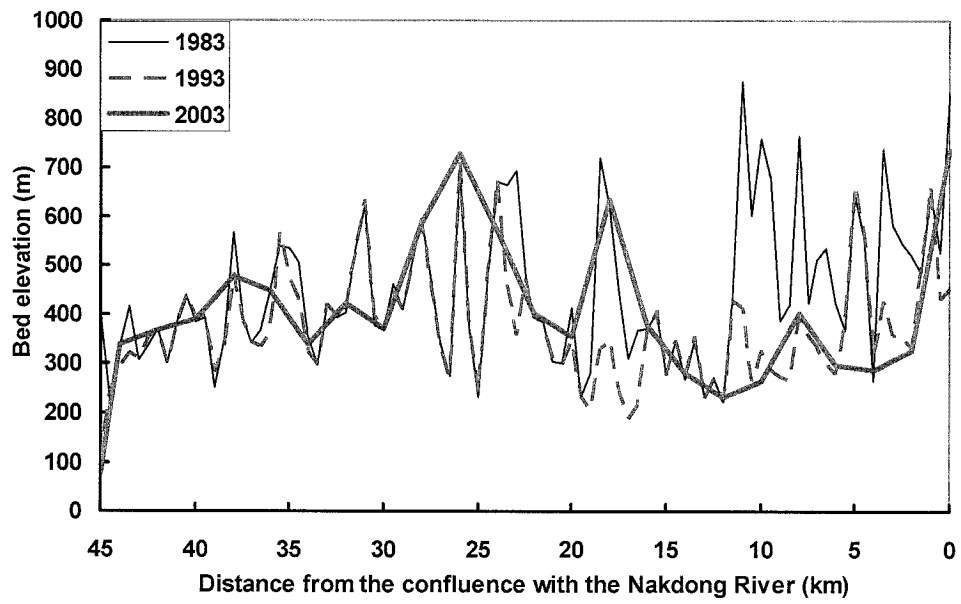
(b) top width
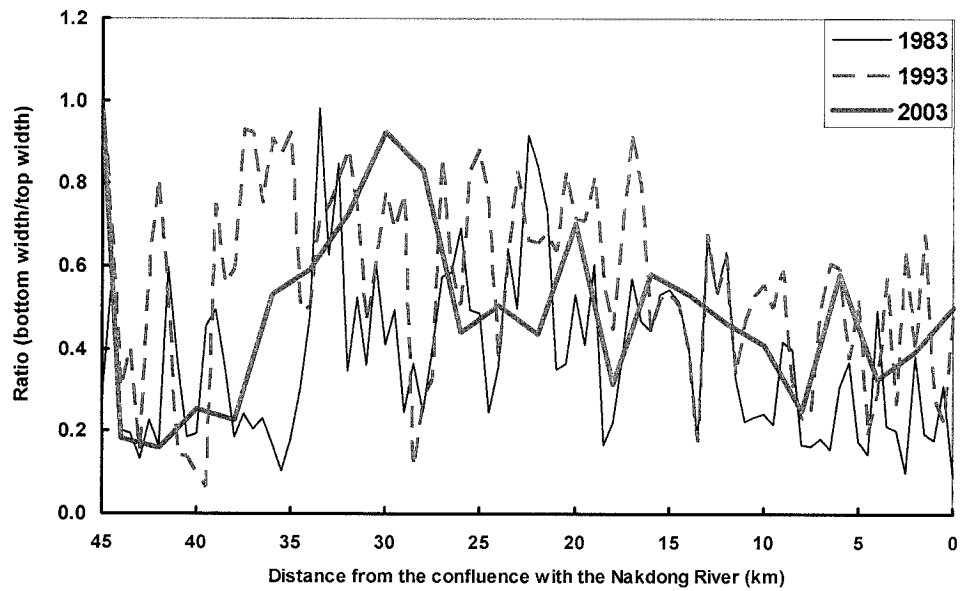
(c) the ratio of bottom width to top width

Figure 4-18. Variation of bottom width (a), top width (b) and the ratio of bottom width to top width (c) along the channel from the confluence with the Nakdong River (0 km) to the Hapcheon Re-regulation Dam (45 km) for 1983, 1993, and 2003

Also, Figure 4-19 and Table 4-15 show the variation of non-vegetated active channel width from the re-regulation dam (45 km) to the confluence with the Nakdong River (0 km) for 1982, 1993, and 2004. These non-vegetated active channel widths measured by aerial photos taken in 1982, 1993 and 2004 were digitized by using ArcView software. From this Figure, the active channel width decreased after dam completion along the whole channel reaches from 321 m in 1982 to 172 m in 2004. The average active channel width of 2004 is just 54% of 1983.
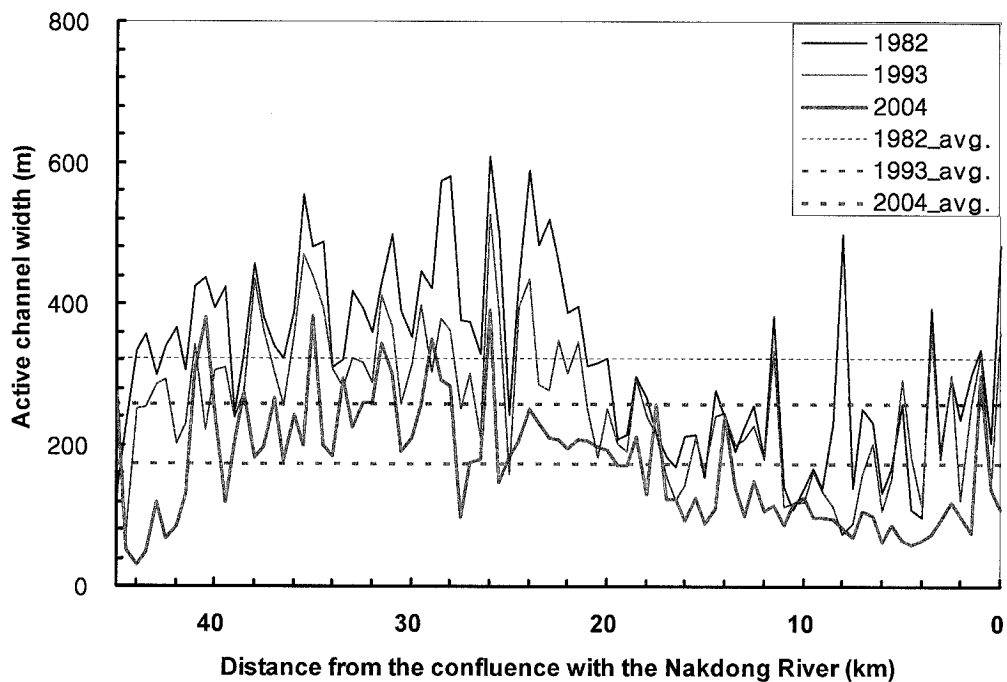
Figure 4-19. Variation of non-vegetated active channel widths from the Hapcheon Re-regulation Dam (45 km) to the confluence with the Nakdong River (0 km) in 1982, 1993, and 2004 measured by digitized aerial photos

Table 4-15. Measured non-vegetated active channel width by digitized aerial photos taken in 1982, 1993 and 2004 (m)

Reach	1982	1993	2004
Sub-reach 1	364.1	297.9 (82 %)	190.1 (52 %)
Sub-reach 2	365.5	285.7 (78 %)	210.8 (58 %)
Sub-reach 3	232.7	193.3 (83 %)	109.3 (47 %)
Entire	321.4	258.2 (80 %)	172.3 (54 %)

* ( ) = % of 1982

The change rates (meters per year) of non-vegetated active channel width are presented in Figure 4-20 along the study reach for each cross-section during the 1993~1982, 2004~1982 and 2004~1993 periods. The average change rate for the entire reach during the period of 2004~1993 was about 1.4 times bigger than the period of 1993~1982.
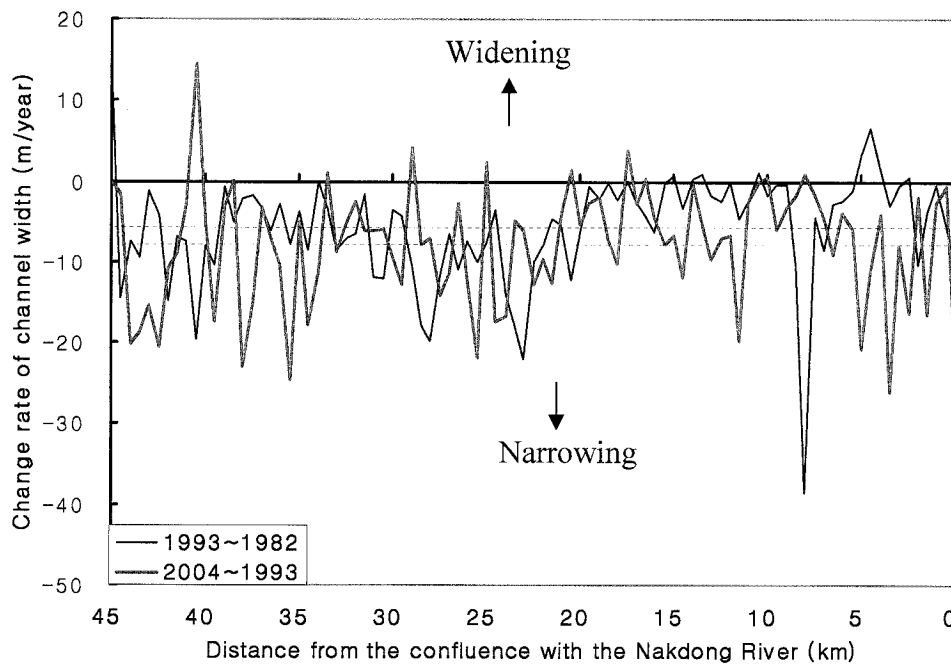
Figure 4-20. Change rate of the non-vegetated active channel width along the study reach during the periods of from 1982 to 1993 and from 1993 to 2004

Channel width/depth ratio

To analyze the width/depth ratio, the bankfull discharges of the pre and post-dam periods were applied for non-uniform flow simulation along the study reach. Applied bankfull discharges (1.58 yr discharge frequency) were 509.8 and 86.3 m^3/s at the Hapcheon Re-regulation Dam for the pre-dam period and post-dam period respectively. Table 4-16 shows width/depth ratios for the each sub-reach and the entire reach in 1983 and 2003. Generally, the width/depth ratios decreased after dam construction, except sub-reach 3. The entire reach decreased from 278.78 in 1983 to 258.13 in 2003.

Table 4-16. Width/depth ratio for the each sub-reach in 1983 and 2003

Reach	Width/depth ratio	
	1983	2003
Sub-reach 1	370.47	248.77
Sub-reach 2	353.46	328.87
Sub-reach 3	113.75	170.36
Entire	278.78	258.13

Sinuosity

The sinuosity for each sub-reach is computed from the digitized aerial photos for the years 1982, 1993 and 2004. The sinuosity was calculated by dividing the thalweg length by the valley length. Figure 4-21 and Table 4-17 show the variation of sinuosity for each reach. The sinuosity of all reaches generally decreased slightly after the dam completion. Sub-reach 2, from the Namjung Bridge (the Hapcheon Water Level Gaging Station) to the Sayang Stream, was the most sinuous. The sinuosity of sub-reach 2 decreased after construction of the Hapcheon Main Dam and re-regulation Dam in 1989. The sinuosity of sub-reach 3 was not changed after the dam completion. Also, we can find that the sinuosity of the entire study reach is over 1.7 from 1982 to 2004.

Table 4-17. Variation of sinuosity of each reach

Year	Reach	Average thalweg length (km)	Valley length (km)	Sinuosity
2004	Sub-reach 1	11.2	7.3	1.53
	Sub-reach 2	19.1	9.5	2.01
	Sub-reach 3	14.8	9.7	1.53
	Entire	45.1	24.9	1.81
1993	Sub-reach 1	11.4	7.3	1.56
	Sub-reach 2	18.9	9.5	1.99
	Sub-reach 3	14.7	9.7	1.52
	Entire	45.0	24.9	1.81
1982	Sub-reach 1	11.8	7.3	1.62
	Sub-reach 2	19.7	9.5	2.07
	Sub-reach 3	15.1	9.7	1.56
	Entire	46.6	24.9	1.87
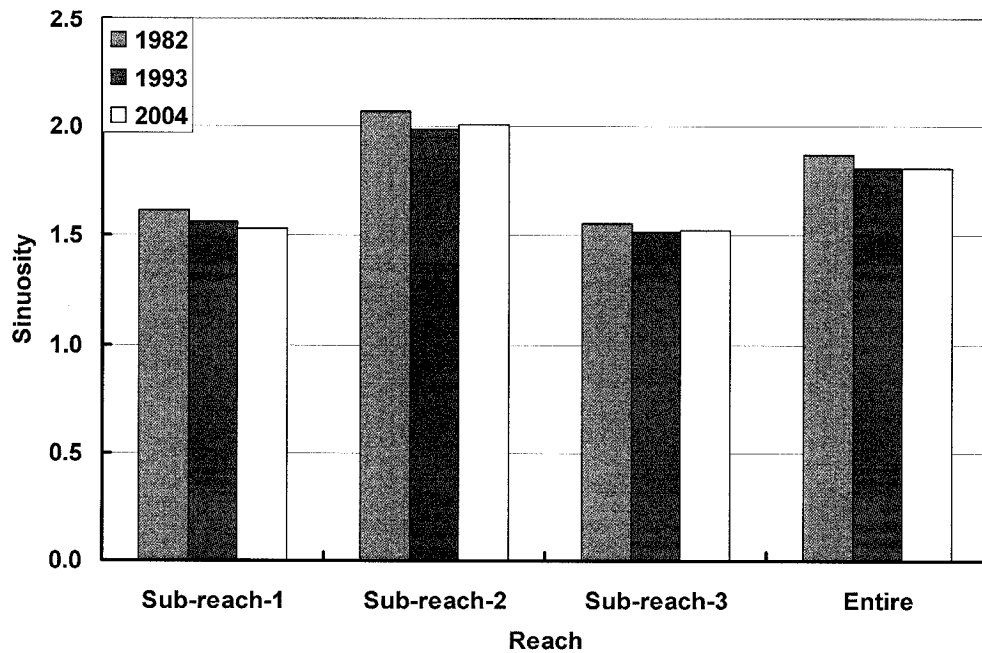
Figure 4-21. Variation of sinuosity of each reach

Channel planform

Figure 4-22 shows planform maps of the non-vegetated active channel of the study reach by digitizing aerial photos taken in 1982, 1993 and 2004. These planform maps were created by using GIS software (ArcView 3.2) as part of this research. Qualitative observations of the planform maps as shown in Figure 4-22 show that the planforms are not much changed through the pre and post-dam period. Most of the rivers in Korea flow through the mountains and artificial channel banks are constructed on both sides and maintained periodically, so these conditions prevent natural change of the channel planform. Only the non-vegetated active channel width was changed with the time due to dam construction by reduced flood peak. The magnified and superimposed channel planform maps are shown in Figure 4-23 for each sub-reach. These channel planforms show clearly that the non-vegetated active channel width decreased after dam construction.
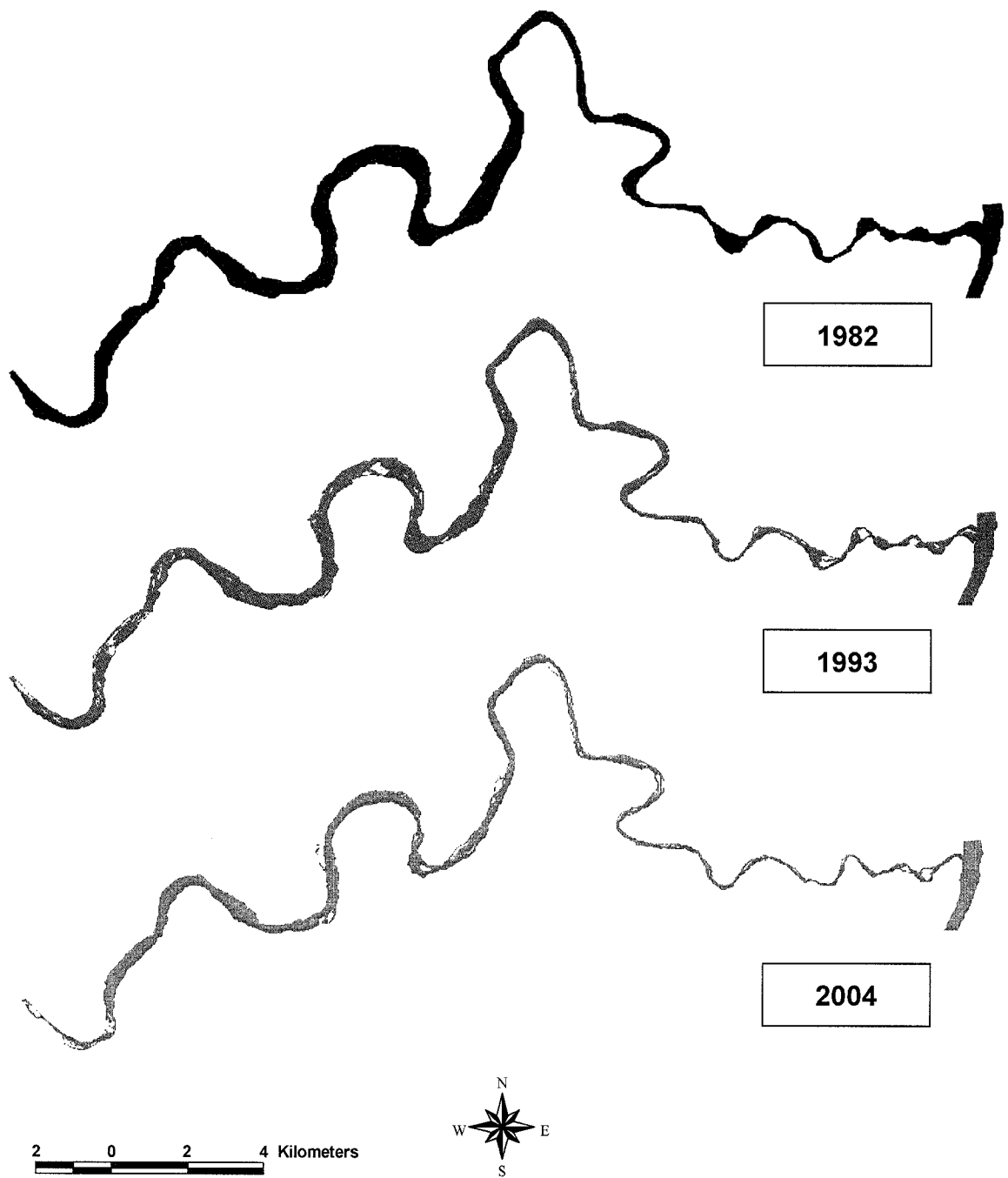
Figure 4-22. Channel planform maps of the non-vegetated active channel of the study reach from aerial photos taken in 1982, 1993 and 2004

72
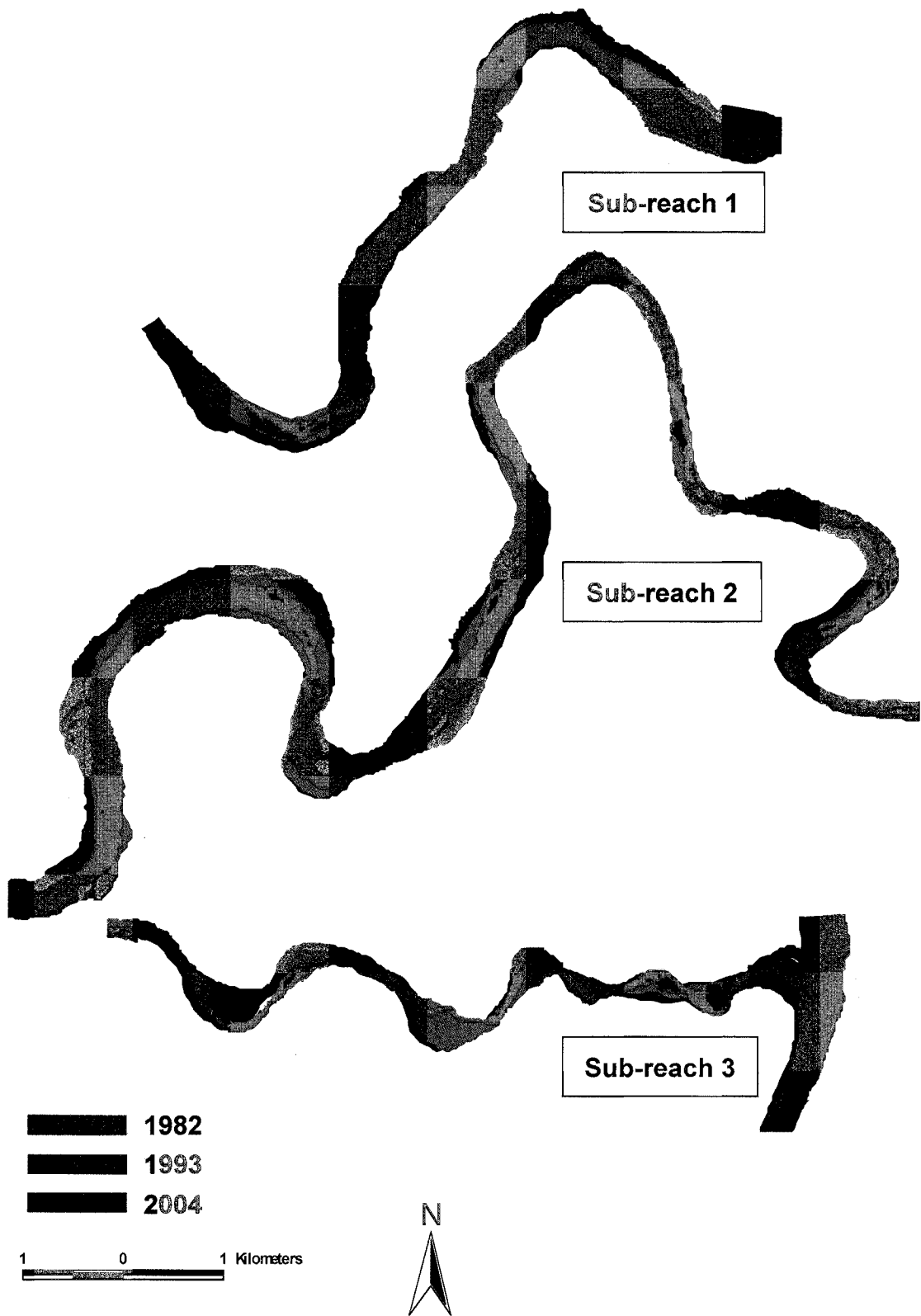
Figure 4-23. Change of non-vegetated active channel for sub-reach 1, 2 and 3 by digitizing aerial photographs taken in 1982, 1993 and 2004

4.6. Field Investigation

A field investigation was completed in January 2007 with simple traditional tools (compass, folding rule, soil auger, shovel) in conjunction with aerial photos stored and displayed in the field on a laptop computer. Field sites were reached on foot from bridges, alternate bars, and other access points. The discharge from the re-regulation dam was 15 m^3/s (from the hydropower station of the re-regulation dam) during the field investigation. The result of the field investigation will show comparisons of the cross-sections measured in 1983 and 2003 with photos taken during field investigation, and aerial photos taken in 1982 and 2004 in order from the Hapcheon Re-regulation Dam to the confluence with the Nakdong River.

Cross-section

This study will focus on the change of the channel bed, shape of the channel and vegetation growth on sand bars. Because the channel bank is artificially constructed and periodically maintained, there is no more natural channel bank changes such as bank erosion in this study reach. Table 4-18 presents a summary of the field evidence of channel changes at the cross-sections from the Hapcheon Re-regulation Dam to the confluence with the Nakdong River. These channel changes on channel width, bed elevation, and bed material size were quantified in the previous section. Predictably, the reach immediately downstream of the re-regulation dam shows the greatest post-dam change. These are fully due to the engineering modifications of the dam and to reservoir construction itself, which locally rerouted the main channel downstream of the re-regulation dam (Figure 4-24~26). Figure 4-24 shows the plots of cross-sections measured in 1983 and 2003 at 44.65 km from the confluence with the Nakdong River (0.35 km downstream from the Hapcheon Re-regulation Dam). The thalweg elevation decreased from 48.06 m to 45.30 m (degraded 2.76 m). The main channel was rerouted and divided into two sub channels after dam construction due to channel scour.

74

Table 4-18. Summary of field evidence of channel response at the cross-sections from the Hapcheon Re-regulation Dam to the confluence with the Nakdong River

Location of cross-section from the confluence	Geomorphic response	Field evidence or indicators
44.65 km (immediately downstream of the re-regulation dam)	- Channel scour	- Thalweg elevation decreased 2.76m (48.06 → 45.3 m)
	- Channel rerouted and divided	- Channel divided into two sub channels
	- Channel narrowing	- 22.4 % of 1982 channel width (227.3 → 50.9 m)
	- Island formation with vegetation growth	- Island formed after the channel rerouted and divided
	- Bed armoring	- Bed material size increased (3.7 → 44mm)
40 km (1 km downstream of the Yongju bridge)	- Channel scour	- Thalweg elevation decreased 3.53m (42.03 → 38.5 m)
	- Channel rerouted and divided	- Channel divided into two sub channels
	- Channel narrowing	- 63.4 % of 1982 channel width (393.4 → 249.5 m)
	- Island formation with vegetation growth	- Island formed after the channel rerouted and divided
	- Bed armoring	- Gravel bed material shown in Figure 4-28 (a) d_{50} was 1.2mm in 2003 survey but it already coarser than before (sand → gravel)
35 km (vicinity of the Hapcheon city)	- Channel scour	- Thalweg elevation decreased 2.24m (34.34 → 32.1 m)
	- Reclaimed playground on left flood plain	- Reclaimed playground at left side sand channel bed as shown in Figure 4-31 and 4-32. (about 120 m wide)
	- Channel narrowing	- 79.8% of 1982 channel width (479.6 → 382.7m)
	- Stable channel	- No island formation and vegetation growth and little change in bed material size (same as sand)
25 km (immediately downstream of the Youngjeon bridge)	- Channel scour	- Thalweg elevation was little change but maximum scour depth is 2.51m (23.25 → 20.74m)
	- Reclaimed playground on right flood plain	- Reclaimed playground at right side sand channel bed as shown in Figure 4-34 and 4-35. (about 50 m wide)
	- Channel narrowing	- 75.8 % of 1982 channel width (241.2 → 182.9 m)
	- Stable channel	- No island formation and vegetation growth and little change in bed material size (same as sand)
1.5 km (just upstream of the Cheongduk bridge)	- Channel scour	- Thalweg elevation was little change but maximum scour depth is 3.21 m (10.81 → 7.6 m)
	- Channel rerouted and divided	- Channel divided into several sub channels (braided) as shown in Figure 4-44
	- Channel narrowing	- 25.0 % of 1982 channel width (299.4 → 74.9 m)
	- Island formation with vegetation growth	- Several islands with perennial vegetation (willow, age 5~10 years)

In Figure 4-24, we can find that the level of left bank was changed in 2003 because it was reconstructed and maintained to prevent flood damage. Figure 4-25 shows a photo taken at the top of re-regulation dam and another taken at approximately 1 km downstream from the re-regulation dam during the field investigation in 2007. These two photos show vegetation expansion on the middle island between two sub channels.
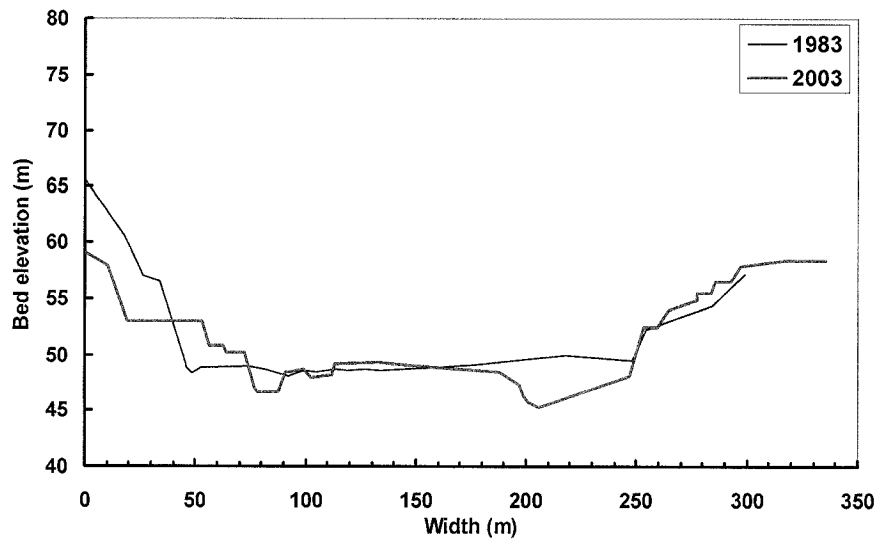
Figure 4-24. Comparison of cross-sections measured in 1983 and 2003 at 44.65 km (0.35 km from the re-regulation Dam from the confluence with the Nakdong River (downstream view)
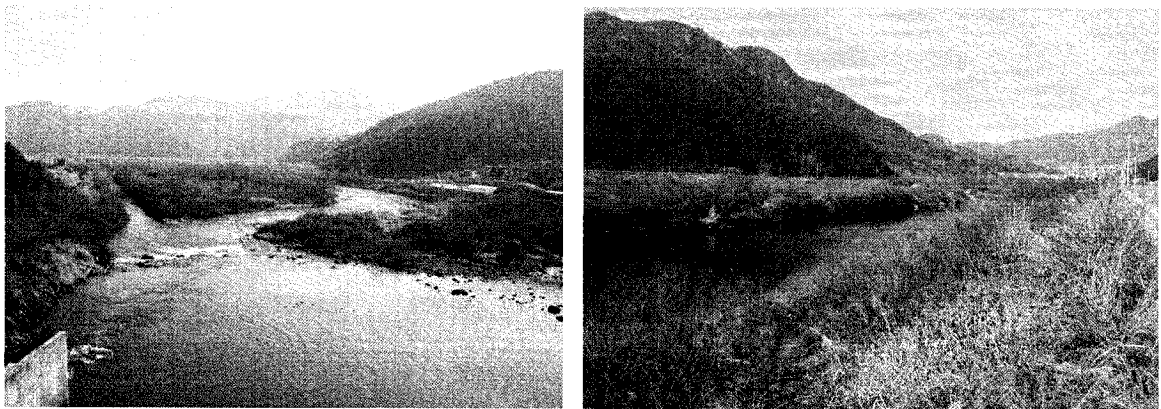
(a) downstream view   (b) upstream view

Figure 4-25. Photos taken at the top of re-regulation dam to the downstream (a) and approximately 1 km downstream from the re-regulation dam to the upstream (b)

76

The aerial photos (Figure 4-26) taken in 1982 and 2004 just below the Hapcheon Re-regulation Dam with non-vegetated active channel boundary area and cross-section survey lines show channel change such as island formation, vegetation expansion, and channel narrowing after the dam construction.

(a) 1982   (b) 2004
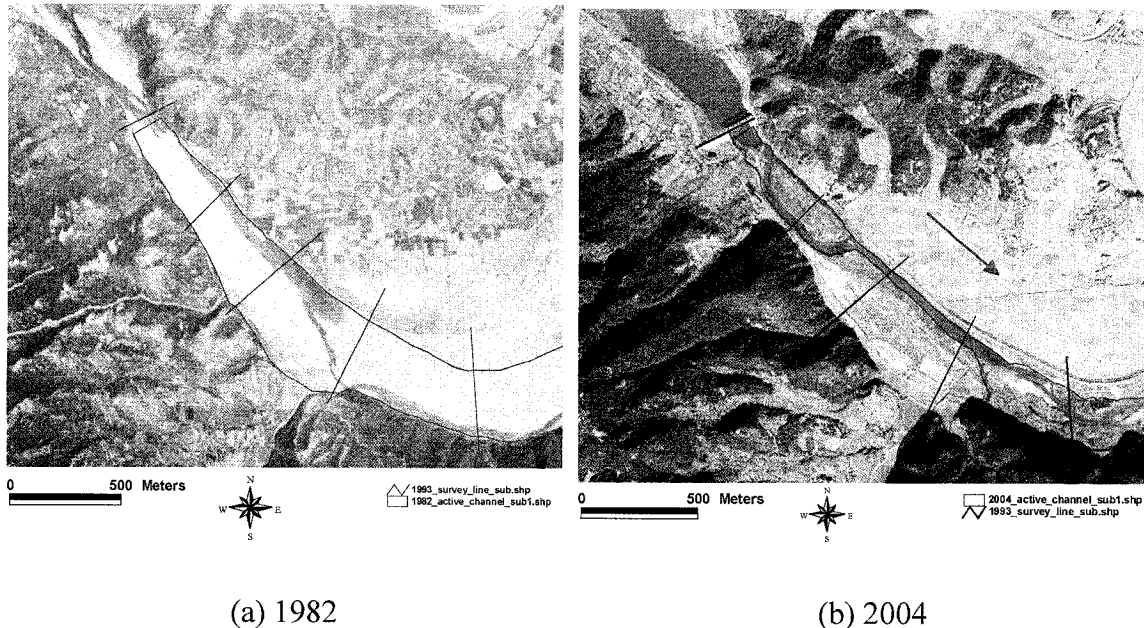
Figure 4-26. Aerial photos taken in 1982 and 2004 at the just below the re-regulation dam with non-vegetated active channel boundary lines and cross-section survey lines

The comparison of the cross-sections measured in 1983 and 2003 at 40 km from the confluence (5 km downstream of the re-regulation dam) shows channel bed scour and the main channel dividing into two sub channels (Figure 4-27). The thalweg elevation decreased 2.76 m (from 48.06 m to 45.30 m) during 1983~2003 period. From Figure 4-28, we can find that the channel bed was already armored and the bed elevation degraded even though the median bed material size, d_{50}, measured in 2003 was 1.7 mm. Because of channel change from sand to gravel during the last three years after measuring the bed material size in 2003, we can also hypothesize that they had been taken into account median bed material size for entire cross-section including both sand bed and gravel bed region in the area of main channel. In addition, the active channel width decreased to 63.4% of 1982 (from 393.4 m to 249.5 m).
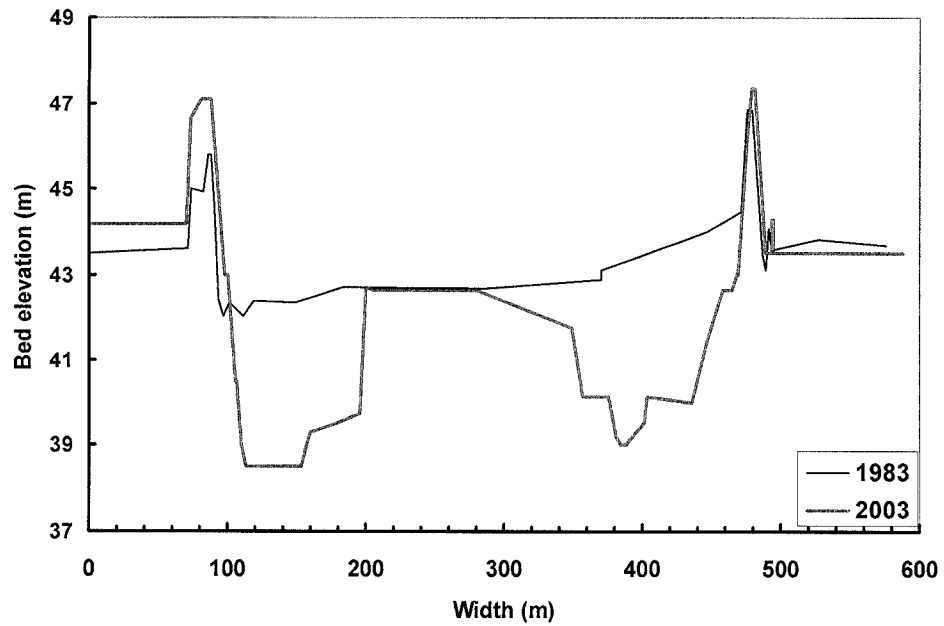
Figure 4-27. Comparison of cross-sections measured in 1983 and 2003 at 40 km (5 km from the re-regulation Dam) from the confluence with the Nakdong River (downstream view)
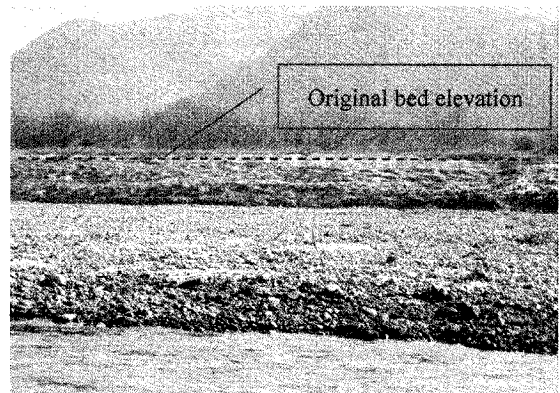
(a) upstream view   (b) side view

Figure 4-28. Gravel bed material (a) and channel scour (b) at 40 km (5 km from the re-regulation Dam) from the confluence with the Nakdong river in the vicinity of left bank side
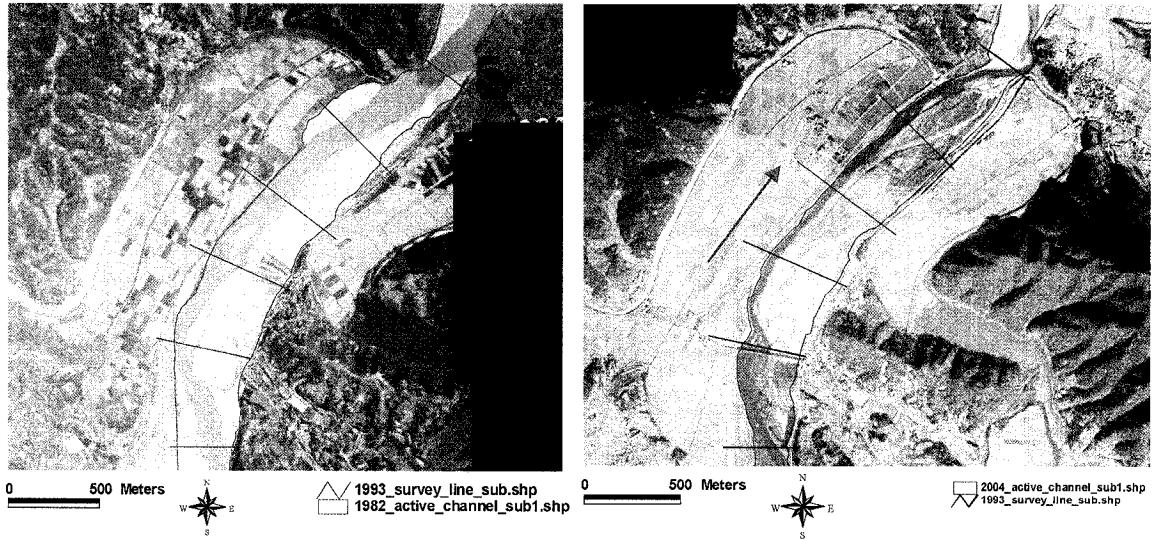
Figure 4-29. Aerial photos taken in 1982 and 2004 at the vicinity of 40 km (5 km downstream from the re-regulation Dam) from the confluence with the Nakdong River with non-vegetated active channel boundary area and cross-section survey lines

The cross-section measured at 35 km (Figure 4-30) from the confluence (10 km downstream from the re-regulation Dam) shows quite stable conditions. Even though the thalweg elevation decreased by 2.24 m (from 34.34 m to 32.10 m), there is no island formation and vegetation growth on sand bars at the main channel, as shown in Figures 4-31 and 32. Only about one third of the entire main channel at the edge of the left bank has been reclaimed as a playground about 120 m wide for the public use on the previous natural floodplain. The primary composition of bed material is sand instead of gravel. There is little change according to the comparison of bed material size measured in 1983 and 2003. In addition, the active channel width also decreased little, to 79.8% of 1982 (from 479.9 m to 382.7 m).
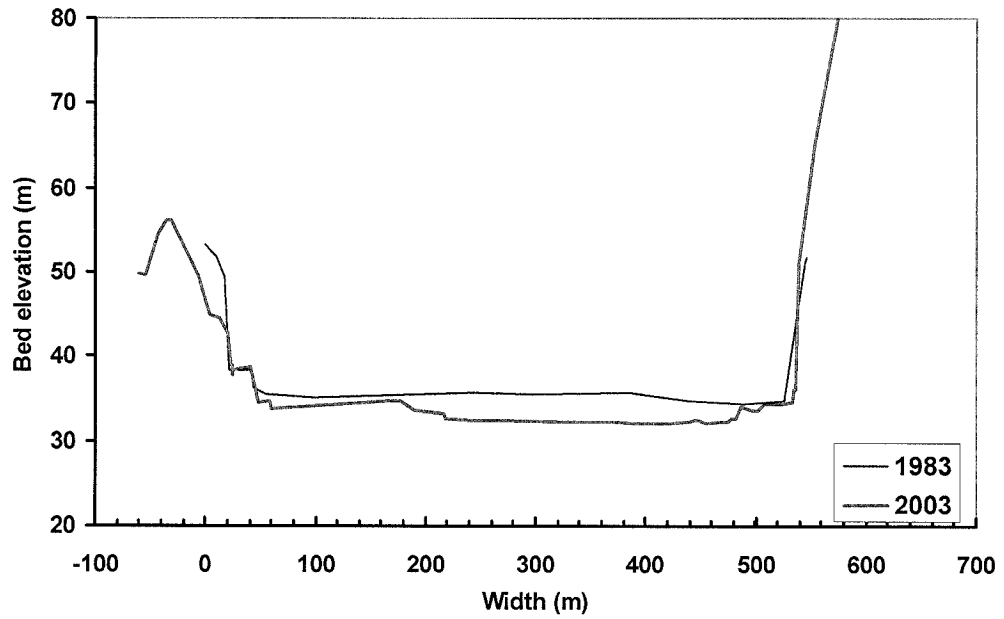
Figure 4-30. Comparison of cross-sections measured in 1983 and 2003 at 35 km (from the 10 km from the re-regulation dam) from the confluence with the Nakdong River (downstream view)
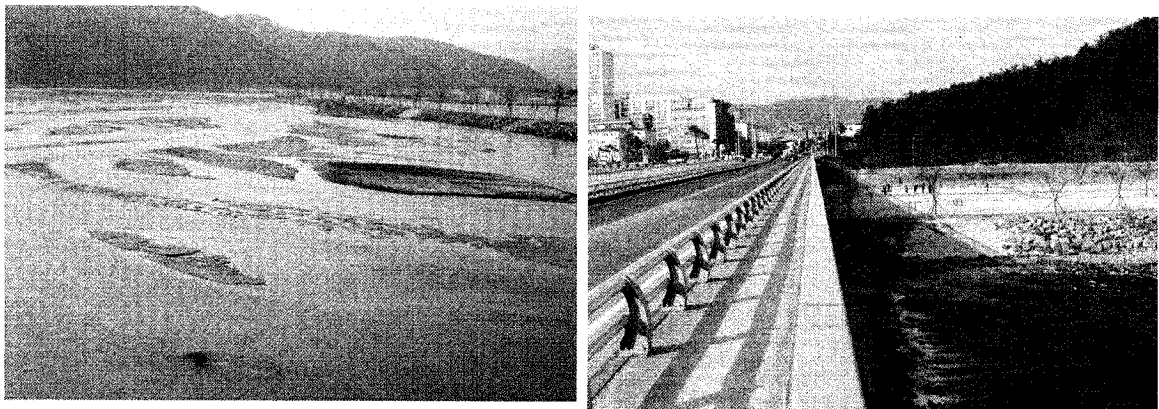
(a) upstream view   (b) side view (left bank, Hapcheon city)

Figure 4-31. Photos taken at 35 km (10 km from the re-regulation dam) from the confluence with the Nakdong River in the vicinity of the Hapcheon city, which is the largest city in the study reach
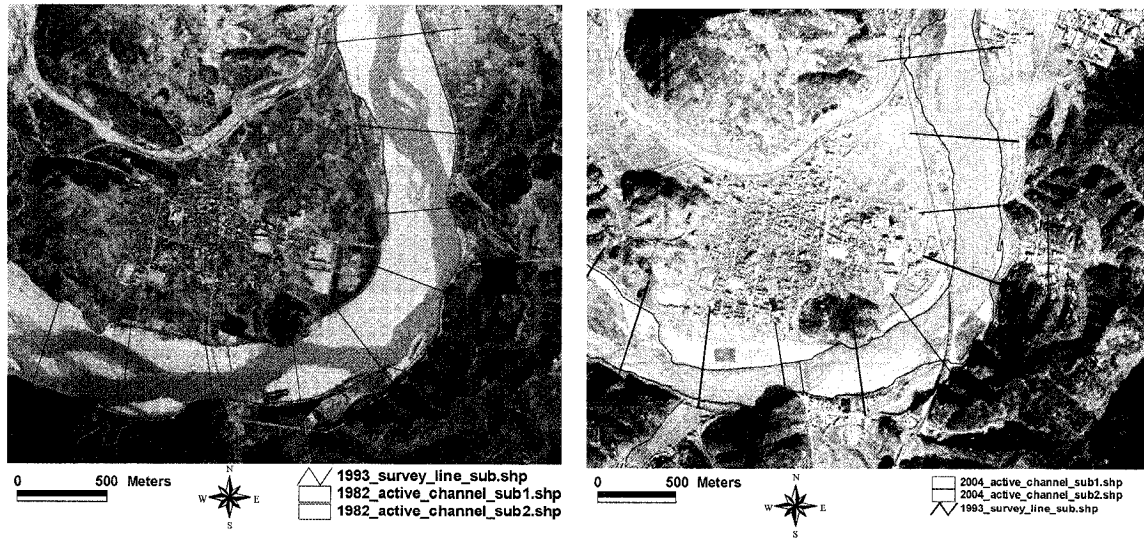
Figure 4-32. Aerial photos taken in 1982 and 2004 in the vicinity of 35 km (Hapcheon city) from the confluence with the Nakdong River (10 km downstream from the re-regulation dam) with non-vegetated active channel boundary area and cross-section survey lines

The cross-sections measured at 25 km (Figure 4-33) from the confluence with the Nakdong river (20 km downstream from the re-regulation dam) of 1983 and 2003 also show quite stable conditions. There is no island formation or significant channel rerouting and vegetation growth on sand bars, as shown in Figures 4-34 and 35. Only bed elevation scoured on the left bank side to a maximum scoured depth of 2.5 m (from 23.25 m to 20.74 m). The edge of the right bank also has been reclaimed as playground about 50 m wide for the public use on the previous natural floodplain. The bed material is composed of sand as in 1983 (Figure 4-34). In addition, the active channel width also decreased to 75.8% of 1982 (from 241.2 m to 182.9 m).
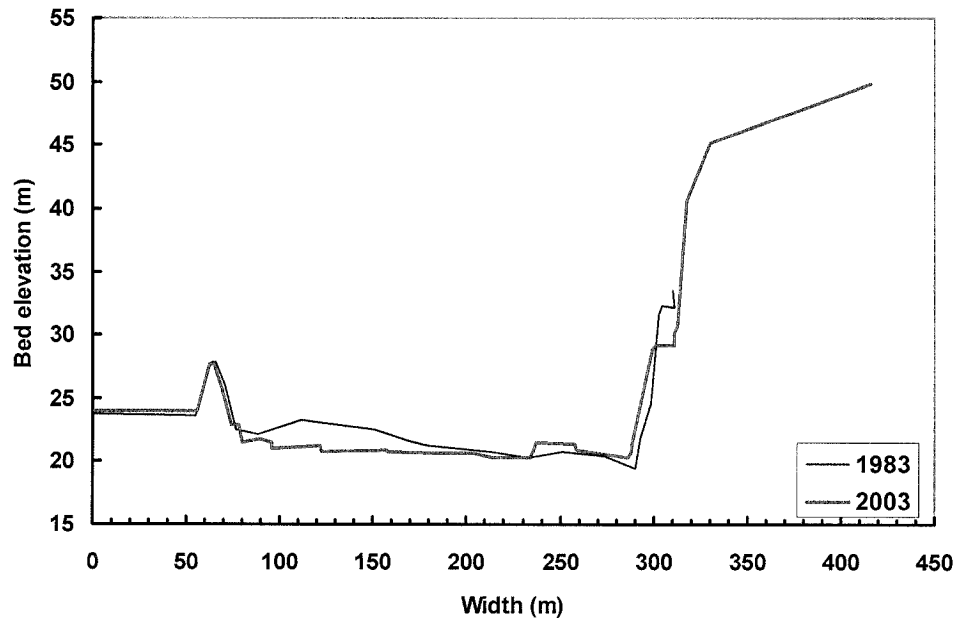
Figure 4-33. Comparison of cross-sections measured in 1983 and 2003 at 25 km (20 km from the re-regulation dam) from the confluence with the Nakdong River (downstream view)

Figure 4-34. Photo taken at 25 km (20 km from the re-regulation dam) from the confluence with the Nakdong River (downstream view)
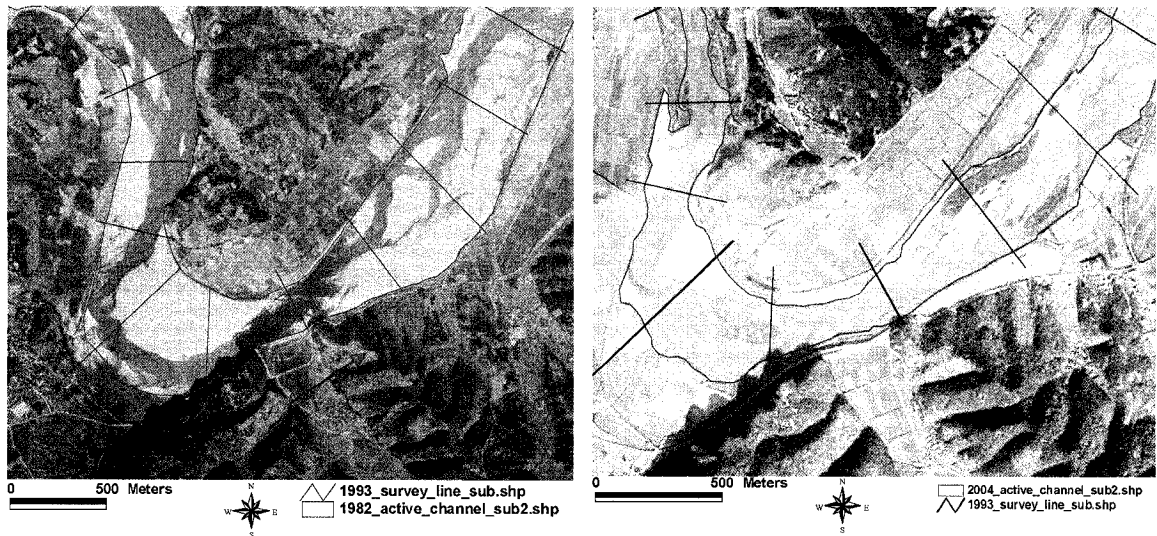
Figure 4-35. Aerial photos taken in 1982 and 2004 at the vicinity of 25 km from the confluence with the Nakdong River (20 km downstream from the re-regulation dam) with non-vegetated active channel boundary area and cross-section survey lines

The cross-sections measured at 1.5 km (Figure 4-36) from the confluence with the Nakdong River (43.5 km downstream from the re-regulation dam) of 1983 and 2003 also show bed elevation scour (maximum scour depth is 3.21 m), and the channel divided into several sub channels and islands with perennial vegetation growth (willows). This cross-section shows the most significant geomorphologic change among other cross-sections in this study reach. Photos shown in Figure 4-37(a), (b) and (c) were taken at the same place (just upstream from the Chungduk Bridge) but at different times (1983, 2004 and 2007) to compare channel geomorphologic change. There were many well developed point bars (alternate bars) before the Hapcheon Dam completion, as shown in Figure 4-37(a). However, the point bar was covered with vegetation and the flow direction changed due to decreasing peak flow after the dam completion (Figure 4-37). Specifically, the alternate bar changed to a middle bar downstream of the Chungduk Bridge, located 1.3 km upstream from the confluence with the Nakdong River. The non-vegetated active channel width also significantly decreased to 25% of 1982 (from 299.4 m to 74.9 m) after dam completion.

83
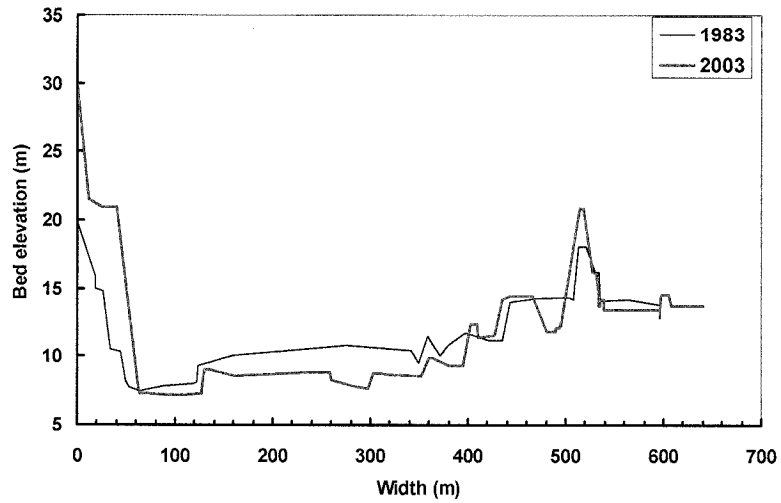
Figure 4-36. Comparison of cross-sections measured in 1983 and 2003 at 1.5 km (43.5 km from the re-regulation dam) from the confluence with the Nakdong River (downstream view)

(a) 1983

(b) 2004

(c) 2007

Figure 4-37. Photos taken in 1983(a), 2004(b), and 2007(c) at 1.5 km (43.5 km from the re-regulation dam) from the confluence with the Nakdong River

Figure 4-38 shows aerial photos taken in 1982 and 2004 in the vicinity of 1.5 km from the confluence with the Nakdong River (43.5 km from the re-regulation dam), with non-vegetated active channel boundary area and cross-section survey lines. From these pictures, we can find that the channel rerouted and islands formed with vegetation growth in 2004 on the channel of previously clear sand bars in 1982. Figure 4-39 shows middle bars (islands) with perennial vegetation growth (mainly 5~10 year old willows) in the channel after the dam completion, as shown in Figure 4-37 (b) and (c), and these sand bars are covered by vegetation.
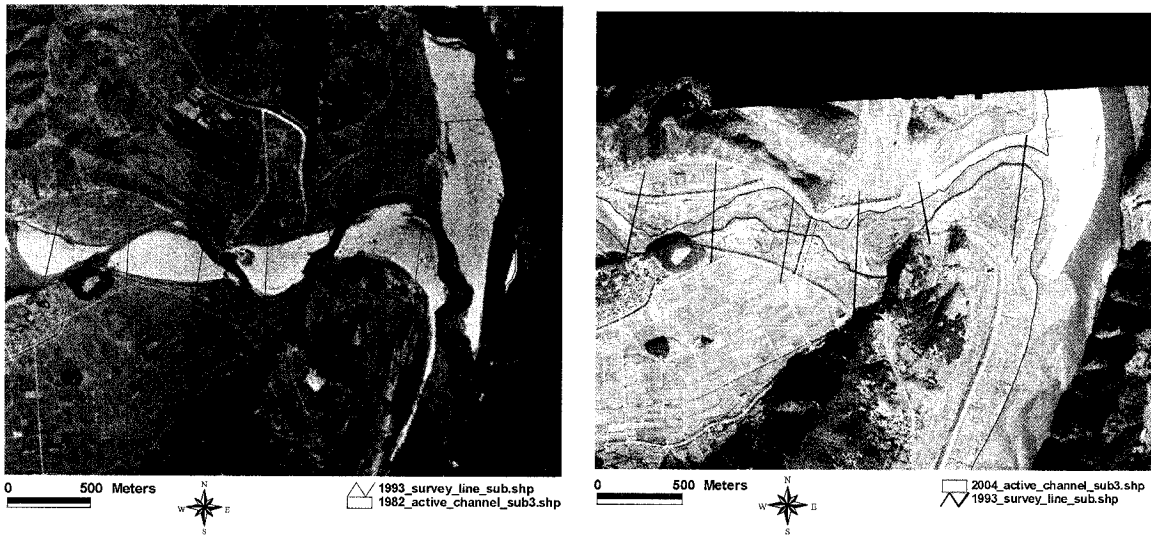
Figure 4-38. Aerial photos taken in 1982 and 2004 in the vicinity of 1.5 km from the confluence with the Nakdong river (43.5 km from the re-regulation dam) with non-vegetated active channel boundary area and cross-section survey lines

Figure 4-39. Island formation with vegetation growth in the vicinity of 1.5 km (43.5 km from the re-regulation dam) from the confluence with the Nakdong River

4.7. Channel Planform

The non-vegetated active channel area was measured from the aerial photos taken in 1982, 1993, and 2004 from the GIS coverage. Figure 4-40 shows sample digitized aerial photos taken in 1982 and 2004 for the active channel area, vegetated area and islands area lines in the vicinity of the Nakdong River for measurement of each area. Table 4-19 is a variation of the active channel area for the study reach. The total active channel area for the entire reach declined over the 20 years. This is consistent with the declining trend. The active channel area of the entire reach decreased from 14.93 km^2 to 8.43 km^2 in 2004. It is 56% of the original 1982 area in 2004. Sub-reach 1 decreased the most, to 50% of the original 1982 area. On the contrary, the vegetated areas for the study reach are consistent with the increasing trend over the study period. Sub-reach 2 increased the most in this study reach. It is increased from 0.40 km^2 in 1993 to 2.09 km^2 in 2004. The trend of the change of vegetated areas is shown in Table 4-19 and Figure 4-41.

Table 4-19. Variation of the active channel areas (km^2) by digitized aerial photos

Reach	1982	1993	2004
Sub-reach 1	3.92	3.13 (80 % of 1982)	1.95 (50 % of 1982)
Sub-reach 2	6.90	5.42 (79 % of 1982)	3.88 (56 % of 1982)
Sub-reach 3	4.11	3.42 (83 % of 1982)	2.51 (61 % of 1982)
Entire	14.93	11.97 (80 % of 1982)	8.34 (56 % of 1982)
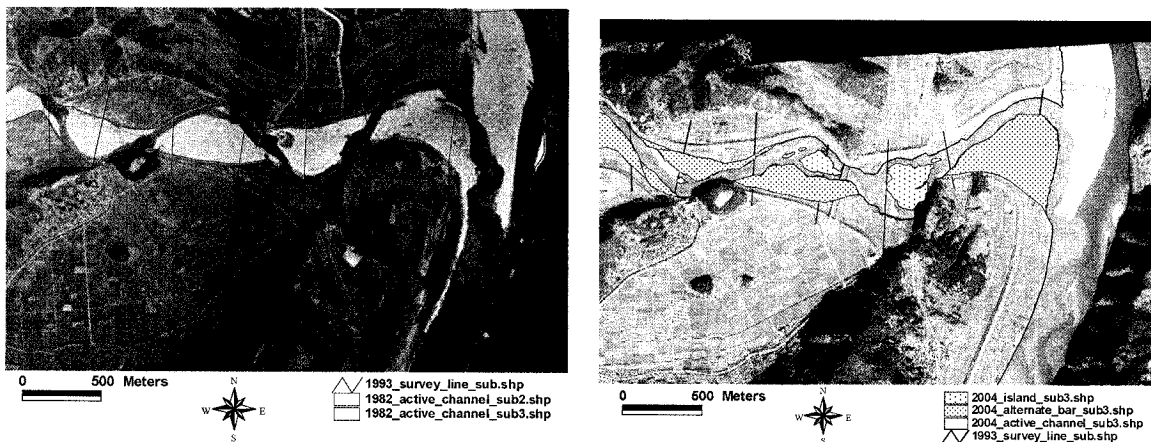
Figure 4-40. Digitized aerial photos taken in 1982 (left) and 2004 (right) with vegetated area, island area, and active channel area lines in the vicinity of the confluence with the Nakdong River

The trend of the change of vegetated areas is shown in Table 4-20 and Figure 4-41. Vegetated area in sub-reach 1 increased the most in the study reach.

Table 4-20. Variation of the vegetated area (km^2) for each sub reach by digitized aerial photos

Reach	1982	1993	2004
Sub-reach 1	-	0.38	1.27
Sub-reach 2	-	0.40	2.09
Sub-reach 3	-	1.06	1.66
Entire	-	1.84	5.02

Island area in the channel also shows a similar pattern of vegetated areas. The island formation is consistent with the increasing trend over the study period. Island area increased in 1993 and 2004 after dam construction, as shown in Table 4-21. As a result, the island area was 0.8 in 1993 and 1.48 in 2004, increasing with the rate 0.073 km^2 /year during 1982~1993 and 0.062 km^2 /year during 1993~2004. Note that the rate of change decreased a little during the 1993~2004 period. Figure 4-43 shows the change of non-vegetated active channel width, vegetated area, and island area in 1982, 1993, and 2004.
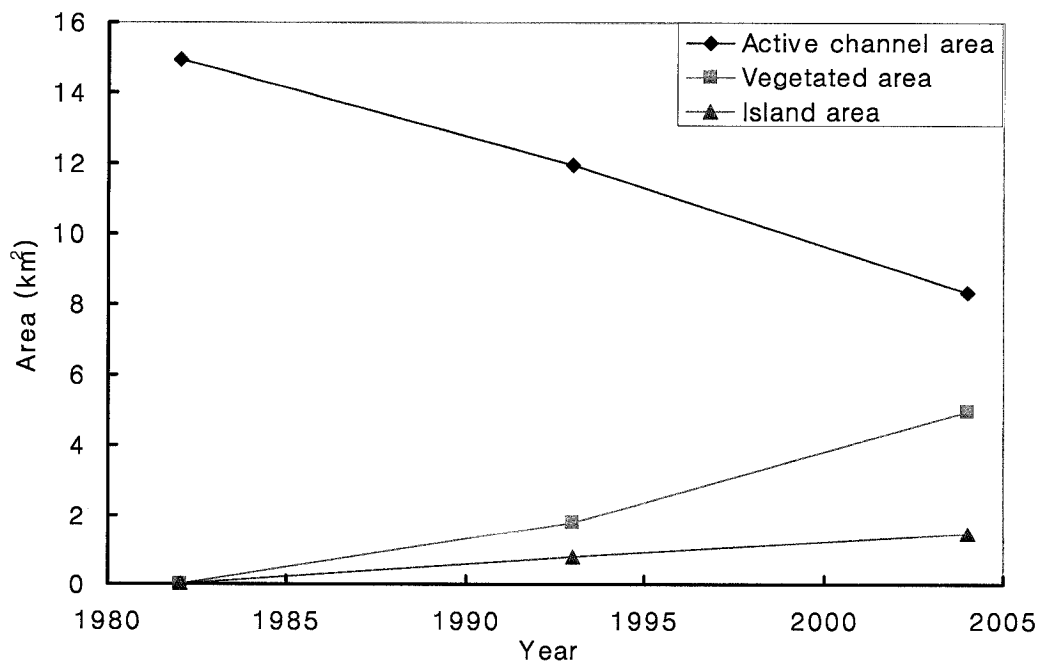
Figure 4-41. Change of non-vegetated active channel width, vegetated area, and island area in 1982, 1993, and 2004

Table 4-21. Variation of island area (km^2) for each sub reach from the aerial photos

Reach	1982	1993	2004
Sub-reach 1	-	0.32	0.73
Sub-reach 2	-	0.26	0.50
Sub-reach 3	-	0.22	0.25
Entire	-	0.80	1.48

4.8. Summary

The data described in Chapter 3 were utilized to quantify and analyze channel changes of the study reach. The water discharge, bed material, bed slope, and channel width were quantified and analyzed to identify historic trends. Sediment transport rates were estimated using empirical equations and compared with measured data from the survey of reservoir sediment deposition of the Hapcheon Main Dam in 2002 (KOWACO, 2002). Also, representative values for each of these variables were identified for use in the stability analysis in the next chapters. Finally, field evidence of channel response at the cross-sections along the study reach was considered to identify channel change from the field investigation.

Water discharge records since 1969 reveal a decline in annual peak discharge after the Hapcheon Main Dam and re-regulation Dam construction. Quantified impacts of Hapcheon Main Dam and re-regulation Dam on the annual water discharge regime included the following items:

(1) The dam attenuated mean annual peak discharges greater than 528 m^3/sec (from 654.7 m^3/sec to 126.3 m^3/sec). The mean annual peak discharge of the post-dam period (1989-2005) was just 19% of the pre-dam period (1969-1981).

(2) The mean daily discharge was greater during the pre-dam period than during the post-dam period (28.7 m^3/sec during pre-dam and 22.1 m^3/sec during post-dam period). The decrease rate was 23% at the Hapcheon Re-regulation Dam gage.

The bankfull discharge (1.58 yr discharge frequency) was estimated by using annual daily peak discharges for the pre-dam (1969-1981) and post-dam (1989-2005) periods. The bankfull discharge of the post-dam period was about 17% of the pre-dam period.

The total sediment loads measured in 1969 and 1970 by FAO and KOWACO (1971) were 1,478 and 477 thousand tons/year, respectively, but these data were estimated from the relationship of precipitation and total sediment transport at the Hapcheon Main Dam site (the Changri gaging station). Another measurement was performed in 2002 was a survey of reservoir sediment deposition of the Hapcheon Main Dam by KOWACO (2002) to evaluate change of the reservoir storage volume. As a result, the estimated sediment volume was 8,279,000 m^3 for the 14-year period 1989-2002. So, the total sediment load was estimated as 946 thousand ton/year at the Hapcheon Main Dam site. Also, the total sediment load was estimated by applying empirical equations such as the Engelund Hansen, Ackers and White, Yang (1973, 1979) and Van Rijn methods at the confluence with the Nakdong River. The estimated total sediment load was 434 thousand tons/year by Yang's (1973) method, which was selected for estimation of sediment transport in this study reach.

The bed material of the study reach changed following construction of the Hapcheon Main Dam and Re-regulation Dam. Prior to dam construction, the channel bed was somewhat coarser in sub-reach 1 than the downstream reaches. The bed of the entire study reach was primarily sand. The average bed material size of the entire study reach was 1.07 mm in 1983. However, following the dam construction, the bed of sub-reach 1, especially just below the re-regulation dam (45-44 km reach) coarsened to gravel size. This means that the channel bed is already armoured in this reach.

The bed slope of sub-reach 1 is somewhat increased after dam completion but the other sub-reaches are decreased. The bed slope of the entire reach declined from 0.000943 in 1983 to 0.000847 in 2003. During the post-dam period, the largest degradational changes occurred along the 45-30 km reach (0~15 km from the re-regulation dam). Average degradation of this reach (45-30 km) is 2.6 m during the 1983-2003 period.

The lateral responses measured in this chapter included non-vegetated active channel width at each aerial survey date, channel width/depth ratio and sinuosity. Width changes

were measured from the non-vegetated active channel digitized from aerial photo taken in 1982, 1993 and 2004. All sub-reaches exhibited a decrease in width with time since 1982. Sub-reach 3 exhibited the greatest change; 53% decrease between 1982 and 2004. Sub-reach 2 was the widest reach for the entire time period. The width of the entire reach was just 54% of the width in 1982. The active channel width decreased after dam construction along the entire study reach from 321 m in 1982 to 172 m in 2004. The rate of change of width between 1993 and 2004 was faster than between 1982 and 1993.

The width/depth ratios also decreased in most of the reaches except sub-reach 3. The width/depth ratio of the entire reach decreased from 279 to 258 from 1982 to 2004, respectively. The sinuosity of all reaches slightly decreased after the dam construction. Also, the total sinuosity of the study reach is over 1.8 through the all years from 1982 to 2004. Sub-reach 2 was the most sinuous reach among the three sub-reaches. According to the planform maps of the non-vegetated active channel (See Figures 4-22 and 4-23), channel planform was relatively unchanged from the pre- to post-dam periods.

According to the field investigation and aerial photos, channel scour and narrowing occurred in most of the cross-sections along the study reach. The reach between 45 km and 40 km from the confluence with the Nakdong River showed the most scour and the channel divided into sub-reaches with vegetation growth. In the middle reach, somewhere approximately between 38 km and 15 km, the channel bed reached relatively stable conditions, although this showed bed scour and channel narrowing. However, the reach at the end of the study reach showed channel division into several sub channels and island formation with establishment of perennial plants such as willow following dam completion.

The total active channel area for the entire reach declined over the 20 years. The active channel width is consistent with the declining trend. It is the 56% of the original 1982 area in 2004. On the contrary, vegetated and island areas are consistent with the increasing trend over the study period.

5 ANALYSIS AND PREDICTION OF CHANNEL CHANGES

Chapter 4 showed how the study reach exhibits both spatial and temporal variability based on channel geomorphologic changes. This chapter presents prediction of the future channel changes based on hydraulic geometry equations, exponential functions, and numerical methods. In addition, this chapter also explores how geomorphic changes including active channel, vegetation, and island area are related to the hydraulic, sedimentologic and channel-form parameters via statistical analysis after the dam construction.

5.1. Statistical Analysis

To conduct statistical analysis for the study reach, the following parameters were selected (Table 5-1). The sub-reach and entire reach averaged values were applied for each parameter. The measured parameters are presented in Chapter 4.

Table 5-1. Variable used in statistical analysis

Symbol of variables	Description of symbols
Q_{peak}	Average peak discharge (m^3/s) for sub-reach and entire reach
Q_{bank}	Bankfull discharge (m^3/s) for sub-reach and entire reach
S	Bed slope(m/m) for sub-reach and entire reach
$Q_{peak}S$	Stream power for peak discharge (m^3/s)
$Q_{bank}S$	Stream power for bankfull discharge (m^3/s)
MI = $S(Q_{bank} / D_{50})^{0.5}$	Mobility index (m/s$^{0.5}$)
D_{50}	Average median bed material size (m)
W_{act}	Non-vegetated active channel width (m)
dW_{act}	Change of non-vegetated active channel width (m/year)
A_{act}	Active channel area (m^2)
dA_{act}	Change of active channel area (m^2/year)
A_{isd}	Island area (m^2)
dA_{isd}	Change of island area (m^2/year)
A_{veg}	Vegetated area (m^2)
dA_{veg}	Change of vegetated area (m^2/year)
P	Sinuosity

Correlation analysis

The correlation model was performed on all of the parameters described in Table 5-1. Table 5-2 is a correlation matrix which summarizes the result of the analysis. Perfect correlations between variables occur when the resulting coefficient (r) is 1 or -1. However, a value of zero signifies no correlation. The results indicated that peak discharge is highly correlated with most of the parameters except the mobility index and bed material size. Conversely, bankfull discharge is correlated with mobility index and average median bed material size. The peak discharge is correlated with planform indices (W_{act}, dW_{act}, A_{act}, dA_{act}, A_{isd}, dA_{isd}, A_{veg}, dA_{veg}, and P). The bed slope correlates well with non-vegetated active channel width, active channel area and island area. The non-vegetated active channel width is correlated with peak discharge, bed slope, stream power ($Q_{peak}S$), mobility index and bed material size. Conversely, non-vegetated active channel width is well correlated with peak discharge, bed slope and stream power, as well as highly correlated with planform indices (A_{act}, dA_{act}, A_{isd}, dA_{isd}, A_{veg}, dA_{veg}, and P). Correlation matrixes of other sub-reaches are presented in APPENDIX C.

Table 5-2. Correlation matrix between reach-averaged parameters by using 1983~2003 data for entire reach. The r-value for the correlation coefficient is listed.

	Q_{peak}	Q_{bank}	S	$Q_{peak}S$	$Q_{bank}S$	MI	D_{50}	W_{act}	dW_{act}	A_{act}	dA_{act}	A_{isd}	dA_{isd}	A_{veg}	dA_{veg}	P
Q_{peak}	1.00															
Q_{bank}	0.28	1.00														
S	0.80	-0.35	1.00													
$Q_{peak}S$	1.00	0.26	0.81	1.00												
$Q_{bank}S$	0.63	0.92	0.04	0.61	1.00											
MI	0.38	-0.78	0.86	0.40	-0.48	1.00										
D_{50}	-0.38	0.78	-0.85	-0.39	0.49	-1.00	1.00									
W_{act}	0.78	-0.39	1.00	0.79	0.00	0.88	-0.88	1.00								
dW_{act}	0.95	-0.03	0.95	0.96	0.36	0.65	-0.64	0.93	1.00							
A_{act}	0.79	-0.37	1.00	0.80	0.02	0.87	-0.86	1.00	0.94	1.00						
dA_{act}	0.97	0.03	0.93	0.97	0.41	0.60	-0.59	0.91	1.00	0.92	1.00					
A_{isd}	-0.85	0.27	-1.00	-0.86	-0.12	-0.81	0.81	-0.99	-0.97	-0.99	-0.95	1.00				
dA_{isd}	-1.00	-0.34	-0.76	-1.00	-0.67	-0.32	0.32	-0.74	-0.93	-0.75	-0.95	0.82	1.00			
A_{veg}	-0.73	0.45	-0.99	-0.74	0.07	-0.91	0.91	-1.00	-0.91	-1.00	-0.88	0.98	0.69	1.00		
dA_{veg}	-0.87	0.22	-0.99	-0.88	-0.17	-0.78	0.78	-0.99	-0.98	-0.99	-0.97	1.00	0.84	0.97	1.00	
P	0.87	-0.23	0.99	0.88	0.16	0.79	-0.79	0.99	0.98	0.99	0.96	-1.00	-0.84	-0.97	-1.00	1.00

Multi regression analysis

Logarithmic based 10 ($\log_{10}$) transformed regressions were performed using variables described in Table 5-1 for two independent variables; change non-vegetated active channel width ($d\text{W}_{act}$) and bed slope (S). $\log_{10}$-transformed regression models are used because they are more accurate than linear regression models (Richard 2000, Richard et al. 2005, and Shafroth et al., 2002). First, each variable individually was regressed against $d\text{W}_{act}$ and S. Then, multiple regression analyses with stepwise selection techniques were applied to different combinations of the measured flow energy, planform and planform changes. The model utilized discharge data from 1969 to 2005 and geometry data from 1983 to 2004. The absolute value of the channel width change was used as the dependent variable in the following models using the reach-averaged and sub-reach-averaged data. The stream power (product of peak discharge and bed slope) was the most significant variable. Therefore, stream power was selected as the first dependent variable and area and the change in area were selected as secondary dependent variables such as active channel area, change of active channel area, vegetated area and island area. The regressed four $\log_{10}$-transformed regression models (Equations 5-1 to 5-4, 3rd order polynomial equations) for the rate change of channel width and one $\log_{10}$-transformed regression model (Equation 5-5) for the bed slope, respectively, are as follows:

$$dW_{act} = -6.51 Q_{peak} S - 3.56 A_{act} + 18.96 \qquad (5\text{-}1)$$

$$dW_{act} = 0.58 Q_{peak} S + 0.62 dA_{act} - 1.86 \qquad (5\text{-}2)$$

$$dW_{act} = 0.03 Q_{peak} S + 0.53 dA_{veg} - 2.36 \qquad (5\text{-}3)$$

$$dW_{act} = 0.35 Q_{peak} S + 0.57 dA_{isd} - 2.12 \qquad (5\text{-}4)$$

$$S = -0.21 A_{act} - 1.43 P - 1.16 \qquad (5\text{-}5)$$

The equations resulting from the multiple regression analyses produced reasonable explained variance (R^2>0.5) values. The regression analyses that resulted in more than 50% (Model R^2) explained variances are presented in Table 5-3. The best regressed equation for the dependent variable, dW_{act}, was equation 5-2 with the independent variables $Q_{peak}S$ and dA_{act}. More detailed literature review, validation of the developed model, and applications are presented in APPENDIX C.

Table 5-3. Results of the multi regression analysis for the flow energy and planform variables best predicting reach-averaged and sub-reach-averaged change rates of the non-vegetated active channel width and bed slope along the study reach

Dependent variables	Independent variables	Partial R^2	P	Model R^2	P
Log_{10} (dW_{act})	$Q_{peak}S$	0.85	0.0256	0.95	<0.0001
	A_{act}	0.11	<0.0001		
	$Q_{peak}S$	0.85	<0.0001	0.99	<0.0001
	dA_{act}	0.99	0.0005		
	$Q_{peak}S$	0.85	0.4160	0.99	<0.0001
	dA_{veg}	0.99	<0.0001		
	$Q_{peak}S$	0.85	0.0701	0.99	<0.0001
	dA_{isd}	0.99	<0.0001		
Log_{10} (S)	A_{act}	0.53	0.0407	0.66	0.0032
	P	0.54	0.0335		

5.2. Future Channel Response

There are many different methods available to estimate future channel response, such as hydraulic geometry equations, exponential functions and numerical approaches. These approaches can predict further lateral and vertical changes in channel width and bed elevation.

Hydraulic geometry equation

Two hydraulic geometry equations were applied for this study reach. To predict equilibrium condition, two calculations for non-uniform flow conditions were conducted using channel geometry files from 1983 and 2003 in HEC-RAS 3.0. The discharge used

was 86.3 m³/s at sub-reach 1 and 109.5 m³/s at sub-reach 3, based on pre-dam bankfull discharge records (1991~2005 period).

Firstly, Lacey's (1929) regime equations were applied for the study reach, as shown in Equations 2-14 to 2-17. Figure 5-1 shows measured and predicted channel width, bed slope, water depth, and flow velocity by using these equations. The measured and predicted values are quite scattered from the perfect agreement lines.
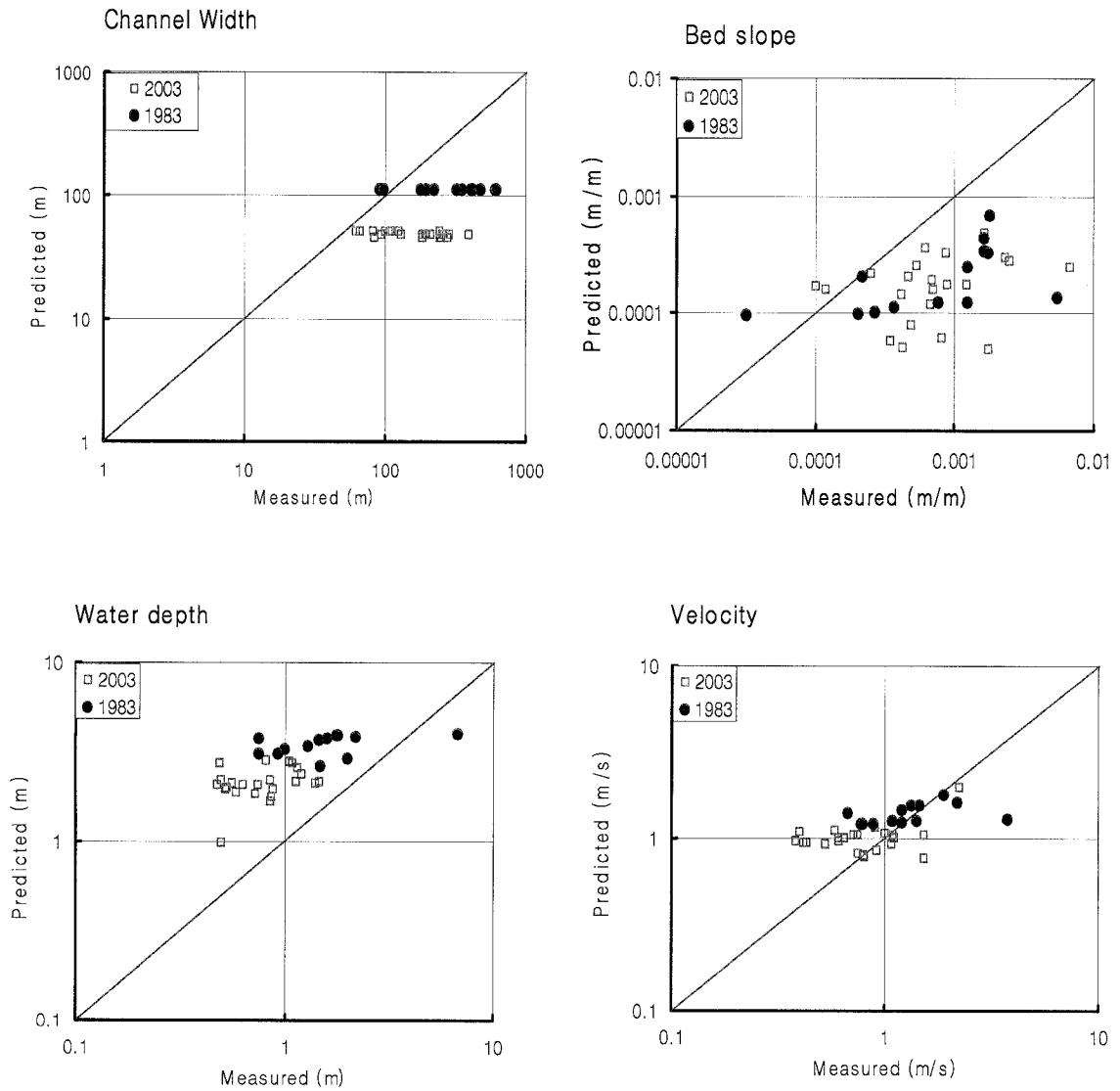
Figure 5-1. Measured and predicted channel width, bed slope, water depth, and flow velocity by using Lacey (1929) regime equations

Secondly, Julien and Wargadalam's (1995) hydraulic geometry equations were applied for the study reach (Equation 2-28 to 32). Figure 5-2 shows predicted and measured channel width, bed slope, water depth, flow velocity and Shields number based on the Julien and Wargadalm (1995) hydraulic geometry equations. The measured and predicted values are quite close to the line of perfect agreement, but the channel is not at equilibrium condition. Table 5-4 shows measured and predicted channel width and bed slope with input data obtained from Julien and Wargadalam's (1995) hydraulic geometry equations. According to the result, both the equilibrium channel width and bed slope will decrease in the future.

Table 5-4. Measured and predicted (by Julien and Wargadalam's (1995) hydraulic geometry equations) channel width and bed slope

Dist.	d_{50} (mm)	$Q(m^3/s)$	Channel Width (m)			Bed slope (m/m)		
			Measured In 2004	Predicted	% error	Measured	Predicted	% error
45.02	44.00	86.3	275.0	33.3	-88	0.01550	0.00623	-60
42	1.20	86.3	83.3	124.1	49	0.00024	0.00017	-30
40	1.70	86.3	249.5	83.2	-67	0.00124	0.00109	-11
38	0.95	86.3	182.2	77.6	-57	0.00227	0.00210	-8
36	0.45	86.3	243.1	111.8	-54	0.00063	0.00044	-30
34	0.79	97.9	184.8	65.9	-64	0.00672	0.00517	-23
32	1.10	97.9	259.9	100.4	-61	0.00084	0.00045	-46
30	0.89	97.9	209.4	80.1	-62	0.00261	0.00160	-39
28	0.40	97.9	283.8	125.5	-56	0.00051	0.00025	-50
26	0.58	97.9	391.4	102.0	-74	0.00108	0.00055	-49
24	0.51	97.9	251.7	108.1	-57	0.00089	0.00053	-40
22	0.50	97.9	194.2	177.3	-9	0.00009	0.00011	22
20	0.82	97.9	192.7	116.0	-40	0.00051	0.00042	-16
18	0.45	97.9	128.7	172.3	34	0.00011	0.00011	-5
16	0.61	97.9	94.0	122.7	30	0.00045	0.00033	-28
14	0.52	109.5	242.7	108.1	-55	0.00110	0.00110	0
12	0.69	109.5	105.7	145.8	38	0.00024	0.00031	26
10	0.20	109.5	124.8	142.3	14	0.00051	0.00075	48
7.95	0.33	109.5	81.9	127.1	55	0.00066	0.00097	48
6	0.12	109.5	62.0	155.0	150	0.00044	0.00064	43
4	0.12	109.5	65.7	112.0	71	0.00198	0.00283	43
2	0.14	109.5	100.2	160.4	60	0.00035	0.00048	37
0	0.15	109.5	108.4	129.4	19	0.00090	0.00057	-37
Avg.			178.9	**116.5**		0.00173	**0.00118**	

- Dist. = Distance from the confluence with the Nakdong River, % error = [(Predicted-Measured)/Measured] ×100

96
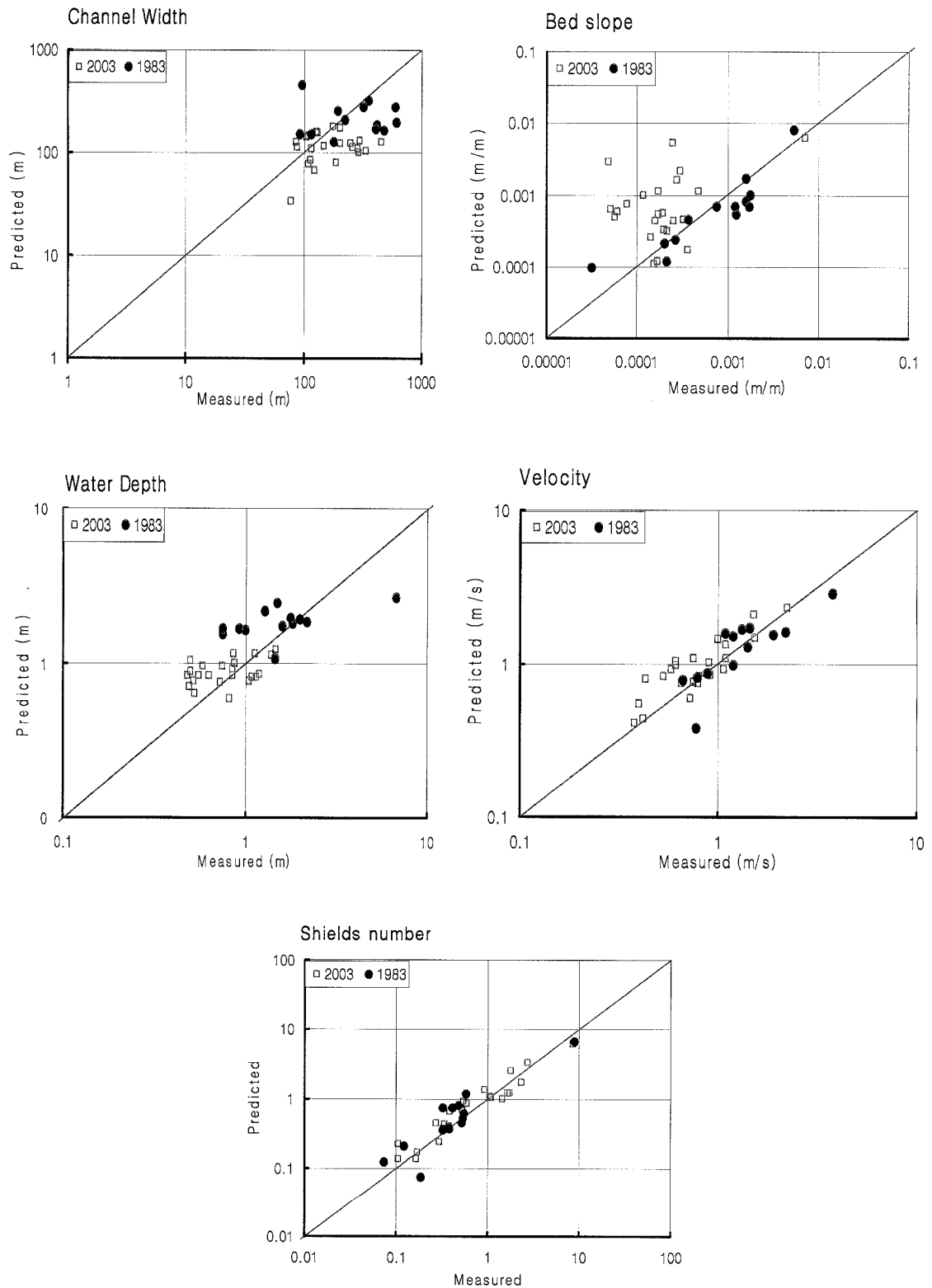
Figure 5-2. Measured and predicted (by Julien and Wargadalam's (1995) hydraulic geometry equations) channel width, bed slope, water depth, flow velocity, and Shields number

Table 5-5 shows the average equilibrium values from Julien and Wargadalam's (1995) hydraulic geometry equations for channel width and bed slope for each sub-reach.

Table 5-5. Estimated equilibrium values by Julien and Wargadalam's (1995) hydraulic geometry equations for channel width and bed slope for each sub-reach average

Reach	Channel Width (m)	Bed slope (m/m)
Sub-reach 1	86.0	0.00200
Sub-reach 2	117.0	0.00095
Sub-reach 3	135.0	0.00096
Entire	116.5	0.00118

Exponential function

An exponential function (Richard, 2000; Richard et al., 2005) was applied to fit the active channel width change per time for the study reach. The hypothesis is that the magnitude of the width vs. time curve increases with deviation from the equilibrium width, W_e:

$$\frac{\Delta W}{\Delta t} = -k_1 (W - W_e) \tag{5-6}$$

Where, ΔW = change in active channel width (m), during the time period Δt;

and Δt = time period (years)

The result is an exponential function:

$$W = W_e + (W_0 - W_e) \cdot e^{-k_1 t} \tag{5-7}$$

where: k_1 = rate constant (slope of regression line) , W_e = Equilibrium width toward which channel is moving, W_o = Channel width at time, t_o; and W = Channel width at time, t.

Plotting the rate of active channel width change vs. the active channel width (Equation 2-21), the rate constant k_1 and the equilibrium width W_e can both be determined empirically from a regression line. The rate constant, k_1, is the slope of the regression line and the intercept is $k_1 W_e$, as shown in Figure 5-3. Data at individual cross-sections for 1982, 1993, and 2004 of the aerial photos were used.
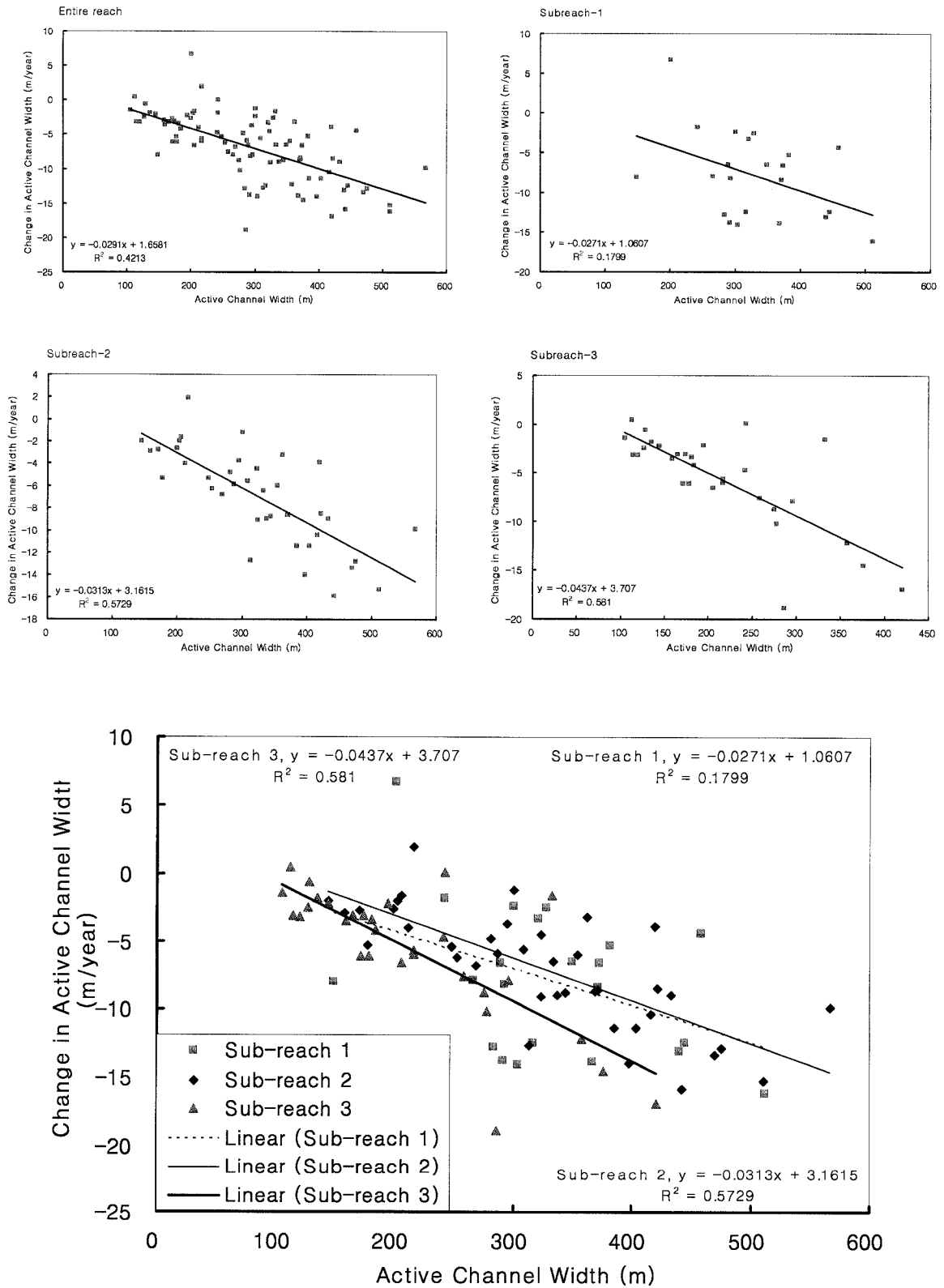
Figure 5-3. Linear regression results of sub-reach data for observed active channel width change (m/year) and observed active channel width (m) for the each study reach

The results of the regressions are summarized in Table 5-6. The k_1 of entire reach was 0.0291 and the equilibrium channel width (W_e) was estimated as 75 m. In addition, the sum-squared error (SSE) between the predicted and observed reach-averaged active channel width was computed.

Table 5-6. Empirical estimation of k_1 and W_e from linear regression of observed active channel width vs. active channel width change data

Reach No.	k_1	$k_1 W_e$	W_e (m)	R^2
Entire	0.0291	1.6581	75	0.42
1	0.0271	1.0607	39	0.18
2	0.0313	3.1615	101	0.57
3	0.0437	3.7070	85	0.58

To determine which method best fit the historic data, the empirically determined k_1 and W_e were input into Equation 5-7 to model the width for the entire reach as a function of time from 1982 to 2004. The result from the equation is plotted in Figure 5-4.

Table 5-7. Measured non-vegetated active channel width by using the exponential equation (Unit : m)

	Year	Sub-reach 1	Sub-reach 2	Sub-reach 3	Entire
	1982	364.1	365.5	232.7	321.4
Observed	1993	297.9	285.7	193.3	258.2
	2004	190.1	210.8	109.3	172.3
	1982	364.1	365.5	232.7	321.4
Predicted	1993	280.4	288.5	176.3	249.0
	2004	218.2	233.9	141.4	196.4
Difference	1982	-	-	-	-
(Obs.-Pre.)	1993	17.6	-2.8	17.1	9.2
	2004	-28.1	-23.1	-32.0	-24.0
Equilibrium width		39.0	101.0	85.0	75.0
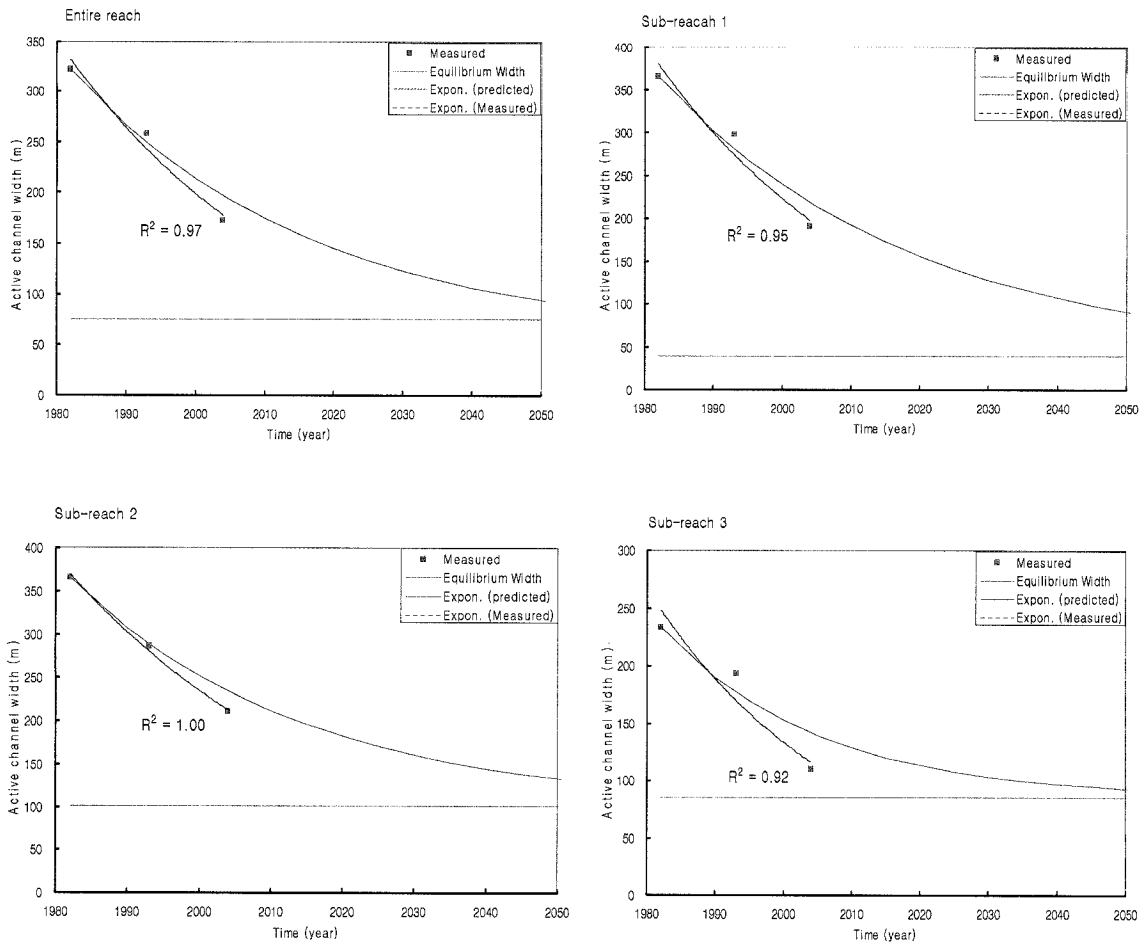
Figure 5-4. Exponential model of width change applied to the each study reach

Table 5-8 shows the comparison of the k_I values estimated from six different rivers: the Rio Grande, Jemez, N. Canadian, Wolf, Arkansas, and Hwang River. The range of the k_I was 0.0219 (Rio Grande River) to 0.111 (Jemez River). The Hwang River's k_I was estimated as 0.0291. The Hwang and Rio Grande River show similar channel narrowing trends in the future.

Table 5-8. Comparison of the k_I values of different rivers

River	Rio Grande	Jemez	N. Canadian	Wolf	Arkansas	Hwang
K_I	0.0219	0.111	0.077	0.1132	0.0380	0.0291

* k_I of the Grande, Jemez, N. Canadian, Wolf, and Arkansas were estimated by Richard et al. (2005) and k_I of the Hwang River was estimated in this study

From equation 5-7, active channel width (W) can describe as following equation 5-8.

$$W = W_e + (W_0 - W_e) \cdot e^{-k_3 t}$$
(5-8)

where: k_3 = rate constant (slope of regression line) , W_e = Equilibrium width toward which channel is moving, W_o = Channel width at time, t_o; and W = Channel width at time, t.

$$\frac{W - W_e}{W_0 - W_e} = e^{-k_3 t}$$
(5-9)

$$\ln\left[\frac{W - W_e}{W_0 - W_e}\right] = -k_3 t$$
(5-10)

Set, $t = X$ and $\ln\left[\dfrac{W - W_e}{W_0 - W_e}\right] = Y$ then equation 5-10 can be described following form.

$$Y = -k_3 X$$
(5-11)

The rate constant k_3 can estimated from equation 5-11, as shown in Figure 5-5.
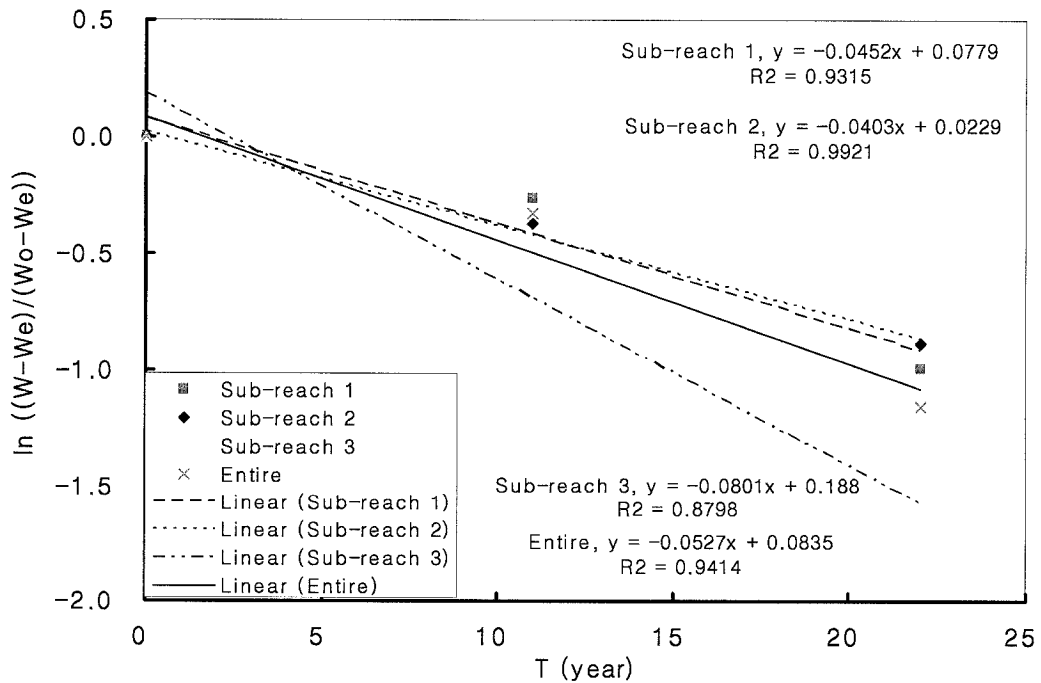
Figure 5-5. Estimated k_3 for each sub-reach of the study reach

102

Table 5-9 summarizes estimated k_3 values from the regression for each sub-reach of the study reach.

Table 5-9. Estimated k_3 for each sub-reach of the study reach

Reach	K_3
Sub-reach 1	0.0452
Sub-reach 2	0.0403
Sub-reach 3	0.0801
Entire	0.0527

5.3. Summary

The statistical analyses using correlation and multiple regression models for the reach-averaged and sub-reach-averaged data sets were performed to determine the relationship between each parameter. These analyses were performed for the 16 parameters shown in Table 5-1. Peak discharge is highly correlated with most of the parameters except mobility index and bed material size. The bed slope correlates well with the most of the parameters, especially with non-vegetated active channel width, active channel area and island area. Also, the non-vegetated active channel width is correlated with peak discharge, bed slope, stream power ($Q_{peak}S$), mobility index and bed material size. From the multi the regression analysis, the four and one $\log_{10}$-transformed regression models (3rd order polynomial equations) were developed for the rate change of channel width and for the bed slope change, respectively. The resulting equations explain more than 65% of the variance.

Three different methods of modeling lateral and vertical movement rates based on measured non-vegetated active channel width changes and bed slope were used to predict future changes and to estimate equilibrium states.

The first method used the Lacey's (1929) regime equations and the second method used Julien and Wargadalam (1995) hydraulic geometry equations, as shown in Figures 5-1 and 5-2. The Julien and Wargadalam (1995) method showed quite close agreement with the line of perfect agreement. However, the channel has not reached equilibrium. The estimated equilibrium channel width was 116.5 m, compared to the 2004 channel

width of 178.9 m. The estimated bed slope was 0.00118, compared to the 2003 bed slope of 0.00168, as shown in Table 5-5.

The third method used the exponential function for the channel width from Richard et al. (2005b). This model showed a good agreement (specially sub-reach 3) with equation 5-6, as shown in Figure 5-3. The estimated equilibrium channel width was 75 m compared to the measured 2004 channel width for the entire reach. From the result of comparing the k_l values with other rivers including the Rio Grande and Arkansas River (Richard et al., 2005b), the range of the k_l values was 0.0219 (the Rio Grande River) to 0.111 (the Jemez River) and 0.0291 for the Hwang River. This means that the Hwang and Rio Grande River show the similar trend of decreasing channel width. In addition, prediction of the future channel width with equation 5-7 showed a good result from comparing between measured and predicted values, as shown in Figure 5-4.

6 ANALYSIS OF THE DOWNSTREAM EFFECTS OF WATER PULSES DUE TO THE RE-REGULATION DAM

Most of the multi-purpose dams in Korea are designed for flood control, water supply and power generation (three hours per day for peak power generation during the non-flood season). Therefore, there is no water flow discharging from the dams during more than 20 hours. For this reason, engineers constructed a re-regulation dam to re-regulate the downstream flow discharge and maintain a minimum flow for the river system. Although the re-regulation dam regulates the discharge from the main dam, flow pulses are still generated by the re-regulation dam operation during flood season. The pulses are caused when the gate opens to pass excess volume of water from the reservoir of the re-regulation dam. These flow pulses may affect and accelerate downstream channel changes such as channel scour, armoring and aggradation. This chapter studies the effects of these flow pulses and how much they affect the downstream channel.

6.1. Unsteady Flow Simulation

The Hapcheon Main Dam and Re-regulation Dam attenuate inflow flood peaks by dam operation. The peak inflow at the main dam was 1,136 m^3/s on July, 2, 2005 at 08:00. During this period, the maximum discharge from the main dam was about 100 m^3/s and the minimum discharge was 0 m^3/s. However, the maximum discharge at the re-regulation dam was about 65 m^3/s due to gate opening and the minimum discharge was about 15 m^3/s, as shown in Figure 6-1, due to power generation. Usually, the maximum discharge from the re-regulation dam is just 20 m^3/s, depending on the water lever of the reservoir of the re-regulation dam. The gate opening is only used to maintain appropriate water level within the reservoir during the flood season from June to September. Figure 6-1 shows a comparison of the inflow discharge into the main dam, out of the main dam and re-regulation dam, and inflow discharge at the main dam during the period from July,

1, 2005 to July, 10, 2005 for 10 days as a typical flood situation (daily pulse). Figure 6-2 shows more clearly the difference of the flow discharges from the main dam and re-regulation dam during the same period, as shown in Figure 6-1.
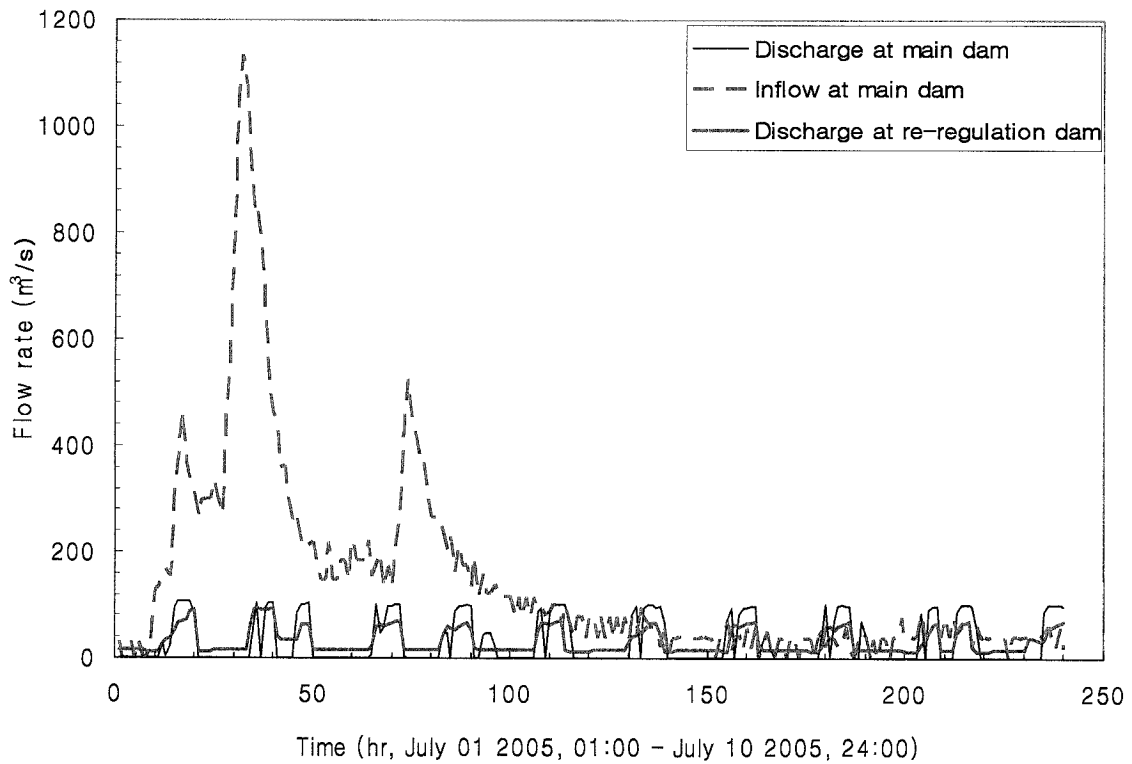
Figure 6-1. Typical inflow and discharge hydrographs at the Hapcheon Main Dam and Re-regulation Dam during typical flood season from July, 1, 2005 to July, 10, 2005

To estimate and evaluate the effects of the pulses on the water level due to discharges from the re-regulation dam along the study reach, an unsteady flow simulation was performed using HEC-RAS (U.S. Army Corps of Engineers, 2002) by applying the 2003 cross-sections data set and the hourly discharge hydrographs from 7/2/2005 07:00 to 7/6/2005 10:00 for the case of daily pulse, and from 8/30/2002 01:00 to 9/3/2002 04:00 for the case of flood peak for the upstream boundary conditions.
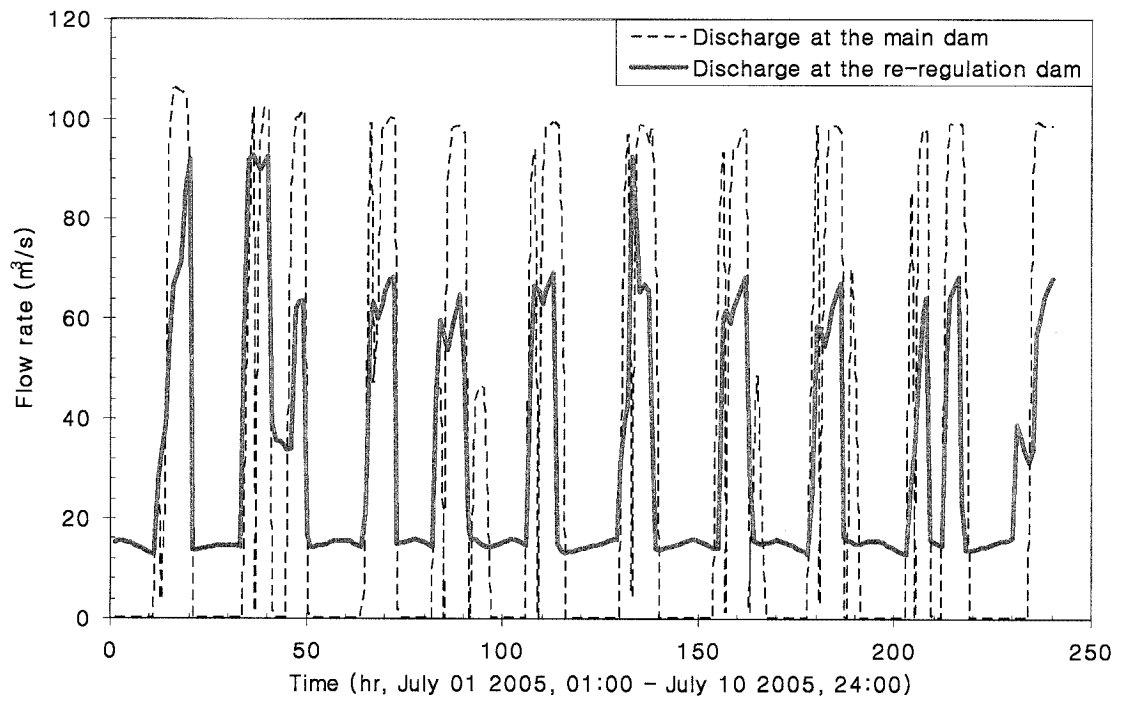
Figure 6-2. Typical discharge hydrograph at the Hapcheon Main Dam and Re-regulation Dam during flood season from July, 1, 2005 to July, 10, 2005

Table 6-1 summarizes the four different cases applied for unsteady flow simulation. Cases 1 and 3 are measured inflow hydrographs as the daily pulse and flood peak situation, and Cases 2 and 4 are average inflow of Cases 1 and 2 for the upstream boundary conditions.

Table 6-1. Cases of unsteady simulation

Case	Flood type	Period	Type of inflow hydrograph	Maximum discharge(m^3/s)	Minimum discharge(m^3/s)
1	Typical	7/2, 2005 07:00 ~ 7/6, 2005 10:00	Daily pulse	92.9	13.2
2			Daily average	33.0	33.0
3	Extreme	8/30, 2002 01:00 ~ 9/3, 2002 04:00	Flood peak	504.0	74.9
4			Flood average	275.1	275.1

Figure 6-3 shows the input hourly discharge hydrographs used in the unsteady flow simulation at the Hapcheon Re-regulation Dam for 100 hours from 7/2/2005 07:00 to 7/6/2005 10:00 for Cases 1 and 2, and from 8/30/2002 01:00 to 9/3/2002 04:00 for Cases 3 and 4. The maximum and minimum discharges are over 92 m³/s and 13 m³/s, respectively, for Case 1 and over 504 m³/s and 74 m³/s, respectively, for Case 3.
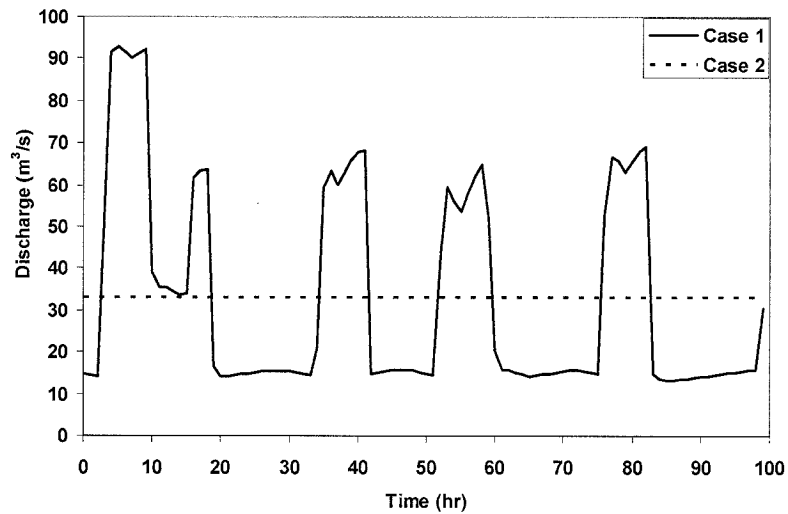
(a) Case 1 and Case 2
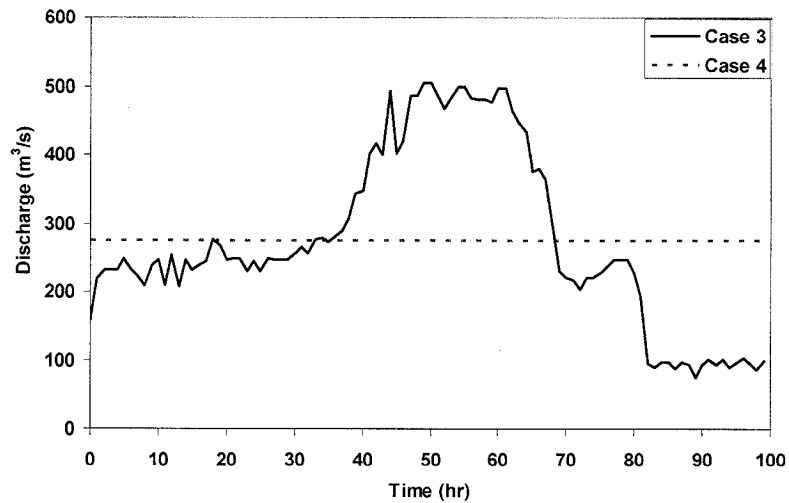
(b) Case 3 and Case 4

Figure 6-3. Input hourly discharge hydrographs for unsteady simulation at the Hapcheon Re-regulation Dam for the period from 7/2/2005 07:00 to 7/6/2005 10:00 (a) and from 8/30/2002 01:00 to 9/3/2002 04:00 (b)

Prior to the unsteady simulation for the four cases, the model was calibrated by using the discharge hydrograph for Case 1. Figure 6-4 shows the plot of measured and simulated water levels at the Jukgo gaging station located 7.2 km from the confluence with the Nakdong River (37.8 km from the re-regulation dam). It shows that the measured and simulated water level follow similar patterns during the simulation time. Therefore, the parameters used in the model run for calibration were applied for the four cases.
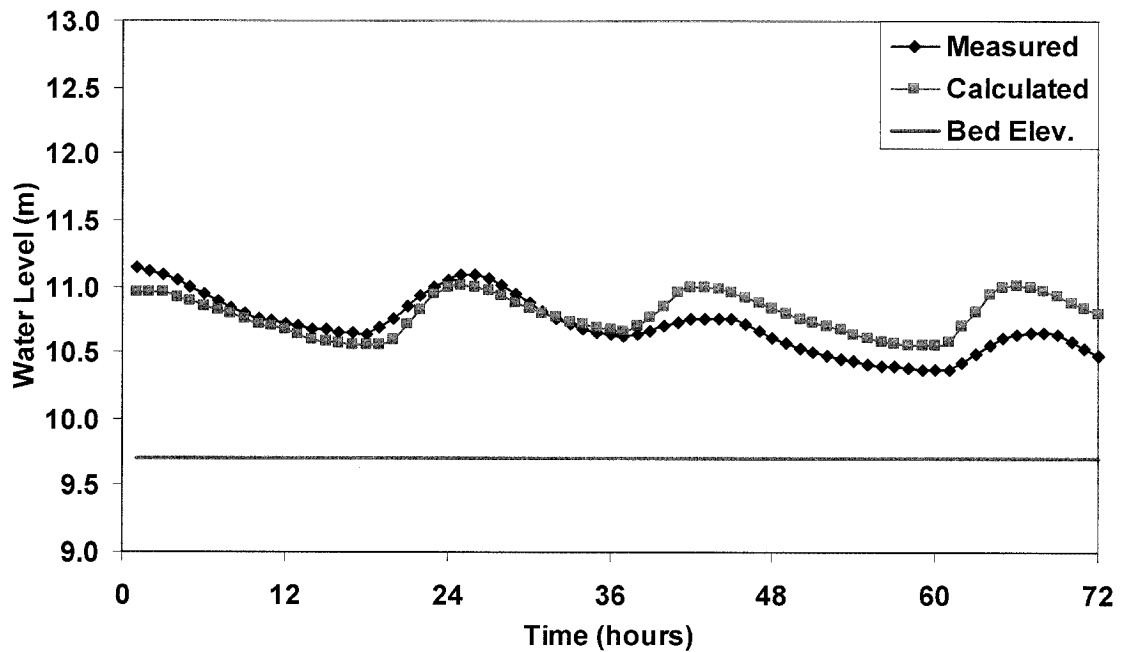
Figure 6-4. Comparison of measured and simulated hourly water levels at the Jukgo water level gaging station (7.2 km from the confluence with the Nakdong River)

Figure 6-5 shows the simulated water depths at the stations of 0, 22, 42, and 44 km from the confluence with the Nakdong River for Cases 1 to 4. The water depths attenuated according as the flow moves downstream (Case 1 in Figure 6-5(a)). The differences of maximum and minimum water depth were about 0.8 m and 0.5 m at 22 km and 0 km, respectively, but it is approximately 1.5 m at 44 and 42 km. However, in Case 2 the water depths were flat along the study reach, as shown in Figure 6-5(b). Cases 3 and 4 show similar results to Cases 1 and 3 (Figure 6-5(c) and 6-5(d)).
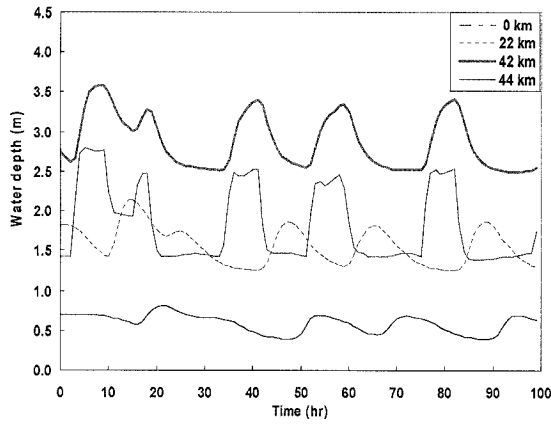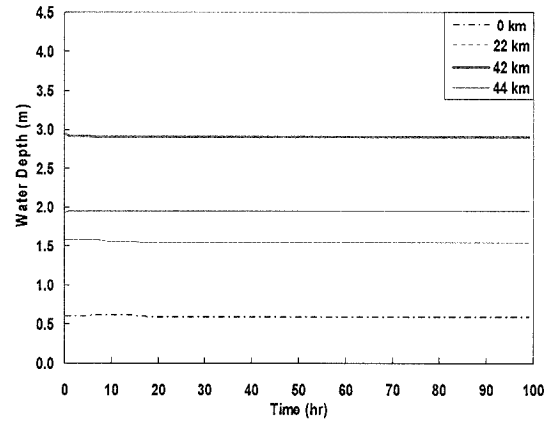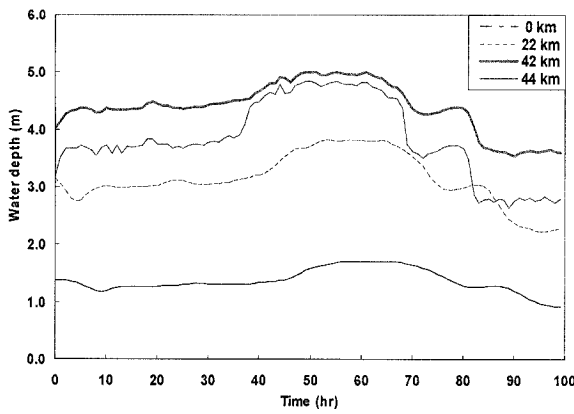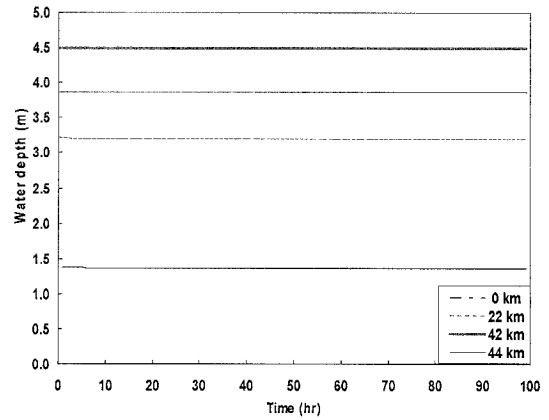
Figure 6-5. Simulated water depths for the Case 1 to 4 at the stations of 0, 22, 42 and 42 km from the confluence with the Nakdong River

To determine the difference in water depth and velocity for the four cases, the average and average difference of the maximum and minimum values were calculated and compared for each flood event (daily pulse, daily average, flood peak, and flood average) using the unsteady flow simulations. The difference between the maximum and minimum water depths and flow velocities for Case 1 for the daily pulse in 2005 (Figures 6-6a, b), and for Case 3, (Figure 6.6c, d). The maximum and minimum differences show similar patterns along the entire study reach.
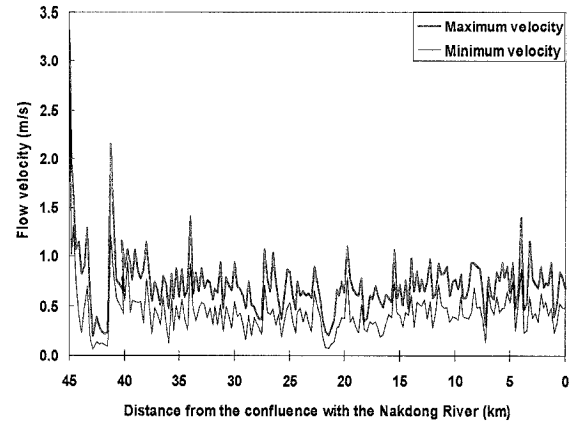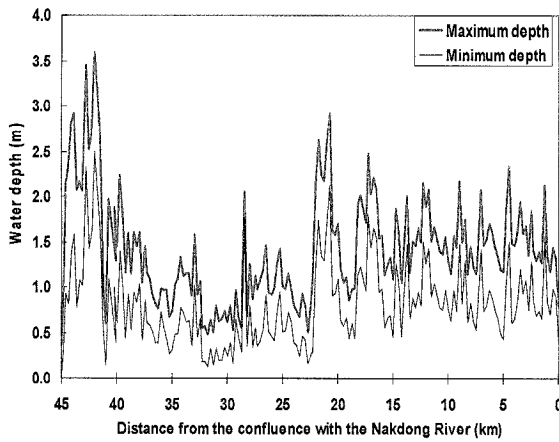
(a) Difference of water depth for the Case 1   (b) Difference of velocity for the Case 1
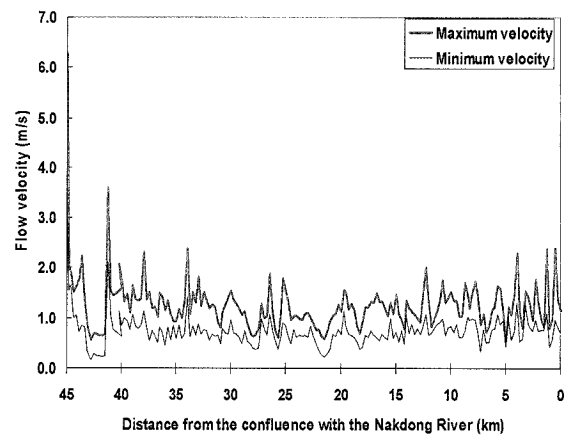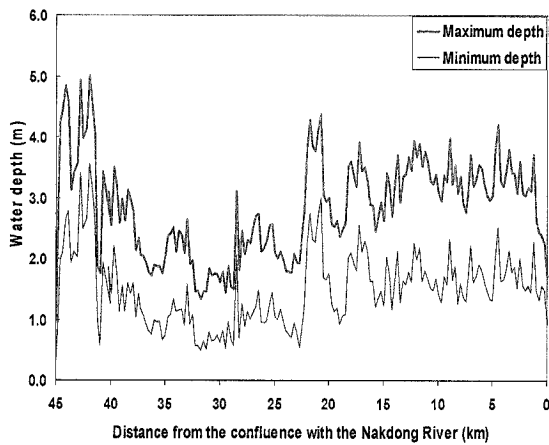
(c) Difference of water depth for the Case 3   (d) Difference of velocity for the Case 3

Figure 6-6. Differences of the maximum and minimum water depths and velocities of the Case1 (a) and (b), and Case 3 (c) and (d) along the study reach

Table 6-2 summarizes the average differences in the maximum and minimum water depths and velocities along the study reach. The average differences of the water depths were 0.62 m for Case 1 and 1.37 m for Case 3. The average differences of the velocities also were 0.30 m/s for Case 1 and 0.54 m/s for Case 3. However, Cases 2 and 4 show little change between the maximum and minimum discharge. This occurred because average discharge values were used for Cases 2 and 4.

Table 6-2. Average and average difference of the maximum and minimum water depths and velocities along the study reach for the each case

Case	Water depth (m)			Velocity (m/s)		
	Maximum	Minimum	difference	maximum	minimum	difference
1	1.42	0.80	0.62	0.74	0.44	0.30
2	1.06	1.03	0.03	0.56	0.55	0.01
3	2.84	1.48	1.36	1.27	0.73	0.54
4	2.26	2.25	0.01	1.05	1.05	0.00

6.2. Incipient Motion Analysis

There are several different approaches to analyze incipient motion, as mentioned in Chapter 2. However, the Shields parameter approach is the most common and widely used, so this approach was selected. The effect caused by the discharge from the Hapcheon Re-regulation Dam was assessed by using incipient motion analysis. The hydraulic parameters for incipient motion analysis were obtained from the unsteady flow simulation. The incipient motion criterion was applied to all four cases. The Shields parameters and critical Shields parameters can be calculated using Equations 2-26 to 32. The summary of the incipient motion analysis for each case is shown in Table 6-3. Figures 6-7 to 6-10 provide plots of the incipient motion analysis for each case. The critical Shields parameters are higher than Shields parameters at 44 and 42 km from the confluence with the Nakdong River (at just below the re-regulation dam) for Cases 1 and 2 of the daily pulse and daily average in 2005, respectively. The Shields parameters for Case 1 show a similar pattern, as seen in the water depths (Figure 6-5(a)) or flow discharge (Figure 6-3(a)), at stations 44, 42, 22, and 0 km (Figure 6-7). The minimum Shields parameters was determined to be very close to the critical Shields parameters in Case 1 at 22 km. Case 2 shows a similar trend in the Shields parameters at each station as seen in Case 1, but these values don't vary along the study reach because Case 2 uses an average discharge of Case 1. The bed material at 44 and 42 km (just below the re-regulation dam) does not move. This suggests that the channel bed is armored 5 km downstream of the re-regulation dam. In Case 3, the Shields parameters are smaller than the critical Shields parameters at most stations except at 44 km during the entire

simulation times and at 42 km after 83 hours of simulation (Figure 6-9). The critical Shields parameters during whole simulation times at 22 and 0 km from the confluence with the Nakdong River are less than the Shields parameter, suggesting bed material movement. Case 4 also shows a similar pattern to Case 3. The Shields parameter is only smaller than the critical Shields parameters at 44 km (Figure 6-10). The channel bed is affected by the flood peak in 2002 at 42, 22 and 0 km in Cases 3 and 4 (Figures 6-9, 6-10).

Table 6-3. Summary of the incipient motion analysis for the different discharges at the stations 44, 42, 22, and 0 km from the confluence with the Nakdong River

Cases applied discharge hydrographs and corresponding Figures	Location of stations (km, the distance from the confluence)	τ_{*c}	Average τ_*	τ_{*c} vs. τ_*
Case 1 (daily pulse) Figure 6-7	44	0.045	0.007	$\tau_{*c} > \tau_*$
	42	0.038	0.017	$\tau_{*c} > \tau_*$
	22	0.031	0.081	$\tau_{*c} < \tau_*$
	0	0.084	1.232	$\tau_{*c} < \tau_*$
Case 2 (daily average) Figure 6-8	44	0.045	0.007	$\tau_{*c} > \tau_*$
	42	0.038	0.017	$\tau_{*c} > \tau_*$
	22	0.031	0.080	$\tau_{*c} < \tau_*$
	0	0.084	1.046	$\tau_{*c} < \tau_*$
Case 3 (flood peak) Figure 6-9	44	0.045	0.034	$\tau_{*c} \approx \tau_*$
	42	0.038	0.100	$\tau_{*c} < \tau_*$
	22	0.031	0.403	$\tau_{*c} < \tau_*$
	0	0.084	2.561	$\tau_{*c} < \tau_*$
Case 4 (flood average) Figure 6-10	44	0.045	0.039	$\tau_{*c} \approx \tau_*$
	42	0.038	0.092	$\tau_{*c} < \tau_*$
	22	0.031	0.440	$\tau_{*c} < \tau_*$
	0	0.084	2.536	$\tau_{*c} < \tau_*$

* Cases indicate the type of discharge hydrograph as shown in Table 6-1. τ_{*c} and τ_* are the critical Shields parameter and Shields parameter, respectively.

Case 1 : Daily pulse
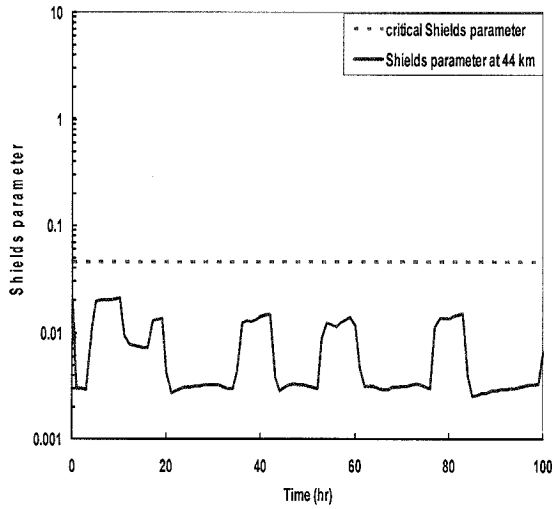
(a) 44 km
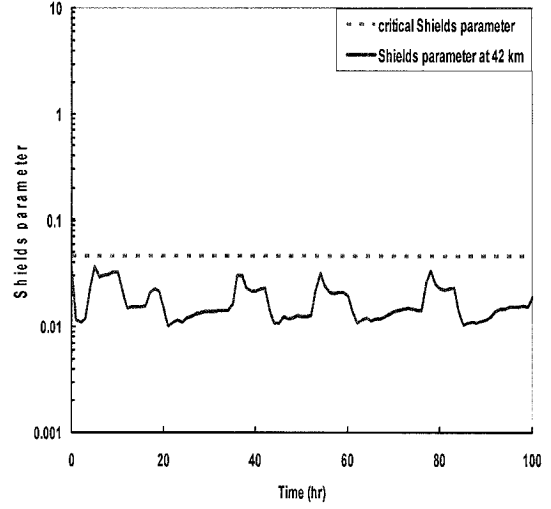
(b) 42 km
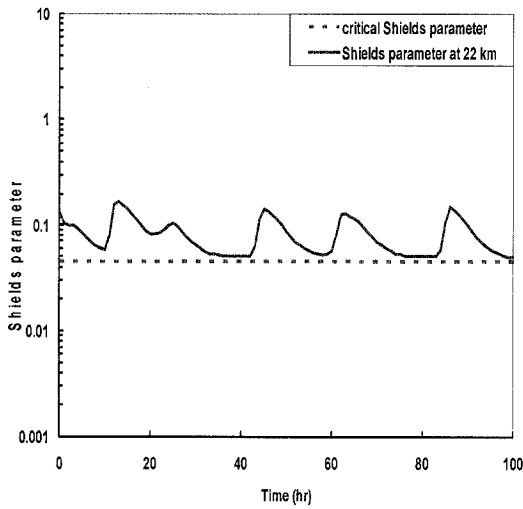
(c) 22 km
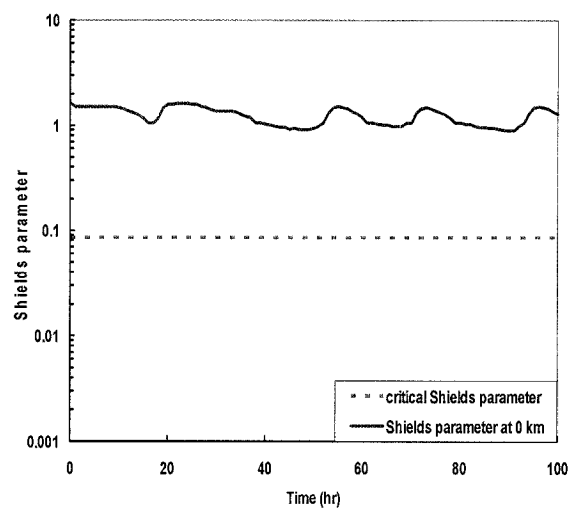
(d) 0 km

Figure 6-7. Critical Shields parameters and Shields parameters at the stations (44, 42, 22, and 0 km from the confluence with the Nakdong River) by unsteady simulation results for case 1 (daily pulse)

Case 2 : Daily average
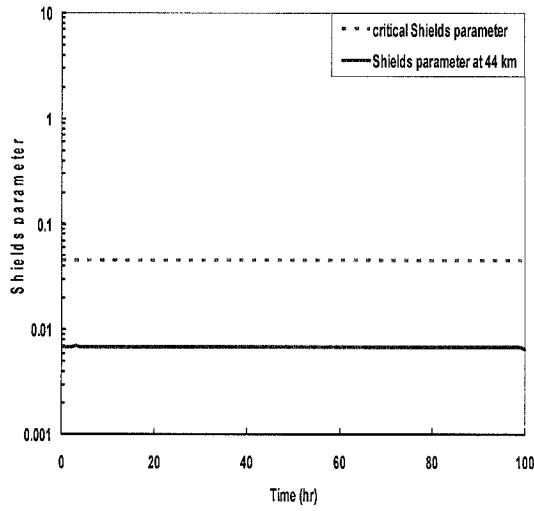
(a) 44 km
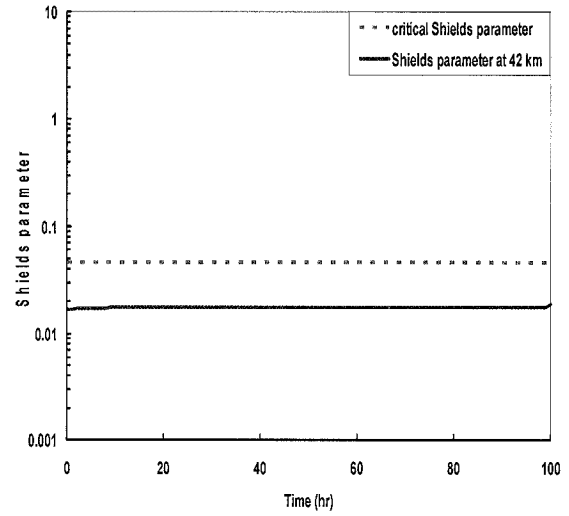
(b) 42 km
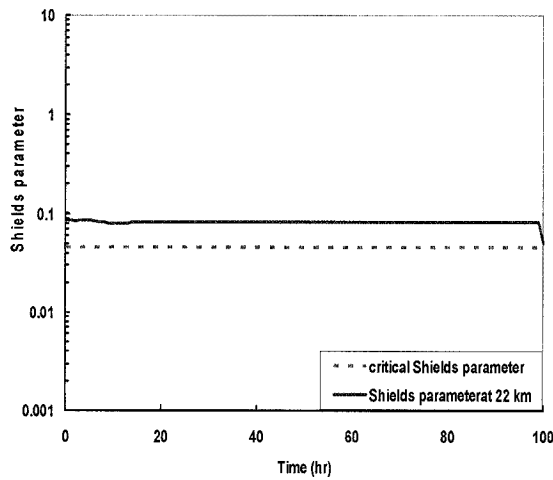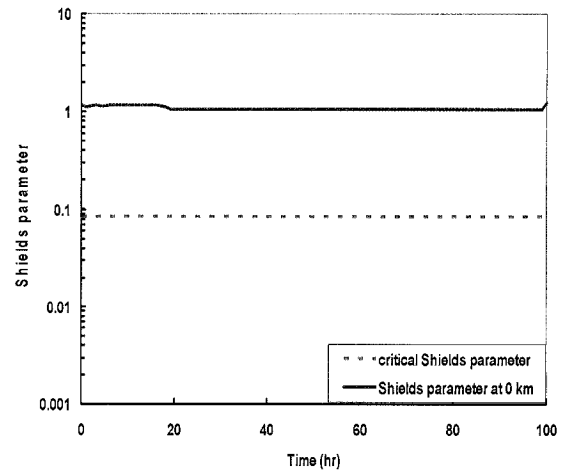
(c) 22 km

(d) 0 km

Figure 6-8. Critical Shields parameters and Shields parameters at the stations (44, 42, 22, and 0 km from the confluence with the Nakdong River) by unsteady simulation results for case 2 (daily average, 33.0 m³/s)

Case 3 : Flood peak
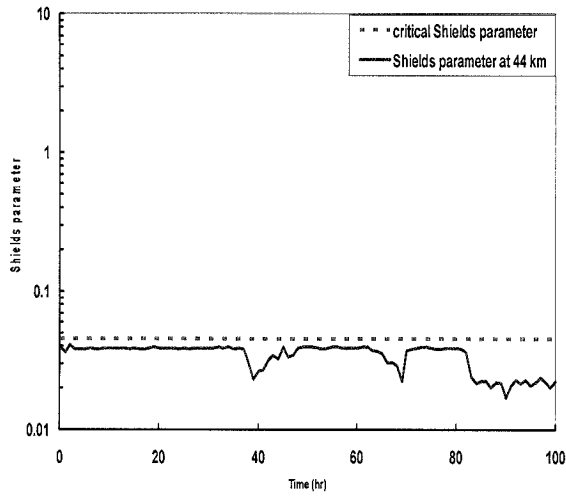
(a) 44 km
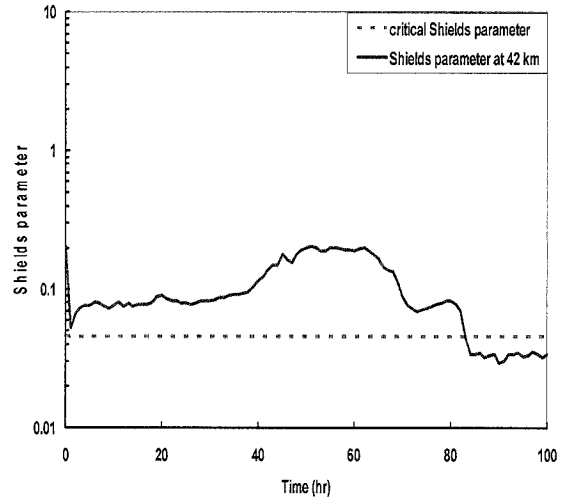
(b) 42 km
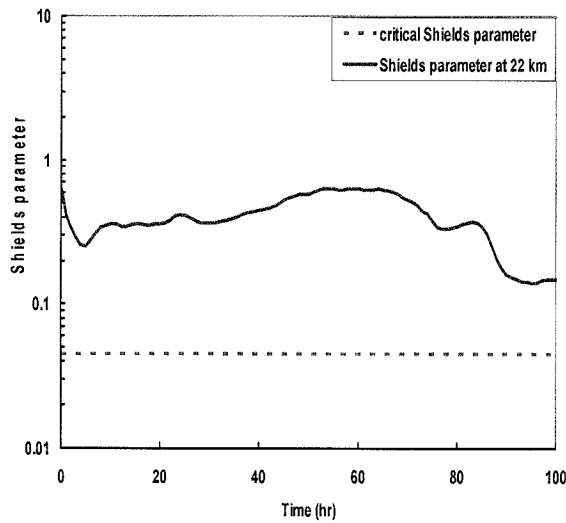
(c) 22 km
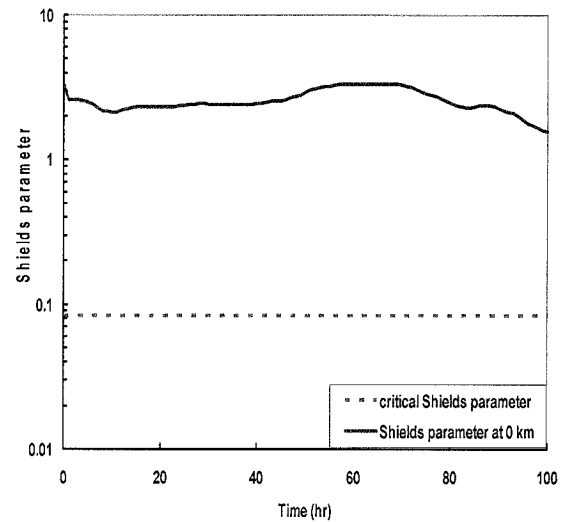
(d) 0 km

Figure 6-9. Critical Shields parameters and Shields parameters at the stations (44, 42, 22, and 0 km from the confluence with the Nakdong River) by unsteady simulation results for case 3 (flood peak)

Case 4 : Flood average
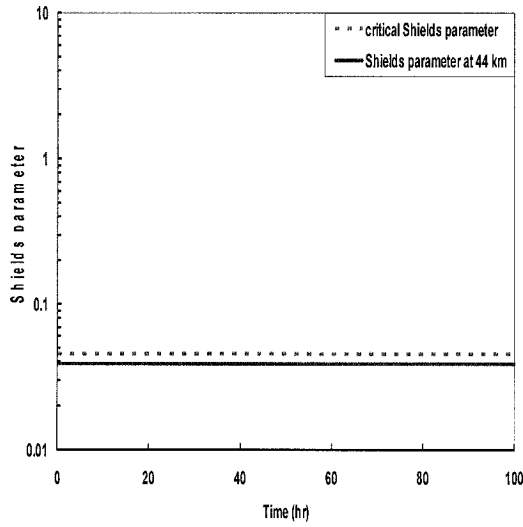
(a) 44 km
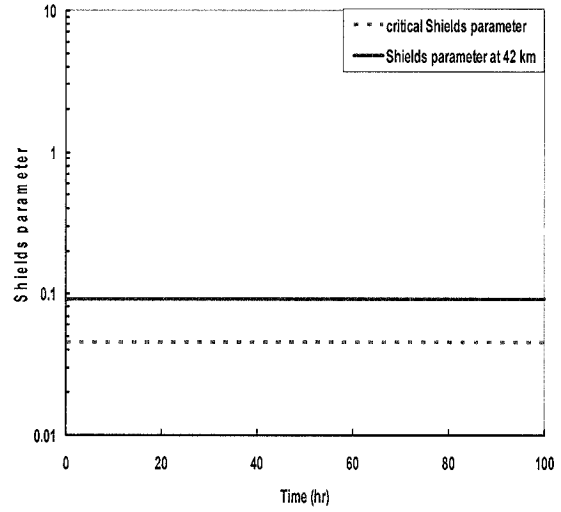
(b) 42 km
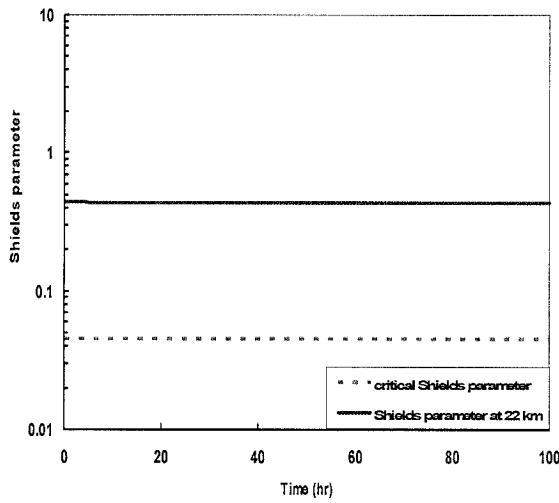
(c) 22 km
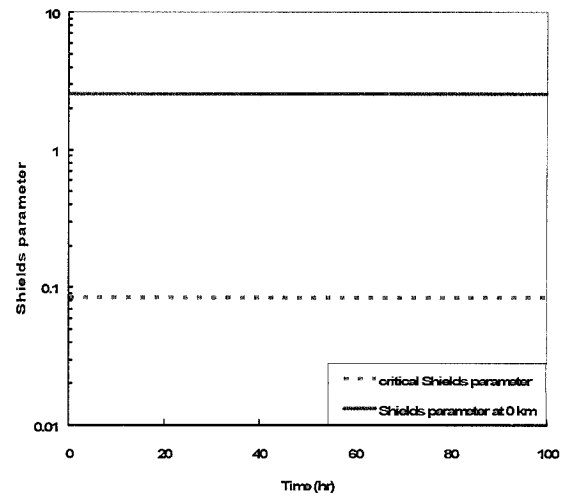
(d) 0 km

Figure 6-10. Critical Shields parameters and Shields parameters at the stations (44, 42, 22, and 0 km from the confluence with the Nakdong River) by unsteady simulation results for case 4 (flood average, 275.1 m^3/s)

Figures 6-11 to 6-14 show the comparisons of the critical Shields parameters and Shields parameters at 9 and 32 hours of the daily pulse (Case 1) and the daily average (Case 2) in 2005 and at 61 and 96 hr of the flood peak (Case 3) and the flood average (Case 4) in 2002, respectively, along the study reach. These times were selected and represent the maximum and minimum discharge times of the hydrograph. A detailed summary of the applied hydrographs and results for each case is shown in Table 6-4. As a result, during the peak flow at 9 hours for Case 1 and 61 hours for Case 3 result in larger Shields parameters than the critical Shields parameters. However, the Shields parameters from 45 to 41 km are lower than the critical Shields parameters, as shown in Figures 6-11 and 6-13. Cases 2 and 4 show similar patterns with Cases 1 and 3 as described before. Case 2 shows that the Shield parameters are larger than the critical Shields parameters along the study reach except from 45 to 41 km, but Case 4 shows that the Shields parameters is always larger than the critical Shields parameter for the entire study reach.

Table 6-4. Summary of the incipient motion analysis for the different discharges along the study reach at the specific times

Cases and corresponding Figures	Time (hr)	Discharge (m^3/s)	τ_{*c}	Average τ_*
Case 1 (daily pulse) Figure 6-11	9	91.4	0.043	2.425
	32	15.0	0.043	1.099
Case 2 (daily average) Figure 6-12	9	33.0	0.056	1.067
	32	33.0	0.056	1.067
Case 3 (flood peak) Figure 6-13	61	496.4	0.042	3.085
	96	96.6	0.042	1.630
Case 4 (flood average) Figure 6-14	61	275.1	0.043	2.425
	96	275.1	0.043	2.425
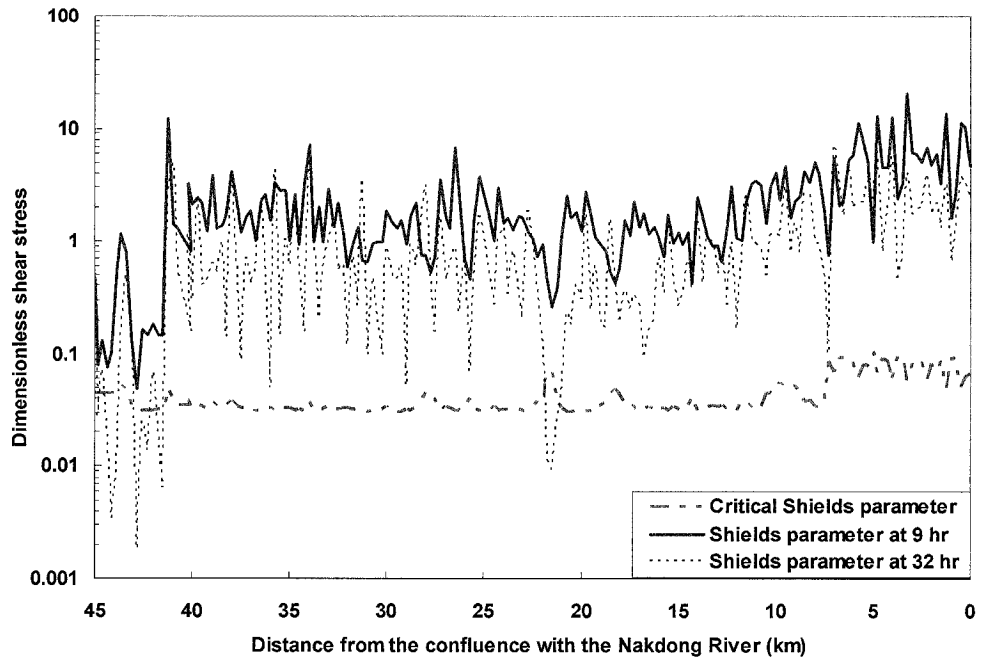
Figure 6-11. Critical Shields parameters and Shields parameters at 9 and 32 hr of the daily pulse for the Case 1 along the study reach
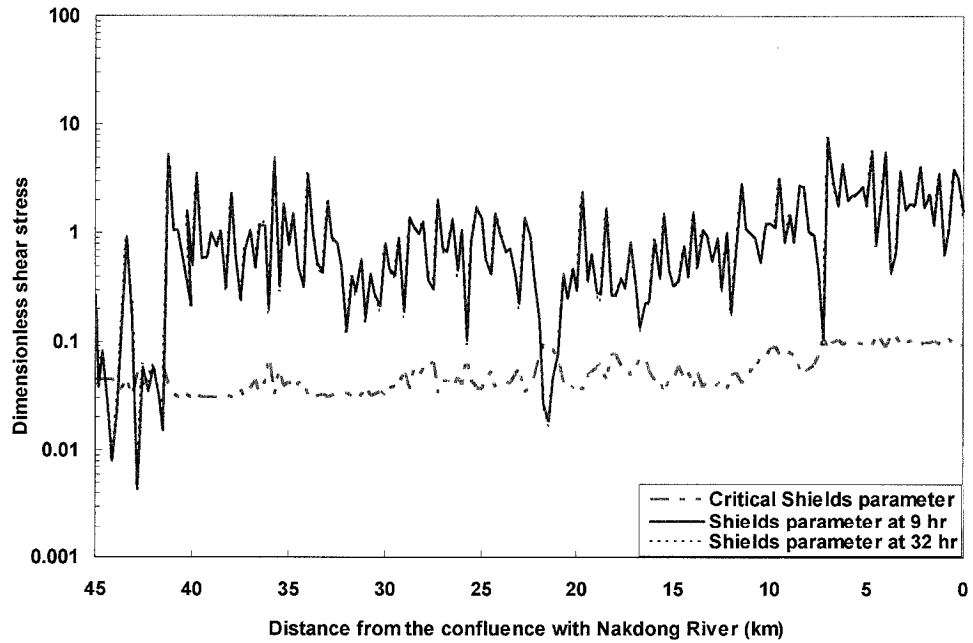
Figure 6-12. Critical Shields parameters and Shields parameters at 9 and 32 hr of the daily average (33.0 m³/s) for the Case 2 along the study reach

119
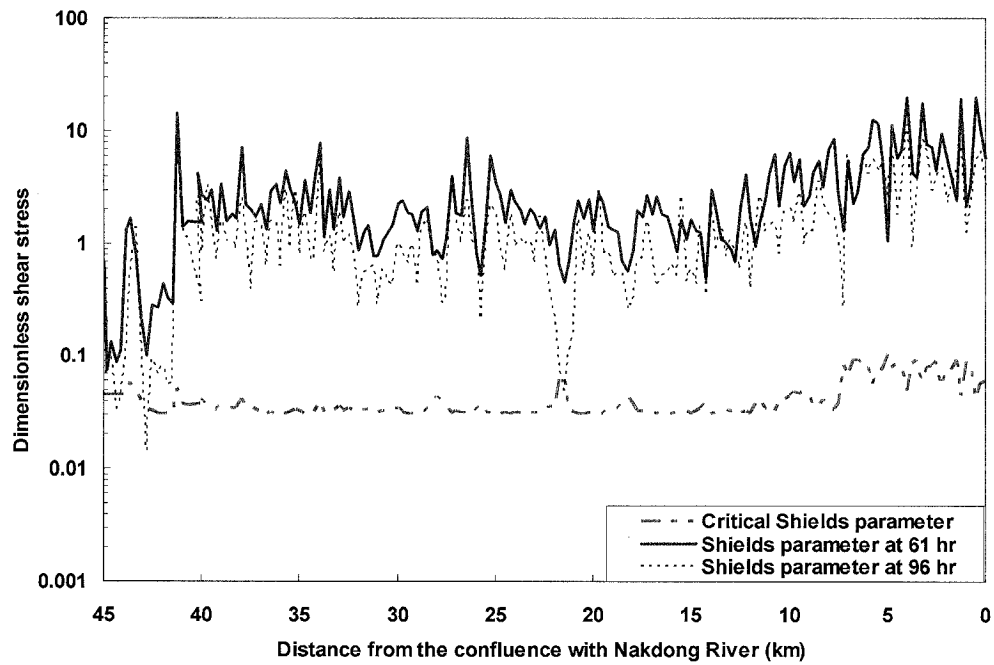
Figure 6-13. Critical Shields parameters and Shields parameters at 61 and 96 hr of the flood peak for the Case 3 along the study reach
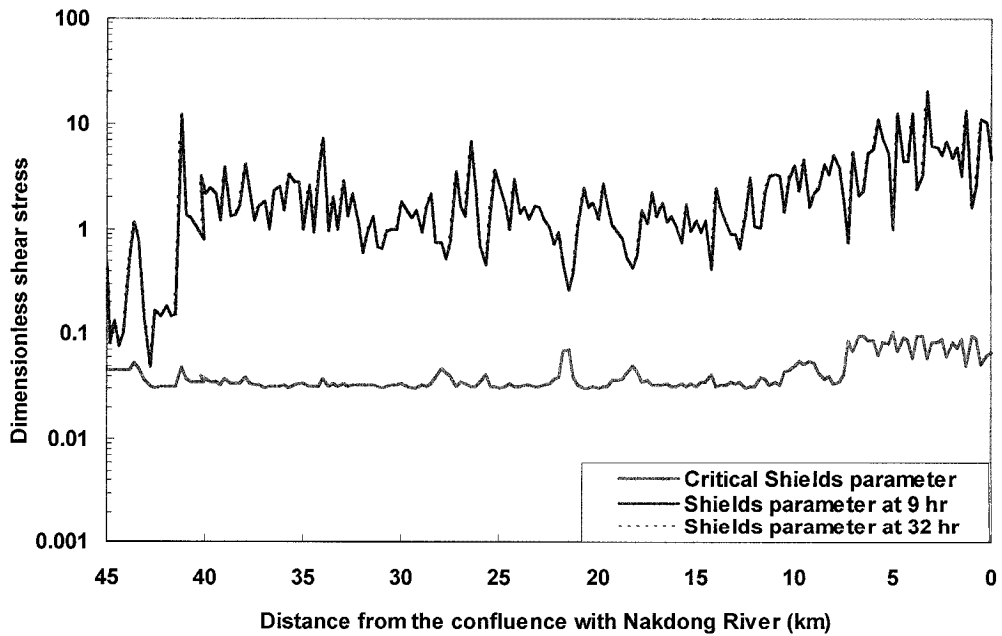
Figure 6-14. Critical Shields parameters and Shields parameters at 61 and 96 hr of the flood average (275.1 m^3/s) for the Case 4 along the study reach

120

6.3. Steady and Unsteady Sediment Transport Modeling

There are many other sediment and water routing models available, such as the HEC-6 (U.S. Army Corps of Engineers or USCOE, 1993), FLUVIAL-12 (Chang, 1998), CONCEPTS (Langendoen, 2000), EFDIC1D (Tetra Tech, 2001), CCHE1D (Wu and Vieira, 2002), GSTARS (Molinas and Yang, 1986; Yang and Simões, 2000; 2002), and GSTAR-1D (USBR, 2006). Among these models, HEC-6 and GSTARS do not have full dynamic modeling capability, so these two models were excluded for this study. The other models have similar modeling capability, including a full dynamic simulation. Finally, GSTAR-1D was selected because it is the model most recently developed by USBR.

Methodology

The simulations use the original 1983 and 2003 measured cross section and bed material gradation data at each cross section, and the daily flow data at Hapcheon Re-regulation Dam. After the closure of the Hapcheon Main Dam, the reservoir trapped more than 99% of the incoming sediment. The model assumes that there is no sediment entering from the upstream boundary at the re-regulation dam. The study reach ends at the confluence with the Nakdong River, where water surface elevations are used as the downstream boundary condition. The model consists of 204 cross sections starting at the re-regulation dam and ending at the confluence with the Nakdong River.

1983-2003 model calibration

Before long term (20 years) simulation of future channel changes, the model was calibrated using the steady flow conditions and by applying a bankfull discharge of 509.8 m³/s for the pre-dam period (1983-1988) and 86.3 m³/s for the post-dam period (1989-2003). The numerical model reproduces the same general shape and magnitude of the cumulative erosion and deposition in the main channel (Figure 6-15). Measured cumulative volume was determined by comparing the change in the cross-sections of 1983 and 2003 for each cross-section. A Minus values indicate erosion and plus values

indicate deposition. From the re-regulation dam to about 18 km from the confluence with the Nakdong River (27 km reach from the re-regulation dam), the field measurements show that the main channel was in a state of dynamic equilibrium and experienced erosion. The numerical model reproduces a similar trend, but predicts that there was less overall degradation along the 27 km. Between 18 km to 9 km from the confluence with the Nakdong River, the field measurements show that the main channel experienced slight erosion and deposition. The numerical model reproduces a similar trend, as shown in Figure 6-15. The other reach (from the 9 km to 0 km) shows degradation in the field measurements but the simulated results show slight aggradation. These differences between the observed and simulated values are due to dredging, which severely altered the channel bed. The dredged depths were more than 10 m in the reach between 5 km and 2.5 km.
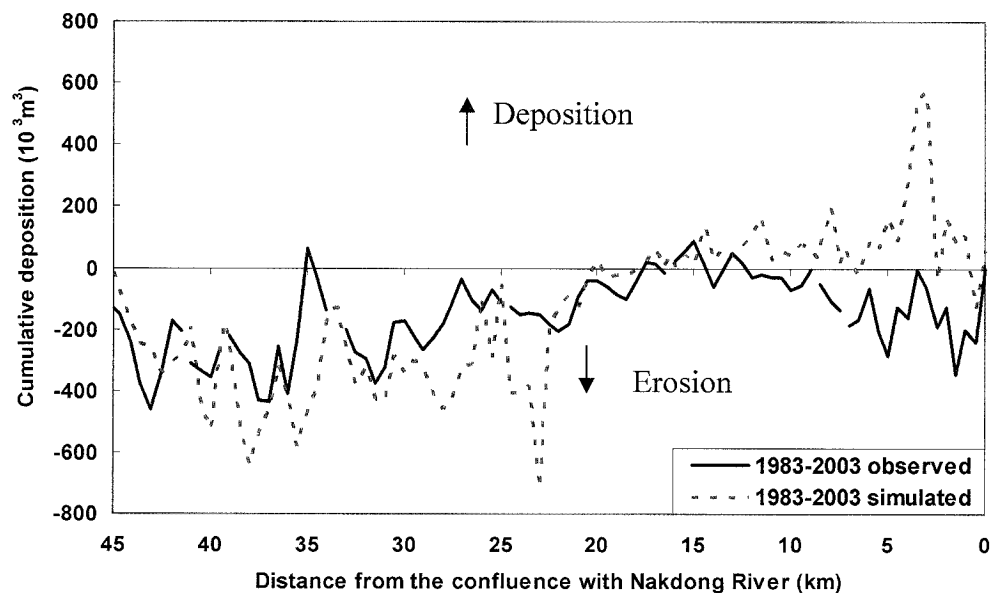
Figure 6-15. Measured and predicted cumulative total volume of sediment from 1983 to 2003

Figure 6-16 shows the measured and predicted thalweg elevation changes from the original thalweg elevation measured in 1983. Figure 6-17 shows measured and predicted thalweg elevations along the study reach. Overall, the model reproduces the thalweg elevation change with similar patterns. However, the simulated thalweg elevation is slightly under estimated (less degradation) compared with measured thalweg elevation

122

from 45 and 20 km reach from the confluence with the Nakdong River and it is a little over estimated (more aggradation) compared with measured thalweg elevation from 20 and 0 km.
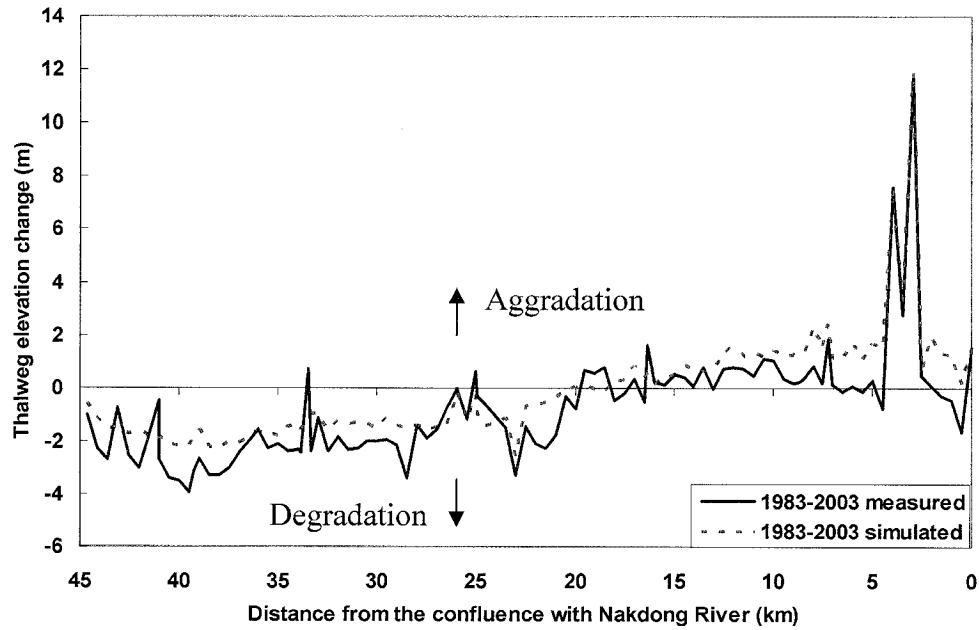
Figure 6-16. Measured and predicted thalweg elevation changes from 1983 to 2003
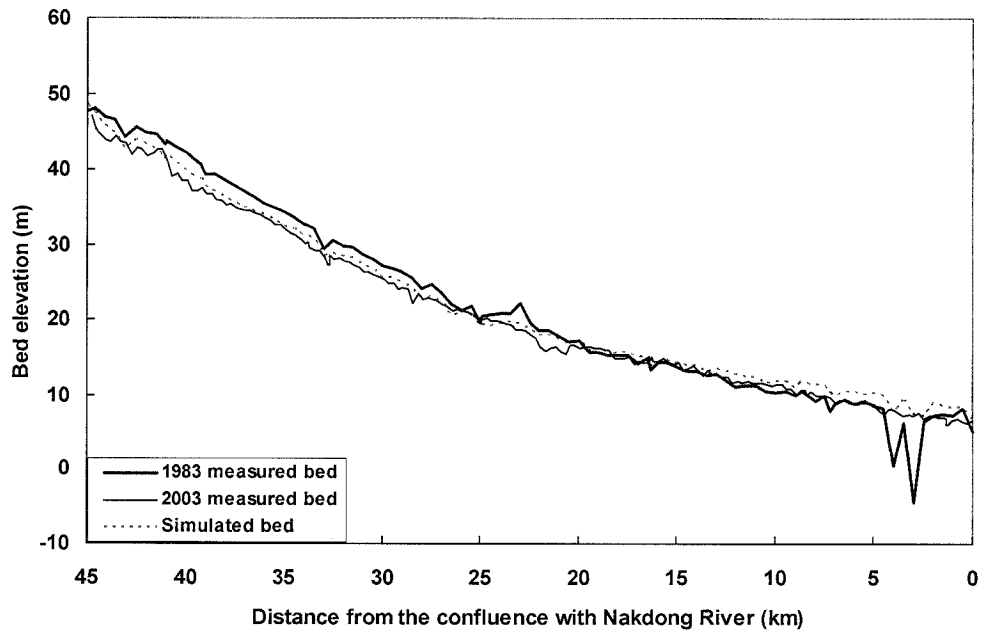
Figure 6-17. Measured and predicted thalweg elevations from 1983 to 2003

2003-2023 Prediction

After model calibration, the calibrated parameters are used for the 2003 to 2023 predictive model. In addition, the model uses 2003 cross-section data, bed gradation, and the average discharge data of the post-dam period (86.3 m^3/s). The predictive discharge data were reproduced based on the historical record at the re-regulation dam from 1989 to 2005. It is hypothesized that the discharge for the next 20 years (2003~2023) will follow the same pattern and values as shown from the previous recorded discharge (1989~2003) at the re-regulation dam. Figure 6-18 shows the future cumulative erosion and deposition in the study channel. Most of the erosion will occur from 45 km to 33 km after 2003. The remaining channel is stable in a state of equilibrium. In addition, most of the erosion and deposition occurred during the first 10 years.
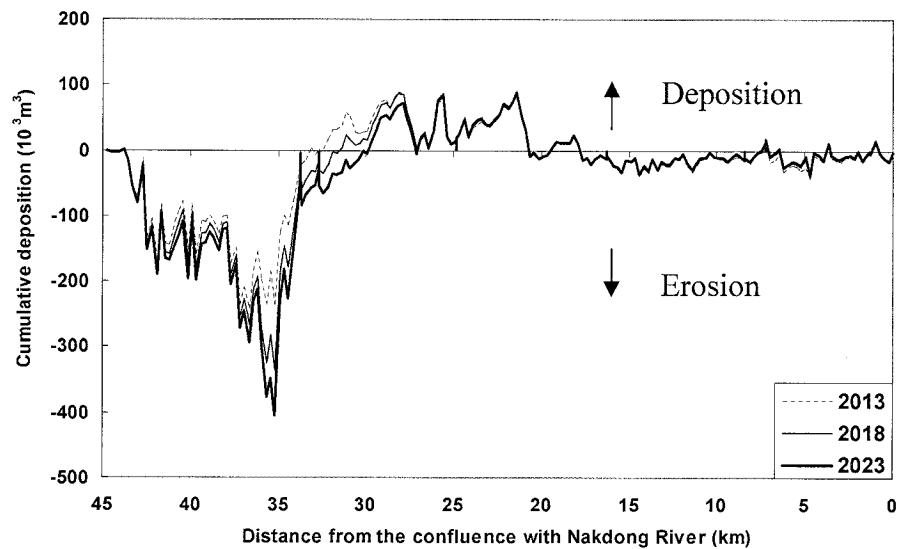
Figure 6-18. Predicted cumulative erosion and deposition of sediment (2003 to 2023)

Figure 6-19 shows the measured and predicted thalweg elevations in 1983, 2003, 2013, 2018 and 2023. The channel eroded in the 45 km to 25 km reach after 1983. The changes in the thalweg elevations stopped varying in 2013. There were few observable changes in the thalweg elevations from 2013 and 2023. Figure 6-20 shows predicted thalweg elevation change from 2003~2013, 2013~2018 and 2018~2023. The maximum

channel scour depth was about 4 m near the re-regulation dam (45 to 25 km) after 1983. The remaining reach is relatively stable.
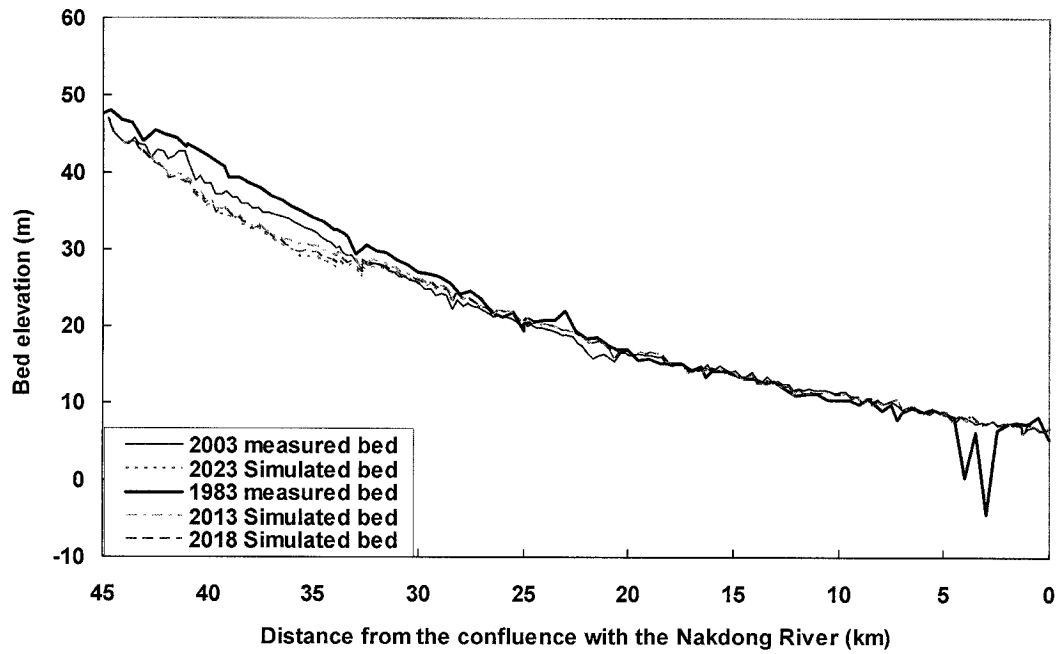
Figure 6-19. Measured (2003) and predicted (2023) thalweg elevations from 2003 to 2023 for 20 years
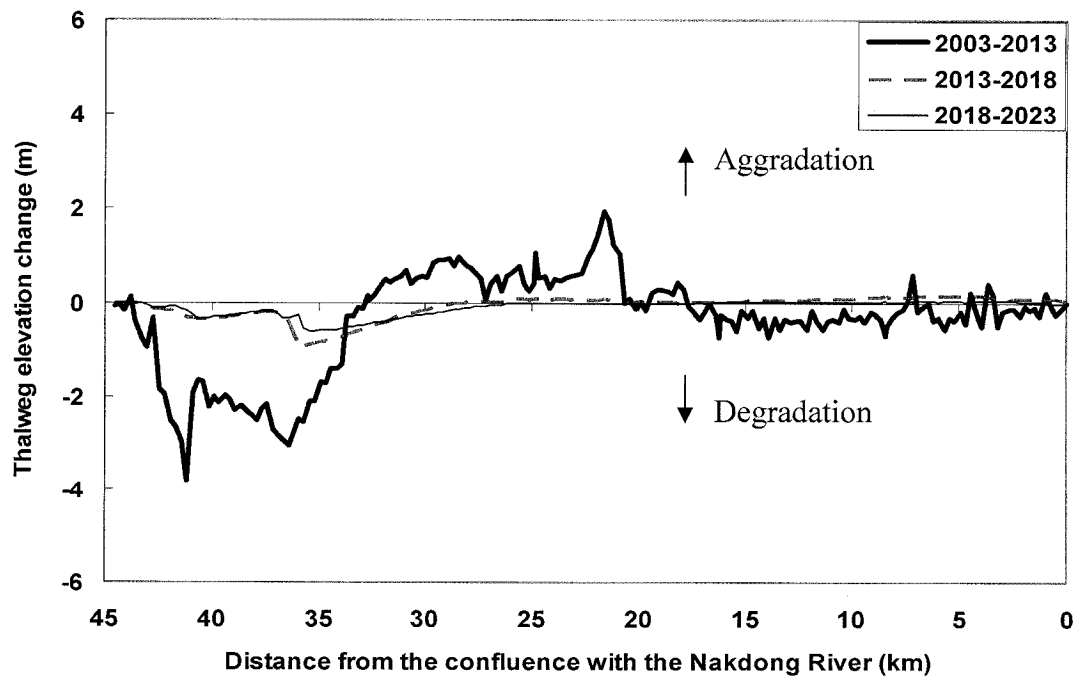
Figure 6-20. Predicted thalweg elevations change for 20 years from 2003

Figure 6-21 represents the median bed material sizes along the study reach of the measured values (1983 and 2003), and the predicted values (2005, 2013 and 2023). The results indicate that most of the bed material changes occur from 45 km to 33 km, just as seen in the thalweg elevation change (Figure 6-20). After 2013, there was very little variation in the bed material. However, the bed material increased an average of 9 mm from about 1 mm in 2003.
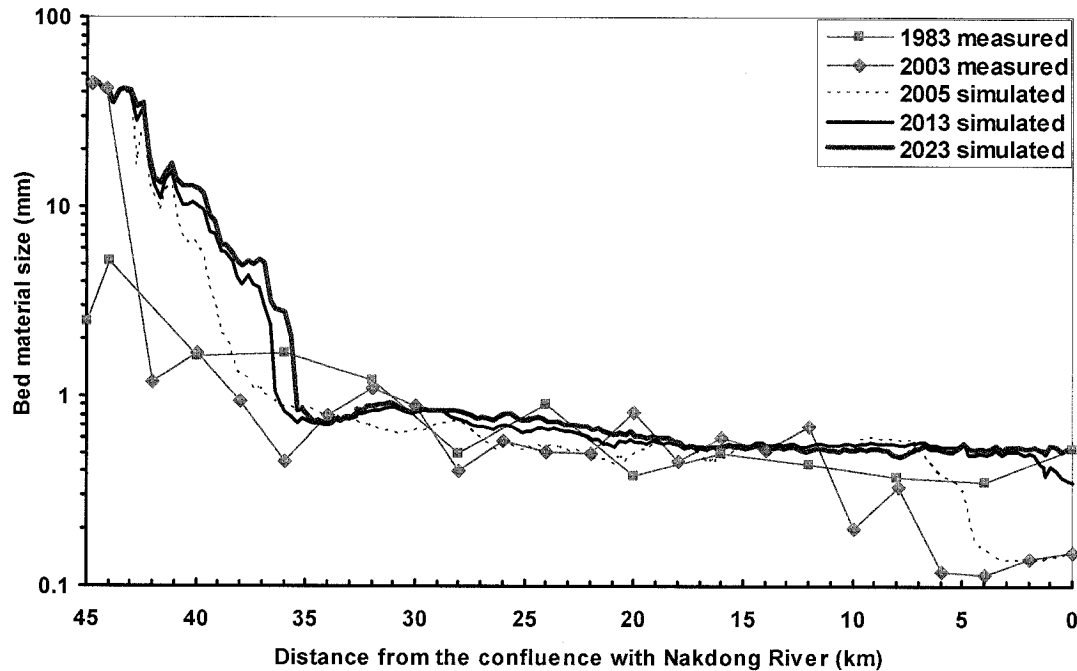
Figure 6-21. Measured (1983 and 2003) and Predicted median bed material size (d_{50}, mm) from 2003 to 2023 for 20 years

Unsteady simulation for the typical and extreme flood events

To analyze the effect caused by the flow pulse and flood, the four cases from the unsteady flow simulation (Section 6.1) were used for the unsteady sediment transport simulation. GSTAR-1D model was used to predict these changes (Table 6-6). The applied parameters are from the 2003 to 2023 predictive model in the previous section. The model used 2003 cross-section data and the bed gradation. The simulation was run for 100 hours in each case. The water surface elevation at the end of study reach (45 km

126

downstream from the Hapcheon Re-regulation Dam) is the downstream boundary condition, and was calculated using HEC-RAS unsteady flow simulation (Section 6-1).

Table 6-5. Cases of unsteady simulations by using the GSTAR-1D

Case	Flood type	Period (100 hrs)	Maximum discharge (m^3/s)	Minimum discharge (m^3/s)
1	Daily pulse	7/2, 2005 07:00 ~	92.9	13.2
2	Daily average	7/6, 2005 10:00	33.0	33.0
3	Flood peak	8/30, 2002 01:00 ~	504.0	74.9
4	Flood average	9/3, 2002 04:00	275.1	275.1

Figure 6-22(a) shows the difference in the cumulative sediment loads (tons) from the daily pulse (Case 1) minus the daily average (Case 2). A positive value suggests that the cumulative sediment loads determined by the daily pulse are larger than the daily average and vice versa for the negative values. From the result, daily pulse (Case 1) affected the entire study reach because the sediment volume of daily pulse (Case 1) is larger than the sediment volume of daily average (Case 2) along the study reach. In the same manner, the difference of the cumulative sediment loads (tons) of the flood peak (Case 3) minus the flood average (Case 4) is shown in Figure 6-22(b). The values are larger than zero along most of the study reach, especially at the reach between 45 and 25 km, but the values are less than zero from 10 km to 0 km.

A summary table is provided for the simulated and measured transport rate for the four cases (Table 6-7). The results indicate that the sediment transport rate (tons/day) due to the daily pulse (Case 1) is 21% larger than those produced by the daily average (Case 2), as shown in Figure 6-23(a). In addition, the sediment transport rate (tons/day) due to the flood peak (Case 3) is 15% larger than those calculated by the flood average (Case 4), as shown in Figure 6-23(b). In addition, Table 6-6 contains the measured sediment transport rate (tons/day) estimated from the reservoir survey (sediment deposition) at the Hapcheon Main Dam in 2002. There is a significant increase in the sediment transport rate by comparing the simulated and measured values (Figure 6-24).

(a) Case 1 and Case 2   (b) Case 3 and Case 4
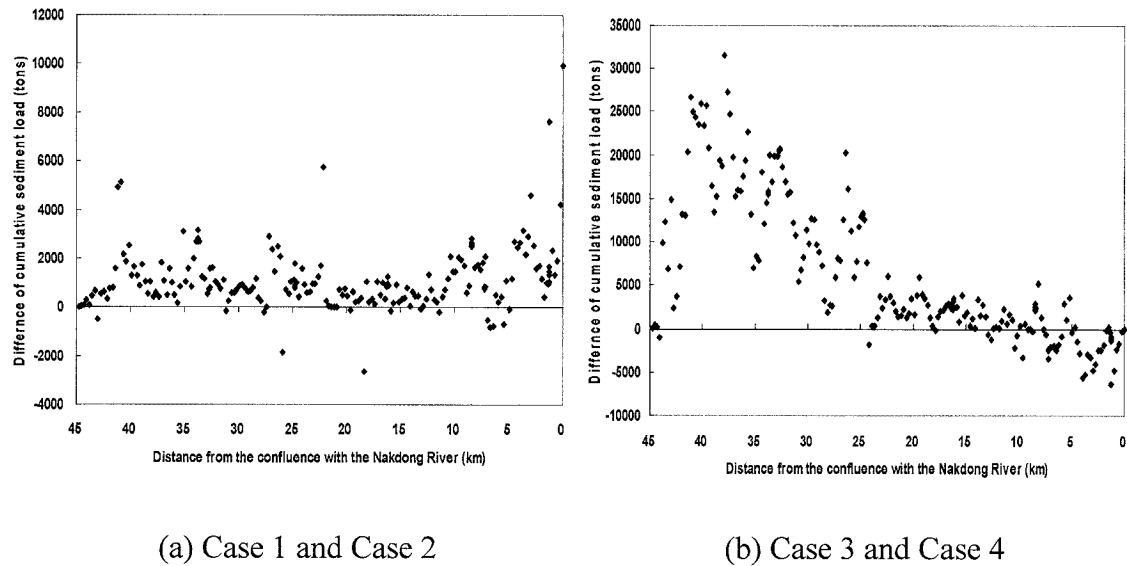
Figure 6-22. Difference of the cumulative sediment load (tons) of the Case 1 minus Case 2 (a) and Case 3 minus Case 4 (b). The plus value represents that the cumulative sediment loads of Case 1 and Case 3 are larger than those of Case 2 and Case 4

Table 6-6. Simulated and measured sediment transport rate for the four cases

	Sediment transport rate (tons/day)			
	Case 1	Case 2	Case 3	Case 4
Simulated	1,594 (121 % of Case 2)	1,316	11,876 (115 % of Case 4)	10,331
Estimated (2002)	1,044	1,044	1,044	1,044
% of simulated and measured	153 %	126 %	1,138 %	990 %

*Simulated: Simulated sediment transport rate due to the daily pulse (Case 1), daily average (Case 2), flood peak (Case 3), and flood average (Case 4) by unsteady simulation using GSTAR-1D sediment transport model

*Estimated (2002): Estimated sediment transport rate from the survey of the reservoir sediment deposition of the Hapcheon Main Dam in 2002

*% of simulated and measured: the percent of simulated sediment transport rate (tons/day) by the measured (2002) sediment transport rate (tons/day)

*(%) of the Case 2 and Case 4: the percent of the sediment transport rate of the daily peak and flood peak (Case 1 and Case 3) by these of the daily average and flood average (Case 2 and Case 4)

(a) Case 1 and Case 2
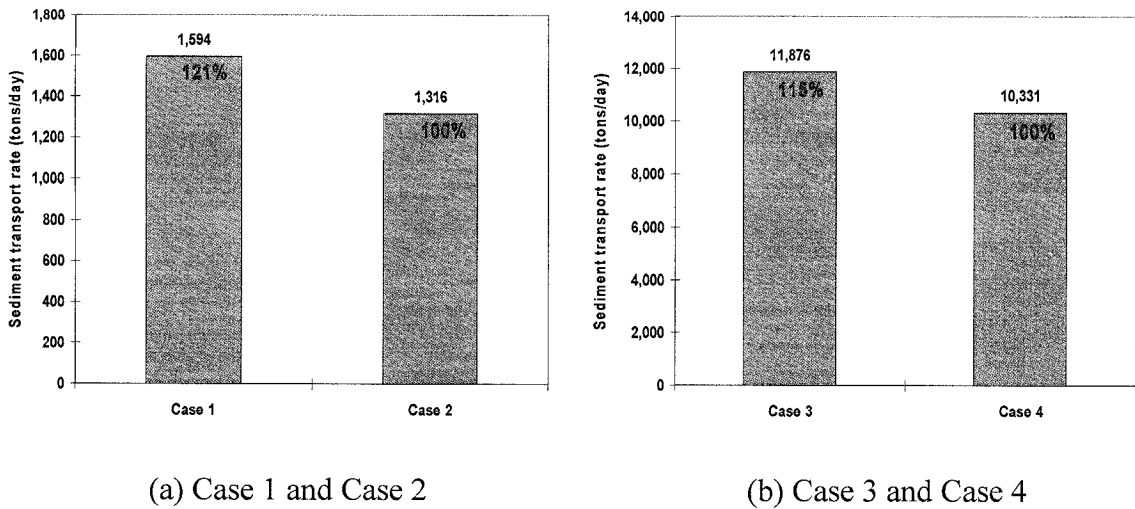
(b) Case 3 and Case 4

Figure 6-23. Comparison of simulated sediment transport rate (tons/day) for Case 1 and Case 2 (a), and Case 3 and Case 4 (b)
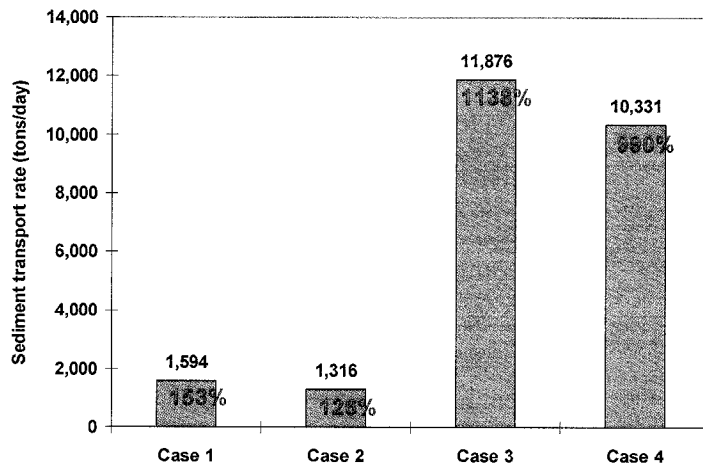
Figure 6-24. Comparison of the simulated sediment transport rates (tons/day) and percent of the simulated and estimated sediment transport rate (1,044 tons/day) from the survey of the reservoir sediment deposition of the Hapcheon Main Dam in 2002

The following analytical method was used to check the simulated sediment transport rate determined by GSTAR-1D based on flow pulses and average flow values (Cases 1 and 2). The analysis assumes that the sediment rating curve is applicable as a first approximation.

$$Q_s = aQ^b \tag{6-1}$$

Where, Q_s = sediment discharge (m^3), Q = flow discharge (m^3), $a = 9.77$, $b = 1.49$ from the estimated sediment-discharge rating curve by Yang's (1973) method in Chapter 4.
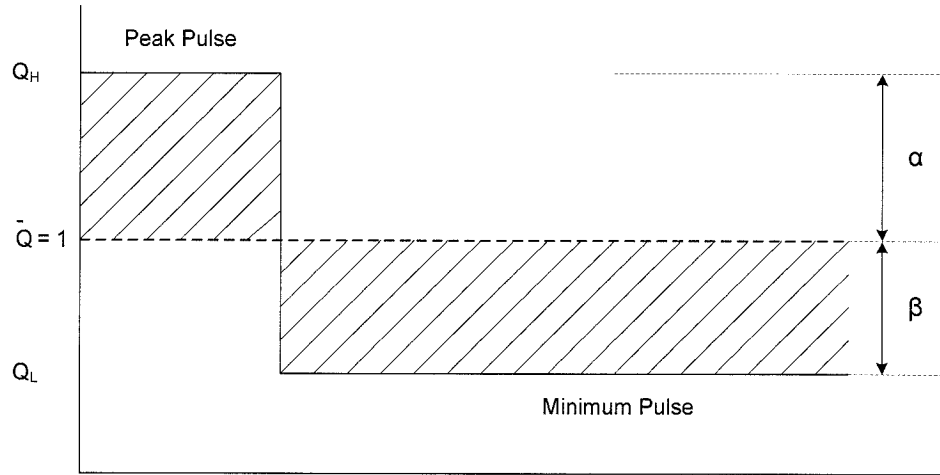
Figure 6-25. Diagram of flow pulse

Sediment volume is estimated based on the following formulae.

$$V_S = \int Q_s dt \tag{6-2}$$

$$\alpha = Q_H - \bar{Q} \tag{6-3}$$

$$\beta = \bar{Q} - Q_L \tag{6-4}$$

Where, V_S = sediment volume, α and β = difference of peak flow pulse, lowest flow pulse from average flow, Q_H = peak pulse flow (m^3), Q_L = minimum pulse flow (m^3), $\bar{Q}$ = average pulse flow (m^3)

Set, $n = 1$ when the duration of pulse (P_d) is 24 hours ($n = 2$ when P_d is 12 hr, $n = 3$ when P_d is 8 hr)

$$\bar{Q} = \frac{Q_H + (n-1)Q_L}{n} \tag{6-5}$$

Rearrange Equation (6-5)

$$Q_H - \bar{Q} = (n-1)\bar{Q} - (n-1)Q_L \tag{6-6}$$

Then, $\qquad\qquad \alpha = (n-1)\beta \tag{6-7}$

$$\frac{Q_H}{Q_L} = \frac{1+\alpha}{1-\beta} = \frac{1+(n-1)\beta}{1-\beta} = \frac{1-\beta+\beta n}{1-\beta} = R \tag{6-8}$$

$$\beta = \frac{R-1}{R+n-1} \tag{6-9}$$

$$V_s = \frac{(1+\alpha)^b + (n-1)(1-\beta)^b}{n} \tag{6-10}$$

Then, the ratio of sediment volume of flow pulse and sediment volume of average flow, K_p is follows.

$$K_p = \frac{V_{s\_pulse}}{V_{s\_avg.}} = \frac{[1+(n-1)\beta)]^b + [(n-1)(1-\beta)^b]}{n} \tag{6-11}$$

Where, V_{s_pulse} = sediment volume of flow pulse (m^3), $V_{s\_avg.}$ = sediment volume of average flow (m^3).

For the Hwang River study reach, the parameters for Case 1:

$Q_H = 64.4$ m^3/s and $Q_L = 14.4$ m^3/s

$n = 3$ (duration of pulse is 8 hr in 24 hr)

$$R = \frac{Q_H}{Q_L} = \frac{64.4}{14.4} = 4.47$$

$$\beta = \frac{R-1}{R+n-1} = \frac{4.47-1}{4.47+3-1} = 0.536$$

$b = 1.49$

$$\therefore K_p = \frac{V_{s\_pulse}}{\overline{V}_{s\_avg.}} = \frac{[1+(n-1)\beta]^b + [(n-1)(1-\beta)^b]}{n}$$

$$= \frac{[1+(3-1)\times 0.536]^{1.49} + [(3-1)\times(1-0.536)^{1.49}]}{3} = 1.20$$

Therefore, the sediment volume of a flow pulse is 20% larger than that of average flow. The result of 1.21 was determined using GSTAR-1D, as shown in Table 6-6 and Figure 6-23(a). Figure 6-26 shows the variation in the ratio of sediment volume by flow pulse to the sediment volume by flow average and the ratio of flow peak and low flow corresponding to the variation of b values. As a result, the ratio of sediment volume by flow pulse and average flow may increase by increasing b values. The ratio of sediment volume is 1 when b value is 1 (Figure 6-26).
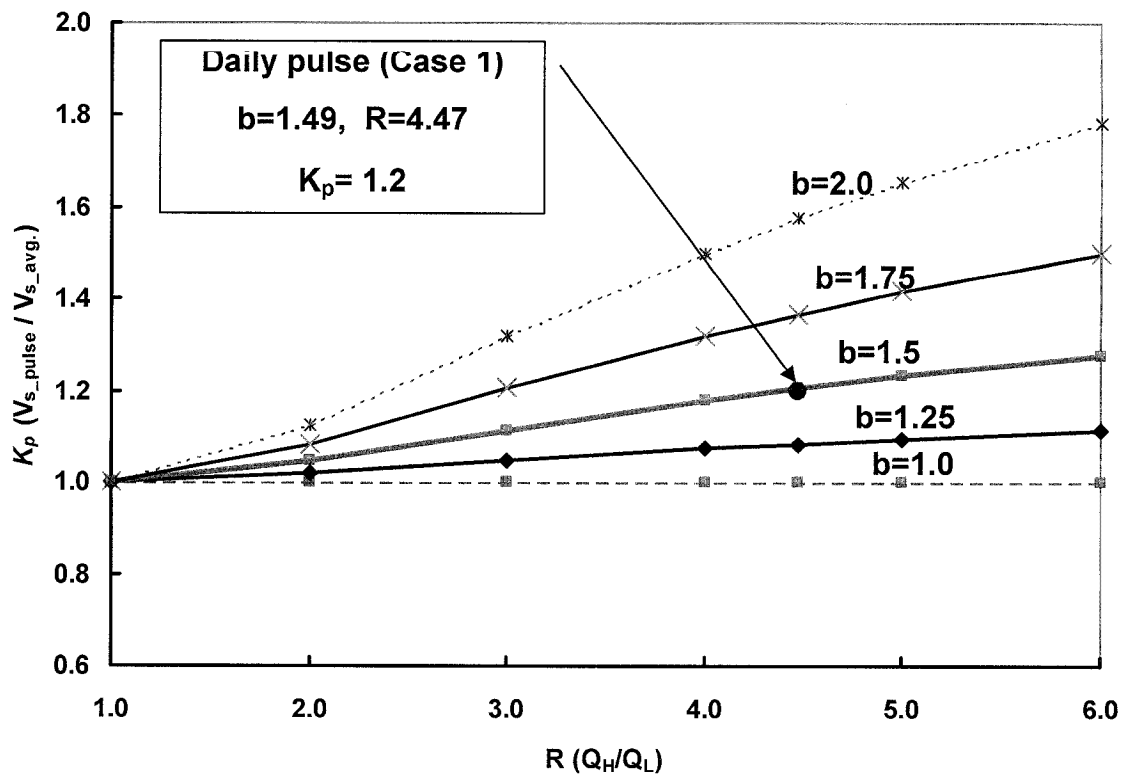
Figure 6-26. Variation of ratio the sediment volume by flow pulse to the sediment volume by average flow corresponding to the variation of b values

The cumulative volumes of erosion and deposition (m^3) by the daily pulse (Case 1) and daily average (Case 2), and by the flood peak (Case 3) and flood average (Case 4) at each cross-section along the study reach are shown in Figures 6-27 and 6-28, respectively. There are few noticeable differences in deposition and erosion from comparing Cases 1 and 2, and Cases 3 and 4, as shown in Figures 6-27 and 6-28.
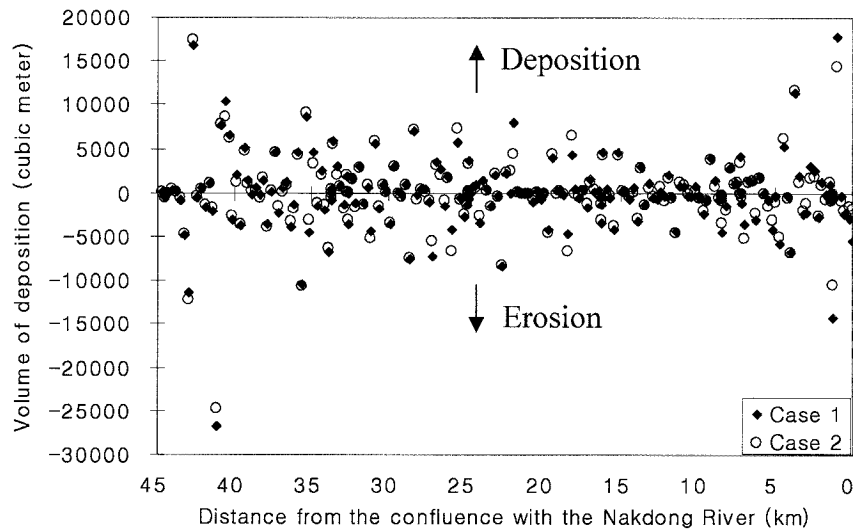
Figure 6-27. The cumulative volumes of erosion and deposition (m^3) by the daily pulse (Case 1) and daily average (Case 2) along the study reach
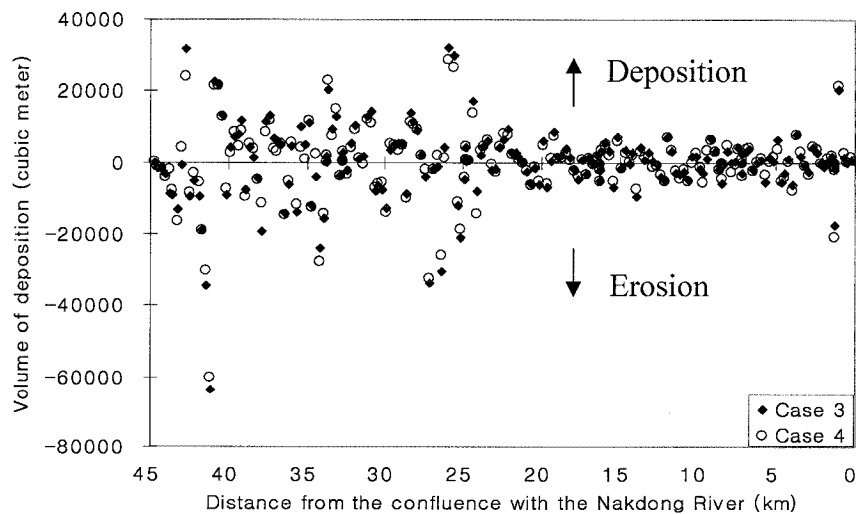
Figure 6-28. The cumulative volumes of erosion and deposition (m^3) by the flood peak (case 3) and flood average (case 4) along the study reach

133

The summary of total cumulative volumes of erosion and deposition (m³) is shown in Table 6-8. The cumulative volumes of erosion and deposition (m³) of Cases 2 and 4 are about 90% of the values determined by Cases 1 and 3.

Table 6-7. Cumulative total volume of erosion and deposition at the entire study reach by each case

	The cumulative total volume of erosion and deposition (thousand m³)			
	Case 1	Case 2	Case 3	Case 4
Erosion	259 (108 % of Case 2)	239	632 (107 % of Case 4)	592
Deposition	245 (106 % of Case 2)	232	632 (107 % of Case 4)	592

- (%) : the percentage of the Case 2 and Case 4 of the Case 1 and Case 3 respectively.

6.4. Summary

The Hapcheon Re-regulation Dam was constructed to re-regulate the peak discharge from the main power station to a value of 15 m³/s for a 24 hours period. Although the re-regulation dam regulates the discharge from the main dam, flow pulses are still generated by the re-regulation dam operation during flood season. The pulses are caused when the gate is opened to pass exceeded water from the reservoir at the re-regulation dam, including discharge from the power station at the re-regulation dam. The flow pulses were analyzed and evaluated.

To estimate and evaluate the effect on the downstream channel by flow pulses, the four cases included daily pulse (Case 1), daily average (Case 2), flood peak (Case 3), and flood average (Case 4) discharge hydrographs applied for unsteady simulation for 100 hours along the study reach. An attenuation of flow occurred at the downstream boundary. The differences in the water depths (Max.-Min.) were 0.62 m for Case 1 and 1.37 m for Case 3.

From the calculated hydraulic parameters, incipient motion analyses were performed by comparing the Shields parameters to the critical Shields parameters for all four cases, at 44, 42, 22 and 0 km from the confluence with the Nakdong River. As a result, Cases 1 and 2 showed that the critical Shields parameters were lower than the Shields parameters except from 44 km to 42 km from the confluence with the Nakdong River (immediately downstream from the re-regulation dam). However, the critical Shields parameters were lower than Shields parameters along most of the study reach in Cases 3 and 4. The critical Shields parameters and Shields parameters at the times of peak and minimum hydrographs were also compared along the study reaches. These values showed a similar trend for the four cases. The flow pulses have greater effect on most study reaches except from 45 km to 42 km because this section of the river bed is already armored due to the dam construction.

To evaluate the dam effect to the downstream channel geometry, a one-dimensional sediment transport model (GSTAR-1D) was selected for this study. The first simulation used the original 1983 measured cross-section and bed material gradation data and the daily flow data from Hapcheon Re-regulation Dam to calculate the model over 20 years (1983 to 2003) as a non-uniform flow condition. These simulation results were compared with measured data in 2003. The numerical model reproduces a similar trend to the measured data in 2003.

After that, the model predicts future channel bed elevation (thalweg elevation) and bed material size change along the study reach for 20 years from 2003 to 2023. The measured data of 2003 were used for this simulation. The bed elevation change mostly occurred from 45 km to 33 km after 2003 from the confluence with the Nakdong River. The maximum scour depth was about 4 m near the re-regulation dam (45 to 25 km) after 1983. These bed elevations will become stable within 10 years (2013) from 2003, as shown in Figure 6-21. The simulated average bed material size will be coarsened in 2023 (from 1 mm to 9 mm) from 43 km to 35 km according to the comparison values measured in 2003. However, the bed material is stable in the remaining portion of the river.

The third simulation performed for the four unsteady flow conditions is presented in Table 6-1. The sediment transport rate (tons/day) due to the daily pulse (Case 1) is 21% larger than those determined by the daily average (Case 2). The sediment transport rate (tons/day) due to the flood peak (Case 3) is 15% larger than those determined by the flood average (Case 4), as shown in Figure 6-25. In addition, daily pulse (Case 1) affected entire reach and flood peak (Case 3) affected about 20~25 km reach below the re-regulation dam according to the Figure 6-22.

7 CONCLUSIONS

This dissertation evaluates and predicts the river channel changes over the 45 km reach of the Hwang River between the Hapcheon Re-regulation Dam and the confluence with the Nakdong River. Historical time series data such as flow rate, aerial photos, cross-section survey, sediment transport, and bed material data were gathered, estimated and applied for this study reach. This is a good example of response in alluvial channel geometry to alterations in water and sediment discharge caused by dam construction. Also, this dissertation quantifies the effects on channel morphology of flow pulses caused by gate opening of the Hapcheon Re-regulation Dam.

A dataset that documents the changing water and sediment regimes and the corresponding lateral and vertical adjustments of the channel from 1982 to 2004 was utilized to quantify historic trends. Also, the flow pulses are simulated using a numerical sediment transport model (GSTAR-1D). The primary conclusions are as follows:

1. The historic analysis revealed significant differences between pre and post-dam hydraulic geometry parameters. During the post-dam period (1989-2005) the peak flows decreased (19.3% of pre-dam period). Following construction of the Hapcheon Main Dam and re-regulation Dam in 1989, the sediment supply was artificially eliminated and the channel bed coarsened from sand to gravel (from 2.16 mm to 44 mm) over the 5 km reach below the re-regulation dam. River channel bed elevation degraded up to 2.6 m over the 20 km reach downstream of the re-regulation dam. The channel adjustment trends toward narrowing and stability increased following construction of the dam.

2. The two methods are used to predict future changes and estimate equilibrium states for this study reach and a statistical analysis is performed to know the relationship with each hydraulic geometry parameter. A sediment transport model is also used to predict future channel changes.

a) The first method used the hydraulic geometry equations of Lacey's (1929) and Julien and Wargadalam (1995), as shown in Figures 5-1 and 5-2. The method of Julien and Wargadalam (1995) showed better results. These results showed the trend of channel narrowing and deepening following the dam completion. The estimated equilibrium channel width was 116.5 m compared to the 2004 channel width of 178.9 m and the estimated bed slope was 0.00117 compared to the 2003 bed slope of 0.00168, as shown in Table 5-1.

b) The second method used the exponential function for the channel width from Richard et al. (2005). This model showed a good agreement (especially sub-reach 3). The estimated equilibrium channel width was 75 m compared to the 2004 channel width for the entire reach. The prediction of the future channel width also showed a good result.

c) Correlation and multiple regression models showed that channel width change rate was significantly associated with measures of flow energy (stream power) and the channel width change, channel width change rate, vegetation expansion change rate and change of islands area. Also, bed slope was significantly associated with measures of active channel area and sinuosity.

d) According to the result of GSTAR-1D model, the thalweg elevation will be in stable/equilibrium condition around 2013~2015 and the simulated thalweg elevation of 2013 is predicted to remain almost identical to that in 2023. In addition, the bed elevation change mostly occurred along the 20 km reach from the re-regulation dam after 1983. The maximum channel scour depth was about 4 m after 1983.

These bed elevations will become stable within 10 years (2013) from 2003. The simulated average bed material size will be coarsened in 2023 (from 1 mm to 9 mm)

3. The effect of flow pulses on channel geometry is examined for the four cases in relation to incipient motion and sediment transport from mathematical model (GSTAR-1D) simulations. Case 1 is daily pulse flow and case 2 is daily average flow (average of Case 1). Case 3 is flood peak and Case 4 is flood average (average of Case 3).

a) According to the incipient motion analysis, the four flow conditions do not affect the 3 km reach downstream from the re-regulation dam because this reach is already armored. The other reaches below 3 km downstream from the re-regulation dam will be affected by the four flow cases.

b) The second simulation was performed for the four unsteady flow conditions as presented in Table 6-1. As a result, the sediment transport rates (tons/day) when applying the daily pulse (Case 1) and flood peak (Case 3) flow were 21% and 15% larger than those of the daily average (Case 2) and flood average (Case 4), respectively. In addition, daily pulse (Case 1) affected entire reach and flood peak (Case 3) affected about 20~25 km reach below the re-regulation dam according to the Figure 6-22.

BIBLIOGRAPHY

Ackers, P., and White, W.R. 1973. "Sediment transport: New approach and analysis." *Journal of Hydraulics Division,* ASCE, vol, 99, no. HY11, Proceeding paper 10167, pp. 2041-2060.

ASCE Task Committee on Hydraulics, Bank Mechanics, and Modelling of River Width Adjustment. 1998. "River Width Adjustment. I: Process and Mechanisms." *Journal of Hydraulic Engineering,* 124 (9).

Assani, A.A., and Petit F. 2004. "Impact of Hydroelectric Power Releases on the Morphology and Sedimentology of the bed of the Warche River (Belgium)." *Earth Surf. Process. Landform.* 29, pp.133-143.

Bagnold, R.A. 1956. The flow of cohesionless grains in fluids." *Philosophical Transactions of the Royal society of London, Series A: Mathematical, Physical and Engineering Sciences* 249: 235-297.

Batalla, R.J., and Martin-Vide, J.P. 2001. "Thresholds of particle entrainment in a poorly sorted sandy gravel-bed river." Catena 44(2001) 223-243.

Bledsoe, B.P. and Watson, C.C. 2001. "Logistic analysis of channel pattern thresholds: meandering, braiding, and incising. *Geomorphology* 38, pp.281-300.

Blench, T. 1957. "Regime behavior of canals and rivers." London, Butterworths.

Blench, T. 1969. "Mobile-bed Fluviology: A regime treatment of canals and rivers." *University of Alberta Press,* Edmonton, Canada, p.168.

Brandt, S.A. 2000a. "Classification of geomorphological feffects downstream of dams." *Catena,* 40, pp.375-401.

Brandt S.A. 2000b. "Prediction of downstream geomorphological changes after dam construction: a stream power approach." *WaterResources Development* **16**: 343–367.

Brebner, A., and Wilson, K.C. 1967. "Determination of the regime equation from relationships for pressurized flow by use of the principle of minimum energy degradation." *Proceedings of the Institution of Civil Engineers,* 36, pp.47-62.

Brierley, G.J., and Fryirs, K.A. 2005. "Geomorphology and River Management: Applications of the river Styles Framework." *Blackwell Publishing.* 398 p.

Brunke, M., and Gonser, T. 1997. "The ecological significance of exchange processes between rivers and ground-water." *Freshwater Biol.* 37, pp.1–33

Buffington, J.M. 1995. "Effects of hydraulic roughness and sediment supply on surface textures of gravel-bedded rivers." *Univ. of Wash., Seattle*, M.S. thesis, 184 p.

Cao, Z., Pender, G., and Meng, J. 2006. "Explicit formulation of the Shields Diagram for incipient motion of sediment." *Journal of Hydraulic Engineering*, Vol. 132, No. 10.

Chang, H.H. 1980. "Geometry of gravel streams." *Journal of Hydraulics Division American Society of Civil Engineers* 106, HY9, pp.1443-56.

Chang, H.C. 1998. "Fluvial-12 mathematical model for erodible channels, Users Manual.".

Chien, N. 1956. "The present status of research on sediment transport." Trans. ASCE, 121:833-68.

Choi, S.U., Yoon, B., Woo, H., and Cho, K. 2004. "Effect of flow regime changes due to damming on the river morphology and vegetation cover in the downstream river reach: a case of Hapcheon Dam on the Hwang River." *Journal of Korea Water Resources Association* 37(1): 55-66. (*in Korean*)

Chorley, R.J. 1966. "The application of statistical methods to geomorphology." In: Dury, G.H.(ed), *Essay in Geomorphology*. American Elsevier Publishing Company, Inc., NY, NY, pp.275-387.

Chorley, R.J., and Kennedy, B.A. 1971. "Physical geography: a systems approach." *London: Prentice –Hall International Inc.*

Church, M. 1978. "Palaeohydrological reconstructions from a Holocene valley fill, In Fluvial Sedimentology." *Can. Soc. Petrol. Geol. Mem.*, vol. 5, edited by A. D. Miall, 743–772, Can. Soc. of Petrol. Geol., Calgary, Alberta, Canada.

Davies, T.R., and Sutherland, A.J. 1980. "Resistance to flow past deformable boundaries." *Earth Surface Processes,* 5, pp.175-9.

Dolan, R., Howard, A., and Gallenson, A. 1974. "Man's impact on the Colorado River in the Grand Canyon." *Am. Sci.* 62, pp.392-401.

Doyle, M.W., Stanley, E.H., and Harbor, J.M. 2002. "Geomorphic analogies for assessing probable channel response to dam removal." *Journal of the American Water Resources Association.* **38**(6):1567-1579.

Doyle, M.W., Stanley, E.H., and Harbor, J.M. 2003. "Channel adjustments following two dam removals in Wisconsin." *Water Resources Research.* **39**(1):art. no.-1011.

Downs, P.W., and Gregory, K.J. 2004. "River Channel management: Towards Sustainable Catchment Hydrosystems." *Oxford University Press Inc.* 395 p.

Dunne, T. 1990. "Hydrology, mechanics, and geomorphic implications or erosion by subsurface flow." *Groundwater geomorphology: Role of subsurface water in earth-surface processes and landforms*, C. G. Higgins and D. R. Coates, eds., Geological Society of America Special Paper 252, Boulder, Colo.

Engelund, F., and Hansen, E. 1972. "A monograph on sediment transport in alluvial streams, Teknisk Forlag, Copenhagen."

Exner, F.M., 1920. "Zur Physik der Dunen, Sitzber. Akad." Wiss Wien, Part IIa, Bd. 129 (in German).

Exner, F.M. 1925. "Uber die Wechselwirkung zwischen Wasser und Geschiebe in Flussen, Sitzber. Akad." Wiss Wien, Part IIa, Bd. 134 (in German).

FAO (Food and Agriculture Organization of the United Nations) and KOWACO (Korea Water Resources Development Corporation). 1971. "Pre-investment Survey of the Nakdong River Basin, Korea: Volume 4-Sediment Transportation in Rivers of the Nakdong Basin."

Ferguson, R.I. 1986. "Hydraulics and hydraulic geometry." *Prog. Phys. Geogr.* 10, pp.1-31.

Friedman, J.M., and Lee, V.J. 2001. "Extreme floods, channel change, and riparian forests along ephemeral streams." *Ecological Monographs*, 72(3), 409-425.

Friedman, J.M., Osterkamp, W.R., and Lewis, W.M. 1996. "Channel narrowing and vegetation development following a Great Plains Flood." *Ecology*, 77(7), 2167-2181.

Fortier, S., and Scobey, F.C. 1926. "Permissible canal velocities," *Transactions of the ASCE*, Vol. 89.

Fox, G.A. 2006. "Sediment transport model for seepage erosion of streambank sediment." *Journal of Hydrologic Engineering*, 11(6).

Gilbert, G.K. 1877. "Report on the geology of the Henry Mountains." Washington DC: United States Geological Survey, Rocky Mountain Region.

Graf, W.L. 1988. "Applications of catastrophe theory in fluvial geomorphology." In Anderson, M.G. (ed.), Modelling geomorphological systems. Chichester: *J. Wiley & Sons*, pp. 33-47.

Graf, W.L. 1999. "Dam nation: a geographic census of American dams and their hydrologic impacts." *Water Resourc. Res.*, 35, 1305-1311.

Grams, P.E., and Schmidt, J.C. 2005. "Equilibrium or indeterminate? Where sediment budgets fail: Sediment mass balance and adjustment of channel form, Green River downstream from Flaming Gorge Dam, Utah and Colorado." *Geomorphology*, 71, pp. 156-186.

Grant, G.E., Schmidt, J.C., and Lewis, S.L. 2003. "A Geological Framework for Interpreting Downstream Effects of Dams on Rivers." *Water Science and Application 7.*

Greimann, B.P., and Huang, Jianchun. 2006. "One-Dimensional Modeling of Incision through Reservoir Deposits"; Hydraulic Engineers, Sedimentation and River Hydraulics Group, Technical Service Center, Bureau of Reclamation, Denver.

Gregory, K.J. 1987. "Environmental effects of river channel change." *Regulated Rivers: Research and Management*, 1:358-63.

Griffiths, G.A. 1984. "Extremal hypotheses for river regime: An illusion of progress?" *Water Resourc. Res.*, 20, pp.113-118.

Grimshaw, D.L., and Lewin, J. 1980. "Reservoir effects on sediment yield." *Journal of Hydrology.* 47, pp.163-171.

Gurnell, A.M., Petts, G.E., Hannah, D.M., Smith, B.P.G., Edwards, P.J., Kollmann, J., Ward, J.V., and Tockner, K. 2001. "Island formation along the gravel-bed Fiume Tagliamento, Italy." *Earth Surface Processes and Landforms*, 26, pp. 31-62.

Hey, R.D. 1979. "Dynamic process–response model of river channel development." *Earth Surface Processes and Landforms* **4**: 59–72.

Hey, R.D. 1982. "Design equations for mobile gravel-bed rivers. In: Hey, R.D., Bathurst, J.C. and Thorne, C.R. (eds), Gravel-bed, Wiley, Chichester, pp.553-574.

Higgins, C.G. 1982. "Drainage systems developed by sapping on Earth and Mars." *Geology*, 10(3), pp.147–152.

Higgins, C.G. 1984. "Piping and sapping: Development of landforms by groundwater outflow." *Groundwater and as a geomorphic agent*, R. G. Lafluer, ed., Allen and Unwin, Inc., Boston.

Hjulstrom, F. 1935. "The morphological activity of rivers as illustrated by rivers Fyris." *Bulletin of the Geological Institute, Uppsala*, Vol. 25, chap 3.

Hook, J.M. 1979. "An analysis of the processes of river bank erosion." *Journal of Hydrology* 42, pp.39-62.

Huang, J.V. and Greimann, B.P. 2006a, "DRAFT User's Manual for GSTAR-1D 1.1.4, Generalized Sediment Transport for Alluvial Rivers – One Dimension, Version 1.1.4." US Department of Interior, Bureau of Reclamation, Technical Service Center, Sedimentation and River Hydraulics Group.

Huang, J.V. and Greimann, B.P. 2006b, "Development and Application of GSTAR-1D." US Department of Interior, Bureau of Reclamation, Technical Service Center, Sedimentation and River Hydraulics Group.

Huang H.Q., and Nanson G.C. 2000. "Hydraulic geometry and maximum flow efficiency as products of the principle of least action." *Earth Surface Processes and Landforms* **25**: 1–16.

Jia, Y. 1990. "Minimum Froude number and equilibrium of alluvial sand rivers." *Earth Surface Processes and Landforms,* 15, pp.199-209.

Jiongxin, X. 1997. "Evolution of mid-channel bars in braided river and complex response to reservoir construction: An example from the middle Hanjiang River, China." *Earth Surface Processes and Landforms,* 22, pp.953–965.

Jiongxin, X. 2001. "Modified Conceptual Model for Predicting the Tendency of Alluvial Channel Adjustment Induced by Human Activities." *Chinese Science Bulletin,* 46.

Jones, J.A. 1997. "Subsurface flow and subsurface erosion." *Process and form in geomorphology,* D. R. Stoddart, ed., Routledge, London.

Johnson, W.C. 1997. "Equilibrium response of riparian vegetation to flow regulation in the Platte River, Nebraska." *Regulated Rivers: Research & Management,* 13, pp.403-415.

Julien, P.Y. 1988. "Downstream Hydraulic Geometry of Noncohesive Alluvial Channels." In: White, W.R. (ed), International Conference on River Regime, 18-20 May, 1988, Hydraulics Research Limited, Wallingford, UK, pp. 9-16.

Julien, P.Y. 1998. "Erosion and Sedimentation." *Cambridge University Press.,* 280 p.

Julien, P.Y. 2002. "River Mechanics." *New York, NY: Cambridge University Press.,* 434 p.

Julien, P.Y. and Wargadalam, J. 1995. "Alluvial Channel Geometry: Theory and Applications." *Journal of Hydraulic Engineering,* 121(4).

Juracek, K.E. 2000. "Channel Stability Downstream from a Dam Assessed Using Aerial Photographs and Stream-gage Information." *Journal of the American Water Resources Association,* 36(3).

144

Karim, M.F. and Holly, F.M. 1986. "Armoring and sorting simulation in alluvial rivers." *Journal of Hydraulic Engineering*, 112(8), pp.705-715.

Karim, M.F., Holly, F.M., and Kennedy, J.F. 1983. "Bed armoring processes in alluvial and application to Missouri River." *IIHR Rep*, No. 269, University of Iowa, Iowa City, Iowa.

Kassem, A., and Chaudhry, M.H. 2002. "Numerical modeling of bed evolution in channel bends." *Journal of Hydraulic Engineering*, 128(5).

Kassem, A., and Chaudhry, M.H. 2005. "Effect of bed armoring on bed topography of channel bend." *Journal of Hydraulic Engineering*, 131(12).

Kellerhals, R. 1967. " Stable channel with gravel-paved beds. Journal of the Waterways and Harbors Division, American Society of Civil Engineers 93 (WW1), Proc. Paper 5091, pp.63-84.

Kennedy, R.G. 1895. "The prevention of silting in irrigation canals." *Minutes of Proc. Inst. Civ. Eng. London*, 119, pp.281-290.

Knighton, A.D. 1998. "Fluvial Forms and Processes: A New Perspective." *Oxford University Press Inc., New York*. 383 p.

Kirkby, M.J. 1977. "Maximum sediment efficiency as a criterion for alluvial channels." In Gregory, K.J. (ed.), *River channel changes*. Chichester: Wiley-Interscience, pp. 429-42.

Komar, P.D., and Wang, C. 1992. "Processes of selective grain transport and the formation of placers on beaches." *J. Geol.*, 95, pp.637–655.

Kondolf, G.M., and Wilcock, P.W. 1992. "The flushing flow problem." *Eos Trans. AGU*, 73, 239.

KOWACO. 2002. "The report of survey of reservoir sediment deposition of Hapcheon dam."

Lacey, G. 1929. "Stable channels in Alluvium." *Minutes Proc. Inst Civ. Eng. London*, 299, pp.259-292.

Lamberti A. 1992. "Dynamic and variational approaches to the river regime relation." In *Entropy and Energy Dissipation in Water Resources*, Singh VP, Fiorentino M (eds). Kluwer: Dordrecht; pp.507–525.

Lane, E.W. 1954. "The importance of fluvial morphology in hydraulic engineering." *United States Department of the Interior Bureau of Reclamation, Denver, Colorado*, Technical Report Hydraulic Laboratory Report no. 372.

Lane, E.W. 1955. "The importance of fluvial morphology in hydraulic engineering." *American Society of Civil Engineers. Proceedings*, 81, pp.62-79.

Langendoen, E.J. 2000. *CONCEPTS – Conservational Channel Evolution and Pollutant Transport System*, USDA-ARS National Sedimentation Laboratory, Research Report No. 16, December.

Lauterbach, D., and Leder, A. 1969. "The influence of reservoir storage on statistical peak flows." *IASH Publ.* 85, pp.821-826.

Lawler, D.M., Glove, J.R., Couperthwaite, J.S., and Leeks, G.J.L. 1999. "Downstream change in river bank erosion rates in Swale-Ouse system, Northern England." Hydrological Processes 13, pp.977-992.

Lenzi, M.A., Mao, L., and Comiti, F. 2006. "When does bedload transport begin in step boulder-bed streams?" *Hydrological Processes*. 20, pp.3517-3533.

Leopold, L.B., and Maddock, T. Jr. 1953. "The Hydraulic Geometry of Stream Channels and Some Physiographic Implications." *USGS Geological Professional Paper, 252*, 57 p.

Li, Z., and Komar, P.D. 1992. "Selective entrainment and transport of mixed size and density sands: Flume experiments simulating the formation of black-sand placers." *J. Sediment. Petrol., 62*, pp.584–590.

Lindley, E.S. 1919. "Regime channels." *Proceedings of the Punjab Engineering Congress* 7, 63.

MacDonald, T.E. 1991. "Inventory and analysis of stream meander problems in Minnesota." M.S. Thesis, Univ. of Minnesota, Minneapolis, MN.

Mackin, J.H. 1948. "Concept of the graded river." *Geol. Soc. Am. Bull.*, 59, pp.463-512.

Malhotra, S.L. 1951. "Effects of barrages and weirs on the regime of rivers." Proc. Int. Assoc. Hydraul. Res., 4th Meeting, pp.335– 347.

Marsh, N.A., Western, A.W., and Grayson, R.B. 2004. "Comparison of methods for predicting incipient motion for sand beds." *Journal of Hydraulic Engineering*, Vol. 130, No. 7.

Martin, C.W., and Johnson, W.C. 1987. "Historical channel narrowing and riparian vegetation expansion in the Medicine Lodge River Basin, Kansas, 1871-1983." *Annals of the Association of American Geographers*, 77(3), pp.436-449.

Meade, R.H., and Parker, R.S. 1985. "Sediment in rivers of the United States." In *National Water Summary 1984*, United States Geological Survey Water-Supply Paper 2275, pp.49-60.

Merritt, D.M., and Cooper, D.J. 2000. "Riparian vegetation and channel change in response to river regulation: a comparative study of regulated and unregulated streams in the Green River Basin, USA." *Regul. Rivers*, 16, pp.543-564.

Meyer-Peter, E., Favre H., and Einstein H.A. 1934. "Neuere Versuchsresultate uber den Geschiebetrieb." *Schweizerische Bauzeitung* 103(13).

Meyer-Peter, E., and Muller, R. 1948. "Formulas for bed-load transport." *Proc. 2d Meeting IAHR*, Stockholm, pp. 39-64.

Milhous, R.T. 1990. "The calculation of flushing flows for gravel and cobble bed rivers." in *Hydraulic Engineering, Proceedings of the 1990 National Conference*, vol. 1, edited by H. H. Chang, pp. 598–603, Am. Soc. Civ. Eng., New York.

Miller, S.N., Youberg, A., Guertin D.P., and Goodrich D.C. 2000. "Channel morphology investigations using Geographic Information System and field research." USDA Forest Service Proceedings RMRS-P-13. 2000.

Miller, T.K. 1991a. "A model of stream channel adjustment: assessment of Rubey's hypothesis." *Journal of Geology* **99**: pp.699–710.

Miller, T.K. 1991b. "An assessment of the equable change principle in at-a-station hydraulic geometry." *Water Resources Research* **27**: 2751–2758.

Ministy of Construction and transportation (MOCT) and Korea Water Resources Corporation (KOWACO). 2004. "A report of investigation for the Nakdong River Basin (in Korean)."

Ministy of Construction and transportation (MOCT). 2003. "A report of master plan for the river improvement project in the Hwang River, Nakdong River basin (in Korean)."

Ministy of Construction. 1993. "A report of analysis for the river bed change in the Hwang River, Nakdong River basin, MOC report (in Korean)."

Ministy of Construction. 1983. "A report of master plan for the river improvement project in the Hwang River, Nakdong River basin (in Korean)."

Mohammadi, M. 2005. "The initiation of sediment motion in fixed bed channels." *Iranian Journal of Science & Technology, Transaction B, Engineering*, Vol. 29, No. B3.

Molinas, A., and C.T. Yang, 1986. "Computer Program User's manual for GSTARS (Generalized Stream Tube model for Alluvial River Simulation)." U.S. Bureau of Reclamation, Technical Service Center, Denver, Colorado.

Montgomery, D.R., Buffington, J.M., Peterson, N.P., Schuett-Hames, D., and Quinn, T. P. 1996. "Streambed scour, egg burial depths and the influence of salmon spawning on bed surface mobility and embryo survival." *Can. J. Fish. Aquat. Sci.*, *53*, pp.1061–1070.

Nanson, G.C., and Hickin, E.J. 1986. "A statistical analysis of bank erosion and channel migration in western Canada." *Geological Society of America Bulletin* 97, pp.497-504.

Page, K., Read, A., Frazier, P., and Mount, N. 2005. "The effect of altered flow regime on the frequency and duration of bankfull discharge: Murrumbidgee river, Australia." *River Research and Applications,* 21, pp.567-578.

Petts, G.E. 1984. "Impounded rivers: perspectives for ecological management." *Chichester: J. Wiley & Sons.*

Petts, G.E. 1979. "Complex response of river channel morphology subsequent to reservoir construction." Prog. Phys. Geogr. 3, pp.329-362.

Petts, G.E., and Gurnell, A.M. 2005. "Dams and geomorphology: Research progress and future directions." *Gemorphology,* 71, pp.27-47.

Phillips, J.D. 1990. "The instability of hydraulic geometry." *Water Resources Research,* 26, pp.739-744.

Phillips, J.D. 1991. "Multiple modes of adjustment in unstable river channel cross-sections." *Journal of Hydrology,* 123, pp.39-49.

Phillips, J.D. 2003. "Sources of nonlinearity and complexity in geomorphic systems." *Progress in Physical Geography,* 27, pp.1-23.

Phillips, J.D., Slattery, M.C., and Musselman, Z.A. 2005. "Channel adjustment of the lower Trinity River, Texas, downstream of Livingston Dam." *Earth Surface Processes and Landforms,* 30, pp.1419-1439.

Phillips, J.D., Slattery, M.C., and Zachary, A.M. 2005. "Channel Adjustments of the lower Tirinity River, Texas, Downstream of Livingston Dam." *Earth Surf. Process. Landforms,* 30, pp.1419-1439.

Pizzuto, J. 2002. "Effects of dam removal on river form and processes." *BioScience,* Vol. 52 No.8.

Pohl, M. 2004. "Channel Bed Mobility Downstream from the Elwha Dams, Washington." *The Professional Geographer*, 56(3), pp.422-431.

Ramette, M. 1979. "Une approche rationelle de la morphologie fluviale." *La Houille Blanche,* 8, pp.491-8.

Rathburn, S.L. 2002. "Modelong pool sediment dynamics in a mountain river." Ph.D. dissertation, Colorado State University.

Renwick, W.H. 1992. "Equilibrium, disequilibrium, and nonequilibrium landforms in the landscape." *Geormophology,* 5, pp.265-76.

Rhoads, B.L. 1992. "Statistical model of fluvial systems." *Geormophology,* 5, pp.433-455.

Richard, G.A. 2000. "Quantification and Prediction of Lateral Channel Adjustments Downstream from Cochiti Dam, Rio Grande, NM." Ph.D. Dissertation. Colorado State University, Fort Collins, CO.

Richard, G.A., and Julien, P.Y. 2005. "Statistical analysis of lateral migration of the Rio Grande, New Mexico." *Geomorphology,* 71, pp.139-155.

Richard, G.A., Julien, P.Y., and Baird, A.C. 2005. "Case Study: Modeling the Lateral Mobility of the Rio Grande below Cochiti Dam, New Mexico." *Journal of Hydraulic Engineering,* 131:11 (931).

Richards, K. 1982. "Rivers: form and process in alluvial channels." *London, Methuen.*

Rosgen, D.L. 2002. "A Stream Channel Stability Assessment Methodology." *Wild Land Hydrology Pagosa Springs.*

Schumm, S.A. 1969. "River metamorphosis." *Journal of the Hydraulics Division,* ASCE, HYI: 255-63.

Schumm, S.A. 1985. "Pattern of alluvial rivers." *Ann.Rev. Earth Planet. Sci.* 13:5-27.

Sear, D.A. 1995. "Morphological and sedimentological changes in a gravel-bed river following 12 years of flow regulation for hydropower." *Regulated Rivers: Research and Management.* **10**(2/4):247-264.

Shafroth, P.B., Stromberg, J.C., and Patten, D.T. 2002. "Riparian vegetation response to altered disturbance and stress regimes." *Ecological Applications,* 12(1), pp.107–123.

Shen, H.W., and Hung, C.S. 1972. "An engineering approach to total bed material load by regression analysis." *Proceedings of the Sediment Symposium,* chap. 14, pp.14-1~14-17.

Shen, H.W., and Lu, J. 1983. "Development and prediction of bed armoring." *Journal of Hydraulic Engineering*, 109(4).

Shields, A. 1936. "Application of similarity principles, and turbulence research to bed-load movement." California Institute of Technology, Pasadena (translated from German).

Shields Jr, F.D., Simon, A., and Steffen, L.J. 2000. "Reservoir Effect on Downstream River Channel Migration." *Environmental Conservation*, 27(1), pp.54-66.

Shvidchenko, A.B. 2001. "Critical shear stress for incipient motion of sand/gravel streambeds." *Water Resources Research*, Vol. 37, No. 8, pp.2773-2283.

Simon, A. 1992. "Energy, time, and channel evolution in catastrophically disturbed fluvial systems." *Geomorphology*, 5 (1992), pp.345-372.

Simon, A., Thomas, R.E., Curini, A., and Shields Jr., F.D. 2002. "Case Study: Channel Stability of the Missouri River, Eastern Montana." *Journal of Hydraulic Engineering*, 128, 10(880).

Simon, A., and Thorne CR. 1996. "Channel adjustment of an unstable coarse-grained stream: opposing trends of boundary and critical shear stress, and the applicability to extremal hypotheses." *Earth Surface Processes and Landforms* **21**: 155–180.

Simons, D.B., and Albertson, M. 1963. "Uniform Water Conveyance channels in Alluvial Material." *Trans. ASCE*, 128(1), pp.65-167.

SLOPE/W users' guide version 4. 1998. GeoSlope International Ltd., Calgary, Alta.

Sophocleous, M. 2002, "Interactions between groundwater and surface water: the state of the science." *Hydrogeology Journal*, 10, pp.52–67.

Tal, M., Gran, K., Murray, A.B., Paola, C., and Hicks, D.M. 2003. "Riparian vegetation as a primary control on channel characteristics in Multi-thread Rivers." Riparian Vegetation and Fluvial Geomorphology: Hydraulic, Hydrologic, and Geotechnical Interaction Water Science and Application.

Tetra Tech, Inc. 2001. "EFDC1D, a one dimensional hydrodynamic and sediment transport mdoel for river and stream networks, model theory and users guide." prepared for US Environmental Protection Agency, Office of Science and Technology, Washington, DC.

Terzaghi, K. 1943. "Theoretical soil mechanics." *Wiley, New York.*

Thorn, C.E., and Welford, M.R. 1994. "The Equilibrium concept in geomorphology." *Annals of the Association of American Geographers,* 84, pp.666-96

Tooth, S., and Nanson, G.C. 2000. "Equilibrium and nonequilibrium conditions in dryland rivers." *Progress in Physical Geography*, 21, pp.183-211.

USBR. 2006. "DRAFT User's Manual for GSTAR-1D 1.1.3." US Department of Interior Bureau of Reclamation Technical Service Center Sedimentation and River Hydraulic Group.

USGS. 1999. "Effects of Flooding on Plant Production Downstream from Glen Canyon Dam." *Gran Canyon Monitoring and Research Program.*

U.S. Army Corps of Engineers. 1993. "The Hydraulic Engineering Center, HEC-6 Scour and Deposition in Rivers and Reservoirs, User's Manual." Mar. 1977 (revised 1993).

U.S. Army Corps of Engineers. 2002. "HEC-RAS River Analysis System Hydraulic Reference Manual." Hydrologic Engineering Center, Davis, CA.

Van Looy, J.A. and Martin, C.W. 2005. "Channel and vegetation change on the Cimarron River, Southwestern Kansas, 1953-2001." *Annals of the Association of American Geographers*, 95(4), pp.727-739.

Van Rijn, L. C. 1984. "Sediment transport, Part I: Bed load transport." *Journal of Hydraulic Engineering* ASCE, 110(10), pp.1431-1456

Vanoni, V.A. ed. 1975. "Sedimentation Engineering." ASCE Task Committee for the Preparation of the Manual on Sedimentation of the Sedimentation Committee of the Hydraulics Division (Reprinted 1977).

Wang, Z., and Hu, C. 2004. "Interactions Between Fluvial Systems and Large Scale Hydro-Projects." *Proceeding of the Ninth International Symposium on River Sedimentation 10/ 18-21, 2004, Yichang, China.*

Ward, J.V., Tockner, K., Edwards, P.J., Kollmann, J., Bretschko, G., Gurnell, A.M., Petts, G.E., and Rossaro, B. 1999. "A reference river system for the Alps: the Fiume Tagliamento." *Regul. Rivers* 15, pp.63-76.

Ward, J.V., Tockner, K., Uehlinger, U., and Malard, F. 2001. "Understanding natural patterns and processes in river corridors as the basis for effective river restoration." *Regul. Rivers* 17, 709.

Wargadalam, J. 1993. "Hydraulic Geometry Equations of Alluvial Channels." Ph.D. Dissertation. Colorado State University, Fort Collins, CO.

Warner, R.F. 1994. "A theory of channel and floodplain responses to alternating regimes and its application to actual adjustments in the Hawkesbury River, Australia." In Kirby: M.J. (ed.), Process models and theoretical geomorphology. Chichester: J. *Wiley & Sons*, pp.173-200.

Watson, C.C., Biedenharn, D.S., and Thorne C.R. 2005. "Stream Rehabilitation Version 1.0." *Cottonwood Research LLC,* 202 p.

Wellmeyer, J.L., Slattery, M.C., and Phillips, J.D. 2005. "Quantifying downstream impacts of impoundment on flow regime and channel planform, lower Trinity River, Texas." *Geomorphology.* 69 (1-4), pp.1-13.

Wharton, G. 1995. "Information from channel geometry-discharge relations." Changing River Channels, John Wiley & Sons Ltd. pp.325-346.

White, C.M. 1940. "The equilibrium of grains on the bed of an alluvial channel", proceeding of the Royal society of London, Series A, vol. 174, pp.332-338.

White, W.R., Bettess, R., and Paris, E. 1982. "Analytical approach to river regime." *Journal of the Hydraulics Division American Society of Civil Engineers,* 108, pp.1179-93.

Williams, G.P., and Wolman, M.G. 1984. "Downstream effects of dams on alluvial rivers." *US Geological Survey, Professional Paper,* 1286, Washington DC.

Wohl, E.E. 2000. "Mountain rivers." Water Resources Monograph 14, American Geophysical Union, Washington, DC, 320 p.

Wohl, E. 2005. "Lecture note of Fluvial Geomorpholgy (G652)." Colorado State University.

Wohl, E.E. 2004. "Limits of Downstream Hydraulic Geometry." *Geology,* 32(10), pp.897-900.

Wohl, E.E., and Rathburn, S. 2003. "Mitigation of Sedimentation Hazards Downstream from Reservoir." *Iternation Journal of Sediment Research,* 18(2), pp.97-106.

Wolman, M.G. 1955. "The natural channel of Brandywine Creek, Pennsylvania." Unites States Geological Survey Professional Paper 271.

Wolman, M.G. 1967. "Two problems involving river channels and their background observations. Northwest." Univ. Stud. Geogr. 14, pp.67-107.

Woo, H. 2002. "River Hydraulics (in Korean)." Chungmoon publishing Co. 844 p.

Woo, H., Lee, D. S., Ahn, H. K., and Lee, C. S. 2004a. "Effect of river channel meander on hydro-geomorphologically induced vegetation expansion on sandbars." *Proceedings of the 6th ICHE,* Brisbane, Australia.

Woo, H., Choi, S.U., and Yoon, B. 2004b. "Downstream effect of dam on river morphology and sandbar vegetation." *Proceedings of the Symposium of the 72nd* Annual ICOLD meeting, Seoul, Korea.

Wu, W., and Vieira, D.A. 2002. "One-Dimensional Channel Network Model CCHE1D Version 3.0 – Technical Manual." *Technical Report No. NCCHE-TR-2002-1*, National Center for Computational Hydroscience and Engineering, The University of Mississippi.

Wynn, T. M., Mostaghimi, S., and Alphin, E.F. 2004. "The Effects of Vegetation on Stream Bank Erosion." 2004 ASAE/CSAE Annual International Meeting Sponsored by ASAE/CSAE Fairmont Chateau Laurier, The Westin, Government Centre Ottawa, Ontario, Canada 1 - 4 August 2004

Xu, J. 1990. "An experimental study of complex response in river channel adjustment downstream from a reservoir." *Earth Surface Processesand Landforms* **15**: 53–53.

Xu, J. 1996. "Channel pattern change downstream from a reservoir: An example of wandering braided rivers." *Geomorphology* pp. 147-158.

Xu, J. 2001. "Modified conceptual model for predicting the tendency of alluvial channel adjustment induced by human activities." *Chinese Science Bulletin* **46**: 51–57.

Yalin, M.S. 1992. "River mechanics." Oxford: Pergamon.

Yang, C.T. 1973. "Incipient motion and Sediment transport." Journal of Hydraulics Division, ASCE, vol. 99, no. HY10, Proceeding Paper 10067, pp.1679-1704.

Yang, C.T. 1976. "Minimum unit stream power and fluvial hydraulics." *Journal of Hydraulics Division American Society of Civil Engineers,* 102, HY7, pp.919-34.

Yang, C.T. 1979. "Unit stream power equation for gravel." *Journal of Hydraulics,* vol. 40, pp.123-138.

Yang, C.T. 1992. "Force, energy, entropy, and energy dissipation rate." In *Entropy and Energy Dissipation in Water Resources,* Singh VP, Fiorentino M (eds). Kluwer: Dordrecht; pp.63–89.

Yang, C.T. 2003. "Sediment transport – Theory and practice." *Krieger Publishing Company, Malabar, Florida,* 396p.

Yang, C.T., and Simões, F.J.M. 2000. "*User's manual for GSTARS 2.1 (Generalized Stream Tube model for Alluvial River Simulation version 2.1)."* U.S. Bureau of Reclamation, Technical Service Center, Denver, Colorado.

Yang, C.T., Song, C.S.S., and Woldenberg, M.J. 1981. "Hydraulic geometry and minimum rate of energy dissipation." *Water Resources Research,* 17, pp.1014-18.

Yang, C.T., and Simões, F.J.M. 2002. *"User's manual for GSTAR3 (Generalized Stream Tube model for Alluvial River Simulation version 3.0). "* U.S. Bureau of Reclamation, Technical Service Center, Denver, Colorado.

Zaslavsky, D., and Kassiff, G. 1965. "Theoretical formulation of piping mechanisms in cohesive soils." *Geotechnique,* 15(3), pp.305–316.

APPENDIX A : HISTORICAL DATA

1. Discharge data

Station	Period	Data type	Agency and Remarks
Changri	1969-1983	Daily	MOCT
Hapcheon Main Dam	1989-Present	Daily	KOWACO (both inflow and outflow data)
	1996-Present	30 min/hourly	"
Hancheon re-regulation Dam	1989-Present	daily	"
	1996-Present	30 min/hourly	"
Hapcheon	1962-Present	hourly/daily	MOCT (many missing and errors)
Jukgo	1962-Present	hourly/daily	"

2. Cross-section data

	No. of cross-section	Interval (m)	Agency
1983	100	500	MOCT
1993	100	500	MOCT
2003	210	250	MOCT

3. Bed material data

	No. of measurement at each cross-section	Interval (km)	Agency
1983	13	4	MOCT
1993	46	1	MOCT
2003	25	2	MOCT

4. Satellite images (dates of photographing)

Route	ETM+	TM			MSS	
1980 (1975)	2000	1995	1990	1985	1980	1975
114-34 (124-34)	6/18/2000	5/12/1995	10/18/1989	5/16/1985	8/28/1979	4/23/1974
114-35 (124-35)	4/18/2001	5/12/1995	10/18/1989	4/30/1985	8/28/1979	4/23/1974
114-36 (124-36)	4/18/2001	5/12/1995	10/18/1989	10/7/1985	8/28/1979	3/22/1974
115-34 (123-34)	5/8/2000	6/1/1994	6/3/1989	10/14/1985	6/5/1981	
115-35 (123-35)	5/8/2000	5/3/1995	6/3/1989	4/24/1986	6/5/1981	2/13/1975
115-36 (123-36)	5/8/2000	6/1/1994	10/9/1989	3/7/1986	6/5/1981	2/13/1975

5. Aerial photographs (1982, 1993, 2004)
- 1982

Number of photo	Location	Date of photographing
27-29	Confluence with the Nakdong River	27-May
27-27	Chungduk Bridge	27-May
27-25	Hwanggang Bridge	27-May
27-23	Youngjun Bridge	27-May
27-21	Hapcheon city	27-May
27-18	Youngju Bridge	28-May
26-24	Naecheon Bridge	26-May
28-19		27-May
28-16	Hapcheon Re-regulation Dam	28-May
28-15	Hapcheon Main Dam	28-May

- 1993

Number of photo	Location	Date of photographing
7-31	Confluence with the Nakdong River	7-Jul
7-29	Chungduk Bridge	7-Jul
7-27	Hwanggang Bridge	7-Jul
6-30	Naecheon Bridge	6-Sep
5-28	Youngjun Bridge	5-Jun
6-26		7-Jul
6-24		6-Jul
7-22	Hapcheon city	7-Jul
7-20	Yongjy Bridge	7-Jul
8-21		8-Jul
8-19	Hapcheon Re-regulation Dam	8-Jul
8-17	Hapcheon Main Dam	8-Jul

- 2004

Number of photo	Location	Date of photographing
250022	Confluence with the Nakdong River	
250020	Hwanggang Bridge	9-Dec
250018	Naecheon Bridge	9-Dec
240016		7-Dec
230014		7-Dec
240014		7-Dec
250014	Youngjun Bridge	9-Dec
240012		7-Dec
250012	Hapcheon city (Namjung bridge)	9-Dec
250010	Immediately downstream of the Hapcheon Re-regulation Dam	9-Dec
260009	Hapcheon Re-regulation Dam	9-Dec
260007		9-Dec
260005	Hapcheon Main Dam	9-Dec

6. Annual peak flow at Changri (Hancheon re-regulation Dam site)

Date	Peak Flow (m³/s)
August 7, 1969	1087.1
July 17, 1970	903.3
August 23, 1971	339.2
July 3, 1972	582.1
August 3, 1973	507.7
May 20, 1974	1132.2
July 31, 1975	1272.0
August 30, 1976	535.9
June 1, 1977	242.3
June 1, 1978	119.8
August 1, 1979	110.2
July 30, 1980	524.5
September 3, 1981	1155.0
August 22, 1989	128.6
June 25, 1990	80.4
April 25, 1991	111.9
February 7, 1992	48.4
August 10, 1993	110.3
January 9, 1994	105.6
August 25, 1995	26.3
August 13, 1996	63.2
December 20, 1997	65.9
September 30, 1998	114.8
September 24, 1999	107.7
September 16, 2000	316.1
June 25, 2001	36.4
September 1, 2002	462.3
September 12, 2003	140.1
August 23, 2004	138.8
September 4, 2005	90.5
Pre-dam average (1969~1981)	654.7
Post-dam average (1989~2005)	126.3
Overall average (1969~2005)	355.3

7. Estimation of discharge frequency

a) Pre-dam period (1969-1981)

Date	Peak Flow (m3/s)	Order	P	Recurrence interval (year)
July 31, 1975	1272.0	1	0.071	14.00
September 3, 1981	1155.0	2	0.143	7.00
May 20, 1974	1132.2	3	0.214	4.67
August 7, 1969	1087.1	4	0.286	3.50
July 17, 1970	903.3	5	0.357	2.80
July 3, 1972	582.1	6	0.429	2.33
August 30, 1976	535.9	7	0.500	2.00
July 30, 1980	524.5	8	0.571	1.75
August 3, 1973	507.7	9	0.643	1.56
August 23, 1971	339.2	10	0.714	1.40
June 1, 1977	242.3	11	0.786	1.27
June 1, 1978	119.8	12	0.857	1.17
August 1, 1979	110.2	13	0.929	1.08

b) Post-dam period (1989-2005)

Date	Peak Flow (m3/s)	Order	P	Recurrence interval (year)
September 1, 2002	462.3	1	0.056	18.00
September 16, 2000	316.1	2	0.111	9.00
September 12, 2003	140.1	3	0.167	6.00
August 23, 2004	138.8	4	0.222	4.50
August 22, 1989	128.6	5	0.278	3.60
September 30, 1998	114.8	6	0.333	3.00
April 25, 1991	111.9	7	0.389	2.57
August 10, 1993	110.3	8	0.444	2.25
September 24, 1999	107.7	9	0.500	2.00
January 9, 1994	105.6	10	0.556	1.80
September 4, 2005	90.5	11	0.611	1.64
June 25, 1990	80.4	12	0.667	1.50
December 20, 1997	65.9	13	0.722	1.38
August 13, 1996	63.2	14	0.778	1.29
February 7, 1992	48.4	15	0.833	1.20
June 25, 2001	36.4	16	0.889	1.13
August 25, 1995	26.3	17	0.944	1.06

c) Overall (1969-2005)

Date	Peak Flow (m3/s)	Order	P	Recurrence interval (year)
July 31, 1975	1272.0	1	0.032	31.00
September 3, 1981	1155.0	2	0.065	15.50
May 20, 1974	1132.2	3	0.097	10.33
August 7, 1969	1087.1	4	0.129	7.75
July 17, 1970	903.3	5	0.161	6.20
July 3, 1972	582.1	6	0.194	5.17
August 30, 1976	535.9	7	0.226	4.43
July 30, 1980	524.5	8	0.258	3.88
August 3, 1973	507.7	9	0.290	3.44
September 1, 2002	462.3	10	0.323	3.10
August 23, 1971	339.2	11	0.355	2.82
September 16, 2000	316.1	12	0.387	2.58
June 1, 1977	242.3	13	0.419	2.38
September 12, 2003	140.1	14	0.452	2.21
August 23, 2004	138.8	15	0.484	2.07
August 22, 1989	128.6	16	0.516	1.94
June 1, 1978	119.8	17	0.548	1.82
September 30, 1998	114.8	18	0.581	1.72
April 25, 1991	111.9	19	0.613	1.63
August 10, 1993	110.3	20	0.645	1.55
August 1, 1979	110.2	21	0.677	1.48
September 24, 1999	107.7	22	0.710	1.41
January 9, 1994	105.6	23	0.742	1.35
September 4, 2005	90.5	24	0.774	1.29
June 25, 1990	80.4	25	0.806	1.24
December 20, 1997	65.9	26	0.839	1.19
August 13, 1996	63.2	27	0.871	1.15
February 7, 1992	48.4	28	0.903	1.11
June 25, 2001	36.4	29	0.935	1.07
August 25, 1995	26.3	30	0.968	1.03

8. Non-vegetated active channel width measured from the aerial photos

Reach	Distance from the confluence(km)	Active channel width (m)		
		1982	1993	2004
Sub-reach 1	45.0	127.4	275.0	275.0
	44.5	227.3	68.8	50.9
	44.0	333.0	250.6	29.5
	43.5	356.3	252.4	47.6
	43.0	298.9	286.1	118.0
	42.5	340.1	292.3	66.4
	42.0	365.2	202.0	83.3
	41.5	304.1	228.2	129.4
	41.0	423.1	340.9	307.3
	40.5	436.0	220.6	379.6
	40.0	393.4	305.0	249.5
	39.5	424.6	310.0	119.3
	39.0	244.8	238.8	205.2
	38.5	328.4	273.7	275.7
	38.0	456.2	434.0	182.2
	37.5	381.2	361.3	196.9
	37.0	340.0	302.0	266.8
	36.5	322.3	255.3	177.8
	36.0	388.6	357.4	243.1
	35.5	554.3	469.0	198.9
	35.0	479.6	438.0	382.7
	34.5	486.3	392.9	198.1
	34.0	308.5	307.5	184.8
	33.5	320.1	281.8	293.3
	33.0	416.5	322.6	225.7
	32.5	392.7	315.2	260.1
	32.0	359.3	286.9	259.9
	31.5	428.5	411.4	343.0
	31.0	498.0	367.7	300.5
	30.5	390.3	256.9	190.3

Reach	Distance from the confluence(km)	Active channel width (m)		
		1982	1993	2004
Sub-reach 2	30.0	352.5	314.1	209.4
	29.5	444.5	397.9	256.7
	29.0	420.6	303.3	349.5
	28.5	573.3	377.7	291.1
	28.0	578.6	360.8	283.8
	27.5	376.2	250.4	96.5
	27.0	373.4	300.7	175.4
	26.5	329.2	208.8	179.9
	26.0	608.5	525.7	391.4
	25.5	497.1	387.4	147.6
	25.0	241.2	157.4	182.9
	24.5	435.3	396.7	205.9
	24.0	588.0	434.0	251.7
	23.5	483.2	286.2	232.2
	23.0	518.0	277.0	209.8
	22.5	458.5	348.8	207.9
	22.0	387.9	300.3	194.2
	21.5	396.7	345.6	207.0
	21.0	310.7	251.5	204.5
	20.5	314.7	181.0	196.4
	20.0	322.0	251.8	192.7
	19.5	208.3	202.0	171.8
	19.0	213.7	191.3	169.8
	18.5	295.5	293.4	212.9
	18.0	266.1	240.1	128.7
	17.5	215.9	215.9	257.7
	17.0	184.8	155.5	123.9
	16.5	168.0	120.6	123.8
	16.0	211.8	142.9	94.0
	15.5	213.2	210.7	125.1
	15.0	154.1	162.1	89.2
	14.5	276.4	239.6	109.4
	14.0	240.9	244.7	242.7
	13.5	189.6	198.8	140.5
	13.0	225.2	206.8	100.1
	12.5	254.5	227.8	149.8
	12.0	181.0	180.3	105.7
	11.5	383.3	332.4	115.5
	11.0	140.2	112.7	85.5

Reach	Distance from the confluence(km)	Active channel width (m)		
		1982	1993	2004
Sub-reach 3	10.5	107.3	117.8	116.5
	10.0	138.0	119.1	124.8
	9.5	167.2	163.0	98.1
	9.0	137.5	133.1	97.6
	8.5	229.1	113.3	94.9
	8.0	497.8	73.7	81.9
	7.5	139.4	88.9	70.0
	7.0	251.8	158.5	106.8
	6.5	232.3	200.3	99.8
	6.0	132.7	106.3	62.0
	5.5	165.6	152.0	87.3
	5.0	257.5	292.6	64.7
	4.5	107.9	180.6	58.2
	4.0	98.0	112.1	65.7
	3.5	392.5	359.4	72.7
	3.0	186.7	180.2	92.9
	2.5	293.3	298.1	118.7
	2.0	235.2	120.4	100.2
	1.5	299.4	255.2	74.9
	1.0	335.2	329.4	299.2
	0.5	203.8	142.8	135.5
	0.0	481.3	359.6	108.4

9. Non-vegetated active channel area (km^2) from the digitized aerial photos

	1982	1993	2004
Active channel area of subreach1	3.9	3.1	1.9
Active channel area of subreach2	6.9	5.4	3.9
Active channel area of subreach3	4.1	3.4	2.5
Entire reach	14.9	12.0	8.3
Area of Islands for subreach1	-	0.3	0.7
Area of Islands for subreach2	-	0.3	0.5
Area of Islands for subreach3	-	0.2	0.2
Entire reach	-	0.8	1.5
Area of vegetated area of subreach1	-	0.38	1.27
Area of vegetated area of subreach2	-	0.40	2.09
Area of vegetated area of subreach3	-	1.06	1.66
Entire reach	-	1.84	5.02

10. Result of sediment transport rate estimation using the five sediment transport equations

Table A-1. Estimated total sediment load (tons/year) by using Engelund and Hansen's (1972) empirical sediment transport equation at confluence with the Nakdong River

Time interval (%)	Interval midpoint (%)	Interval, Δp (%)	Discharge, Q (m^3/s)	Sediment, Q_s (tons/day)	days	Sediment load (tons/year)
(1)	(2)	(3)	(4)	(5)	(6)	(7)
0.00-0.02	0.01	0.02	462.3	133,284	0.073	9,730
0.02-0.1	0.06	0.08	316.9	76,349	0.292	22,294
0.1-0.5	0.3	0.4	120.1	18,232	1.46	26,618
0.5-1.5	1	1	109.4	15,888	3.65	57,991
1.5-5.0	3.25	3.5	72.1	8,588	12.775	109,715
5-15	10	10	44.9	4,269	36.5	155,834
15-25	20	10	29.2	2,263	36.5	82,586
25-35	30	10	22.8	1,571	36.5	57,325
35-45	40	10	19.7	1,266	36.5	46,205
45-55	50	10	16.2	948	36.5	34,620
55-65	60	10	14.4	797	36.5	29,096
65-75	70	10	11.8	594	36.5	21,688
75-85	80	10	8.2	347	36.5	12,675
85-95	90	10	5.0	167	36.5	6,108
95-98.5	96.25	3.5	1.0	16	12.775	199
Total						672,700

$$Q_s = 15.565Q^{1.4757}$$
$$R^2 = 0.9979$$
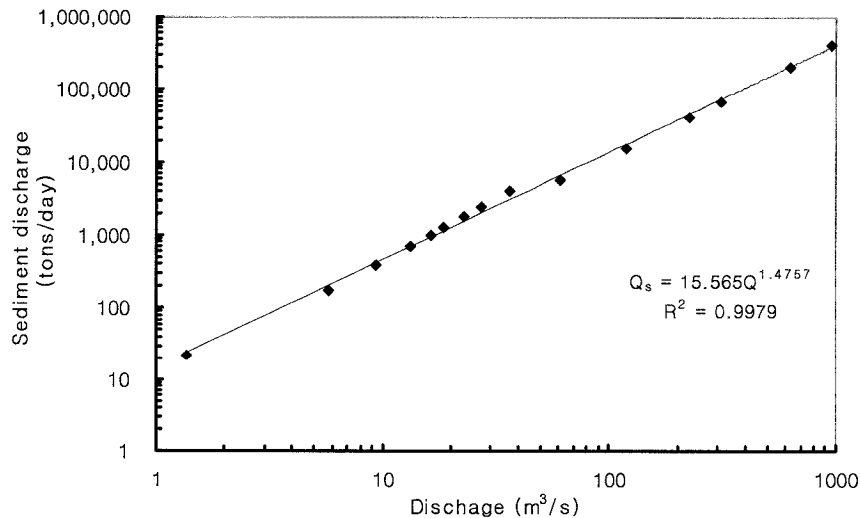
Figure A-1. Sediment – discharge rating curve at confluence with the Nakdong River by Engelund and Hansen's (1972) method

164

Table A-2. Estimated total sediment load (tons/year) by using Ackers and White's (1973) empirical sediment transport equation at confluence with Nakdong River

Time interval (%)	Interval midpoint (%)	Interval, Δp (%)	Discharge, Q (m³/s)	Sediment, Q_s (ton/day)	days	Sediment load *(tons/year)*
(1)	(2)	(3)	(4)	(5)	(6)	(7)
0.00-0.02	0.01	0.02	462.3	582,530	0.073	42,525
0.02-0.1	0.06	0.08	316.9	286,957	0.292	83,792
0.1-0.5	0.3	0.4	120.1	46,496	1.46	67,885
0.5-1.5	1	1	109.4	39,037	3.65	142,487
1.5-5.0	3.25	3.5	72.1	17,864	12.775	228,209
5-15	10	10	44.9	7,349	36.5	268,248
15-25	20	10	29.2	3,280	36.5	119,705
25-35	30	10	22.8	2,062	36.5	75,269
35-45	40	10	19.7	1,568	36.5	57,226
45-55	50	10	16.2	1,086	36.5	39,654
55-65	60	10	14.4	871	36.5	31,795
65-75	70	10	11.8	600	36.5	21,887
75-85	80	10	8.2	303	36.5	11,060
85-95	90	10	5.0	120	36.5	4,374
95-98.5	96.25	3.5	1.0	6	12.775	75
Total						1,194,200

$$Q_s = 5.8585Q^{1.8753}$$
$$R^2 = 0.9903$$
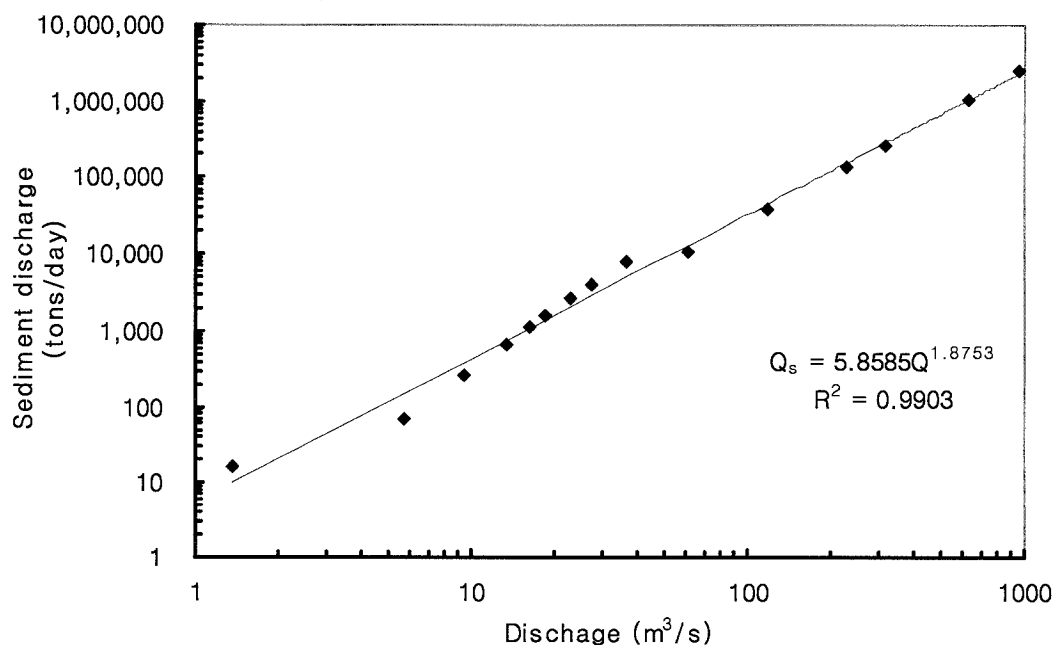
Figure A-2. Sediment – discharge rating curve at confluence with the Nakdong River by Ackers and White's (1973) method

165

Table A-3. Estimated total sediment load (tons/year) by using Yang's (1973) empirical sediment transport equation at confluence with the Nakdong River

Time interval (%)	Interval midpoint (%)	Interval, Δp (%)	Discharge, Q (m^3/s)	Sediment, Qs (tons/day)	days	Sediment load (tons/year)
(1)	(2)	(3)	(4)	(5)	(6)	(7)
0.00-0.02	0.01	0.02	462.3	89,492	0.07	6,533
0.02-0.1	0.06	0.08	316.9	51,051	0.29	14,907
0.1-0.5	0.3	0.4	120.1	12,061	1.46	17,609
0.5-1.5	1	1	109.4	10,500	3.65	38,325
1.5-5.0	3.25	3.5	72.1	5,650	12.78	72,176
5-15	10	10	44.9	2,794	36.5	101,983
15-25	20	10	29.2	1,474	36.5	53,792
25-35	30	10	22.8	1,020	36.5	37,237
35-45	40	10	19.7	821	36.5	29,965
45-55	50	10	16.2	614	36.5	22,404
55-65	60	10	14.4	515	36.5	18,805
65-75	70	10	11.8	383	36.5	13,986
75-85	80	10	8.2	223	36.5	8,141
85-95	90	10	5.0	107	36.5	3,902
95-98.5	96.25	3.5	1.0	10	12.78	125
Total						439,900

$Q_s = 9.77Q^{1.49}$
$R^2 = 0.995$

Figure A-3. Sediment – discharge rating curve at confluence with the Nakdong River by Yang's (1973) method

166

Table A-4. Estimated total sediment load (tons/year) by using Yang's (1979) empirical sediment transport equation at confluence with the Nakdong River

Time interval (%)	Interval midpoint (%)	Interval, Δp (%)	Discharge, Q (m³/s)	Sediment, Q_s (ton/day)	days	Sediment load *(tons/year)*
(1)	(2)	(3)	(4)	(5)	(6)	(7)
0.00-0.02	0.01	0.02	462.3	104,262	0.073	7,611
0.02-0.1	0.06	0.08	316.9	59,979	0.292	17,514
0.1-0.5	0.3	0.4	120.1	14,481	1.46	21,142
0.5-1.5	1	1	109.4	12,633	3.65	46,109
1.5-5.0	3.25	3.5	72.1	6,861	12.775	87,646
5-15	10	10	44.9	3,429	36.5	125,156
15-25	20	10	29.2	1,826	36.5	66,652
25-35	30	10	22.8	1,271	36.5	46,394
35-45	40	10	19.7	1,026	36.5	37,456
45-55	50	10	16.2	771	36.5	28,127
55-65	60	10	14.4	649	36.5	23,671
65-75	70	10	11.8	484	36.5	17,683
75-85	80	10	8.2	284	36.5	10,377
85-95	90	10	5.0	138	36.5	5,029
95-98.5	96.25	3.5	1.0	13	12.775	167
Total						540,700
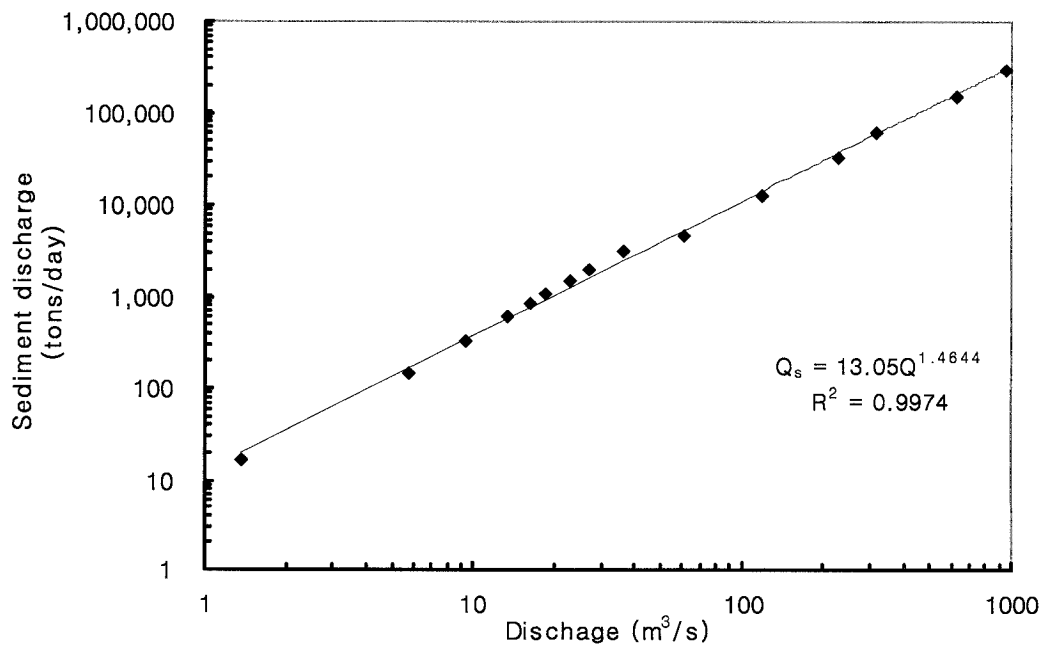
Figure A-4. Sediment – discharge rating curve at confluence with the Nakdong River by Yang's (1979) method

Table A-5. Estimated total sediment load (tons/year) by using Van Rijn's (1984) empirical sediment transport equation at confluence with the Nakdong River

Time interval (%)	Interval midpoint (%)	Interval, Δp (%)	Discharge, Q (m^3/s)	Sediment, Q_s (ton/day)	days	Sediment load *(tons/year)*
(1)	(2)	(3)	(4)	(5)	(6)	(7)
0.00-0.02	0.01	0.02	462.3	309,778	0.073	22,614
0.02-0.1	0.06	0.08	316.9	171,637	0.292	50,118
0.1-0.5	0.3	0.4	120.1	37,624	1.46	54,930
0.5-1.5	1	1	109.4	32,519	3.65	118,693
1.5-5.0	3.25	3.5	72.1	16,943	12.775	216,452
5-15	10	10	44.9	8,078	36.5	294,861
15-25	20	10	29.2	4,122	36.5	150,446
25-35	30	10	22.8	2,799	36.5	102,175
35-45	40	10	19.7	2,227	36.5	81,299
45-55	50	10	16.2	1,640	36.5	59,873
55-65	60	10	14.4	1,364	36.5	49,800
65-75	70	10	11.8	999	36.5	36,474
75-85	80	10	8.2	566	36.5	20,643
85-95	90	10	5.0	261	36.5	9,523
95-98.5	96.25	3.5	1.0	21	12.775	269
Total						1,268,200

$$Q_s = 21.056Q^{1.5639}$$
$$R^2 = 0.9719$$
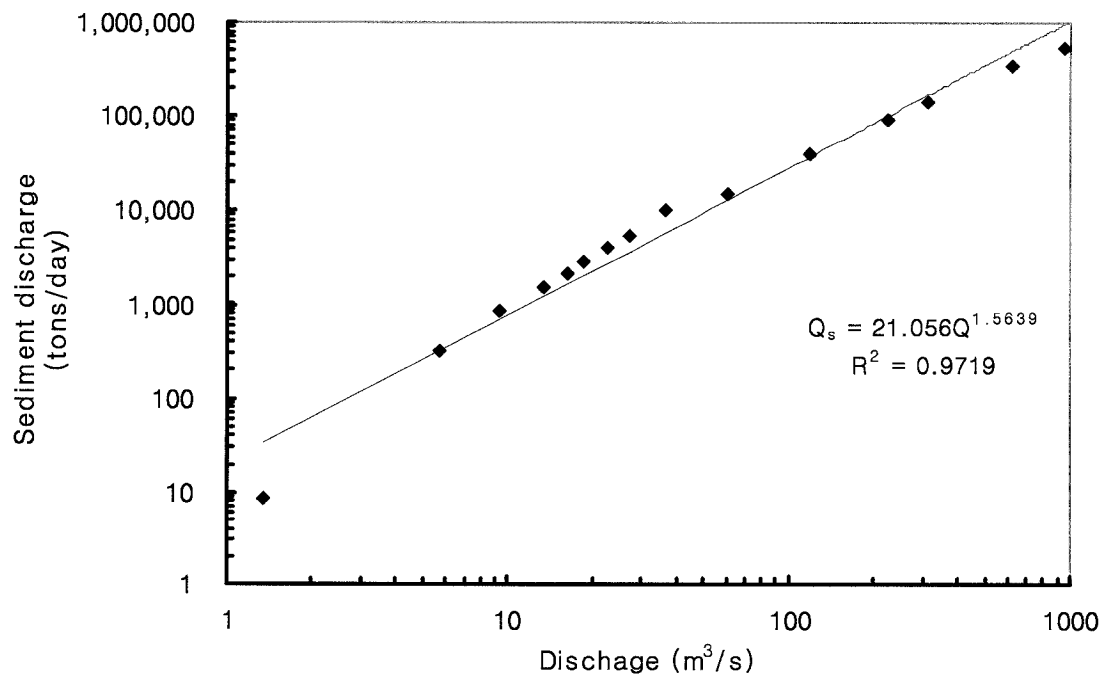
Figure A-5. Sediment – discharge rating curve at confluence with the Nakdong River by Van Rijn's (1984) method
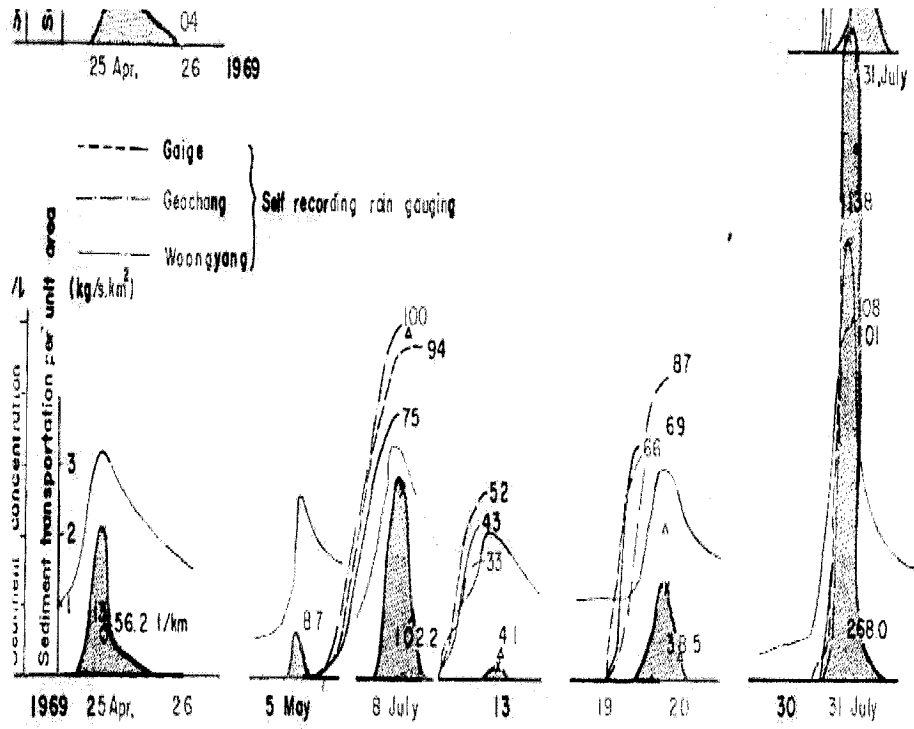
Figure A-6. Example of the Hydro-, Rain-, Sediment (Concentration + Transport) Graph (FAO/UNDP and KOWACO, 1971)

169

11. Sediment transport equations

1. Engelund and Hansen (1972)

$$C_w = 0.05 \left(\frac{G}{G-1}\right) \frac{VS_f}{[(G-1)gd_s]^{1/2}} \left[\frac{R_h S_f}{(G-1)d_s}\right]^{0.5}$$

Where, d_s = grain size, S_f = friction slope, R_h = hydraulic radius, V = depth – averaged velocity, g = gravitational acceleration, and G = specific gravity of sediment

2. Ackers and White (1973)

$$C_w = c_{AW2} G \frac{d_s}{h} \left(\frac{V}{u_*}\right)^{c_{AW1}} \left[\frac{c_{AW5}}{c_{AW3}} - 1\right]^{c_{AW4}}$$

Where, d_s =grain size, h = flow depth, V =depth –averaged velocity, and G =specific gravity of sediment

In which c_{AW1}, c_{AW2}, c_{AW3}, and c_{AW4} depend on the dimensionless particle diameter $d_* = [(G-1)g/v^2]^{1/3} d_s$. The relationships for c_{AW1}, c_{AW2}, c_{AW3}, and c_{AW4} obtained using flume data for particle sizes ranging from 0.04 mm to 4.0 mm are

1. for $1.0 < d_* < 60.0$,

c_{AW1} = 1.0 - 0.56 $\log d_*$

$\log c_{AW2}$ = 2.86 $\log d_*$ - $(\log d_*)^2$ – 3.53

$c_{AW3} = \dfrac{0.23}{d_*^{1/2}} + 0.14$

$c_{AW4} = \dfrac{9.66}{d_*} + 1.34$

2. for $d_* > 60.0$,

c_{AW1} = 0, c_{AW2} = 0.025, c_{AW3} = 0.17, c_{AW4} = 1.50

3. Yang (1973)

$$\log C_{ppm} = 5.435 - 0.286 \log\frac{\omega d_s}{v} - 0.457 \log\frac{u_*}{\omega}$$

$$+ \left(1.799 - 0.409 \log\frac{\omega d_s}{v} - 0.314 \log\frac{u_*}{\omega}\right)$$

$$\times \log\left(\frac{VS}{\omega} - \frac{V_c S}{\omega}\right)$$

(4) Yang (1979)

$$\log C_{ppm} = 6.681 - 0.633 \log \frac{\omega d_s}{v} - 4.816 \log \frac{u_*}{\omega}$$

$$+ \left(2.784 - 0.305 \log \frac{\omega d_s}{v} - 0.282 \log \frac{u_*}{\omega} \right)$$

$$\times \log \left(\frac{VS}{\omega} - \frac{V_c S}{\omega} \right)$$

Where, ω = fall velocity, V = depth –averaged velocity, V_c = average flow velocity at incipient motion, S = bed slope, v = kinematic viscosity, and VS = unit stream power

(5) Van Rijn (1984)
- Suspended load

$$\frac{q_{sb}}{\sqrt{(s-1)gD^3}} = 0.053 \frac{T^{2.1}}{D_*^{0.3}}$$

Where, q_{sb} = suspended load (m^3/s/m), T, D_* = dimensionless stage of transport and particle size respectively,

- Bed load

$$q_{ss} = FVdC_a; \quad 0.3 < Z' < 3, \quad 0.01 < a/d \ (=\eta_a) < 0.1$$

Where, $\displaystyle F = \frac{\eta_a^{Z'} - \eta_a^{1.2}}{(1-\eta_a)^{Z'}(1.2 - Z')}$, $\quad Z$ = Rouse number, $\quad Z' = Z + \phi$,

$\displaystyle \phi = 2.5 \left(\frac{\omega_o}{u_*} \right)^{0.8} \left(\frac{C_a}{C_o} \right)^{0.4}$; $\dfrac{\omega_r}{u_*} < 1.0$, C_a = sediment concentration at an average

elevation above bed elevation, C_o = sediment concentration at maximum elevation above the bed elevation.

- Total load

$$q_s = q_{sb} + q_{ss}$$

APPENDIX B : SEDIMENT TRANSPORT MODEL

1. Description of GSTAR-1D model

GSTAR-1D, a one-dimensional hydraulic and sediment transport model selected for application to the study reach. The model was selected because GSTAR-1D model have capabilities steady and unsteady flow simulation with mobile boundary conditions. Also, GSTAR-1D is the most recent model developed in the GSTAR series. The unsteady simulation capability is the most important for this study because it is need to unsteady simulation for the flow fluctuation by the re-regulation dam operation to analyze the effect of this flow fluctuation to the downstream channel geometry. But, HEC-6 and GSTARS series don't have unsteady flow simulation capability. The other models have unsteady simulation capability and generally have many of the same capabilities each other. Therefore, GSTAR-1D selected for this study reach because it is the most recent developed model and well suited for a simulation of the downstream channel geomophological change by dam construction.

GSTAR-1D is a hydraulic and sediment transport numerical model developed to simulate flows in rivers and channels with or without movable boundaries. Some of the model's capabilities are (Huang and Greimann , 2006a):

• Computation of water surface profiles in a single channel or multi-channel looped networks.

• Steady and unsteady flows.

• Subcritical flows in a steady hydraulic simulation.

• Subcritical, supercritical, and transcritical flows in an unsteady hydraulic simulation.

• Steady and unsteady sediment transport.

• Transport of cohesive and non-cohesive sediments.

- Cohesive sediment aggregation, deposition, erosion, and consolidation.

- Sixteen different non-cohesive sediment transport equations that are applicable to a wide range of hydraulic and sediment conditions.

- Cross stream variation in hydraulic roughness.

- Exchange of water and sediment between main channel and floodplains.

- Fractional sediment transport, bed sorting, and armoring.

- Computation of width changes using theories of minimum stream power and other minimizations.

- Point and non-point sources of flow and sediments.

- Internal boundary conditions, such as time-stage tables, rating curves, weirs, bridges, and radial gates.

GSTAR-1D uses the standard step method to solve the energy equation for steady gradually varied flows. The energy equation for steady gradually varied flow between downstream cross-section 1 and upstream cross-section 2 is expresses as:

$$Z_2 + \beta_2 \frac{V_2^2}{2g} - Z_1 - \beta_1 \frac{V_1^2}{2g} = h_f + h_c \qquad \text{(B-1)}$$

Where, Z_1, Z_2 = water surface elevations at cross sections 1 and 2, respectively; V_1, V_2 = average velocities at cross sections 1 and 2, respectively; β_1, β_2 = velocity distribution coefficients at cross sections 1 and 2, respectively; g = gravitational acceleration; h_f = friction loss between cross sections 1 and 2, and h_c = contraction or expansion losses between cross sections 1 and 2.

GSTAR-1D also has the ability to simulate unsteady flow. The theoretical basis for the unsteady flow solution is described below. One-dimensional river flows are described by the de St. Venant equations,

173

$$\frac{\partial(A + A_d)}{\partial t} + \frac{\partial Q}{\partial x} = q_{lat} \tag{B-2}$$

$$\frac{\partial Q}{\partial t} + \frac{\partial(\beta Q^2 / A)}{\partial x} + gA\frac{\partial Z}{\partial x} = -gAS_f \tag{B-3}$$

where: Q = discharge (m3/s), A = cross section area (m²), A_d = ineffective cross section area (m²), q_{lat} = lateral inflow per unit length of channel (m²/s), t = time independent variable (s), x = spatial independent variable (m), g = gravity acceleration (m/s²), β = velocity distribution coefficients, Z = water surface elevation (m), S_f= energy slope ($= \dfrac{Q|Q|}{K^2}$), and K = conveyance (m³/s).

GSTAR-1D simulates the physical processes important to both cohesive and non-cohesive sediment transport. There are three major components of sediment transport:

1. Sediment Routing

2. Bed Material Mixing

3. Cohesive Sediment Consolidation

There are two types of sediment routing available in GSTAR-1D: unsteady sediment routing and Exner equation routing. The unsteady sediment routing computes the changes to the suspended sediment concentration with time. The Exner equation routing ignores changes to the suspended sediment concentration over time. Unsteady sediment routing can be used when unsteady flow is being simulated and suspended concentrations change rapidly. In most other cases, Exner equation routing can be used.

The Exner equation (Exner, 1920; 1925) was derived assuming that changes to the volume of sediment in suspension are much smaller than the changes to the volume of sediment in the bed, which is generally true for long-term simulations where steady flow is being simulated. The mass conservation equation for sediment reduces to,

$$\frac{\partial Q_s}{\partial x} + \varepsilon\frac{\partial A_d}{\partial t} - q_s = 0 \tag{B-4}$$

Where, ε = volume of sediment in a unit bed layer volume (one minus porosity); A_d = volume of bed sediment per unit length; Q_s = volumetric sediment discharge; and q_s = lateral sediment inflow per unit length.

When simulating unsteady flow, the changes in suspended concentration cannot always be ignored. To compute the changes in suspended sediment concentration, the convection-diffusion equation with a source term for sediment erosion/deposition is used. If floodplains are being simulated, the sediment transport is two-dimensional (2D) and the cross-stream component of sediment transport in the y-direction is responsible for the transfer of sediment into and out of the floodplain. If floodplains are not simulated, the transport in the y-direction is ignored. The 2D depth-averaged convection-diffusion equation for a particular sediment size class is:

$$\frac{\partial(hC)}{\partial t} + \frac{\partial(huC)}{\partial x} + \frac{\partial(hvC)}{\partial y} = \frac{\partial}{\partial x}(D_x h \frac{\partial C}{\partial x}) + \frac{\partial}{\partial y}(D_y h \frac{\partial C}{\partial y}) + \Omega \qquad \text{(B-5)}$$

Where, h = depth; C = depth-averaged sediment concentration of one constituent; t = time; u, v = depth-averaged velocity components in the horizontal streamwise and transverse directions, x and y, respectively; D_x, D_y = diffusion coefficients in the x and y directions, respectively; and Ω = source (erosion) and sink (deposition) terms for one sediment constituent.

2. Model Applicability

The GSTAR-1D model was applied to a reach of the Rio Grande, from Cochiti Dam to Isleta Diversion Dam from 1972 to 1992 and from 1992 to 2002 by Huang and Griemann (2006b) to assess the model applicability. In this study, the bed profile and sediment cumulative erosion are compared with the field measurement data. The agreement between measurement and simulation was good, although the model tended to over predicted cumulative total volume of sediment in the middle region of the study reach. Also, Griemman and Huang (2006) applied GSTAR-1D to simulate a laboratory experiment of incision through a reservoir delta deposit. The model was shown to predict the vertical incision and downstream sediment load with reasonable accuracy if the erosion width is specified correctly.

3. Upstream flow boundary condition (100 hr) for the four cases

- Case 1 (daily pulse), Case 2 (daily average), and Case 3 (flood peak), Case 4 (Flood average)

No.	Date	Time	Flow discharge (m³/s)		Date	Time	Flow discharge (m³/s)	
			Case 1	Case 2			Case 3	Case 4
0	7/2/2005	7:00	14.7	33.0	8/30/2002	1:00	158.0	275.1
1	7/2/2005	8:00	14.5	33.0	8/30/2002	2:00	219.1	275.1
2	7/2/2005	9:00	14.3	33.0	8/30/2002	3:00	231.5	275.1
3	7/2/2005	10:00	52.6	33.0	8/30/2002	4:00	231.5	275.1
4	7/2/2005	11:00	91.6	33.0	8/30/2002	5:00	231.5	275.1
5	7/2/2005	12:00	92.9	33.0	8/30/2002	6:00	248.8	275.1
6	7/2/2005	13:00	91.7	33.0	8/30/2002	7:00	231.8	275.1
7	7/2/2005	14:00	90.0	33.0	8/30/2002	8:00	223.0	275.1
8	7/2/2005	15:00	91.4	33.0	8/30/2002	9:00	210.1	275.1
9	7/2/2005	16:00	92.4	33.0	8/30/2002	10:00	240.0	275.1
10	7/2/2005	17:00	39.2	33.0	8/30/2002	11:00	246.9	275.1
11	7/2/2005	18:00	35.6	33.0	8/30/2002	12:00	210.2	275.1
12	7/2/2005	19:00	35.4	33.0	8/30/2002	13:00	254.1	275.1
13	7/2/2005	20:00	34.7	33.0	8/30/2002	14:00	207.9	275.1
14	7/2/2005	21:00	33.6	33.0	8/30/2002	15:00	246.7	275.1
15	7/2/2005	22:00	34.0	33.0	8/30/2002	16:00	231.9	275.1
16	7/2/2005	23:00	61.7	33.0	8/30/2002	17:00	240.0	275.1
17	7/2/2005	0:00	63.3	33.0	8/30/2002	18:00	244.6	275.1
18	7/3/2005	1:00	63.6	33.0	8/30/2002	19:00	277.5	275.1
19	7/3/2005	2:00	16.7	33.0	8/30/2002	20:00	267.6	275.1
20	7/3/2005	3:00	14.2	33.0	8/30/2002	21:00	246.6	275.1
21	7/3/2005	4:00	14.3	33.0	8/30/2002	22:00	248.3	275.1
22	7/3/2005	5:00	14.5	33.0	8/30/2002	23:00	248.9	275.1
23	7/3/2005	6:00	14.7	33.0	8/30/2002	0:00	230.3	275.1
24	7/3/2005	7:00	14.9	33.0	8/31/2002	1:00	244.1	275.1
25	7/3/2005	8:00	15.2	33.0	8/31/2002	2:00	230.1	275.1
26	7/3/2005	9:00	15.4	33.0	8/31/2002	3:00	248.1	275.1
27	7/3/2005	10:00	15.5	33.0	8/31/2002	4:00	247.6	275.1
28	7/3/2005	11:00	15.5	33.0	8/31/2002	5:00	247.3	275.1
29	7/3/2005	12:00	15.4	33.0	8/31/2002	6:00	247.0	275.1
30	7/3/2005	13:00	15.4	33.0	8/31/2002	7:00	255.9	275.1
31	7/3/2005	14:00	15.0	33.0	8/31/2002	8:00	264.9	275.1
32	7/3/2005	15:00	14.7	33.0	8/31/2002	9:00	256.4	275.1
33	7/3/2005	16:00	14.4	33.0	8/31/2002	10:00	276.0	275.1
34	7/3/2005	17:00	21.1	33.0	8/31/2002	11:00	277.8	275.1
35	7/3/2005	18:00	59.5	33.0	8/31/2002	12:00	273.0	275.1
36	7/3/2005	19:00	63.3	33.0	8/31/2002	13:00	280.4	275.1
37	7/3/2005	20:00	60.1	33.0	8/31/2002	14:00	290.1	275.1
38	7/3/2005	21:00	62.6	33.0	8/31/2002	15:00	308.4	275.1
39	7/3/2005	22:00	65.7	33.0	8/31/2002	16:00	344.3	275.1
40	7/3/2005	23:00	67.9	33.0	8/31/2002	17:00	348.1	275.1
41	7/3/2005	0:00	68.3	33.0	8/31/2002	18:00	401.0	275.1
42	7/4/2005	1:00	14.8	33.0	8/31/2002	19:00	417.2	275.1

43	7/4/2005	2:00	15.1	33.0	8/31/2002	20:00	399.2	275.1
44	7/4/2005	3:00	15.3	33.0	8/31/2002	21:00	494.3	275.1
45	7/4/2005	4:00	15.6	33.0	8/31/2002	22:00	402.2	275.1
46	7/4/2005	5:00	15.8	33.0	8/31/2002	23:00	419.7	275.1
47	7/4/2005	6:00	15.7	33.0	8/31/2002	0:00	486.9	275.1
48	7/4/2005	7:00	15.6	33.0	9/1/2002	1:00	486.9	275.1
49	7/4/2005	8:00	15.2	33.0	9/1/2002	2:00	503.9	275.1
50	7/4/2005	9:00	14.8	33.0	9/1/2002	3:00	504.0	275.1
51	7/4/2005	10:00	14.4	33.0	9/1/2002	4:00	486.3	275.1
52	7/4/2005	11:00	43.7	33.0	9/1/2002	5:00	466.6	275.1
53	7/4/2005	12:00	59.7	33.0	9/1/2002	6:00	482.7	275.1
54	7/4/2005	13:00	56.1	33.0	9/1/2002	7:00	498.9	275.1
55	7/4/2005	14:00	53.7	33.0	9/1/2002	8:00	498.8	275.1
56	7/4/2005	15:00	58.1	33.0	9/1/2002	9:00	482.0	275.1
57	7/4/2005	16:00	61.8	33.0	9/1/2002	10:00	481.3	275.1
58	7/4/2005	17:00	64.8	33.0	9/1/2002	11:00	481.0	275.1
59	7/4/2005	18:00	52.1	33.0	9/1/2002	12:00	476.0	275.1
60	7/4/2005	19:00	20.3	33.0	9/1/2002	13:00	496.4	275.1
61	7/4/2005	20:00	15.8	33.0	9/1/2002	14:00	496.4	275.1
62	7/4/2005	21:00	15.7	33.0	9/1/2002	15:00	463.1	275.1
63	7/4/2005	22:00	15.2	33.0	9/1/2002	16:00	446.5	275.1
64	7/4/2005	23:00	14.7	33.0	9/1/2002	17:00	433.7	275.1
65	7/4/2005	0:00	14.3	33.0	9/1/2002	18:00	375.0	275.1
66	7/5/2005	1:00	14.4	33.0	9/1/2002	19:00	379.1	275.1
67	7/5/2005	2:00	14.7	33.0	9/1/2002	20:00	364.2	275.1
68	7/5/2005	3:00	14.8	33.0	9/1/2002	21:00	290.7	275.1
69	7/5/2005	4:00	15.1	33.0	9/1/2002	22:00	230.4	275.1
70	7/5/2005	5:00	15.4	33.0	9/1/2002	23:00	220.6	275.1
71	7/5/2005	6:00	15.7	33.0	9/1/2002	0:00	216.1	275.1
72	7/5/2005	7:00	15.8	33.0	9/2/2002	1:00	202.9	275.1
73	7/5/2005	8:00	15.5	33.0	9/2/2002	2:00	220.4	275.1
74	7/5/2005	9:00	15.1	33.0	9/2/2002	3:00	220.4	275.1
75	7/5/2005	10:00	14.7	33.0	9/2/2002	4:00	228.9	275.1
76	7/5/2005	11:00	52.9	33.0	9/2/2002	5:00	237.6	275.1
77	7/5/2005	12:00	66.7	33.0	9/2/2002	6:00	246.3	275.1
78	7/5/2005	13:00	65.6	33.0	9/2/2002	7:00	246.3	275.1
79	7/5/2005	14:00	63.0	33.0	9/2/2002	8:00	246.3	275.1
80	7/5/2005	15:00	65.8	33.0	9/2/2002	9:00	227.3	275.1
81	7/5/2005	16:00	67.8	33.0	9/2/2002	10:00	194.4	275.1
82	7/5/2005	17:00	69.2	33.0	9/2/2002	11:00	94.5	275.1
83	7/5/2005	18:00	14.9	33.0	9/2/2002	12:00	90.6	275.1
84	7/5/2005	19:00	13.5	33.0	9/2/2002	13:00	97.9	275.1
85	7/5/2005	20:00	13.2	33.0	9/2/2002	14:00	97.9	275.1
86	7/5/2005	21:00	13.4	33.0	9/2/2002	15:00	87.4	275.1
87	7/5/2005	22:00	13.5	33.0	9/2/2002	16:00	97.8	275.1
88	7/5/2005	23:00	13.7	33.0	9/2/2002	17:00	94.2	275.1
89	7/5/2005	0:00	13.9	33.0	9/2/2002	18:00	74.9	275.1
90	7/6/2005	1:00	14.1	33.0	9/2/2002	19:00	94.1	275.1
91	7/6/2005	2:00	14.3	33.0	9/2/2002	20:00	100.9	275.1
92	7/6/2005	3:00	14.5	33.0	9/2/2002	21:00	93.8	275.1

93	7/6/2005	4:00	14.7	33.0	9/2/2002	22:00	100.7	275.1
94	7/6/2005	5:00	15.0	33.0	9/2/2002	23:00	90.1	275.1
95	7/6/2005	6:00	15.2	33.0	9/2/2002	0:00	96.9	275.1
96	7/6/2005	7:00	15.5	33.0	9/3/2002	1:00	103.7	275.1
97	7/6/2005	8:00	15.7	33.0	9/3/2002	2:00	95.0	275.1
98	7/6/2005	9:00	15.8	33.0	9/3/2002	3:00	86.3	275.1
99	7/6/2005	10:00	30.6	33.0	9/3/2002	4:00	99.9	275.1

4. Sample input and output files of the GSTAR-1D

(a) Input file for Case 1

```
YTT    Hwang River 2003 for future channel adjustment forecasting (Case 1, daily pulse)
YTT
*** HWANG  for steady flow simulation     1          1****************************************
***     NKI(J)        b.c.        for     internal     station
***     nriv    nf    nlay
YNR        1     11     2
***     isolve (2=diffusive, 4=dynamic)  isolves    EPSY    F1 (implicity factor)  XFACT  METRIC   YZ
YSL        4                        1    1.00E-04   0.6             1        1     1
***     KFLP    qmin
YFP       0      0
***     THE    iHotSt
YTM      100     0
***     TDT     DT    DTPLT   xcplt
YDT       0    0.01    10      1
***     Start of River 1
***     KU(J)
UFB        2
***     T1     ST1
U02       0    14.70
U02       1    14.50
U02       2    14.30
U02       3    52.60
U02       4    91.60
U02       5    92.90
U02       6    91.70
U02       7    90.00
U02       8    91.40
U02       9    92.40
U02      10    39.20
U02      11    35.60
U02      12    35.40
U02      13    34.70
U02      14    33.60
U02      15    34.00
U02      16    61.70
U02      17    63.30
U02      18    63.60
U02      19    16.70
U02      20    14.20
U02      21    14.30
U02      22    14.50
U02      23    14.70
U02      24    14.90
U02      25    15.20
U02      26    15.40
U02      27    15.50
U02      28    15.50
U02      29    15.40
U02      30    15.40
U02      31    15.00
```

```
U02    32   14.70
U02    33   14.40
U02    34   21.10
U02    35   59.50
U02    36   63.30
U02    37   60.10
U02    38   62.60
U02    39   65.70
U02    40   67.90
U02    41   68.30
U02    42   14.80
U02    43   15.10
U02    44   15.30
U02    45   15.60
U02    46   15.80
U02    47   15.70
U02    48   15.60
U02    49   15.20
U02    50   14.80
U02    51   14.40
U02    52   43.70
U02    53   59.70
U02    54   56.10
U02    55   53.70
U02    56   58.10
U02    57   61.80
U02    58   64.80
U02    59   52.10
U02    60   20.30
U02    61   15.80
U02    62   15.70
U02    63   15.20
U02    64   14.70
U02    65   14.30
U02    66   14.40
U02    67   14.70
U02    68   14.80
U02    69   15.10
U02    70   15.40
U02    71   15.70
U02    72   15.80
U02    73   15.50
U02    74   15.10
U02    75   14.70
U02    76   52.90
U02    77   66.70
U02    78   65.60
U02    79   63.00
U02    80   65.80
U02    81   67.80
U02    82   69.20
U02    83   14.90
U02    84   13.50
U02    85   13.20
U02    86   13.40
U02    87   13.50
U02    88   13.70
U02    89   13.90
U02    90   14.10
U02    91   14.30
U02    92   14.50
U02    93   14.70
U02    94   15.00
U02    95   15.20
U02    96   15.50
U02    97   15.70
U02    98   15.80
U02    99   30.60
DFB     3
***    TN      SLFI (5 = normanl depth, 3 = time, discharge  stage)
D03     0   7.27
D03     1   7.27
D03     2   7.27
D03     3   7.27
D03     4   7.27
D03     5   7.28
D03     6   7.28
D03     7   7.28
D03     8   7.29
D03     9   7.29
```

D03	10	7.28
D03	11	7.28
D03	12	7.27
D03	13	7.25
D03	14	7.23
D03	15	7.22
D03	16	7.22
D03	17	7.26
D03	18	7.38
D03	19	7.45
D03	20	7.49
D03	21	7.51
D03	22	7.51
D03	23	7.49
D03	24	7.47
D03	25	7.44
D03	26	7.42
D03	27	7.40
D03	28	7.39
D03	29	7.39
D03	30	7.39
D03	31	7.39
D03	32	7.38
D03	33	7.37
D03	34	7.36
D03	35	7.34
D03	36	7.31
D03	37	7.28
D03	38	7.25
D03	39	7.22
D03	40	7.20
D03	41	7.17
D03	42	7.16
D03	43	7.15
D03	44	7.13
D03	45	7.13
D03	46	7.12
D03	47	7.12
D03	48	7.12
D03	49	7.13
D03	50	7.17
D03	51	7.27
D03	52	7.36
D03	53	7.40
D03	54	7.41
D03	55	7.41
D03	56	7.39
D03	57	7.38
D03	58	7.36
D03	59	7.33
D03	60	7.30
D03	61	7.26
D03	62	7.23
D03	63	7.21
D03	64	7.19
D03	65	7.17
D03	66	7.16
D03	67	7.18
D03	68	7.23
D03	69	7.30
D03	70	7.37
D03	71	7.39
D03	72	7.40
D03	73	7.39
D03	74	7.38
D03	75	7.37
D03	76	7.35
D03	77	7.32
D03	78	7.29
D03	79	7.26
D03	80	7.23
D03	81	7.20
D03	82	7.18
D03	83	7.16
D03	84	7.15
D03	85	7.14
D03	86	7.13
D03	87	7.12
D03	88	7.12
D03	89	7.12

```
D03     90     7.13
D03     91     7.17
D03     92     7.26
D03     93     7.36
D03     94     7.40
D03     95     7.41
D03     96     7.41
D03     97     7.39
D03     98     7.38
D03     99     7.36
***     # int. BC
INF         0
***     NKQF(J) non-point flow source
LNF         0
**** *********************************************************************************
**** station: 180
****
****
**** cross section   1 of 211 at original   1
****      FLDST        ZDI        QDI
*XIN       0          0          0
****    location      bec       ninterp     iHotC
*XST    44943.00       0          0          0
****    station   elevation    data
*XSP     0.00       80.00      10.00      80.00      30.00      66.00      40.00      66.00      50.00      66.00
*XSP    52.00       52.00     130.00      52.00     132.00      66.00     170.00      66.00
****    locl_dead   locr_dead    hdead
*XIX     0.00       50.00      66.00     132.00     170.00      66.00
****    locl_lev    locr_lev     hlev
*XLX     0.00       50.00      66.00     132.00     170.00      66.00
****    xloc_rcoef    rcoef
*XRH     0.000       0.035     50.000      0.035    132.000      0.035
****     bankl       bankr
*XOX    50.00      132.00
****    expansion   contraction
*XFL     0.30        0.10
****    GIS Cut Line
****       xl    yl    xr    yr
*XSL     5000       0    5000    280
****       xl    yl    xr    yr
*XSL     5000       0    5000    280
*XSL
*** ***********************************************************************************
*** station: 179
***
***
*** cross section   2 of 211 at original   2
***      FLDST        ZDI        QDI
XIN       0          0          0
***    location      bec       ninterp     iHotC
XST    44763.00       0          0          0
***    station   elevation    data
XSP     0.00       99.20      30.00      88.50      33.20      88.50      70.00      65.50      90.00      57.20
XSP   100.00       53.20     119.50      47.50     121.00      47.00     161.00      47.00     162.00      48.20
XSP   165.50       48.70     188.00      48.70     190.00      48.40     222.00      48.40     223.50      48.50
XSP   264.00       48.50     273.00      53.20     290.50      53.20     295.00      55.60     299.00      55.60
XSP   301.00       57.10     350.00      70.20     400.20      81.03
***    locl_dead   locr_dead    hdead
XIX     0.00      100.00      60.00     295.00     400.20      60.00
***    locl_lev    locr_lev     hlev
XLX     0.00      100.00      60.00     295.00     400.20      60.00
***    xloc_rcoef    rcoef
XRH     0.000       0.035    100.000      0.035    295.000      0.035
***     bankl       bankr
XOX   100.00      295.00
***    expansion   contraction
XFL     0.30        0.10
***    GIS Cut Line
***       xl    yl    xr    yr
XSL     5000       0    5000    280
XSL
*** ***********************************************************************************
*** station: 178
***
***
*** cross section   3 of 211 at original   3
***      FLDST        ZDI        QDI
XIN       0          0          0
***    location      bec       ninterp     iHotC
XST    44573.00       0          0          0
```

181

```
***      station    elevation    data
XSP      0.00      64.00       28.00    62.70    30.00    61.10    57.00    57.80    65.90    52.91
XSP     97.30      52.91       97.50    53.01   100.00    53.01   103.00    50.80   109.90    50.80
XSP    110.60      50.20      119.00    50.20   123.40    47.10   125.00    46.70   134.40    46.70
XSP    135.00      47.10      137.80    48.40   139.80    48.40   146.30    48.73   149.30    47.90
XSP    158.50      48.20      160.00    49.20   179.70    49.30   191.70    49.10   234.70    48.40
XSP    244.00      47.30      245.50    46.30   247.50    45.80   252.50    45.30   293.60    48.10
XSP    300.00      52.40      306.50    52.40   311.50    53.90   323.90    54.90   324.40    55.42
XSP    330.40      55.42      332.40    56.50   339.40    56.50   344.00    57.90   364.00    58.40
XSP    382.00      58.40
***    locl_dead  locr_dead   hdead
XIX      0.00     100.00       55.00   323.90   382.00    55.00
***    locl_lev   locr_lev    hlev
XLX      0.00     100.00       55.00   323.90   382.00    55.00
***    xloc_rcoef  rcoef
XRH      0.000      0.035     100.000    0.035  323.900    0.035
***      bankl      bankr
XOX    100.00     323.90
***    expansion  contraction
XFL      0.30       0.10
***    GIS Cut Line
***      xl    yl    xr    yr
XSL     5000    0   5000   280
XSL
```

Abbreviated channel cross-section data (Station No. 177 ~ 2)

```
*** ****************************************************************************************
*** station: 1
***
***
*** cross section 210 of 211 at original 210
***     FLDST      ZDI       QDI
XIN       0         0         0
***    location    bec      ninterp    iHotC
XST    220.00       0         0          0
***    station   elevation   data
XSP      0.00      22.03       5.00    22.03    20.00    10.77   133.00    10.77   153.00    21.26
XSP    160.00      21.26      180.00    13.53   200.00    10.77   205.00     7.20   206.00     6.40
XSP    226.00       6.40      227.00     7.20   237.00     7.20   239.00     7.00   245.00     7.00
XSP    270.20       7.10      285.40     7.10   296.20     7.10   302.40     7.20   303.90     8.26
XSP    368.20       8.10      440.60     7.75   492.00     7.70   544.00     7.20   552.60    11.23
XSP    605.00      11.40      608.20    12.60   617.00    12.80   642.10    13.10   658.70    13.50
XSP    684.40      20.00      692.10    21.24   704.70    20.27   720.30    22.03   800.00    22.03
***    locl_dead  locr_dead   hdead
XIX      0.00     160.00       25.00   692.10   800.00    25.00
***    locl_lev   locr_lev    hlev
XLX      0.00     160.00       25.00   692.10   800.00    25.00
***    xloc_rcoef  rcoef
XRH      0.000      0.025     160.000    0.025  692.100    0.025
***      bankl      bankr
XOX    160.00     692.10
***    expansion  contraction
XFL      0.30       0.10
***    GIS Cut Line
***      xl    yl    xr    yr
XSL     5000    0   5000   280
XSL
*** ****************************************************************************************
*** station: 0
***
***
*** cross section 211 of 211 at original 211
***     FLDST      ZDI       QDI
XIN       0         0         0
***    location    bec      ninterp    iHotC
XST      0.00       0         0          0
***    station   elevation   data
XSP      0.00      12.24      113.50    12.24   121.30     7.04   127.60     7.04   148.50    13.86
XSP    188.20      13.86      188.50    13.62   191.70    13.62   228.00    13.69   248.00    21.26
XSP    255.00      21.26      275.00    13.69   300.00    13.69   308.00     7.80   311.20     7.05
XSP    313.00       6.90      333.20     6.90   349.50     6.75   357.00     6.75   417.20     6.92
XSP    431.60       6.92      434.80     8.14   447.20     8.10   511.60    10.69   551.80    10.69
XSP    558.00       8.35      611.40     7.83   642.60     7.75   713.80     7.34   758.90     7.35
XSP    822.70       7.58      862.40    10.49   867.40    10.49   883.50    11.59   935.00    13.10
XSP    935.20      13.40      949.50    13.50   955.80    14.33   964.10    15.80   980.70    19.82
```

```
XSP     990.00      21.92    1001.50    21.92    1018.10    19.00    1027.00    18.91    1061.00    14.40
XSP    1100.00      14.40
***    locl_dead   locr_dead    hdead
XIX      0.00      255.00    25.00    990.00    1100.00    25.00
***    locl_lev    locr_lev    hlev
XLX      0.00      255.00    25.00    990.00    1100.00    25.00
***    xloc_rcoef    rcoef
XRH      0.000      0.025    255.000    0.025    990.000    0.025
***    bankl       bankr
XOX    255.00      990.00
***    expansion   contraction
XFL      0.30        0.10
***    GIS Cut Line
***       xl     yl    xr    yr
XSL     5000      0   5000   280
XSL
***    End of River 1 (from the example 1)
***    Start Sediment Transport Input
***    theta   ntsedf  nrespone
YST      1       2      1
***    drl    dru    bdin
YSG     0.01  0.0625     0        ! silt     0.03
YSG     0.0625  0.25     0        ! fsnd     0.13
YSG     0.25    0.5      0        ! msnd     0.35
YSG     0.5     1        0        ! csnd     0.71
YSG      1      2        0        ! vcsnd    1.41
YSG      2      4        0        ! vfgrv    2.83
YSG      4      8        0        ! fgrv     5.66
YSG      8      16       0        ! mgrv    11.31
YSG     16      32       0        ! cgrv    22.63
YSG     32      64       0        ! vcgrv   45.25
YSG     64     128       0        ! scob    90.51
***    Start of River 1               3
***    nts
USB      4
***    TSI     QSI
US4      0     50.0
US4     100    50.0
***    QI     PISED
***            1       2       3       4       5       6       7       8       9      10      11
USS    1.000    0.0000  0.0000  0.0098  0.0196  0.0294  0.0588  0.1275  0.2549  0.2549  0.1275  0.1176
USS   10.000    0.0000  0.0000  0.0098  0.0196  0.0294  0.0588  0.1275  0.2549  0.2549  0.1275  0.1176
USS   50.000    0.0000  0.0039  0.0079  0.0158  0.0315  0.0630  0.1260  0.2520  0.2520  0.1260  0.1221
USS  100.000    0.0000  0.0039  0.0079  0.0158  0.0315  0.0630  0.1260  0.2520  0.2520  0.1260  0.1221
USS  200.000    0.0000  0.0039  0.0079  0.0158  0.0315  0.0630  0.1260  0.2520  0.2520  0.1260  0.1221
USS  500.000    0.0000  0.0039  0.0079  0.0158  0.0315  0.0630  0.1260  0.2520  0.2520  0.1260  0.1221
***    NKQS(J) non-point flow source
LNS      0
***    ii
BP1      1  4  12  20  28  36  44  60  68  76  84  96  104  112  120  132  140  148  156  168  179  187  195  210
***    PTMP
***    Layer     2
***    silt/clay vfs    fs      s      cs     vcs     vfg     fg      g      cg     vcg
BPL      0.0000  0.0000  0.0000  0.0000  0.0000  0.0000  0.0000  0.0000  0.0000  1.0000  0.0000
BPL      0.0000  0.0000  0.0000  0.1000  0.0000  0.1000  0.0000  0.0000  0.1000  0.7000  0.0000
BPL      0.0000  0.1000  0.1000  0.3000  0.2000  0.0000  0.1000  0.1000  0.1000  0.0000  0.0000
BPL      0.0000  0.1000  0.1000  0.2000  0.2000  0.1000  0.1000  0.1000  0.1000  0.0000  0.0000
BPL      0.0000  0.0000  0.2000  0.3000  0.3000  0.1000  0.1000  0.0000  0.0000  0.0000  0.0000
BPL      0.0000  0.2000  0.4000  0.3000  0.1000  0.0000  0.0000  0.0000  0.0000  0.0000  0.0000
BPL      0.0000  0.0000  0.2000  0.6000  0.2000  0.0000  0.0000  0.0000  0.0000  0.0000  0.0000
BPL      0.0000  0.1000  0.1000  0.4000  0.3000  0.1000  0.0000  0.0000  0.0000  0.0000  0.0000
BPL      0.0000  0.0000  0.2000  0.4000  0.3000  0.1000  0.0000  0.0000  0.0000  0.0000  0.0000
BPL      0.0000  0.3000  0.3000  0.3000  0.1000  0.0000  0.0000  0.0000  0.0000  0.0000  0.0000
BPL      0.0000  0.1000  0.3000  0.5000  0.1000  0.0000  0.0000  0.0000  0.0000  0.0000  0.0000
BPL      0.0000  0.1000  0.3000  0.4000  0.2000  0.0000  0.0000  0.0000  0.0000  0.0000  0.0000
BPL      0.0000  0.2000  0.3000  0.4000  0.1000  0.0000  0.0000  0.0000  0.0000  0.0000  0.0000
BPL      0.0000  0.0000  0.2000  0.5000  0.2000  0.1000  0.0000  0.0000  0.0000  0.0000  0.0000
BPL      0.0000  0.2000  0.4000  0.3000  0.1000  0.0000  0.0000  0.0000  0.0000  0.0000  0.0000
BPL      0.0000  0.0000  0.4000  0.5000  0.1000  0.0000  0.0000  0.0000  0.0000  0.0000  0.0000
BPL      0.0000  0.0000  0.5000  0.4000  0.1000  0.0000  0.0000  0.0000  0.0000  0.0000  0.0000
BPL      0.0000  0.0000  0.3000  0.5000  0.2000  0.0000  0.0000  0.0000  0.0000  0.0000  0.0000
BPL      0.0000  0.7000  0.2000  0.1000  0.0000  0.0000  0.0000  0.0000  0.0000  0.0000  0.0000
BPL      0.0000  0.4000  0.4000  0.2000  0.0000  0.0000  0.0000  0.0000  0.0000  0.0000  0.0000
BPL      0.0000  0.9000  0.1000  0.0000  0.0000  0.0000  0.0000  0.0000  0.0000  0.0000  0.0000
BPL      0.0000  1.0000  0.0000  0.0000  0.0000  0.0000  0.0000  0.0000  0.0000  0.0000  0.0000
BPL      0.0000  0.8000  0.1000  0.1000  0.0000  0.0000  0.0000  0.0000  0.0000  0.0000  0.0000
BPL      0.0000  0.7000  0.2000  0.1000  0.0000  0.0000  0.0000  0.0000  0.0000  0.0000  0.0000
***    ttin    temp
TMP      0    10.00
***    Erosion    and      Deposition Limits
```

```
FI2        0
***     crosmin_e crosmax_e crosmin_d crosmax_d   botmin    botmax
FIM     -99999    99999    -99999    99999      0    99999
***     nstube  wfrac
STU        1    0.8
***     imin  ilength
SMN        0    0
***     ised
SEQ        6
***     xc
SA2        0    5000
***     angle1(abangle2(benalt   alphad  alphas  blength  wt dep  dlong   dtrans
SAT       35    35     10    0.25     1     0     0     0     0
SAT       35    35     10    0.25     1     0     0     0     0
***     ii
CS2        0
***     stdep_f stdep_p   concEq  er_lim
CSD      0.02   0.02      1    0.1
***     ii
CE2        0
***     stpero  er_stme  stmero  er_mass
CER      0.04  0.2500    2.84    1.07
***     fall velocity
CF0      1.00
***     densC_I densC_f densC_e  time_e
CSC    1300.00  1600.00  1400.00  1650.00
***     xc
CD2        0
***     densityClay0
CDI     1600.00
***     end message
END
```

(b) Output file for Case 1

```
# XC Time Series Data
# t=time(hr)
# q        = discharge (cfs or m^3/s)
# z        = current water surface elevation (ft or m)
# zba      = average bed elevation of the main channel (ft or m)
# conc     = concentration (-)
TITLE="XC Time Series"
VARIABLES= t,q0001,z0001,zba0001,conc0001
ZONE T=" XC Time Series Data"
#          |              xc   1              |
#     tt        q        z        zba       conc
  0.0000000E+00 0.147000E+02 0.473534E+02 0.210051-300 0.000000E+00
  0.1000000E-01 0.146990E+02 0.473530E+02 0.492035E+02 0.000000E+00
  0.2000000E-01 0.146970E+02 0.473524E+02 0.492035E+02 0.000000E+00
  0.3000000E-01 0.146950E+02 0.473518E+02 0.492035E+02 0.000000E+00
  0.4000000E-01 0.146930E+02 0.473513E+02 0.492035E+02 0.000000E+00
  0.5000000E-01 0.146910E+02 0.473508E+02 0.492035E+02 0.000000E+00
  0.6000000E-01 0.146890E+02 0.473504E+02 0.492035E+02 0.000000E+00
  0.7000000E-01 0.146870E+02 0.473500E+02 0.492035E+02 0.000000E+00
  0.8000000E-01 0.146850E+02 0.473497E+02 0.492035E+02 0.000000E+00
  0.9000000E-01 0.146830E+02 0.473494E+02 0.492035E+02 0.000000E+00
  0.1000000E+00 0.146810E+02 0.473491E+02 0.492035E+02 0.000000E+00
  0.1100000E+00 0.146790E+02 0.473489E+02 0.492035E+02 0.000000E+00
  0.1200000E+00 0.146770E+02 0.473487E+02 0.492035E+02 0.000000E+00
  0.1300000E+00 0.146750E+02 0.473486E+02 0.492035E+02 0.000000E+00
  0.1400000E+00 0.146730E+02 0.473484E+02 0.492035E+02 0.000000E+00
  0.1500000E+00 0.146710E+02 0.473483E+02 0.492035E+02 0.000000E+00
  0.1600000E+00 0.146690E+02 0.473481E+02 0.492035E+02 0.000000E+00
  0.1700000E+00 0.146670E+02 0.473480E+02 0.492035E+02 0.000000E+00
  0.1800000E+00 0.146650E+02 0.473479E+02 0.492035E+02 0.000000E+00
  0.1900000E+00 0.146630E+02 0.473477E+02 0.492035E+02 0.000000E+00
  0.2000000E+00 0.146610E+02 0.473476E+02 0.492035E+02 0.000000E+00
  0.2100000E+00 0.146590E+02 0.473474E+02 0.492035E+02 0.000000E+00
  0.2200000E+00 0.146570E+02 0.473473E+02 0.492035E+02 0.000000E+00
  0.2300000E+00 0.146550E+02 0.473471E+02 0.492035E+02 0.000000E+00
  0.2400000E+00 0.146530E+02 0.473470E+02 0.492035E+02 0.000000E+00
  0.2500000E+00 0.146510E+02 0.473468E+02 0.492035E+02 0.000000E+00
  0.2600000E+00 0.146490E+02 0.473466E+02 0.492035E+02 0.000000E+00
  0.2700000E+00 0.146470E+02 0.473465E+02 0.492035E+02 0.000000E+00
  0.2800000E+00 0.146450E+02 0.473463E+02 0.492035E+02 0.000000E+00
  0.2900000E+00 0.146430E+02 0.473462E+02 0.492035E+02 0.000000E+00
  0.3000000E+00 0.146410E+02 0.473460E+02 0.492035E+02 0.000000E+00
  0.3100000E+00 0.146390E+02 0.473459E+02 0.492035E+02 0.000000E+00
  0.3200000E+00 0.146370E+02 0.473458E+02 0.492035E+02 0.000000E+00
  0.3300000E+00 0.146350E+02 0.473456E+02 0.492035E+02 0.000000E+00
  0.3400000E+00 0.146330E+02 0.473455E+02 0.492035E+02 0.000000E+00
  0.3500000E+00 0.146310E+02 0.473454E+02 0.492035E+02 0.000000E+00
  0.3600000E+00 0.146290E+02 0.473452E+02 0.492035E+02 0.000000E+00
  0.3700000E+00 0.146270E+02 0.473451E+02 0.492035E+02 0.000000E+00
  0.3800000E+00 0.146250E+02 0.473450E+02 0.492035E+02 0.000000E+00
  0.3900000E+00 0.146230E+02 0.473449E+02 0.492035E+02 0.000000E+00
  0.4000000E+00 0.146210E+02 0.473448E+02 0.492035E+02 0.000000E+00
  0.4100000E+00 0.146190E+02 0.473447E+02 0.492035E+02 0.000000E+00
  0.4200000E+00 0.146170E+02 0.473446E+02 0.492035E+02 0.000000E+00
  0.4300000E+00 0.146150E+02 0.473444E+02 0.492035E+02 0.000000E+00
  0.4400000E+00 0.146130E+02 0.473443E+02 0.492035E+02 0.000000E+00
  0.4500000E+00 0.146110E+02 0.473442E+02 0.492035E+02 0.000000E+00
  0.4600000E+00 0.146090E+02 0.473441E+02 0.492035E+02 0.000000E+00
  0.4700000E+00 0.146070E+02 0.473440E+02 0.492035E+02 0.000000E+00
  0.4800000E+00 0.146050E+02 0.473439E+02 0.492035E+02 0.000000E+00
  0.4900000E+00 0.146030E+02 0.473439E+02 0.492035E+02 0.000000E+00
  0.5000000E+00 0.146010E+02 0.473438E+02 0.492035E+02 0.000000E+00
  0.5100000E+00 0.145990E+02 0.473437E+02 0.492035E+02 0.000000E+00
  0.5200000E+00 0.145970E+02 0.473436E+02 0.492035E+02 0.000000E+00
  0.5300000E+00 0.145950E+02 0.473435E+02 0.492035E+02 0.000000E+00
  0.5400000E+00 0.145930E+02 0.473434E+02 0.492035E+02 0.000000E+00
```

```
0.5500000E+00  0.145910E+02  0.473433E+02  0.492035E+02  0.000000E+00
0.5600000E+00  0.145890E+02  0.473432E+02  0.492035E+02  0.000000E+00
0.5700000E+00  0.145870E+02  0.473432E+02  0.492035E+02  0.000000E+00
0.5800000E+00  0.145850E+02  0.473431E+02  0.492035E+02  0.000000E+00
0.5900000E+00  0.145830E+02  0.473430E+02  0.492035E+02  0.000000E+00
0.6000000E+00  0.145810E+02  0.473429E+02  0.492035E+02  0.000000E+00
0.6100000E+00  0.145790E+02  0.473429E+02  0.492035E+02  0.000000E+00
0.6200000E+00  0.145770E+02  0.473428E+02  0.492035E+02  0.000000E+00
0.6300000E+00  0.145750E+02  0.473427E+02  0.492035E+02  0.000000E+00
0.6400000E+00  0.145730E+02  0.473426E+02  0.492035E+02  0.000000E+00
0.6500000E+00  0.145710E+02  0.473426E+02  0.492035E+02  0.000000E+00
0.6600000E+00  0.145690E+02  0.473425E+02  0.492035E+02  0.000000E+00
0.6700000E+00  0.145670E+02  0.473424E+02  0.492035E+02  0.000000E+00
0.6800000E+00  0.145650E+02  0.473424E+02  0.492035E+02  0.000000E+00
0.6900000E+00  0.145630E+02  0.473423E+02  0.492035E+02  0.000000E+00
0.7000000E+00  0.145610E+02  0.473422E+02  0.492035E+02  0.000000E+00
0.7100000E+00  0.145590E+02  0.473422E+02  0.492035E+02  0.000000E+00
0.7200000E+00  0.145570E+02  0.473421E+02  0.492035E+02  0.000000E+00
0.7300000E+00  0.145550E+02  0.473421E+02  0.492035E+02  0.000000E+00
0.7400000E+00  0.145530E+02  0.473420E+02  0.492035E+02  0.000000E+00
0.7500000E+00  0.145510E+02  0.473419E+02  0.492035E+02  0.000000E+00
0.7600000E+00  0.145490E+02  0.473419E+02  0.492035E+02  0.000000E+00
0.7700000E+00  0.145470E+02  0.473418E+02  0.492035E+02  0.000000E+00
0.7800000E+00  0.145450E+02  0.473418E+02  0.492035E+02  0.000000E+00
0.7900000E+00  0.145430E+02  0.473417E+02  0.492035E+02  0.000000E+00
0.8000000E+00  0.145410E+02  0.473416E+02  0.492035E+02  0.000000E+00
0.8100000E+00  0.145390E+02  0.473416E+02  0.492035E+02  0.000000E+00
0.8200000E+00  0.145370E+02  0.473415E+02  0.492035E+02  0.000000E+00
0.8300000E+00  0.145350E+02  0.473415E+02  0.492035E+02  0.000000E+00
0.8400000E+00  0.145330E+02  0.473414E+02  0.492035E+02  0.000000E+00
0.8500000E+00  0.145310E+02  0.473414E+02  0.492035E+02  0.000000E+00
0.8600000E+00  0.145290E+02  0.473413E+02  0.492035E+02  0.000000E+00
0.8700000E+00  0.145270E+02  0.473413E+02  0.492035E+02  0.000000E+00
0.8800000E+00  0.145250E+02  0.473412E+02  0.492035E+02  0.000000E+00
0.8900000E+00  0.145230E+02  0.473412E+02  0.492035E+02  0.000000E+00
0.9000000E+00  0.145210E+02  0.473411E+02  0.492035E+02  0.000000E+00
0.9100000E+00  0.145190E+02  0.473411E+02  0.492035E+02  0.000000E+00
0.9200000E+00  0.145170E+02  0.473410E+02  0.492035E+02  0.000000E+00
0.9300000E+00  0.145150E+02  0.473410E+02  0.492035E+02  0.000000E+00
0.9400000E+00  0.145130E+02  0.473409E+02  0.492035E+02  0.000000E+00
0.9500000E+00  0.145110E+02  0.473409E+02  0.492035E+02  0.000000E+00
0.9600000E+00  0.145090E+02  0.473408E+02  0.492035E+02  0.000000E+00
0.9700000E+00  0.145070E+02  0.473408E+02  0.492035E+02  0.000000E+00
0.9800000E+00  0.145050E+02  0.473407E+02  0.492035E+02  0.000000E+00
0.9900000E+00  0.145030E+02  0.473407E+02  0.492035E+02  0.000000E+00
0.1000000E+01  0.145010E+02  0.473406E+02  0.492035E+02  0.000000E+00
0.1010000E+01  0.144990E+02  0.473406E+02  0.492035E+02  0.000000E+00
0.1020000E+01  0.144970E+02  0.473405E+02  0.492035E+02  0.000000E+00
0.1030000E+01  0.144950E+02  0.473405E+02  0.492035E+02  0.000000E+00
0.1040000E+01  0.144930E+02  0.473404E+02  0.492035E+02  0.000000E+00
0.1050000E+01  0.144910E+02  0.473404E+02  0.492035E+02  0.000000E+00
0.1060000E+01  0.144890E+02  0.473404E+02  0.492035E+02  0.000000E+00
0.1070000E+01  0.144870E+02  0.473403E+02  0.492035E+02  0.000000E+00
0.1080000E+01  0.144850E+02  0.473403E+02  0.492035E+02  0.000000E+00
0.1090000E+01  0.144830E+02  0.473402E+02  0.492035E+02  0.000000E+00
0.1100000E+01  0.144810E+02  0.473402E+02  0.492035E+02  0.000000E+00
0.1110000E+01  0.144790E+02  0.473401E+02  0.492035E+02  0.000000E+00
0.1120000E+01  0.144770E+02  0.473401E+02  0.492035E+02  0.000000E+00
0.1130000E+01  0.144750E+02  0.473400E+02  0.492035E+02  0.000000E+00
0.1140000E+01  0.144730E+02  0.473400E+02  0.492035E+02  0.000000E+00
0.1150000E+01  0.144710E+02  0.473400E+02  0.492035E+02  0.000000E+00
0.1160000E+01  0.144690E+02  0.473399E+02  0.492035E+02  0.000000E+00
0.1170000E+01  0.144670E+02  0.473399E+02  0.492035E+02  0.000000E+00
0.1180000E+01  0.144650E+02  0.473398E+02  0.492035E+02  0.000000E+00
0.1190000E+01  0.144630E+02  0.473398E+02  0.492035E+02  0.000000E+00
0.1200000E+01  0.144610E+02  0.473397E+02  0.492035E+02  0.000000E+00
0.1210000E+01  0.144590E+02  0.473397E+02  0.492035E+02  0.000000E+00
0.1220000E+01  0.144570E+02  0.473397E+02  0.492035E+02  0.000000E+00
0.1230000E+01  0.144550E+02  0.473396E+02  0.492035E+02  0.000000E+00
0.1240000E+01  0.144530E+02  0.473396E+02  0.492035E+02  0.000000E+00
```

```
0.1250000E+01 0.144510E+02 0.473395E+02 0.492035E+02 0.000000E+00
0.1260000E+01 0.144490E+02 0.473395E+02 0.492035E+02 0.000000E+00
0.1270000E+01 0.144470E+02 0.473395E+02 0.492035E+02 0.000000E+00
0.1280000E+01 0.144450E+02 0.473394E+02 0.492035E+02 0.000000E+00
0.1290000E+01 0.144430E+02 0.473394E+02 0.492035E+02 0.000000E+00
0.1300000E+01 0.144410E+02 0.473393E+02 0.492035E+02 0.000000E+00
0.1310000E+01 0.144390E+02 0.473393E+02 0.492035E+02 0.000000E+00
0.1320000E+01 0.144370E+02 0.473392E+02 0.492035E+02 0.000000E+00
0.1330000E+01 0.144350E+02 0.473392E+02 0.492035E+02 0.000000E+00
0.1340000E+01 0.144330E+02 0.473392E+02 0.492035E+02 0.000000E+00
0.1350000E+01 0.144310E+02 0.473391E+02 0.492035E+02 0.000000E+00
0.1360000E+01 0.144290E+02 0.473391E+02 0.492035E+02 0.000000E+00
0.1370000E+01 0.144270E+02 0.473390E+02 0.492035E+02 0.000000E+00
0.1380000E+01 0.144250E+02 0.473390E+02 0.492035E+02 0.000000E+00
0.1390000E+01 0.144230E+02 0.473390E+02 0.492035E+02 0.000000E+00
0.1400000E+01 0.144210E+02 0.473389E+02 0.492035E+02 0.000000E+00
0.1410000E+01 0.144190E+02 0.473389E+02 0.492035E+02 0.000000E+00
0.1420000E+01 0.144170E+02 0.473388E+02 0.492035E+02 0.000000E+00
0.1430000E+01 0.144150E+02 0.473388E+02 0.492035E+02 0.000000E+00
0.1440000E+01 0.144130E+02 0.473388E+02 0.492035E+02 0.000000E+00
0.1450000E+01 0.144110E+02 0.473387E+02 0.492035E+02 0.000000E+00
0.1460000E+01 0.144090E+02 0.473387E+02 0.492035E+02 0.000000E+00
0.1470000E+01 0.144070E+02 0.473386E+02 0.492035E+02 0.000000E+00
0.1480000E+01 0.144050E+02 0.473386E+02 0.492035E+02 0.000000E+00
0.1490000E+01 0.144030E+02 0.473386E+02 0.492035E+02 0.000000E+00
0.1500000E+01 0.144010E+02 0.473385E+02 0.492035E+02 0.000000E+00
0.1510000E+01 0.143990E+02 0.473385E+02 0.492035E+02 0.000000E+00
0.1520000E+01 0.143970E+02 0.473384E+02 0.492035E+02 0.000000E+00
0.1530000E+01 0.143950E+02 0.473384E+02 0.492035E+02 0.000000E+00
0.1540000E+01 0.143930E+02 0.473384E+02 0.492035E+02 0.000000E+00
0.1550000E+01 0.143910E+02 0.473383E+02 0.492035E+02 0.000000E+00
0.1560000E+01 0.143890E+02 0.473383E+02 0.492035E+02 0.000000E+00
0.1570000E+01 0.143870E+02 0.473383E+02 0.492035E+02 0.000000E+00
0.1580000E+01 0.143850E+02 0.473382E+02 0.492035E+02 0.000000E+00
0.1590000E+01 0.143830E+02 0.473382E+02 0.492035E+02 0.000000E+00
0.1600000E+01 0.143810E+02 0.473381E+02 0.492035E+02 0.000000E+00
0.1610000E+01 0.143790E+02 0.473381E+02 0.492035E+02 0.000000E+00
0.1620000E+01 0.143770E+02 0.473381E+02 0.492035E+02 0.000000E+00
0.1630000E+01 0.143750E+02 0.473380E+02 0.492035E+02 0.000000E+00
0.1640000E+01 0.143730E+02 0.473380E+02 0.492035E+02 0.000000E+00
0.1650000E+01 0.143710E+02 0.473379E+02 0.492035E+02 0.000000E+00
0.1660000E+01 0.143690E+02 0.473379E+02 0.492035E+02 0.000000E+00
0.1670000E+01 0.143670E+02 0.473379E+02 0.492035E+02 0.000000E+00
0.1680000E+01 0.143650E+02 0.473378E+02 0.492035E+02 0.000000E+00
0.1690000E+01 0.143630E+02 0.473378E+02 0.492035E+02 0.000000E+00
0.1700000E+01 0.143610E+02 0.473377E+02 0.492035E+02 0.000000E+00
0.1710000E+01 0.143590E+02 0.473377E+02 0.492035E+02 0.000000E+00
0.1720000E+01 0.143570E+02 0.473377E+02 0.492035E+02 0.000000E+00
0.1730000E+01 0.143550E+02 0.473376E+02 0.492035E+02 0.000000E+00
0.1740000E+01 0.143530E+02 0.473376E+02 0.492035E+02 0.000000E+00
0.1750000E+01 0.143510E+02 0.473376E+02 0.492035E+02 0.000000E+00
0.1760000E+01 0.143490E+02 0.473375E+02 0.492035E+02 0.000000E+00
0.1770000E+01 0.143470E+02 0.473375E+02 0.492035E+02 0.000000E+00
0.1780000E+01 0.143450E+02 0.473374E+02 0.492035E+02 0.000000E+00
0.1790000E+01 0.143430E+02 0.473374E+02 0.492035E+02 0.000000E+00
0.1800000E+01 0.143410E+02 0.473374E+02 0.492035E+02 0.000000E+00
0.1810000E+01 0.143390E+02 0.473373E+02 0.492035E+02 0.000000E+00
0.1820000E+01 0.143370E+02 0.473373E+02 0.492035E+02 0.000000E+00
0.1830000E+01 0.143350E+02 0.473372E+02 0.492035E+02 0.000000E+00
0.1840000E+01 0.143330E+02 0.473372E+02 0.492035E+02 0.000000E+00
0.1850000E+01 0.143310E+02 0.473372E+02 0.492035E+02 0.000000E+00
0.1860000E+01 0.143290E+02 0.473371E+02 0.492035E+02 0.000000E+00
0.1870000E+01 0.143270E+02 0.473371E+02 0.492035E+02 0.000000E+00
0.1880000E+01 0.143250E+02 0.473371E+02 0.492035E+02 0.000000E+00
0.1890000E+01 0.143230E+02 0.473370E+02 0.492035E+02 0.000000E+00
0.1900000E+01 0.143210E+02 0.473370E+02 0.492035E+02 0.000000E+00
0.1910000E+01 0.143190E+02 0.473369E+02 0.492035E+02 0.000000E+00
0.1920000E+01 0.143170E+02 0.473369E+02 0.492035E+02 0.000000E+00
0.1930000E+01 0.143150E+02 0.473369E+02 0.492035E+02 0.000000E+00
0.1940000E+01 0.143130E+02 0.473368E+02 0.492035E+02 0.000000E+00
```

```
0.1950000E+01 0.143110E+02 0.473368E+02 0.492035E+02 0.000000E+00
0.1960000E+01 0.143090E+02 0.473367E+02 0.492035E+02 0.000000E+00
0.1970000E+01 0.143070E+02 0.473367E+02 0.492035E+02 0.000000E+00
0.1980000E+01 0.143050E+02 0.473367E+02 0.492035E+02 0.000000E+00
0.1990000E+01 0.143030E+02 0.473366E+02 0.492035E+02 0.000000E+00
0.2000000E+01 0.143010E+02 0.473366E+02 0.492035E+02 0.000000E+00
0.2010000E+01 0.144915E+02 0.473374E+02 0.492035E+02 0.000000E+00
0.2020000E+01 0.148745E+02 0.473404E+02 0.492035E+02 0.000000E+00
0.2030000E+01 0.152575E+02 0.473452E+02 0.492035E+02 0.000000E+00
0.2040000E+01 0.156405E+02 0.473511E+02 0.492035E+02 0.000000E+00
0.2050000E+01 0.160235E+02 0.473576E+02 0.492035E+02 0.000000E+00
0.2060000E+01 0.164065E+02 0.473644E+02 0.492035E+02 0.000000E+00
0.2070000E+01 0.167895E+02 0.473711E+02 0.492035E+02 0.000000E+00
0.2080000E+01 0.171725E+02 0.473776E+02 0.492035E+02 0.000000E+00
0.2090000E+01 0.175555E+02 0.473839E+02 0.492035E+02 0.000000E+00
0.2100000E+01 0.179385E+02 0.473899E+02 0.492035E+02 0.000000E+00
0.2110000E+01 0.183215E+02 0.473956E+02 0.492035E+02 0.000000E+00
0.2120000E+01 0.187045E+02 0.474012E+02 0.492035E+02 0.000000E+00
0.2130000E+01 0.190875E+02 0.474066E+02 0.492035E+02 0.000000E+00
0.2140000E+01 0.194705E+02 0.474120E+02 0.492035E+02 0.000000E+00
0.2150000E+01 0.198535E+02 0.474172E+02 0.492035E+02 0.000000E+00
0.2160000E+01 0.202365E+02 0.474224E+02 0.492035E+02 0.000000E+00
0.2170000E+01 0.206195E+02 0.474277E+02 0.492035E+02 0.000000E+00
0.2180000E+01 0.210025E+02 0.474329E+02 0.492035E+02 0.000000E+00
0.2190000E+01 0.213855E+02 0.474381E+02 0.492035E+02 0.000000E+00
0.2200000E+01 0.217685E+02 0.474434E+02 0.492035E+02 0.000000E+00
0.2210000E+01 0.221515E+02 0.474487E+02 0.492035E+02 0.000000E+00
0.2220000E+01 0.225345E+02 0.474540E+02 0.492035E+02 0.000000E+00
0.2230000E+01 0.229175E+02 0.474593E+02 0.492035E+02 0.000000E+00
0.2240000E+01 0.233005E+02 0.474647E+02 0.492035E+02 0.000000E+00
0.2250000E+01 0.236835E+02 0.474701E+02 0.492035E+02 0.000000E+00
0.2260000E+01 0.240665E+02 0.474755E+02 0.492035E+02 0.000000E+00
0.2270000E+01 0.244495E+02 0.474809E+02 0.492035E+02 0.000000E+00
0.2280000E+01 0.248325E+02 0.474863E+02 0.492035E+02 0.000000E+00
0.2290000E+01 0.252155E+02 0.474917E+02 0.492035E+02 0.000000E+00
0.2300000E+01 0.255985E+02 0.474971E+02 0.492035E+02 0.000000E+00
0.2310000E+01 0.259815E+02 0.475025E+02 0.492035E+02 0.000000E+00
0.2320000E+01 0.263645E+02 0.475079E+02 0.492035E+02 0.000000E+00
0.2330000E+01 0.267475E+02 0.475133E+02 0.492035E+02 0.000000E+00
0.2340000E+01 0.271305E+02 0.475187E+02 0.492035E+02 0.000000E+00
0.2350000E+01 0.275135E+02 0.475240E+02 0.492035E+02 0.000000E+00
0.2360000E+01 0.278965E+02 0.475293E+02 0.492035E+02 0.000000E+00
0.2370000E+01 0.282795E+02 0.475347E+02 0.492035E+02 0.000000E+00
0.2380000E+01 0.286625E+02 0.475400E+02 0.492035E+02 0.000000E+00
0.2390000E+01 0.290455E+02 0.475452E+02 0.492035E+02 0.000000E+00
0.2400000E+01 0.294285E+02 0.475505E+02 0.492035E+02 0.000000E+00
0.2410000E+01 0.298115E+02 0.475557E+02 0.492035E+02 0.000000E+00
0.2420000E+01 0.301945E+02 0.475609E+02 0.492035E+02 0.000000E+00
0.2430000E+01 0.305775E+02 0.475661E+02 0.492035E+02 0.000000E+00
0.2440000E+01 0.309605E+02 0.475713E+02 0.492035E+02 0.000000E+00
0.2450000E+01 0.313435E+02 0.475764E+02 0.492035E+02 0.000000E+00
0.2460000E+01 0.317265E+02 0.475815E+02 0.492035E+02 0.000000E+00
0.2470000E+01 0.321095E+02 0.475866E+02 0.492035E+02 0.000000E+00
0.2480000E+01 0.324925E+02 0.475916E+02 0.492035E+02 0.000000E+00
0.2490000E+01 0.328755E+02 0.475966E+02 0.492035E+02 0.000000E+00
0.2500000E+01 0.332585E+02 0.476016E+02 0.492035E+02 0.000000E+00
0.2510000E+01 0.336415E+02 0.476066E+02 0.492035E+02 0.000000E+00
0.2520000E+01 0.340245E+02 0.476115E+02 0.492035E+02 0.000000E+00
0.2530000E+01 0.344075E+02 0.476165E+02 0.492035E+02 0.000000E+00
0.2540000E+01 0.347905E+02 0.476213E+02 0.492035E+02 0.000000E+00
0.2550000E+01 0.351735E+02 0.476262E+02 0.492035E+02 0.000000E+00
0.2560000E+01 0.355565E+02 0.476310E+02 0.492035E+02 0.000000E+00
0.2570000E+01 0.359395E+02 0.476358E+02 0.492035E+02 0.000000E+00
0.2580000E+01 0.363225E+02 0.476406E+02 0.492035E+02 0.000000E+00
```

Abbreviated following result

4. Summary of GSTAR-1D simulation result (steady condition)

(a) Observed and simulated bed elevation

Distance from the confluence (km)	Bed elevation (El.m)			
	Measured (2003)	Simulated (2013)	Simulated (2018)	Simulated (2023)
44.8	47.0	47.0	47.0	47.0
44.6	45.3	45.2	45.2	45.2
44.3	44.7	44.6	44.6	44.6
44.1	43.9	43.8	43.7	43.7
43.8	43.7	43.8	43.8	43.8
43.6	44.4	44.0	44.0	44.0
43.3	43.7	42.9	42.9	42.9
43.0	43.4	42.4	42.4	42.3
42.8	42.0	41.7	41.5	41.4
42.5	42.9	41.0	40.9	40.8
42.2	42.7	40.8	40.6	40.5
41.9	41.8	39.3	39.1	39.0
41.7	42.2	39.6	39.3	39.2
41.4	42.7	39.7	39.4	39.3
41.2	42.6	38.8	38.5	38.3
40.9	41.0	39.1	38.7	38.5
40.7	39.0	37.3	37.0	36.6
40.4	39.5	37.8	37.4	37.1
40.2	38.5	36.3	35.9	35.6
39.9	38.5	36.5	36.1	35.8
39.7	37.2	35.1	34.7	34.4
39.4	37.1	35.2	34.8	34.5
39.2	37.5	35.4	35.1	34.8
38.9	36.7	34.4	34.1	33.8
38.7	36.8	34.6	34.3	34.0
38.4	36.0	33.7	33.5	33.2
38.2	35.9	33.5	33.3	33.1
37.9	35.3	32.8	32.5	32.3
37.7	35.4	33.1	32.9	32.7
37.4	34.8	32.6	32.4	32.2
37.2	34.8	32.1	31.9	31.7
36.9	34.5	31.7	31.4	31.2
36.7	34.4	31.5	31.2	30.9
36.4	34.2	31.1	30.7	30.3
36.2	33.9	31.1	30.4	30.1
36.0	33.5	31.0	30.0	29.8
35.7	33.1	30.6	29.6	29.1
35.4	32.7	30.6	29.7	29.1
35.2	32.6	30.5	29.6	29.0
34.9	32.1	30.4	29.6	29.0
34.7	31.5	29.8	28.9	28.3
34.4	31.2	29.8	29.0	28.4
34.2	30.8	29.4	28.6	28.0
33.9	30.2	28.9	28.2	27.6

189

33.8	30.3	29.6	28.9	28.4
33.8	30.3	29.6	28.9	28.4
33.8	30.3	29.6	28.9	28.4
33.8	30.3	29.6	28.9	28.4
33.7	29.5	29.2	28.5	28.0
33.4	29.2	28.9	28.2	27.7
33.2	29.2	29.1	28.5	28.0
32.9	28.2	28.1	27.5	27.0
32.7	27.3	27.5	26.9	26.4
32.7	27.3	27.5	26.9	26.4
32.7	27.3	27.4	26.9	26.4
32.7	27.3	27.4	26.9	26.4
32.7	28.6	28.7	28.1	27.7
32.4	28.1	28.2	27.7	27.3
32.2	28.2	28.5	28.0	27.6
31.9	27.9	28.4	28.0	27.6
31.7	27.7	28.1	27.7	27.4
31.4	27.2	27.7	27.3	27.0
31.2	27.0	27.5	27.2	26.9
30.9	26.4	27.1	26.8	26.5
30.7	26.3	26.7	26.5	26.2
30.4	26.0	26.5	26.3	26.0
30.2	25.7	26.3	26.1	25.8
29.9	25.4	25.9	25.8	25.5
29.7	24.8	25.6	25.5	25.3
29.4	24.8	25.7	25.6	25.4
29.2	24.1	25.0	24.9	24.8
28.9	24.2	25.1	25.1	24.9
28.7	24.0	24.8	24.7	24.6
28.4	22.2	23.2	23.2	23.0
28.2	23.4	24.2	24.2	24.1
27.9	22.7	23.4	23.4	23.3
27.7	23.0	23.6	23.6	23.6
27.4	22.7	23.2	23.2	23.1
27.2	22.5	22.5	22.6	22.5
26.9	22.0	22.4	22.4	22.4
26.7	21.7	22.3	22.3	22.2
26.4	21.1	21.4	21.4	21.4
26.2	21.4	21.9	22.0	22.0
25.9	21.2	21.9	21.9	21.9
25.6	21.0	21.8	21.8	21.8
25.4	20.6	21.0	21.1	21.0
25.2	20.2	20.4	20.5	20.5
24.9	20.3	20.7	20.8	20.8
24.9	20.0	21.0	21.1	21.1
24.9	20.0	21.0	21.1	21.1
24.8	20.0	21.0	21.1	21.1
24.8	20.0	21.0	21.1	21.1
24.7	20.2	20.7	20.8	20.8
24.4	19.9	20.4	20.5	20.5

24.2	19.8	20.1	20.2	20.1
23.9	19.7	20.2	20.3	20.3
23.7	19.5	20.0	20.0	20.0
23.4	19.3	19.8	19.9	19.9
23.2	18.8	19.4	19.4	19.4
22.9	18.8	19.4	19.4	19.4
22.7	18.6	19.2	19.3	19.3
22.4	17.9	18.9	18.9	18.9
22.2	17.5	18.6	18.7	18.7
21.9	16.4	17.8	17.9	17.8
21.7	15.9	17.9	17.9	17.9
21.4	16.3	18.1	18.1	18.1
21.2	16.4	17.6	17.6	17.6
20.9	15.9	16.9	16.9	16.9
20.7	15.5	15.5	15.5	15.5
20.4	16.7	16.8	16.8	16.8
20.2	16.6	16.4	16.4	16.4
19.9	16.3	16.3	16.3	16.3
19.7	16.5	16.3	16.3	16.3
19.4	16.4	16.6	16.6	16.6
19.2	16.2	16.4	16.4	16.4
18.9	16.3	16.6	16.6	16.6
18.7	16.1	16.4	16.4	16.4
18.4	16.0	16.1	16.2	16.2
18.2	15.0	15.4	15.4	15.4
17.9	14.9	15.2	15.2	15.2
17.7	15.0	14.9	14.9	14.9
17.4	15.1	14.9	14.9	14.9
17.2	14.2	13.8	13.8	13.8
16.9	14.5	14.3	14.3	14.3
16.7	14.3	14.3	14.3	14.3
16.4	14.4	14.1	14.2	14.2
16.3	15.1	14.4	14.4	14.4
16.3	15.1	14.4	14.4	14.4
16.2	15.1	14.4	14.4	14.4
16.2	15.1	14.4	14.4	14.4
16.2	14.6	14.3	14.3	14.3
15.9	14.5	14.1	14.2	14.2
15.7	14.8	14.4	14.4	14.5
15.4	14.4	13.8	13.8	13.8
15.2	14.1	14.0	14.0	14.0
14.9	14.3	13.9	14.0	14.0
14.7	13.4	13.2	13.3	13.3
14.4	13.5	13.0	13.0	13.1
14.2	14.0	13.7	13.7	13.7
13.9	13.3	12.6	12.6	12.6
13.7	12.7	12.4	12.4	12.4
13.4	13.4	12.8	12.8	12.9
13.2	12.9	12.5	12.6	12.6
12.9	12.8	12.4	12.4	12.4

12.7	12.5	12.1	12.1	12.1
12.4	12.5	12.1	12.2	12.2
12.2	11.7	11.1	11.2	11.2
11.9	11.9	11.7	11.8	11.8
11.7	11.6	11.2	11.3	11.3
11.4	12.0	11.4	11.4	11.5
11.2	11.6	11.2	11.3	11.3
10.9	11.6	11.2	11.3	11.3
10.6	11.6	11.2	11.3	11.3
10.4	11.6	11.4	11.5	11.5
10.2	11.3	10.9	11.0	11.0
9.9	11.4	11.0	11.1	11.2
9.7	11.4	11.1	11.2	11.3
9.4	10.9	10.5	10.6	10.6
9.2	10.9	10.7	10.8	10.8
8.9	10.1	9.9	10.0	10.0
8.7	10.7	10.3	10.4	10.5
8.5	10.7	10.0	10.1	10.2
8.5	10.7	10.0	10.1	10.2
8.4	10.7	10.0	10.1	10.2
8.4	10.7	10.0	10.1	10.2
8.4	10.2	9.7	9.8	9.8
8.1	10.5	10.2	10.3	10.3
7.9	10.0	9.8	9.9	9.9
7.6	10.1	9.9	10.0	10.0
7.4	10.1	10.1	10.2	10.2
7.2	9.7	10.3	10.4	10.4
7.2	9.7	10.3	10.4	10.4
7.2	9.7	10.3	10.4	10.4
7.2	9.7	10.3	10.4	10.4
7.0	9.0	8.8	8.9	9.0
6.7	9.5	9.4	9.5	9.6
6.5	9.3	9.3	9.4	9.5
6.2	9.0	8.6	8.7	8.8
6.0	9.0	8.6	8.8	8.8
5.7	9.0	8.4	8.5	8.6
5.5	9.0	8.7	8.8	8.8
5.2	9.0	8.6	8.7	8.8
5.0	8.9	8.7	8.8	8.9
4.7	8.1	7.6	7.8	7.8
4.5	7.5	7.7	7.9	7.9
4.2	8.3	8.1	8.2	8.2
4.0	8.0	7.5	7.7	7.7
3.7	7.7	8.1	8.3	8.3
3.5	7.4	7.5	7.6	7.7
3.2	7.5	7.0	7.1	7.2
3.0	7.3	7.1	7.2	7.3
2.7	7.6	7.5	7.5	7.6
2.5	7.0	6.9	7.0	7.0
2.2	7.3	7.0	7.1	7.1

2.0	7.3	7.2	7.3	7.3
1.7	7.1	6.9	7.0	7.0
1.5	7.1	7.0	7.1	7.1
1.3	6.9	6.6	6.7	6.7
1.3	6.9	6.6	6.7	6.7
1.3	6.9	6.6	6.7	6.7
1.3	6.9	6.6	6.7	6.7
1.3	6.1	5.8	5.9	6.0
1.3	6.1	5.8	5.9	6.0
1.3	6.1	5.8	5.9	6.0
1.3	6.1	5.8	5.9	5.9
1.0	6.8	7.0	7.1	7.1
0.7	6.9	6.8	6.9	6.9
0.5	6.5	6.2	6.3	6.3
0.2	6.4	6.3	6.3	6.3
0.0	6.8	6.7	6.7	6.7

(b) Observed and simulated Cumulative volumes of deposition and erosion

Distance from The confluence (km)	Cumulative volume of deposition and erosion (10^3 m^3)	
	Observed (1983~2003)	Simulated (1983~2003)
45.0	-12.2	-131.1
44.7	-77.0	-153.7
44.2	-171.5	-243.8
43.7	-248.7	-376.2
43.1	-255.9	-461.9
42.6	-341.0	-342.7
42.0	-309.5	-172.3
41.5	-286.3	-207.4
41.1	-206.4	
41.0	-192.3	-309.4
40.5	-447.6	-336.6
40.0	-524.0	-357.4
39.5	-262.4	-266.4
39.3	-174.7	
39.0	-243.8	-222.0
38.5	-512.7	-276.7
38.0	-638.5	-312.1
37.5	-540.3	-431.6
37.0	-458.4	-435.1
36.5	-318.8	-255.3
36.1	-410.0	-409.1
35.5	-582.4	-236.4
35.0	-456.6	61.4

34.5	-397.4	-33.2
34.0	-174.6	-135.2
33.9	-140.0	
33.5	-125.7	-160.2
33.4	-147.7	
33.0	-260.2	-203.2
32.5	-381.1	-276.1
32.0	-320.4	-298.4
31.5	-426.4	-374.9
31.0	-436.4	-327.3
30.5	-284.3	-177.0
30.0	-343.2	-169.5
29.5	-299.1	-224.0
29.0	-324.3	-264.2
28.5	-417.6	-226.1
28.0	-463.5	-182.8
27.5	-423.0	-111.1
27.0	-323.0	-36.8
26.5	-309.9	-107.4
26.0	-98.4	-138.1
25.5	-292.3	-74.4
25.0	-52.2	-112.6
25.0	-73.9	
24.5	-405.6	-128.9
24.0	-406.6	-153.2
23.5	-382.1	-147.5
23.0	-714.9	-154.4
22.5	-184.8	-183.0
22.0	-136.7	-208.6
21.5	-90.8	-181.4
21.0	-125.1	-91.3
20.5	-28.4	-42.3
20.0	22.2	-40.5
19.5	-32.0	-60.2
19.0	-22.2	-86.9
18.5	-29.4	-100.3
18.0	-6.7	-44.8
17.5	19.8	15.5
17.0	60.2	11.5
16.5	0.9	-15.7
16.3	41.5	
16.0	1.3	21.2
15.5	43.6	54.4
15.0	14.0	88.9
14.5	139.1	7.9

14.0	22.4	-63.4
13.5	68.3	-7.6
13.0	36.3	46.6
12.5	73.5	13.7
12.0	105.1	-31.7
11.5	169.0	-22.3
11.0	21.6	-30.4
10.5	54.4	-33.7
10.0	43.1	-71.1
9.5	76.1	-58.9
9.0	61.1	-9.8
8.7	34.0	
8.5	74.6	-52.9
8.0	196.1	-108.9
7.5	19.3	-134.7
7.2	68.9	
7.0	24.7	-186.0
6.5	-24.2	-165.1
6.0	91.8	-66.8
5.5	63.1	-204.5
5.0	161.6	-286.6
4.5	87.1	-125.0
4.0	289.8	-160.3
3.5	550.6	-5.7
3.0	571.5	-67.8
2.5	-36.3	-193.9
2.0	160.0	-125.0
1.5	78.5	-347.7
1.0	105.7	-203.9
0.5	-127.3	-239.3
0.0	58.0	0.0

APPENDIX C : STATISTICAL ANALYSIS AND CHANNEL PATTERN

1. Review of Statistical Analysis

This section deal with the relationship among hydraulic, sedimentologic and channel-form parameters through statistical analysis using a correlation and multi regression model. Statistical methods dominated quantitative analyses of fluvial systems since 1950's (Rhoads, 1992). He assessed the utility of statistical models by examining methodological issues associated with empirical analysis of hydraulic and channel geometry relationships. Also, Chorley (1966) mentioned about the importance of the evaluating operating variables for geological, geographical and geomorphic phenomena simultaneously. Other studies have used statistical analyses to identify relationships. Shafroth et al. (2002) analyzed the relationship between channel width and flood power, and water flows (summer flow and intermittency). They found that the three independent variables were all statistically significant, and the signs of the coefficients indicates that channels were wider when flood power was higher, average summer flows were lower, and where flow was intermittent. Also, many researchers studied about the relationship between lateral migration and other hydraulic parameters including sedimentologic parameters. Hook (1979), Nanson and Hickin (1986), MacDonald (1991), Lawler et al. (1999), and Richard et al. (2005) found the lateral migration rates increase with flow energy in meandering rivers. Bledsoe and Watson (2002) found that measures of stream power were significantly correlated with the degree of lateral stability in river channels measured by the transition to braiding. Miller et al., (2000) developed the linear regression models to use the prediction of channel width and cross-section area as a function of watershed properties.

2. Correlation matrixes for sub-reaches

Table C-1. Correlation matrix for Sub-reach 1

	Q_{peak}	Q_{bank}	S	$Q_{peak}S$	$Q_{bank}S$	MI	D_{50}	W_{act}	dW_{act}	A_{act}	dA_{act}	A_{isd}	dA_{isd}	A_{veg}	dA_{veg}	P
Q_{peak}	1.00															
Q_{bank}	0.87	1.00														
S	0.12	0.24	1.00													
$Q_{peak}S$	0.94	0.91	0.36	1.00												
$Q_{bank}S$	0.83	0.96	0.41	0.95	1.00											
MI	0.65	0.77	0.51	0.80	0.85	1.00										
D_{50}	-0.22	-0.19	0.13	-0.19	-0.17	-0.38	1.00									
W_{act}	0.56	0.46	-0.14	0.41	0.34	0.01	-0.25	1.00								
dW_{act}	0.89	0.75	0.06	0.81	0.70	0.56	-0.49	0.67	1.00							
A_{act}	0.21	-0.10	-0.65	0.00	-0.20	-0.25	-0.24	0.35	0.31	1.00						
dA_{act}	0.68	0.54	0.50	0.67	0.55	0.53	-0.18	0.46	0.69	-0.22	1.00					
A_{isd}	-0.62	-0.49	-0.38	-0.60	-0.50	-0.55	0.44	-0.51	-0.70	0.12	-0.93	1.00				
dA_{isd}	-0.69	-0.54	-0.38	-0.66	-0.54	-0.57	0.31	-0.31	-0.64	0.23	-0.92	0.88	1.00			
A_{veg}	-0.55	-0.43	-0.40	-0.54	-0.45	-0.42	0.23	-0.63	-0.62	0.08	-0.87	0.93	0.70	1.00		
dA_{veg}	-0.61	-0.48	-0.50	-0.61	-0.50	-0.49	0.19	-0.55	-0.60	0.15	-0.93	0.94	0.82	0.96	1.00	
P	0.13	0.10	-0.72	-0.09	-0.10	-0.17	-0.28	0.44	0.11	0.34	-0.05	-0.10	-0.07	-0.09	-0.04	1.00

Table C-2. Correlation matrix for Sub-reach 2

	Q_{peak}	Q_{bank}	S	$Q_{peak}S$	$Q_{bank}S$	MI	D_{50}	W_{act}	dW_{act}	A_{act}	dA_{act}	A_{isd}	dA_{isd}	A_{veg}	dA_{veg}	P
Q_{peak}	1.00															
Q_{bank}	1.00	1.00														
S	-0.59	-0.57	1.00													
$Q_{peak}S$	1.00	1.00	-0.57	1.00												
$Q_{bank}S$	1.00	1.00	-0.55	1.00	1.00											
MI	0.81	0.83	-0.01	0.83	0.84	1.00										
D_{50}	-0.38	-0.41	-0.52	-0.41	-0.43	-0.85	1.00									
W_{act}	0.74	0.76	0.10	0.76	0.78	0.99	-0.90	1.00								
dW_{act}	0.89	0.91	-0.17	0.90	0.92	0.99	-0.76	0.96	1.00							
A_{act}	0.76	0.78	0.08	0.77	0.79	1.00	-0.89	1.00	0.97	1.00						
dA_{act}	0.92	0.93	-0.23	0.93	0.94	0.98	-0.72	0.95	1.00	0.95	1.00					
A_{isd}	-0.78	-0.80	-0.04	-0.80	-0.81	-1.00	0.88	-1.00	-0.98	-1.00	-0.96	1.00				
dA_{isd}	-0.96	-0.96	0.33	-0.96	-0.97	-0.95	0.64	-0.91	-0.99	-0.92	-0.99	0.93	1.00			
A_{veg}	-0.67	-0.70	-0.19	-0.69	-0.71	-0.98	0.94	-1.00	-0.94	-0.99	-0.91	0.99	0.86	1.00		
dA_{veg}	-0.77	-0.79	-0.05	-0.79	-0.81	-1.00	0.88	-1.00	-0.98	-1.00	-0.96	1.00	0.93	0.99	1.00	
P	0.95	0.96	-0.31	0.96	0.97	0.95	-0.65	0.91	0.99	0.92	1.00	-0.94	-1.00	-0.87	-0.93	1.00

Table C-3. Correlation matrix for Sub-reach 3

|	Q_{peak}	Q_{bank}	S	$Q_{peak}S$	$Q_{bank}S$	MI	D_{50}	W_{act}	dW_{act}	A_{act}	dA_{act}	A_{isd}	dA_{isd}	A_{veg}	dA_{veg}	P
Q_{peak}	1.00															
Q_{bank}	1.00	1.00														
S	0.56	0.58	1.00													
$Q_{peak}S$	1.00	1.00	0.58	1.00												
$Q_{bank}S$	1.00	1.00	0.60	1.00	1.00											
MI	1.00	1.00	0.59	1.00	1.00	1.00										
D_{50}	-0.66	-0.64	0.25	-0.64	-0.62	-0.63	1.00									
W_{act}	0.84	0.85	0.92	0.85	0.86	0.86	-0.14	1.00								
dW_{act}	1.00	1.00	0.57	1.00	1.00	1.00	-0.65	0.85	1.00							
A_{act}	0.82	0.84	0.93	0.84	0.85	0.84	-0.11	1.00	0.83	1.00						
dA_{act}	0.99	1.00	0.64	1.00	1.00	1.00	-0.58	0.89	1.00	0.88	1.00					
A_{isd}	-0.84	-0.86	-0.92	-0.85	-0.87	-0.86	0.15	-1.00	-0.85	-1.00	-0.89	1.00				
dA_{isd}	-1.00	-1.00	-0.56	-1.00	-1.00	-1.00	0.66	-0.84	-1.00	-0.82	-0.99	0.84	1.00			
A_{veg}	-0.59	-0.61	-1.00	-0.61	-0.63	-0.62	-0.22	-0.94	-0.60	-0.95	-0.67	0.93	0.59	1.00		
dA_{veg}	-0.62	-0.65	-1.00	-0.65	-0.67	-0.66	-0.17	-0.95	-0.64	-0.96	-0.70	0.95	0.63	1.00	1.00	
P	0.70	0.73	0.98	0.72	0.74	0.73	0.07	0.98	0.72	0.98	0.78	-0.98	-0.71	-0.99	-0.99	1.00

3. Validation of the regressed equations

Four models were developed to describe the historic changes in the active channel change rate (m/year). These models validated using 1983~2003 data of the study reach. As a result, the second equation of the active channel width change rate shows the best result. The average absolute error of the difference with predicted and observed values was 10% at the sub-reach 3 and 25% at the entire reach as shown in Table C-1. However, the other equations showed the absolute errors are more than 148% except sub-reach 1 and sub-reach 2 of the equation 1. Therefore, it is clear that only equation 2 is applicable for the prediction of future active channel change rate. Figure C-1 shows the validation results of the active channel width change rate for 1983~2003 of the sub-reach and entire reach by the equation (C-2). Also, one model developed to describe the historic changes in the bed slope change (m/m). The model validated using 1983~2003 data (Table C-2). The average absolute errors of predicted and measured values are the range 10%~12% in the sub-reach and entire reach. Therefore, it is applicable the prediction of the bed slope for future bed slope change. Figure C-2 shows the validation result of bed slope for 1983~2003 of the sub-reach and entire reach by the equation (C-5).
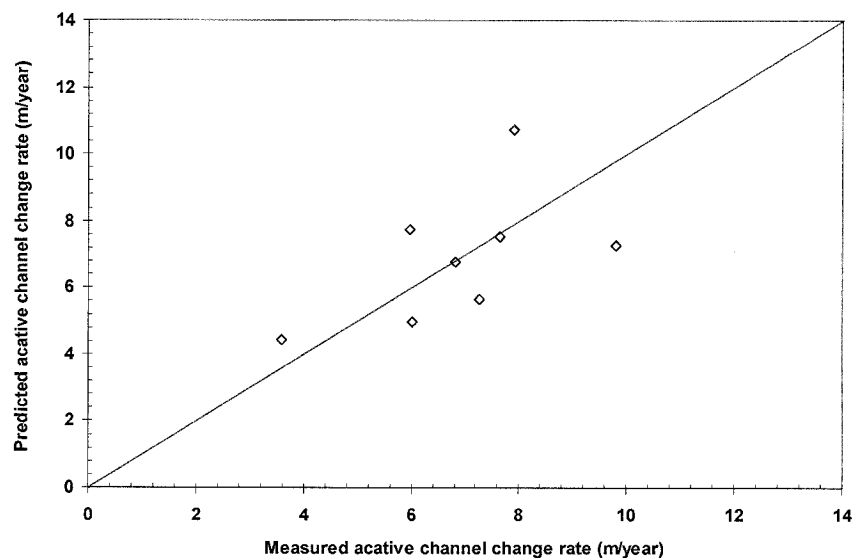
Figure C-1. Validation result of active channel width change rate for 1983~2003 of the sub-reach and entire reach by the equation (C-2)

198

Table C-1. Validation of active channel width change rate model using 1983~1993 and 1993~2003 active channel width change rate results

Equation	Reach	Period	Observed (m/year)	Predicted (m/year)	Error (pred-obs)/obs	Average absolute error
Equation (C-1): $dW_{act} = -6.51 Q_{peak} S - 3.56 A_{act} + 18.96$	1	1983~1993	6.02	8.78	31 %	
		1993~2003	9.80	10.47	6 %	19 %
	2	1983~1993	7.26	22.56	68 %	
		1993~2003	6.81	12.51	46 %	57 %
	3	1983~1993	3.58	8.69	59 %	
		1993~2003	7.63	0.50	-1413 %	736 %
	Entire	1983~1993	5.96	4.95	-20 %	
		1993~2003	7.89	1.92	-312 %	166 %
Equation (C-2): $dW_{act} = 0.58 Q_{peak} S + 0.62 dA_{act} - 1.86$	1	1983~1993	6.02	4.97	-21 %	
		1993~2003	9.80	7.29	-34 %	28 %
	2	1983~1993	7.26	5.66	-28 %	
		1993~2003	6.81	6.78	0 %	14 %
	3	1983~1993	3.58	4.42	19 %	
		1993~2003	7.63	7.52	-2 %	10 %
	Entire	1983~1993	5.96	7.74	23 %	
		1993~2003	7.89	10.72	26 %	25 %
Equation (C-3): $dW_{act} = 0.03 Q_{peak} S + 0.53 dA_{veg} - 2.36$	1	1983~1993	6.02	1.05	-474 %	
		1993~2003	9.80	1.66	-489 %	481 %
	2	1983~1993	7.26	1.07	-580 %	
		1993~2003	6.81	2.31	-195 %	387 %
	3	1983~1993	3.58	1.81	-97 %	
		1993~2003	7.63	1.35	-465 %	281 %
	Entire	1983~1993	5.96	2.38	-150 %	
		1993~2003	7.89	3.21	-146 %	148 %
Equation (C-4): $dW_{act} = 0.35 Q_{peak} S + 0.57 dA_{isd} - 2.12$	1	1983~1993	6.02	1.40	-329 %	
		1993~2003	9.80	1.77	-454 %	392 %
	2	1983~1993	7.26	1.07	-577 %	
		1993~2003	6.81	1.12	-507 %	542 %
	3	1983~1993	3.58	1.13	-218 %	
		1993~2003	7.63	0.42	-1699 %	958 %
	Entire	1983~1993	5.96	1.89	-215 %	
		1993~2003	7.89	1.95	-305 %	260 %
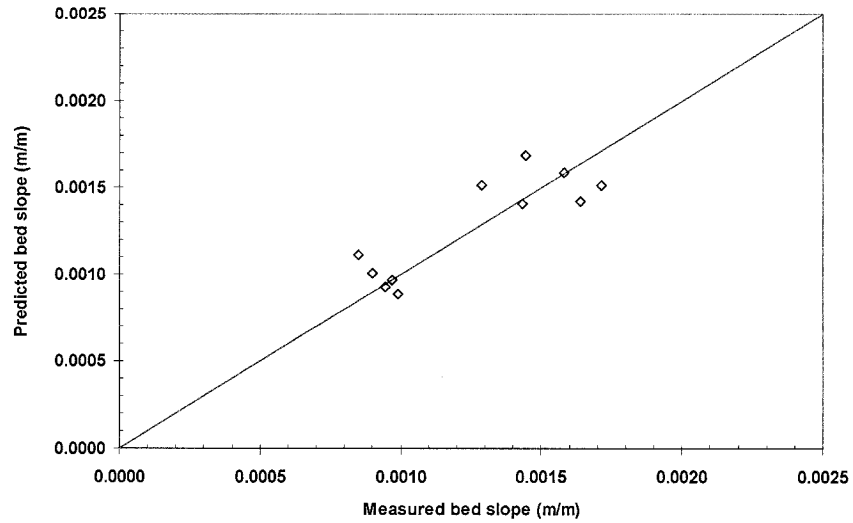
Figure C-2. Validation result of bed slope for 1983~2003 of the sub-reach and entire reach by the equation (C-5)

Table C-2. Validation of bed slope model using 1983~2003 bed slope results

| Equation	Reach	Period	Observed (m/m)	Predicted (m/m)	Error (pred-obs)/obs	Average absolute error
Equation (C-5): $S = -0.21A_{act} - 1.43P - 1.16$	1	1983	0.0014340	0.0014068	-2 %	
		1993	0.0017133	0.0015145	-13 %	
		2003	0.0014452	0.0016880	14 %	10 %
	2	1983	0.0009889	0.0008892	-11 %	
		1993	0.0009674	0.0009686	0 %	
		2003	0.0008497	0.0011166	24 %	12 %
	3	1983	0.0016375	0.0014177	-16 %	
		1993	0.0012882	0.0015130	15 %	
		2003	0.0015810	0.0015864	0 %	10 %
	Entire	1983	0.0009430	0.0009299	-1 %	
		1993	0.0008981	0.0010059	11 %	
		2003	0.0008466	0.0011122	24 %	12 %

4. Predict the rate of change active channel width and bed slope

The regression equation (C-6) was used to predict the rate of change of active channel width, dW_{act}. Equation C-6 can then be used to estimate the active channel width at the end of the time period as follows:

$$W_{act2} = W_{act1} - (\Delta t \cdot dW_{act})$$

$$W_{act2} = W_{act1} - [\Delta t \cdot (0.58 Q_{peak} S + 0.62 dA_{act} - 1.86)] \qquad \text{(C-6)}$$

Where: W_{act1} = active channel width at beginning of time period, W_{act2} = active channel width at end of time period (m), Δt = length of time period (years), dW_{act} = rate of change of active channel width (m/year), $Q_{peak} S$ = stream power (m³/s), and dA_{act} = active channel area change rate (m²/year)
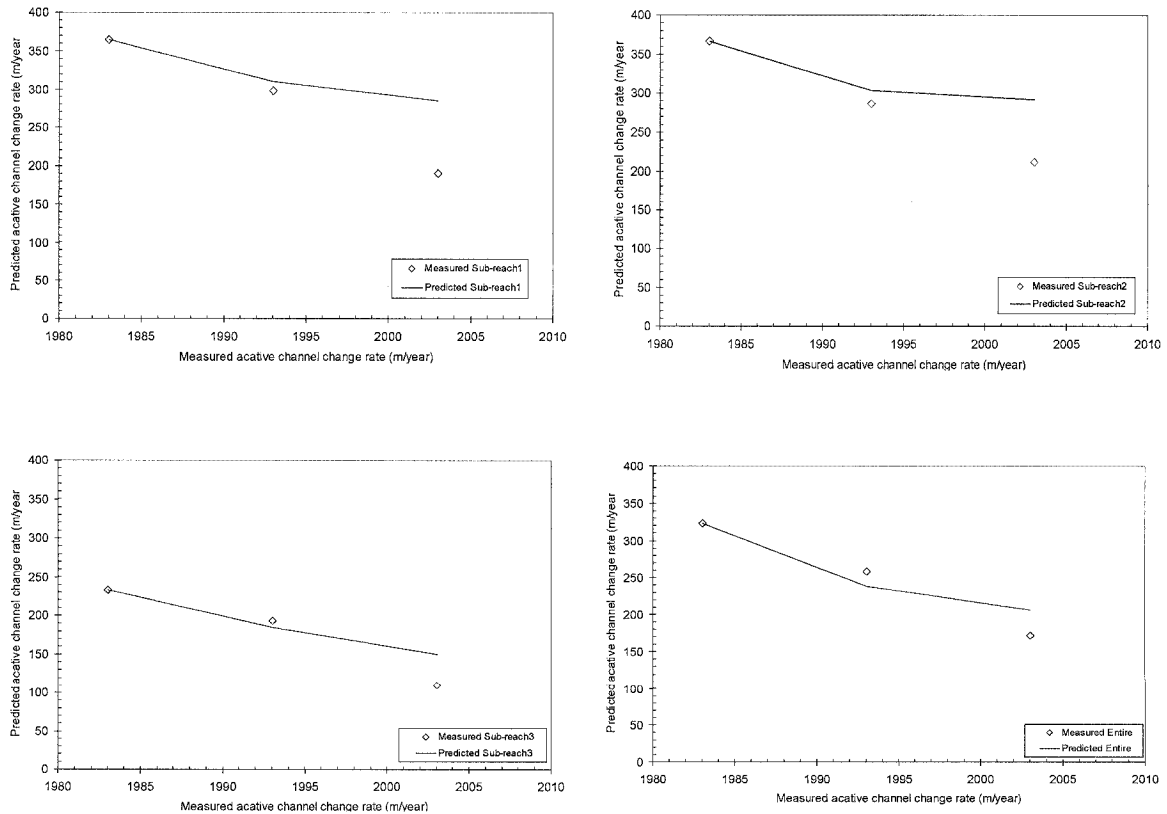
Figure C-3. Regression equations of the active channel width change rate (m/year) applied to the sub-reach and entire reach for the study reach.

Generally, the sub-reach 3 and entire reach showed the best result by applying equation C-6 as shown in Figure C-3.

The regression equation (C-7) was used to predict the bed slope change, S. Equation 5-17 can then be used to estimate the bed slope at the end of the time period as follows:

$$S_2 = S_1 - (\Delta t \cdot S)$$

$$S_2 = S_1 - [\Delta t \cdot (-0.21 A_{act} - 1.43 P - 1.16)] \qquad\qquad (C-7)$$

Where: S_2 = bed slope at beginning of time period, S_2 = bed slope at end of time period (m), Δt = length of time period (years), A_{act} = active channel area (m/year), P = sinuosity

Generally, the sub-reach1 and 3 showed the best result by applying equation C-7 as shown in Figure C-4.
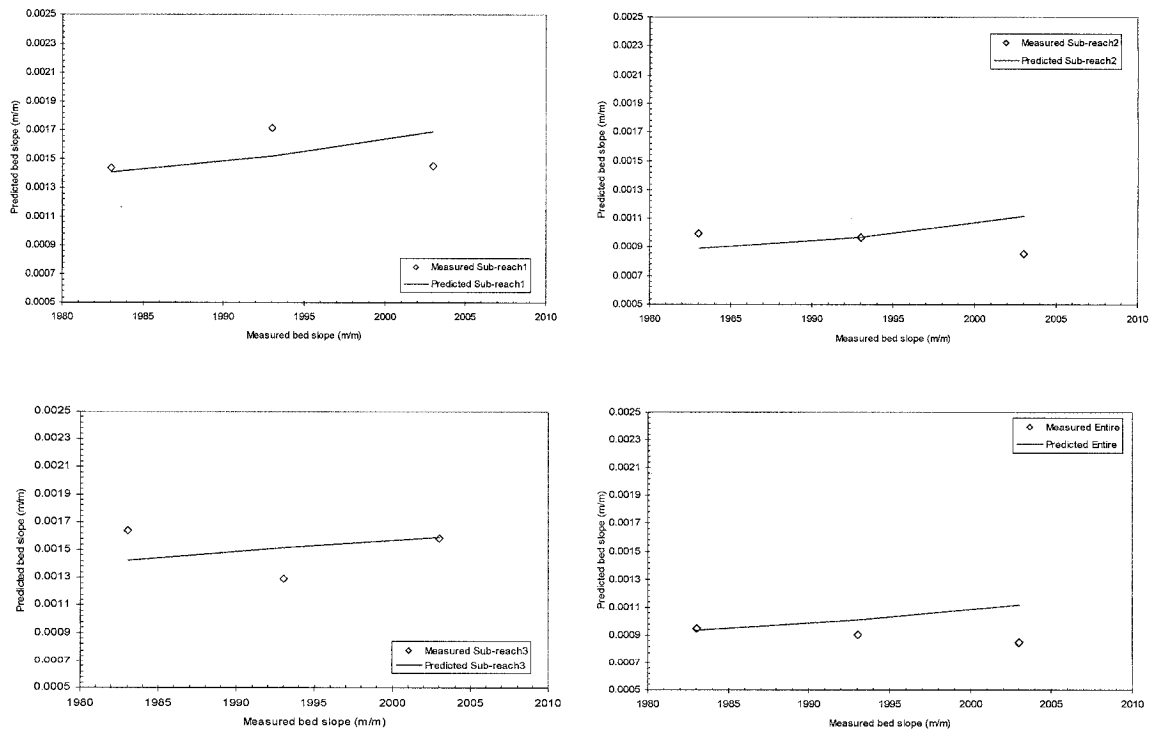
Figure C-4. Regression equations of the bed slope change (m/m) applied to the sub-reach and entire reach for the study reach.

5. Channel Pattern (Meandering, Braiding, and Incising)

To evaluate the state of channel pattern of the study reach, Logistic analysis method by Bledsoe and Watson (2001) was applied. The relationship of this analysis is between median bed material size, D_{50} (mm), and stream power, $SQ^{0.5}$ ($m^{1.5}/s^{0.5}$) as shown in Figure C-5.
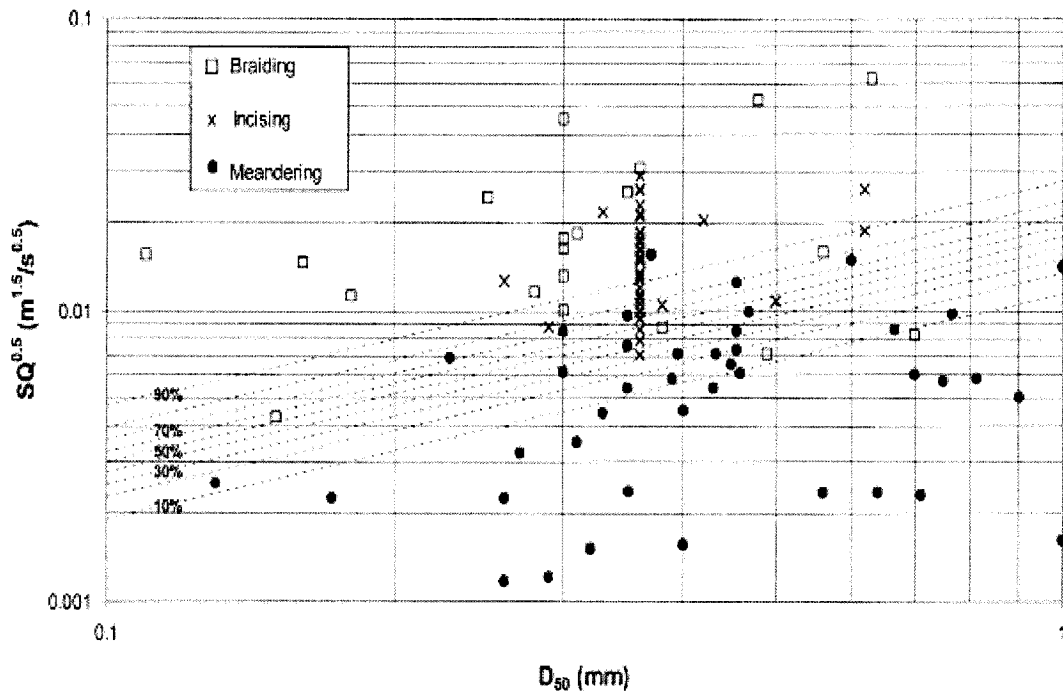
Figure C-5. Probability of incising or braiding a s a function of $SQ^{0.5}$ and D_{50} for streams with sand beds (model 21, n= 109). Discharge is represented by annual flood as first priority then bankfull (Bledsoe and Watson, 2001, Figure 2).

Figure C-6 shows the relationship of $SQ^{0.5}$ and D_{50} for the study reach by applying sub-reach average values for 1983 and 2003. As a result, the channel pattern was between braiding and incising in 1983. However, the channel pattern was between incising and meandering in 2003.
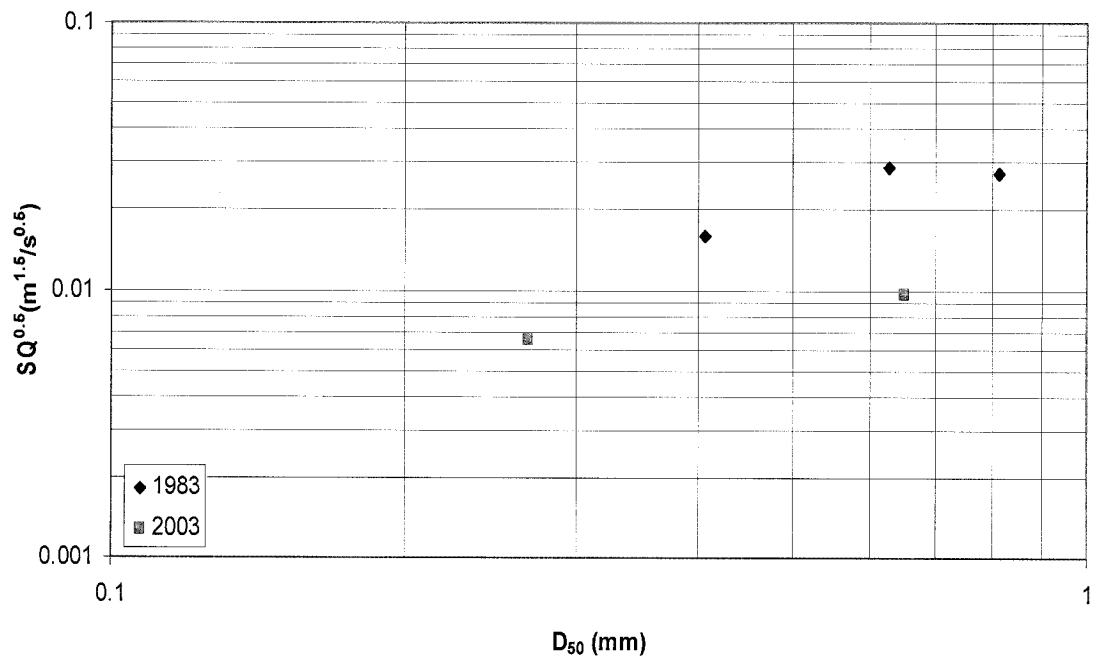
Figure C-6. Relationship of $SQ^{0.5}$ and D_{50} for the study reach by applying sub-reach average values for 1983 and 2003.

APPENDIX D : CONCEPTUAL MODEL OF CHANNEL CHANGES AFTER DAM CONSTRUCTION

1. Review

Conceptual model offer a powerful alternative to the more rigorous, time- and labor intensive modeling efforts required of numerical models. A conceptual model offers general guidelines to assist in understanding and predicting physical processes operating within a system that affect such responses as channel sediment pattern. A conceptual model can also provide insight into the interaction of processes operating at various length and time scales, and the importance of scale in assessing sedimentation patterns following a sediment release (Rathburn, 2002).

There are numerous studies related to the conceptual model to understand and predict channel adjustment on the downstream channel geometry by dam construction. Xu (1990) developed a descriptive model generalizing the complex response in river adjustment downstream from a reservoir by using experimental study. The model included considerable detail on the response of channel geometry and planform, and postulates a three-stage processes by which the river adjusts its channel to the post-dam flow regime. The first stage characterized by clear-water scour, where width/depth ratios of the channel and channel gradient both decrease. In stage two, a reverse tendency appears, that is, width/depth ratios increases and sinuosity decreases. The rate at which gradient decreases becomes very slow. Finally, in stage three, equilibrium is achieved again and width/depth ratios, sinuosity, and bed slope become constants, meaning the system enters a new stable state. The time needed for this sequence is unclear and no doubt varies considerably among rivers. Rathburn (2002) developed the conceptual model of channel response at the scale of a channel reach to a sediment release for the transporting the introduced load, aggrading portion of the channel, and degrading or incising the deposited sediment. In this model, the key factors for the creating or changing slope, pools, channel bed, and bars were the critical Shields parameter and

Shield parameters by comparing the its magnitude. Phillips (2003) developed the conceptual model of the complex interrelationships between key geomorphological factors downstream of a dam.

Dams and reservoirs construction influence the two primary factors-water and sediment-that determine the shape, size, and overall morphology of a river, they represent fundamental interventions in the fluvial system (Grant et al., 2003). According to this concept, they developed the conceptual model of hierarchical linkages influencing channel and valley floor morphology for the basin scale and channel and reach scale.

Conceptual models are more common for lowland alluvial rivers (Wohl, 2000). There are many studies related development of conceptual model for the channel adjustment by dam construction. The components of the developing model of channel adjustment to changes in flow regime and sediment loads were supported by many of the reports on channel changes below dams (Petts and Gurnell, 2005). Schumm (1969) concluded that channel degradation may only be the most immediate result of dam construction from observation on the North Platte River, and that, in time, a complete transformation, or metamorphosis, of channel morphology may be a consequence of river impoundment. By the end of the 1970's, there was established a complex response model of channel adjustment along rivers below dams. This model included different final states caused by different combinations of changes in flow regime and sediment loads and different rates and temporal sequences of changes. Also, Schumm (1985) developed the conceptual model for South Platte River and Arkansas River at Bent's Old Fort.

Petts (1979) found that channel changes from the 14 regulated rivers in Britain were found to be highly variable but were dominated by four general types: including (I) degraded reaches immediately below the dams, and channel of reduced capacity either (II) through meandering reaches or (III) below tributary confluences. Channel changes in these rivers were found to be discontinuous and often localized and a fourth type, an accommodation adjustment, was common. In the latter cases, the regulated clear water releases are not competent to erode the coarse bed sediments or the cohesive, well vegetated banks and sediment yields from all sources are too low to effect sedimentation. Under such conditions, the only impact of a dam is a change in stage-discharge

relationship, with a marked reduction in the frequency of the bankfull flow reflecting the inherited channel dimensions. A rare, extreme flood may be required to initiate channel in these reaches (Petts and Gurnell, 2005).

Brandt (2000a) devised the typology for the effects of dams on downstream geomorphology consisting of nine cases. He thinks that it is possible to estimate resulting cross-sectional geomorphology and longitudinal extent of changes by this typology. Additionally, he proposed a classification scheme for distinguishing geomorphic effects downstream of dams based loosely on Lane's (1955) conceptualization of the balance between grain size, sediment load, discharge, and channel slope.

In predicting downstream effects of moderate to large-sized dams, considered here as dams larger than approximately 10^7 m^3 of storage (Graf, 1999), virtually all sediment is assumed to be trapped by the reservoir. Also, the trap efficiency of large reservoir is commonly greater than 99 %, whereas smaller reservoirs generally have lower values (Williams and Wolman, 1984). In this case, downstream impacts due to truncated sediment supply from upstream are most directly influenced by the rate which sediment is re-supplied to the channel from tributaries, hillslopes, and channel erosion (Grant et al., 2003). Wolman (1967) made observations about the response of river channels below dams. First, at the larger scale, variations of channel response between and along rivers were related to the degree of flood regulation. At a pre- to post-dam discharge ratio of 0.9 or higher all channels experienced degradation while for ratios below 0.75, channels tended to aggradation. Secondly, at the local scale, different sites along a single river can change in different ways. For sites below Garrison Dam on the Missouri River, USA, he observed that some had enlarged cross-sections (by either increased width or increased depth) and others had reduced cross-sections. Thirdly, channel response may change from degradation to aggradation over time after dam closure or even experience several cycles of erosion and sedimentation. Wolman cited phases of aggradation and degradation of the channel-bed below Fort Peck Dam on the Missouri River, USA. Also, Malhotra (1951) had reported initially rapid channel degradation below dams on the Indus River, India followed after 20–30 years by aggradation. Previous mentioned Xu's (1990) descriptive model generalizing the complex response in river adjustment

downstream from a reservoir by using experimental study model focuses on channel responses, the general conceptual model developed below in concerned with fundamental variables related to sediment supply and transport capacity, and is focused on sediment loads rather than the channel response (Phillips, 2003). The interpretation of such complex patterns of change required the development of a new conceptual framework (Petts and Gurnell, 2005).

A framework developed to understand and predict the geological effects both water flow and sediment transport regimes of river channel in ways that influence channel morphology downstream from dams. Here presented a simple conceptual model derived from this framework that may useful for predicting certain directions and magnitudes of downstream effects including illustrating these points for this study reach.

2. A Framework for Geomorphic Effects by Dam

As a means of exploring how geology affects channel response of dams, here begin examining the role of geology mainly based on the Hwang River study reach below the Hapcheon Re-regulation Dam. As many studies mentioned, dams influence the two primary factors, water and sediment (Xu, 1990; schumm, 1969; Petts and Gurnell, 2005). In this study reach, water flow and sediment decreasing were the most important factors including flow pulses by the operation of re-regulation dam.

Due to change of these input conditions, channel bed scoured especially immediately downstream of the dam and followed channel bed particle diameter increase, bed slope decrease, sinuosity decrease and w/h ratio decrease. After that, non-vegetated active channel width decrease including active channel area decrease. On the contrary, the island formation (area) and vegetated area increase by active channel width and area decreasing. Finally, equilibrium condition achieved by bed slope, particle diameter and active channel width become constants. It means that river channel system enters a stable state as shown in flow diagram of Figure D-1.
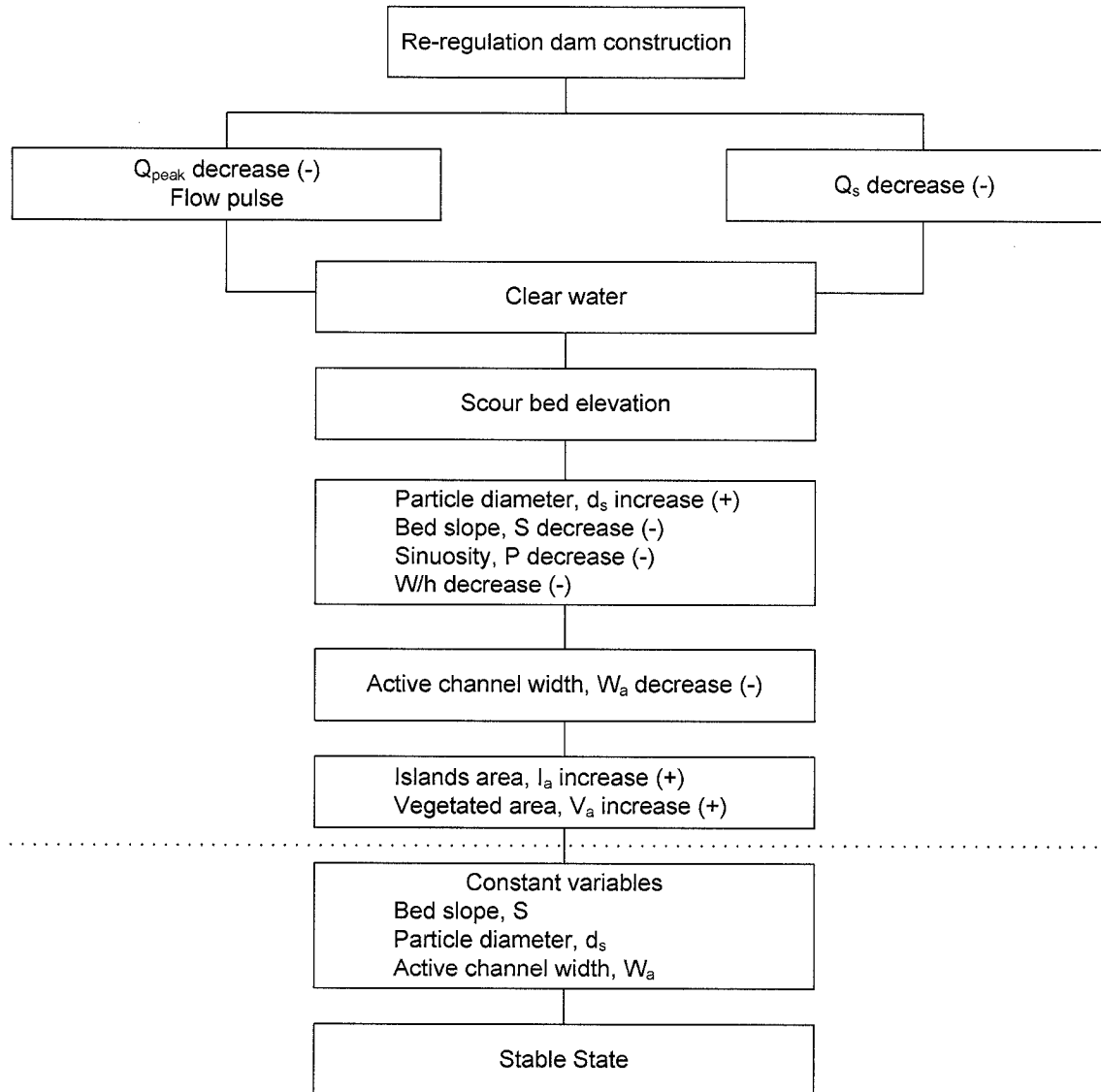
Figure D-1. Flow diagram and framework for the downstream channel adjustment by dam construction

3. Basic equations for Conceptual Model

Here I present a conceptual and analytical model for predicting geomorphic response of rivers to dams based on quantitative analysis of Julien and Wargdalam (1995) hydraulic geometry equations as previous mentioned in chapter 2.

From the downstream hydraulic geometry equations developed by Julien and Wargadalam (1995) for non-cohesive alluvial channel, bed slope presented as following equation:

$$S = 12.4 Q^{\frac{-1}{3m+2}} d_s^{\frac{5}{6m+4}} \tau_*^{\frac{6m+5}{6m+4}} \tag{D-1}$$

The relationship of Equation (D-1) among channel slope S, dominant discharge Q, grain size d_s, and Shields parameter τ_* can be rewritten as

$$SQ^{\frac{1}{3m+2}} = 12.4 d_s^{\frac{5}{6m+4}} \tau_*^{\frac{6m+5}{6m+4}} \tag{D-2}$$

After considering that the sediment discharge Q_s is proportional to the Shields number τ_*, we find that the product of slope and discharge on the left-hand side of Equation (D-2) must be balanced by the product of grain size and sediment discharge on the right-hand side of Equation (D-2), which is kwon as Lane's (1955) relationship (Julien, 2002). The Lanes balance is as follows:

$$QS \propto Q_s d_s \tag{D-3}$$

This qualitative relationship states that equilibrium conditions exist between hydraulic conditions, water flow and bed slope, on the left side of relation and sediment conditions, sediment and bed material size, on the left-hand side of relation. From this qualitative relationship, a quantitative relationship between hydraulic and sediment variables is possible after defining a sediment transport relationship. It is important to use a bed-sediment discharge because riverbed changes are induced by erosion and/or sedimentation of bed material. Meyer-Peter and Muller (1948) developed a complex bedload formula based on the median bed material size, d_{50}. From this formula, Chien (1956) demonstrated that the elaborate original formulation can be reduced to the following simple form:

$$\frac{q_{bv}}{\sqrt{(G-1)gd_s^3}} = 8(\tau_* - \tau_{*c})^{3/2} \qquad \qquad \text{(D-4)}$$

Where, q_{bv} =uint bed load discharge by volume (m²/s), G =Specific gravity of sediment, d_s = grain diameter (m), τ_* and τ_{*c} = Shields parameter and critical Shields parameter

Julien (2002) approximated this formula (equation D-4) for sands, where $0.1 < \tau_* < 1$, is

$$q_{bv} \approx 18\sqrt{g}d_s^{3/2}\tau_*^2 \qquad \qquad \text{(D-5)}$$

Accordingly, the bed load discharge by volume is $Q_{bv} = q_{bv}W$, and from relations (2-14~18) and (D-5) we obtain following formula (Julien, 2002).

$$Q_{bv} \cong 0.77Q^{\frac{6+4}{5+6m}}d_s^{\frac{-2.5+5m}{5+6m}}S^{\frac{7+10m}{5+6m}} \qquad \qquad \text{(D-6)}$$

Where, Q_{bv} = bed load discharge by volume (m³/s), Q = dominant discharge (m³/s), d_s = grain diameter (m), S = Bed slope

Specially for $m = 1/6$, this reduces to

$$Q_{bv}d_s^{0.28} \cong 0.77Q^{1.11}S^{1.44} \qquad \qquad \text{(D-7)}$$

Equation (D-7) shows the dominant role played by the channel slope S in the conveyance of sediment in alluvial channel. From this equation, we can get following equations to assess the effect of sediment discharge Q_{bv} on the downstream hydraulic geometry of sand-bed streams after substituting bed slope S into Julien and Wargadalm (1995) hydraulic geometry equations.

$$h \approx 0.19 Q^{0.46} d_s^{0.13} Q_{bv}^{-0.12} \qquad\qquad\qquad \text{(D-8)}$$

$$W \approx 1.3 Q^{0.62} d_s^{-0.15} Q_{bv}^{-0.15} \qquad\qquad\qquad \text{(D-9)}$$

$$V \approx 4 Q^{-0.08} d_s^{0.02} Q_{bv}^{0.27} \qquad\qquad\qquad \text{(D-10)}$$

$$S \approx 1.2 Q^{-0.77} d_s^{0.19} Q_{bv}^{0.69} \qquad\qquad\qquad \text{(D-11)}$$

$$\tau_* \approx 0.14 Q^{-0.31} d_s^{-0.67} Q_{bv}^{0.57} \qquad\qquad\qquad \text{(D-12)}$$

Where, h = bankfull flow depth (m), W = channel width (m), V = flow velocity (m/s), S = bed slope, τ_* = Shields parameter

From above equations, we can thus infer that an increase in dominant discharge is expected to cause a significant increase in bankfull channel width and in flow depth, a significant decrease in slope, and a less-pronounced decrease in Shields parameter. Also, an increase in dominant sediment discharge corresponds to a significant increase in slope and Shields parameter, a less-pronounced increase in velocity, and slight decreases in channel width and flow depth. The effects of increases in grain size are comparatively less significant, except for a decrease in Shields parameter. In summary, we can expect the following dynamic responses of alluvial systems to perturbations in water and sediment discharges (Julien, 2002).

$$Q^+ \rightarrow W^+ h^+ S^- \tau_*^- \qquad\qquad\qquad \text{(D-13)}$$

$$Q_{bv}^+ \rightarrow S^+ \tau_*^+ V^+ \qquad\qquad\qquad \text{(D-14)}$$

$$d_s \rightarrow \tau_*^- \qquad\qquad\qquad \text{(D-15)}$$

Water discharge is primarily affected variable to the parameters, flow depth and channel width, in equation (D-8) and (D-9), and sediment discharge is primarily affected variable to the parameters, in equation (D-10) and (D-12) but each variable is inversely

proportional. Also, these two variables affect to parameter, Shields parameter, as similar portion in equation (D-11) and grain diameter of channel bed is primary variable.

4. Conceptual Model for Downstream Effects of Dam

Here I present a conceptual and analytical model for predicting geomorphic response of rivers to dams based on quantitative analysis of Julien and Wargdalam (1995) hydraulic geometry equations as mentioned in chapter 2. To know the channel response after dam completion, above relations applied by introducing dimensionless ratio of post-dam flow depth to pre-dam flow depth (h*) and post-dam channel width to pre-dam channel width (W*), and dimensionless ratio of post-dam flow velocity to pre-dam flow velocity (V*) and post-dam bed slope and pre-dam bed slope (S*) as follows.

$$h^* = \frac{h_{post}}{h_{pre}}$$
(D-16)

$$W^* = \frac{W_{post}}{W_{pre}}$$
(D-17)

$$V^* = \frac{V_{post}}{V_{pre}}$$
(D-18)

$$S^* = \frac{S_{post}}{S_{pre}}$$
(D-19)

Where, h^* = dimensionless ratio of post-dam flow depth (h_{post}) to pre-dam flow depth (h_{pre}), W^* = dimensionless ratio of post-dam channel width (W_{post}) to pre-dam channel width (W_{pre}), V^* = dimensionless ratio of post-dam flow velocity (V_{post}) to pre-dam flow velocity (V_{pre}), S^* = dimensionless ratio of post-dam bed slope (S_{post}) to pre-dam bed slope (S_{pre})

These variables estimated from the equations (D-8 to12) for pre and post-dam period. The variables h^*, W^* and V^*, S^* will be plot as h^*-W^* and V^*-S^* relations to know the

213

effect of the variables change pre and post-dam period as shown in Figure 7-2. In response domain for predicted channel adjustments in relation to the dimensionless variables x* and y*, the region 1 represents that two dimensionless variables increase (+) after dam construction by changing bed load discharge by volume Q_{bv} , dominant discharge Q and grain diameter of channel bed d_s . In the same way, the region 2 represents that the dimensionless variables x* and y* decrease (-) at the same time and the region 3 and 4 represent that the one variable increase (+) then the other variable decrease (-) and vice versa.
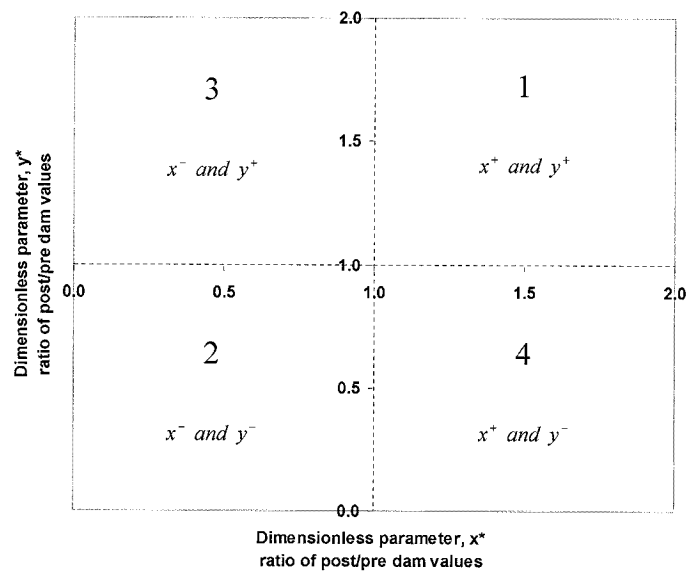

Figure D-2. Response domain for predicted channel adjustments in relation to the dimensionless variable x* and y*

This suggests that plots of individual dams in four dimensionless variables can be describing tendency and state of change. It can be possibly inferred through from this response domain that flow depth decrease and channel width narrow, and flow velocity decrease and bed slope decrease by decreasing dominant discharge and/or bed load discharge due to dam construction in response domain 2 as referred in large number of studies and observations (William and Wolman, 1984; Graf, 1999; Page et al., 2005). In the contrary, flow depth increase and channel width widen, and flow velocity increase

and bed slope increase by increasing dominant discharge and bed load discharge in response domain 1, for example dam removal as referred in large number of studies and observations (Sear, 1995; Pizzuto, 2002; Doyle et al., 2002, 2003). The response domain 3 and 4 represent the variables increase or decrease due to increasing or decreasing dominant discharge and bed load discharge. In the next section, example is examined how the geologic setting affects the direction and magnitude of downstream response.

5. Application of Conceptual Model

By this analysis, interpreting the downstream effects of dams will strongly depend on the downstream channel change by both change of dominant discharge and bed load discharge. Table D-1 and Figure D-3 show the longitudinal change of several dimensionless variables for the Hwang River below the Hapcheon Re-regulation Dam of 45 km long to the confluence with the Nakdong River. Selected locations from the confluence were cross-sections where the bed grain diameter data were available in this reach. Most of the dimensionless variables are less than 1 especially all of flow depth (h) and channel width (W) were less than this value. This means of less than 1 that variables decreased in post-dam period.
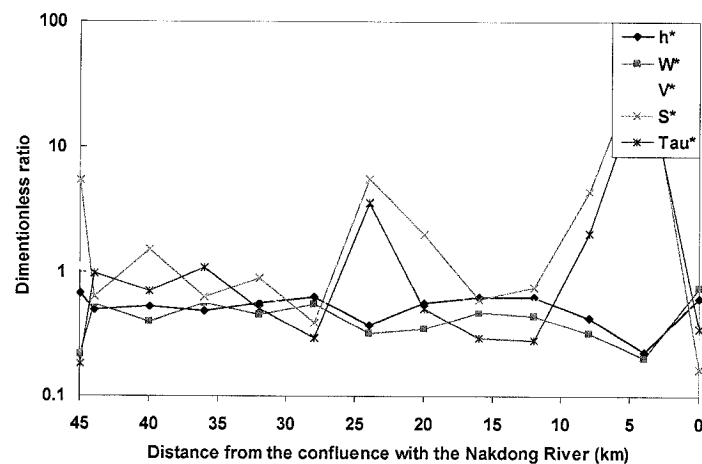

Figure D-3. Longitudinal change of dimensionless variables for the Hwang River below the Hapcheon Re-regulation Dam

Table D-1. Summary of calculation of each dimensionless variable for the Hwang River below the Hapcheon Re-regulation Dam

Sub-reach	Location (km)	Q^*	Q_{bv}^*	h^*	W^*	V^*	S^*	τ_*^*	d_{50}^*
1	36	0.17	0.05	0.49	0.57	0.60	0.63	1.09	0.28
	40	0.17	0.08	0.53	0.40	0.78	1.49	0.70	1.13
	44	0.17	0.01	0.50	0.56	0.60	0.64	0.98	0.32
	45	0.17	1.52	0.68	0.22	1.10	5.35	0.19	20.39
2	16	0.17	0.06	0.64	0.48	0.55	0.61	0.30	1.32
	20	0.17	0.28	0.57	0.35	0.84	1.97	0.51	2.20
	24	0.17	1.21	0.38	0.33	1.36	5.53	3.56	0.59
	28	0.17	0.04	0.64	0.56	0.48	0.40	0.30	0.86
	32	0.17	0.08	0.57	0.46	0.65	0.89	0.51	1.00
3	0	0.17	0.01	0.63	0.76	0.36	0.17	0.35	0.29
	4	0.17	71.52	0.23	0.21	3.53	59.05	39.90	0.34
	8	0.17	0.76	0.43	0.33	1.20	4.34	2.03	0.92
	12	0.17	0.07	0.64	0.45	0.59	0.75	0.29	1.68

- Location(km): the distance from the confluence with the Nakdong river to Hapcheon Re-regulation Dam

Figure D-4 shows Downstream change for the Hwang River below the Hapcheon Re-regulation Dam plotted on the response domain from Figure D-2 for the V*-S* and h*-W* as function of dominant discharge, bed load discharge and grain diameter. Because bed load discharge significantly affected to both flow velocity and bed slope however, dominant discharge significantly affected to both flow depth and channel width. In case of relation, V*-S*, most of the values were plotted in response domain III but some of the values were plotted in response domain II because flow velocity only significantly influenced by bed load discharge but bed slope influenced by both dominant discharge and bed load discharge with nearly same portion as inverse proportion each other. So, it should be change depends on grain diameter. However, in case of relation, h*-W*, all variables were plotted in response domain III because these two dimensionless variables were mainly effected by dominant discharge as described in previous section. These results show similar pattern with measured values as described in previous chapter 4.
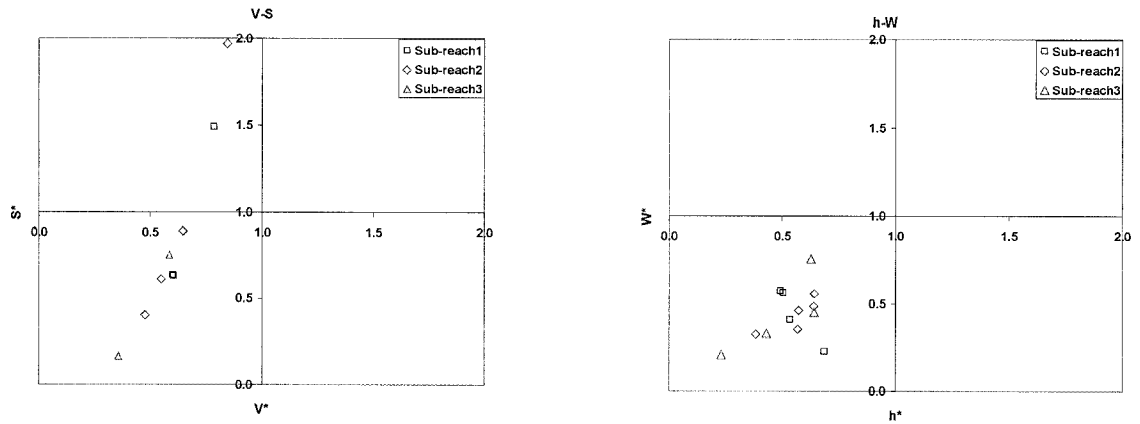
Figure D-4. Downstream change for the Hwang River below the Hapcheon Re-regulation Dam plotted on the response domain from Figure 7-2 for the V*-S* and h*-W* as function of dominant discharge, bed load discharge and grain diameter